Host Cellular Regulatory Networks in Dengue Virus-Human Interactions

A thesis presented for the degree of Doctor of Philosophy

at the University of Glasgow

By

Suzana Misbah

MRC-University of Glasgow
Centre for Virus Research
Institute of Infection Immunity and Inflammation
College of Medical Veterinary and Life Sciences
University of Glasgow

November 2015

AUTHOR'S DECLARATION

I declare that, except where explicit reference is made to the contribution of others, this thesis is the result of my own work and has not been submitted for any other degree at the University of Glasgow or any other institution.

Suzana Misbah
November 2015

ACKNOWLEDGEMENTS

First of all, I would like to express my gratitude to my supervisor, Dr. Alain Kohl for giving me the opportunity to join his research team and carry out this project. Thanks for providing invaluable guidance and tremendous support throughout my PhD. I would also like to thank my co-supervisor, Prof. Juergen Haas, for his research input and suggestions, and for providing access to his lab facilities at the Division of Pathway Medicine, University of Edinburgh during the yeast two-hybrid studies. Special thanks to Juergen's research group, Dr. Samantha Griffiths, Dr. Ramya Gundurao and Rui Chen for their kind assistance throughout the studies.

My appreciation also goes to my PhD assessors, Dr. Chris Boutell and Dr. Arvind Patel for their kind advice and encouragement. I am very grateful to Dr. Andrew Davidson, University of Bristol, for his generosity in providing the dengue virus replicons and his PhD student Amjad Yousuf for helping with the infectious dengue virus work. I wish to thank Dr. Jamel Mankouri, University of Leeds, for the Kv1.3 gene construct. I would also like to thank the Ministry of Higher Education Malaysia and the Universiti Malaysia Terengganu for providing the IPTA Academic Training Scheme sponsorship to pursue my PhD at the University of Glasgow.

My sincere appreciation goes to all my lab members especially to Steph and Mel, for their consistent input throughout my PhD. Thanks for all the help since I started in the lab and for the ideas, suggestions and critical proof-reading of this thesis. Special thanks to Isabelle for helping me with the dengue virus qRT-PCR, Esther for her brilliant ideas, Claire for cheering me up during the hard times, Siwi for the PhD companionship, Margus, Emilie, Joy and Tim. Thanks for the lovely times we spent together over these years!

I would also like to thank my parents Hj. Misbah Ghazali & Hjh. Raunah Mohd. Seh for their advice and constant support. I would never have managed to complete this PhD without their du'a. Last but not least, I wish to express my deepest appreciation to the people for whom I dedicated my life, my beloved husband Yazri Tahir and my cheeky boy Arif Hazim for their love, patience and endless support. This thesis is as much theirs as it is mine. Thanks for always being there whenever I need you and for giving me the strength to accomplish this journey.

ABSTRACTS

Dengue fever is one of the most important mosquito-borne diseases worldwide and is caused by infection with dengue virus (DENV). The disease is endemic in tropical and sub-tropical regions and has increased remarkably in the last few decades. At present, there is no antiviral or approved vaccine against the virus. Treatment of dengue patients is usually supportive, through oral or intravenous rehydration, or by blood transfusion for more severe dengue cases. Infection of DENV in humans and mosquitoes involves a complex interplay between the virus and host factors. This results in regulation of numerous intracellular processes, such as signal transduction and gene transcription which leads to progression of disease. To understand the mechanisms underlying the disease, the study of virus and host factors is therefore essential and could lead to the identification of human proteins modulating an essential step in the virus life cycle. Knowledge of these human proteins could lead to the discovery of potential new drug targets and disease control strategies in the future.

Recent advances of high throughput screening technologies have provided researchers with molecular tools to carry out investigations on a large scale. Several studies have focused on determination of the host factors during DENV infection in human and mosquito cells. For instance, a genome-wide RNA interference (RNAi) screen has identified host factors that potentially play an important role in both DENV and West Nile virus replication (Krishnan et al. 2008). In the present study, a high-throughput yeast two-hybrid screen has been utilised in order to identify human factors interacting with DENV non-structural proteins. From the screen, 94 potential human interactors were identified. These include proteins involved in immune signalling regulation, potassium voltage-gated channels, transcriptional regulators, protein transporters and endoplasmic reticulum-associated proteins. Validation of fifteen of these human interactions revealed twelve of them strongly interacted with DENV proteins. Two proteins of particular interest were selected for further investigations of functional biological systems at the molecular level.

These proteins, including a nuclear-associated protein BANP and a voltage-gated potassium channel Kv1.3, both have been identified through interaction with the DENV NS2A. BANP is known to be involved in NF-κB immune signalling pathway, whereas, Kv1.3 is known to play an important role in regulating passive flow of potassium ions upon changes in the cell transmembrane potential.

This study also initiated a construction of an *Aedes aegypti* cDNA library for use with DENV proteins in Y2H screen. However, several issues were encountered during the study which made the library unsuitable for protein interaction analysis. In parallel, innate immune signalling was also optimised for downstream analysis. Overall, the work presented in this thesis, in particular the Y2H screen provides a number of human factors potentially targeted by DENV during infection. Nonetheless, more work is required to be done in order to validate these proteins and determine their functional properties, as well as testing them with infectious DENV to establish a biological significance. In the long term, data from this study will be useful for investigating potential human factors for development of antiviral strategies against dengue.

TABLE OF CONTENTS

AUTHOR'S DECLARATION 2
ACKNOWLEDGEMENTS 3
ABSTRACTS 4
TABLE OF CONTENTS 6
LIST OF TABLES 10
LIST OF FIGURES 11
ABBREVIATIONS 13
CHAPTER 1: INTRODUCTION 15
1.1 Dengue disease 15
1.1.1 Global distribution 15
1.1.2 Importance of dengue 18
1.2 Dengue virus 19
1.2.1 Structure and genome organisation 19
1.2.2 Replication cycle 22
1.2.3 Protein functions 24
1.3 Dengue virus-host factors 29
1.3.1 Cell surface receptors 29
1.3.2 Screening of DENV host factors 31
1.4 Mosquito host 35
1.4.1 Life cycle and behaviour 35
1.4.2 Routes of transmission 37
1.4.3 Vector competence and control strategies 38
1.5 Human host 39
1.5.1 Clinical manifestation 39
1.5.2 Laboratory diagnostics 39
1.5.3 Prevention and treatment 40
1.5.4 Vaccination strategies 41
1.5.5 Human innate immunity 42
1.6 Hypotheses and aims of study 48
CHAPTER 2: MATERIALS AND METHODS 49
2.1 Cell culture techniques 49
2.1.1 Cell lines 49
2.1.2 Propagation of cells 50
2.1.3 Seeding of cells 50
2.1.4 Cryopreservation of cells 51
2.1.5 Recovery of frozen cells 51
2.2 Nucleic acid techniques 52

2.2.1 RNA isolation 52
2.2.2 RT-PCR 52
2.2.3 Polymerase chain reaction 53
2.2.4 KOD PCR 53
2.2.5 Agarose gel electrophoresis 54
2.2.6 Purification of DNA from PCR products 54
2.2.7 Purification of DNA from agarose gels 55
2.2.8 Quantitation of nucleic acids 55
2.2.9 Transformation of plasmids 55
2.2.10 Mini-scale plasmid purification 56
2.2.11 Large-scale plasmid purification 56
2.2.12 Plasmid restriction digestion 57
2.2.13 DNA Ligation 57
2.2.14 DNA sequencing 58
2.2.15 Bacterial glycerol stock 58
2.3 Protein techniques 58
2.3.1 Protein sample preparation 58
2.3.2 Protein quantification 59
2.3.3 Protein electrophoresis 59
2.3.4 Protein transfer 59
2.3.5 Immunoblotting 60
2.4 Yeast two-hybrid interaction analysis 61
2.4.1 MGC cDNA library, plasmids and yeast strains 61
2.4.2 Dengue virus replicons 62
2.4.3 Determination of DENV transmembrane domains 64
2.4.4 Gateway cloning technology 64
2.5 Yeast two-hybrid protein-protein interaction assay 70
2.5.1 Production of competent yeast AH109 72
2.5.2 Transformation of DENV bait constructs 72
2.5.3 Yeast two-hybrid screen 72
2.5.4 Sequencing of human open reading frames 73
2.5.5 Protein-protein interaction analysis 74
2.5.6 Storage of yeast 75
2.6 Replication of DENV replicon 75
2.6.1 *In vitro* transcription 75
2.6.2 Transfection of DNA and RNA 75
2.6.3 Dual luciferase assay 76
2.7 Functional assays 77
2.7.1 LUMIER assay 77

2.7.2 Co-immunoprecipitation assay 79
2.7.3 siRNA gene silencing 80
2.7.4 Immunostaining 80
2.7.5 Interferon reporter assay 81
2.7.6 Cell proliferation assay 83
2.7.7 BANP and Kv1.3 effect on dengue virus replication 83
2.8 Construction of *Ae. aegypti* cDNA library 85
2.8.1 Preparation of cDNA 88
2.8.2 Production of competent yeast Y187 90
2.8.3 Co-transformation and *in vivo* recombination in yeast 91
2.8.4 Determination of cDNA library titre 91
2.8.5 Harvest of Aag2 cDNA library 92
2.8.6 Mosquito innate immune signalling 92
2.9 Commonly Used Solutions 94
CHAPTER 3: DENGUE VIRUS-HUMAN PROTEIN-PROTEIN INTERACTIONS 96
3.1 Introduction 96
3.2 Objectives 99
3.3 Results 100
3.3.1 Generation of DENV bait constructs 100
3.3.2 Yeast two-hybrid screen 106
3.3.3 Confirmation of interactions 118
3.4 Discussion 123
CHAPTER 4: FUNCTIONAL ANALYSIS OF BANP PROTEIN IN DENGUE VIRUS INFECTION 127
4.1 Introduction 127
4.1.1 MAR elements 127
4.1.2 MAR-binding proteins 128
4.1.3 BANP/SMAR1 128
4.1.4 Relevance of study 130
4.2 Objectives 133
4.3 Results 134
4.3.1 BANP amino acid sequences 134
4.3.2 Confirmation of BANP-NS2A interaction 134
4.3.3 Localisation of BANP and NS2A 140
4.3.4 Assessment of cell viability 144
4.3.5 Effect of BANP on type I interferon response 146
4.3.6 Effect of BANP knockdown in DENV infection 154
4.3.7 Effect of BANP knockdown and overexpression in DENV production 159

4.4 Discussion 162
4.5 Conclusion 168
CHAPTER 5: FUNCTIONAL ANALYSIS OF Kv1.3 IN DENGUE VIRUS INFECTION ... 169
5.1 Introduction 169
5.1.1 Voltage-gated potassium channel Kv1 169
5.1.2 Potassium-gated channel Kv1.3 169
5.2 Objectives 173
5.3 Results 174
5.3.1 Confirmation of Kv1.3-NS2A interaction 174
5.3.2 Cellular localisation of Kv1.3 and NS2A 179
5.3.3 Kv1.3 effect on cell viability 182
5.3.4 Effect of Kv1.3 blockade on DENV-2 infection 183
5.3.5 Effect of Kv1.3 on dengue virus replication 188
5.4 Discussion 190
5.5 Conclusion 193
CHAPTER 6: ESTABLISHMENT OF *Ae. aegypti* cDNA LIBRARY 194
6.1 Introduction 194
6.2 Objectives 197
6.3 Results 198
6.3.1 Construction of *Ae. aegypti* cDNA library 198
6.3.2 Mosquito immune signaling pathways 203
6.3.3 Replication of DENV replicon in mosquito cells 211
6.4 Discussion 214
6.5 Conclusion 222
CHAPTER 7: CONCLUDING REMARKS 223
APPENDIX 228
REFERENCES 233

LIST OF TABLES

Table 1.1: Advantages and disadvantages of yeast two-hybrid assay. 34
Table 2.1: Cell lines used in this study. 49
Table 2.2: Number of seeded cells used for experiments. 51
Table 2.3: Standard PCR parameters. 53
Table 2.4: KOD PCR parameters. 54
Table 2.5: List of antibodies used for immunoblotting. 60
Table 2.6: Gateway donor and destination vectors used in this study. 61
Table 2.7: Transmembrane prediction software used in this study. 64
Table 2.8: DENV gene-specific primers for Gateway cloning. 67
Table 2.9: attB universal primers used in this study. 68
Table 2.10: Sequencing primers for gene insert in pDONR207 entry vector. 68
Table 2.11: Sequencing primers for gene insert in pGBKT7 yeast vector. 69
Table 2.12: Primer sequences for gene insert in yeast pGADT7. 74
Table 2.13: Primers sequences for MGC human insert in pDONR223. 78
Table 2.14: siRNA sequences of human BANP and β-galactosidase. 80
Table 2.15: List of plasmids used in this study. 82
Table 2.16: Potassium channel inhibitors used in this study. 84
Table 2.17: Primer and probe sequences used for qRT-PCR. 85
Table 2.18: Oligonucleotide sequences for construction of Aag2 cDNA library. . 89
Table 2.19: LD-PCR parameters. 89
Table 2.20: Reporter plasmids used in mosquito innate immune signalling. 93
Table 3.1: List of DENV bait gene constructs used in this study. 101
Table 3.2: List of the human proteins interacting with DENV or Flaviviruses. .. 111
Table 3.3: List of the human proteins interacting with DENV or implicated in replication of other viruses. 112
Table 3.4: Summary of the key functional description of enriched Gene Ontology terms. 116
Table 3.5: List of interactions tested by LUMIER assay. 119
Table 5.1: List of relevant information describing the potassium channel blockers. 184

LIST OF FIGURES

Figure 1.1: Global distribution of dengue countries (WHO, 2014). 17
Figure 1.2: Dengue virion structures. 20
Figure 1.3: A schematic representation of DENV polyprotein. 21
Figure 1.4: A schematic diagram of DENV replication cycle. 23
Figure 1.5: Mosquito life cycle. 36
Figure 1.6: Host cellular innate immune responses during DENV infection. 44
Figure 1.7: Subversion of antiviral responses during DENV infection. 47
Figure 2.1: DENV-2 New Guinea C replicons used in this study. 62
Figure 2.2: A schematic map of DENV bait construct in pGBKT7 yeast vector. .. 63
Figure 2.3: A schematic diagram of the Gateway cloning system. 65
Figure 2.4: PCR amplification of DENV genes incorporating *att*B sites. 66
Figure 2.5: A schematic diagram of the yeast two-hybrid system. 71
Figure 2.6: A schematic diagram of LUMIER assay. 77
Figure 2.7: A schematic diagram of the SMART technology. 86
Figure 2.8: A schematic diagram of the homologous recombination in yeast. ... 87
Figure 3.1: A schematic diagram of the DENV gene constructs. 102
Figure 3.2: Amplification of DENV genes. 103
Figure 3.3: Enzymatic digestion of DENV bait constructs. 105
Figure 3.4: Graphical representation of the DENV-human protein-protein interaction network. 108
Figure 3.5: A Venn diagram representing the overlap DENV-human proteins. .. 110
Figure 3.6: Enriched Gene Ontology annotation terms of the human proteins. 117
Figure 3.7: Interactions between Protein A-tagged human proteins and the *RLuc*-tagged DENV NS proteins by LUMIER assay. 121
Figure 3.8: Interactions between *RLuc*-tagged human proteins and the Protein A-tagged DENV NS proteins by LUMIER assay. 122
Figure 4.1: Regulation of NF-κB transactivation by SMAR1. 132
Figure 4.2: Sequence similarities of BANP isoforms and SMAR1. 136
Figure 4.3: Over-expression of BANP and the endogenous BANP. 137
Figure 4.4: Validation of BANP and NS2A interaction by co-IP. 139
Figure 4.5: Expression of DENV NS2A in HEK293 cells. 140
Figure 4.6: Cellular localisation of BANP and NS2A in HEK293 cells. 143
Figure 4.7: Effect of over-expressed BANP and NS2A on HEK293 cell viability. . 145
Figure 4.8: Poly(I:C)-induced interferon response in HEK293 cells. 147

Figure 4.9: Overexpression of BANP inhibits IFN-β production. 149
Figure 4.10: Co-expression of BANP-NS2A inhibits IFN-β. 151
Figure 4.11: Inhibition of IFN-β-mediated gene expression. 153
Figure 4.12: *FFLuc* expression of DENV replicon in mammalian cell lines. 155
Figure 4.13: Expression of *FFLuc* in BHK-21 cells. 157
Figure 4.14: Expression of *FFLuc* in HEK293 cells. 157
Figure 4.15: Validation of BANP knockdown in HEK293 cells. 158
Figure 4.16: DENV replication in BANP overexpression and knockdown. 160
Figure 4.17: mRNA expression of BANP knockdown. 161
Figure 5.1: Schematic diagram of a voltage-gated K^+ channel. 170
Figure 5.2: Expression of Kv1.3-EGFP and its native form in HEK293 cells. 175
Figure 5.3: mRNA gene expression of endogenous Kv1.3 by RT-PCR. 175
Figure 5.4: Interaction of Kv1.3-EGFP and NS2A by co-IP/pull-down assay. 177
Figure 5.5: Interaction of Kv1.3 and NS2A detected with anti-Kv1.3 by co-immunoprecipitation/pull-down assay. 178
Figure 5.6: Cellular localisation of Kv1.3 and NS2A detected by immunofluorescence staining. 181
Figure 5.7: Effect of over-expressed Kv1.3 on HEK293 cell viability. 182
Figure 5.8: Effect of potassium channel blockers on cell viability. 185
Figure 5.9: Effect of MgTx on *FFLuc* expression from DENV-2 replicon. 187
Figure 5.10: Gene expression of DENV-2 capsid region in HEK293 cells exhibiting Kv1.3 blockade. 189
Figure 6.1: 28S and 18S ribosomal RNA profile analysis of Aag2 cells. 198
Figure 6.2: Amplification of Aag2 mosquito cDNA by LD-PCR. 200
Figure 6.3: Amplification of mosquito gene fragments. 202
Figure 6.4: Activation of JAK/STAT, IMD and Toll immune signaling pathways. 205
Figure 6.5: Activation of Toll through co-stimulation with pJL195. 207
Figure 6.6: Activation of Toll through pre-stimulation with pJL195. 208
Figure 6.7: Toll activation through ectopic stimulation with *Bacillus* sp. 210
Figure 6.8: Expression of DENV NS proteins in Aag2 and C6/36 cells. 212
Figure 6.9: Expression of DENV NS proteins in mosquito cells. 213

ABBREVIATIONS

AD	Activation domain
ADE	Antibody dependent enhancement
att	Attachment site
BANP	BTG3-associated nuclear protein
bp	Base pair
cDNA	complementary DNA
co-IP	Co-immunoprecipitation
DAPI	4', 6'-diamino-2-phenylindole hydrochloride
DBD	DNA binding domain
DENV	Dengue virus
DF	Dengue fever
DHF	Dengue hemorrhagic fever
DMSO	Dimethyl sulphoxide
DNA	Deoxyribonucleic acid
ds	Double-stranded
DSN	Duplex-specific nuclease
DSS	Dengue shock syndrome
E	Envelope
EGFP	Enhanced green fluorescent protein
ER	Endoplasmic reticulum
FFLuc	*Firefly luciferase*
IFN	Interferon
IgG	Immunoglobulin G
JAK/STAT	Janus kinase/Single transducers and activators of transcription
kb	Kilobase
kDa	KiloDalton
LD-PCR	Long distance-polymerase chain reaction
LRR	Leucine-rich repeat
LUMIER	LUminescence-based Mammalian IntERactome
MGC	Mammalian gene collection
ml	Millilitre
MMLV RT	Moloney Murine Leukemia Virus Reverse Transcriptase

MW	Molecular weight
µg	Microgram
µl	Microlitre
ng	Nanogram
NS	Non-structural
ORF	Open reading frame
p.t	post-transfection
PBS	Phosphate buffered saline
PCR	Polymerase chain reaction
prM	pre-Membrane
qRT-PCR	Quantitative RT-PCR
RLuc	*Renilla luciferase*
RNA	Ribonucleic acid
rpm	Revolutions per minute
RT-PCR	Reverse transcriptase PCR
siRNA	Small interfering RNA
SMART	Switching mechanism at 5' end of RNA template
TMD	Transmembrane domain
U	Units
WHO	World Health Organization
Y2H	Yeast two-hybrid

CHAPTER 1: INTRODUCTION

1.1 Dengue disease

1.1.1 Global distribution

Dengue fever (DF) is the most common mosquito-borne viral disease which contributes to a global health concern (WHO 2012). The disease may progress into life threatening forms; dengue haemorrhagic fever (DHF) and dengue shock syndrome (DSS). Dengue is caused by infection with dengue virus (DENV), which is transmitted to humans by *Aedes* mosquitoes, particularly *Aedes aegypti* and *Aedes albopictus* (Gubler 1998). The disease is now endemic in more than 100 countries, particularly in South East Asia, Western Pacific, and the Americas (WHO 2011) (http://apps.searo.who.int/pds_docs/B4751.pdf) (Figure 1.1). The disease is estimated to cause 390 million infections per year (Bhatt et al. 2013). Epidemiological data across the countries show an increasing trend of dengue cases and an expansion of dengue geographical regions in recent years (Teixeira et al. 2013; Mia et al. 2013; Arima & Matsui 2011).

DENV may have evolved from a sylvatic cycle involving non-human primates, approximately 500 years ago and was later introduced into human populations (Wang et al. 2000; Holmes & Twiddy 2003). As early as the 18th century, epidemics of dengue-like illness were reported in Asia, North America and Africa which was likely due to international sea-trade (Wilder-Smith & Gubler 2008; Gubler 2006). Epidemics were infrequent at that time with 10-40 year intervals due to the mode of transportation across the sea (Gubler 2002). In 1943, DENV was first isolated from the blood of an infected person by passage through mouse brain, during an epidemic in Japan (Hotta 1952).

During World War II, there was a dramatic change in the epidemiology of dengue in South East Asia which resulted in an expansion of the geographical distribution of dengue and an increase in *Aedes* mosquito populations (Gubler 1997). Most countries in South East Asia have higher prevalence of dengue, which consequently led to the emergence of DHF (Gubler 1997). The first confirmed DHF were documented in the Philippines in 1953–1954, and spread through Thailand and Malaysia in 1958, followed by Singapore and Vietnam in the 1960s (Gubler 2002). Since then, major dengue outbreaks occurred at regular frequencies in the region

which began to spread globally to the Western regions. After World War II, intensive vector control programs and collaborative efforts with the yellow fever disease were implemented in the Americas, including the use of dichlorodiphenyltrichloroethane (DDT), which successfully eradicated *Aedes* populations and reduced the spread of DENV (Gubler 2002).

During the 1980-1990s however, rapid expansion of human settlements, deforestation of land for cultivation, and development of modern transportation have facilitated the movement of people across countries. As a consequence, there was a dramatic geographical expansion of epidemic DHF in Asia, involving India, Pakistan, Sri Lanka, the Maldives, and China (Gubler 1997). Since then, dengue has been re-introduced from Asia to the West Pacific and the Americas, a contributing factor was a decline in the vector control enforcements in the Americas (Gubler 2002; Gubler & Clark 1995). In 2010, 187,333 dengue cases have been documented in South East Asia countries including India, Philippines, Thailand, Indonesia and Myanmar (WHO 2011). The rate of dengue reported cases in this region has increased over the last decade with severe cases 18 times higher compared to the Americas (Shepard et al. 2013; WHO 2011).

Several factors associated with human activities contributed to an increase in the number of dengue cases. The factors include uncontrolled urbanisation, international travel and increased human population (Arima et al. 2013; Gubler 1998). The dynamic distribution of dengue has also been aided by environmental factors, such as temperature, rainfall and seasonal variations which greatly affect the mosquito population (Halstead 2008). Thus considerable efforts in managing the vector control and understanding DENV transmission strategies may greatly reduce the incidence of dengue in the future.

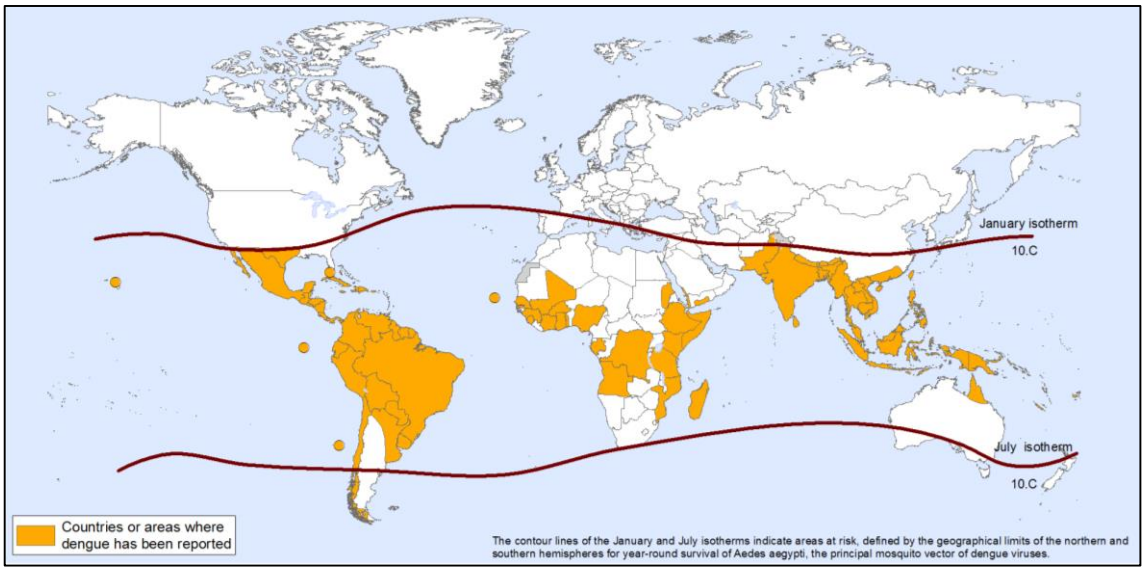

Figure 1.1: Global distribution of dengue countries (WHO, 2014).

Highlighted in orange are countries reporting dengue cases in 2013. Two lines across the map denote the border line of dengue-infected regions. Data source: WHO.(http://gamapserver.who.int/mapLibrary/Files/Maps/Global_DengueTransmission_ITHRiskMap.png).

1.1.2 Importance of dengue

Dengue is a disease of significant importance and has become an international public health concern. An estimated 500,000 DHF patients were hospitalised and a case-fatality rate of approximately 0.5-2.5% has been reported in South East Asia in 1985-2009 (WHO, 2011). In recent years, transmission of dengue has significantly increased in urban and semi-urban areas across the world (Messina et al. 2014). This is facilitated by the highly efficient *Aedes* mosquito vector transmitting the virus, resulting in a local spread within a community or to a different geographical region. Treatment of patients, environmental management of the mosquito vectors and disease prevention programs have imposed a massive economic burden for the governments and communities. For example, an estimation of the cost of dengue illness in America is $2.1 billion every year (Shepard et al. 2011), and US$950 million annually in twelve countries in South East Asia (Shepard et al. 2013). This indicates that dengue poses a significant impact on the health care system and greatly contributes to an economic burden in affected countries.

DENV can subvert immune responses which contributes to its efficient capability to invade human hosts (Muñoz-Jordán 2010). Further, the existence of five DENV serotypes complicates treatment of dengue and hampers the development of an effective vaccine (Guzman et al. 2013). In dengue endemic areas, limited sensitivity of early dengue diagnostic tools and the cross-reactivity of antibodies to previous DENV infections may lead to improper care and increased the risk of death (Hunsperger et al. 2009). This is also worrisome because clinical features of mild DF resembles clinical symptoms of other viral infections which leads to misdiagnosis of dengue and can lead to mortality in dengue patients (Lahiri et al. 2008). Taken together, dengue poses a significant threat and economic burden to many countries. Due to this reason, dengue has become a priority for collaborative scientific research and disease preventive programs under several international organisations including the World Health Organisation (WHO), United Nations Children's Fund (UNICEF), the World Bank, United Nations Environment Programme (UNEP) and the Research and Training in Tropical Diseases (TDR) (WHO 2011).

1.2 Dengue virus

1.2.1 Structure and genome organisation

DENV belongs to the genus *Flavivirus* of the family *Flaviviridae* and has five closely related serotypes; DENV-1, DENV-2, DENV-3, DENV-4 (Gubler 1998), and the most recently described DENV-5 (Mustafa et al. 2014; Normile 2013). Mature DENV is a spherical virion of approximately 50 nm in diameter (Zhang et al. 2003) (Figure 1.2). DENV has a positive-sense single-stranded RNA genome of ~11 kb in length, which is flanked by highly structured 5′ and 3′ untranslated regions (UTRs) (Halstead 2007). Similar to other Flaviviruses, DENV RNA is capped at the 5' end and lacks a poly(A) tail at the 3' end.

DENV genome encodes a single open reading frame (ORF) which is translated into a large polyprotein precursor consisting of three structural proteins; capsid (C), pre-membrane (prM), envelope (E), and seven non-structural (NS) proteins; NS1, NS2A, NS2B, NS3, NS4A, NS4B, NS5 (Figure 1.3) (Lindenbach & Rice 2003). DENV has a nucleocapsid core containing the viral genome and multiple copies of C proteins, surrounded by an envelope derived from the host lipid bilayer (Kuhn et al. 2002). Fitting crystal structures into cryo-electron microscopy (cryo-EM) map revealed 180 copies of the E glycoproteins organised as 90 dimers in a herringbone pattern on the surface of the lipid bilayer (Kuhn et al. 2002). Similarly, 180 copies of membrane (M) protein are present on the surface, partly integrating with E proteins. Parts of the E and M proteins are anchored to the virus lipid bilayer exposing the α-helices on the virus envelope (Zhang et al. 2003).

All four DENV serotypes share ~65% of their genome homology, with some genetic variations within a single serotype (Westaway and Blok, 1997). DENV serotypes differ from one another by 25-40% at the amino acid level. Each serotype is further separated into different genotypes that have a small divergence of ~3% (Westaway and Blok, 1997).

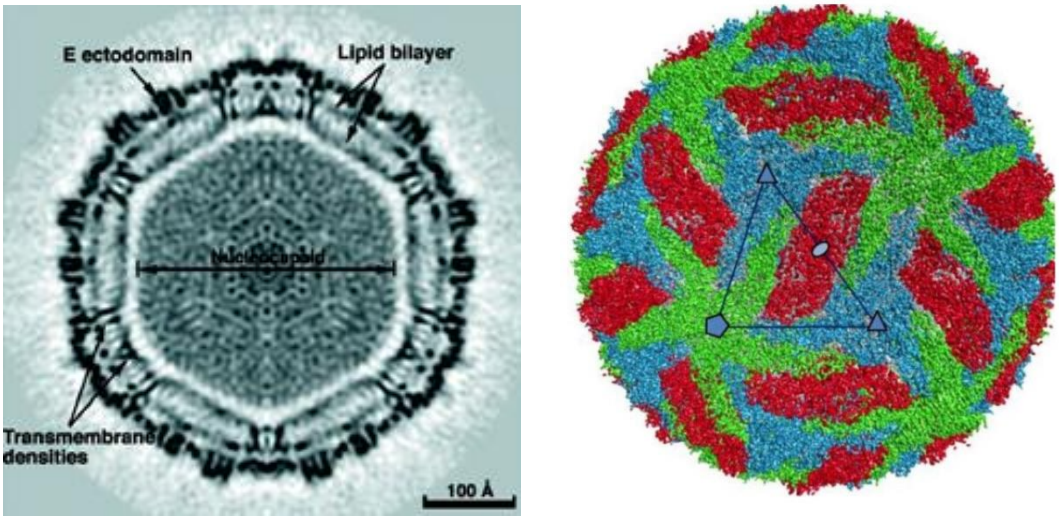

(a) **(b)**

Figure 1.2: Dengue virion structures.

(a) The virus was visualised by cryo-EM with X-ray structures fitted. The virus is spherical which consists of an icosahedral nucleocapsid core surrounded by a lipid bilayer envelope. E and M transmembrane proteins are partly embedded in the envelope where the E ectodomain spans to the outer membrane leaflet. (b) Surface rendering of the cryo-EM density map. Similar colours of E-M heterodimers are equivalent by icosahedral symmetry. Different colours of E-M heterodimers are quasi-equivalent in which the green demonstrates 5-fold axes of the icosahedral symmetry, blue 3-fold and red 2-fold. Symmetry axes are marked by a pentagon, small triangles and an oval, respectively. The large triangle indicates an asymmetric unit, which consists all parts of three E-M dimers. Figures (a) adapted from Zhang et al. (2003), (b) from (Zhang et al. 2013).

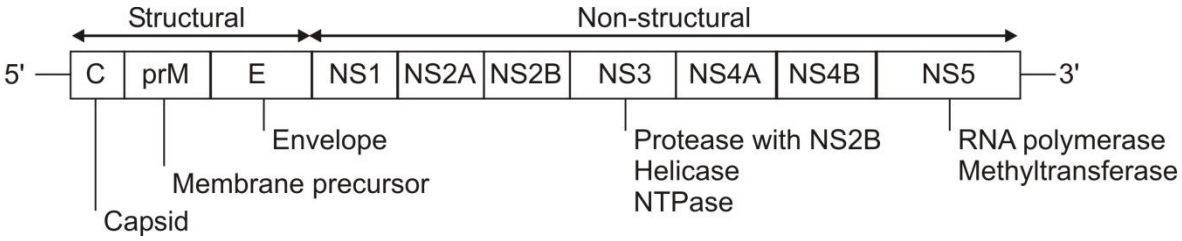

Figure 1.3: A schematic representation of DENV polyprotein.

The viral genome encodes three structural proteins; capsid (C), pre-membrane (prM), envelope (E), and seven non-structural proteins; NS1, NS2A, NS2B, NS3, NS4A, NS4B, NS5. C, prM and E are associated with the viral structure. NS1 is involved in RNA replication, NS2A participates in replication and assembly, NS2B serves as a cofactor for NS3 which is a serine protease, RNA helicase, 5'-RNA triphosphatase, and nucleoside triphosphatase. NS4A and NS4B participate in viral replication, and NS5 serves as a methyltransferase and RNA-dependent RNA polymerase.

1.2.2 Replication cycle

DENV initiates an infection by entering the host cell through receptor-mediated endocytosis (Figure 1.4). Several host cell receptors have been described for DENV (Section 1.3.1). Upon entry, the viral E glycoproteins undergo trimerisation triggered by the acidic environment of the host cellular endosomal compartment (Modis et al. 2004; Allison et al. 1995). This results in fusion of the E glycoprotein to the endosomal membranes and uncoating of C protein that releases the viral genome into the cytoplasm. Following this process, translation of the viral proteins, genome replication and assembly of viral particles occur in the infected cell through manipulation of the host cell machinery. The single-stranded positive-sense RNA genome is translated into a single polyprotein which is subsequently cleaved into individual proteins by the viral and host proteases (Kuhn et al. 2002).

Replication of the viral genome occurs in endoplasmic reticulum (ER)-derived membrane where the positive-sense RNA is used to make a newly synthesised negative-strand RNA, which serves as a template for synthesis of more single-stranded (ss) positive-strand RNA. The genomic RNA is subsequently enclosed in the C proteins, forming a nucleocapsid. The nucleocapsid core buds through the ER membrane, therefore acquiring an envelope that contains the major E glycoprotein, and the precursor membrane protein, prM. The immature viruses are transported through the Golgi network, and undergo proteolytic cleavage of prM to M protein by the host protease furin (Elshuber et al. 2003; Stadler et al. 1997). Mature infectious viruses are then released from the infected cell by exocytosis and are capable of infecting other neighbouring cells.

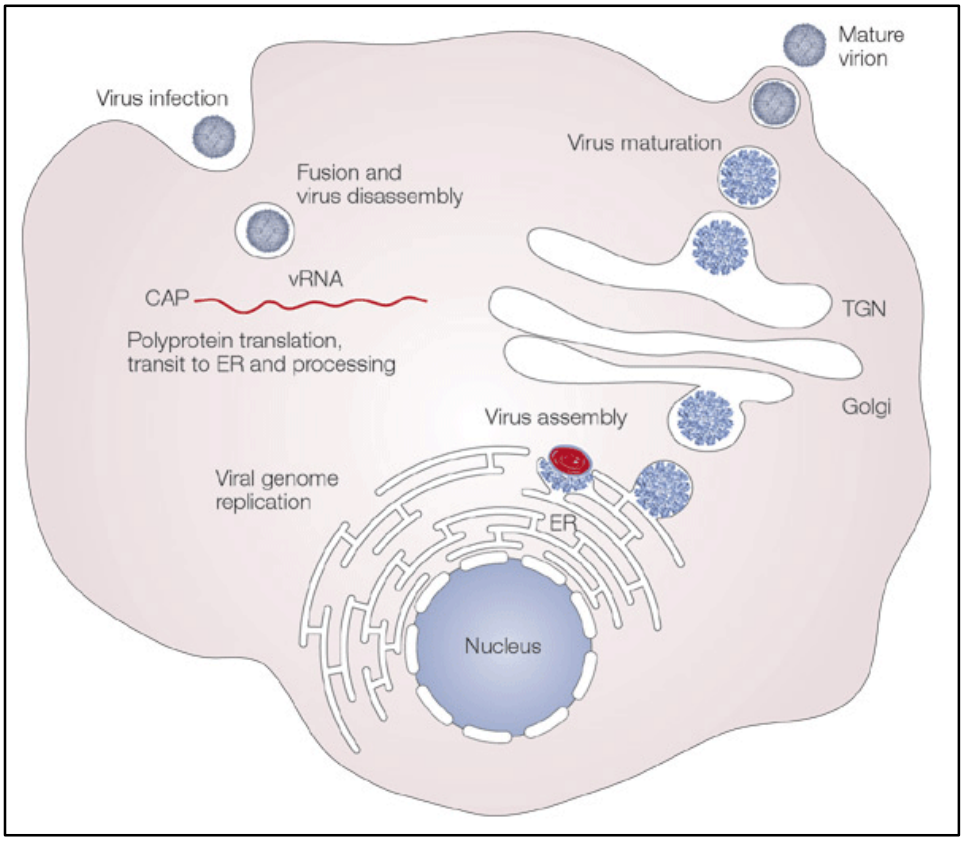

Figure 1.4: A schematic diagram of DENV replication cycle.

In short, the cycle begins upon internalisation of the virus through endocytosis, followed by synthesis of the viral RNA and protein translation mediated by the viral and host machinery. Upon maturation in the trans-Golgi network (TGN), the virus is released by exocytosis. Figure adapted from Mukhopadhyay et al. (2005).

1.2.3 Protein functions

1.2.3.1 Envelope

DENV E glycoprotein (~53 kDa) plays a vital role in viral attachment and membrane fusion for viral entry (Kuhn et al. 2002). Crystal structures revealed three distinct domains (I, II and III) of E ectodomain which are connected by hinges (Modis et al. 2004; Modis et al. 2003). At low pH conditions in endosomes, conserved histidine residues within domain I and domain III become protonated, leading to E conformational changes and exposure of the fusion peptide (Nayak et al. 2009; Fritz et al. 2008). Fusion of the viral and endosomal membranes subsequently occurs, followed by the release of the viral genome into the cytoplasm. The E protein contains two N-glycosylation sites at Asn67 and Asn153 which participate in conformational changes during membrane fusion (Modis et al. 2005). Domain III has been shown to be involved in receptor binding (Crill & Roehrig 2001), thus it serves as a molecular target for antiviral strategy against dengue.

1.2.3.2 Membrane

M protein is the mature form of prM, consisting of 75 amino acids (~9 kDa). The protein is associated with E protein on the external surface of DENV. In the immature virion, prM forms prM-E heterocomplex (Kuhn et al. 2002). Some parts of the prM cover E protein preventing a premature fusion during travel in the acidic environment of Golgi network (Guirakhoo et al. 1992). During virus egress, the host furin cleaves prM, forming M-E heterodimers on the mature virus. This process is essential for maturation of virus and requires a reduced pH environment. It has been shown that alterations in intracellular pH produced non-infectious virions (Yu et al. 2008). Similarly, a prM mutant failed to undergo cleavage, thus resulting in immature, non-infectious virions (Elshuber et al. 2003). M protein is capable of forming dimers and tetramers but the protein is found in its monomeric form entering the cellular secretory pathway (Wong et al. 2012). Apart from its structural association with E, prM/M is capable of eliciting a protective immune response in mice and has pro-apoptotic properties (Brabant et al. 2009; Catteau et al. 2003; Bray & Lai 1991). The protein has been shown to interact with several host proteins during virus entry and release (Brault et al. 2011; Gao et al. 2010; Duan et al. 2008).

1.2.3.3 Capsid

DENV C is a small (~12 kDa), dimeric protein which contains a highly hydrophobic region. C is responsible for encapsidation prior to virus maturation. It has been shown that the C protein interacts with the viral genetic material through the positively charged basic residues during virus assembly (Ma et al. 2004; Lindenbach & Rice 2003). This process is complex and is believed to involve NS proteins (Kummerer & Rice 2002). Although DENV C protein acts as a structural component of the virus particle, it has additional functions in the virus life cycle. Interaction between DENV and the host immune response may contribute to DENV-mediated apoptosis. For example, DENV C localised in the nucleus interacts with an apoptotic regulator and transcriptional repressor, human death-domain associated (Daxx) protein in order to induce Fas-mediated apoptosis in HepG2 cells (Netsawang et al. 2010).

Furthermore, DENV C is found associated with lipid droplets (Carvalho et al. 2012; Samsa et al. 2009). A novel finding by Faustino et al. (2014) shows that C protein interacts with very low density lipoprotein surfaces in a potassium-dependent manner. Such an interaction produces lipoviroparticles, which are a novel way to release the newly synthesised virions to the extracellular surroundings (Faustino et al. 2014).

1.2.3.4 NS1

NS1 protein (~50 kDa) exists as a monomer and is secreted in mature form as a soluble hexadimer (Flamand et al. 1999). The protein forms a lipoprotein particle with an open-barrel protein shell and a lipid-rich central channel (Gutsche et al. 2011). During viral infection, NS1 is found circulating in the bloodstream of virus-infected patients beginning the onset of fever and its high concentration in the blood is associated with severity of dengue (Libraty et al. 2002; Alcon et al. 2002). Since NS1 is secreted, it plays a role as a molecular target for antibody recognition, therefore it is used as a molecular marker for diagnosis of dengue (Kassim et al. 2011; Singh et al. 2010).

Furthermore, NS1 has been found on cellular membranes associated with lipid rafts and within intracellular organelles of virus-infected cells (Welsch et al. 2009; Avirutnan et al. 2007). Binding of NS1 to the cellular surface induces complement activation, which contributes to vascular leakage which leads to DHF/DSS (Avirutnan et al. 2006). Increasing data support the involvement of NS1 in virus replication, although the specific functional role of NS1 is not fully understood (Lindenbach & Rice 1999; Mackenzie et al. 1996; Muylaert et al. 1996). NS1 contains highly conserved cysteine (Cys) residues and two glycosylation sites at asparagine (Asn) residues; Asn130 and Asn207 (Wallis et al. 2004; Pryor & Wright 1994). Recent data suggest mutation of these residues impaired RNA synthesis and reduced virus growth (Fan et al. 2014).

NS1 interacts with ribosomal protein RPL18 in Huh-7 cells, which is shown to be important during DENV replication (Cervantes-Salazar et al. 2015). Further to this, NS1 has been reported to interact with vimentin and hnRNP C1/C2 in DENV-infected cells (Kanlaya et al. 2010b; Noisakran et al. 2008). This interaction complex dissociates during vimentin disruption, which reduced dengue NS1 expression and viral replication. Secreted NS1 has also been shown to interact with the complement component 1 (C1q) which suggests its important role in the human complement system and immune evasion during DENV infection (Silva et al. 2013).

1.2.3.5 NS2A

NS2A is a transmembrane protein (~22 kDa) and its function in DENV life cycle is not fully understood. NS2A is involved in virus replication where it can bind to the 3' UTR and components of the replication complex (Mackenzie et al. 1998). Studies on Flaviviruses show that NS2A has a functional role in virus assembly since mutation of NS2A disrupts this process (Leung et al. 2008; Kummerer & Rice 2002). This is supported by recent structural analysis and mutagenesis of the ER membrane-spanning region of DENV NS2A which affects the virus assembly and RNA synthesis (Xie et al. 2015; Xie et al. 2013). Another important role of NS2A is its capability to antagonize host immune responses and block dsRNA-activated protein kinase PKR (Tu et al. 2012; Liu et al. 2006; Muñoz-Jordan et al. 2003).

1.2.3.6 NS2B

NS2B is small, hydrophobic protein (~14 kDa) about which very little is known. NS2B functions as a serine protease cofactor and acts as an activator by forming a heterodimeric complex with NS3 (Falgout et al. 1991). The protease component of NS2B/NS3 interacts with the host signal peptidase which catalyses proteolytic processing of DENV polyprotein (Falgout et al. 1991). This subsequently cleaves the NS region of NS2A/NS2B, NS2B/NS3, NS3/NS4A and NS4B/NS5 junctions (Yusof 2000; Arias et al. 1993; Falgout et al. 1991). NS2B/NS3 protease complex has also been reported to inhibit type I interferon (IFN) response by inhibiting the phosphorylation of Interferon Regulatory Factor 3 (IRF3) (Rodriguez-Madoz et al. 2010).

1.2.3.7 NS3

NS3 (~70 kDa) is a cytoplasmic protein which has multifunctional properties including RNA helicase, 5′-terminal RNA triphosphatase and serine protease. RNA helicase activity of NS3 has been associated with unwinding of the viral genome during RNA replication (Bartholomeusz & Wright 1993). The 5′-RNA triphosphatase activity in NS3 plays a role in 5'-capping of the RNA (Bartelma & Padmanabhan 2002). A site-directed mutagenesis study by Shafee & AbuBakar (2003) suggests the possible involvement of the NS3 protease and NS2B/NS3 protease precursor in apoptosis during DENV-2 infection, although the specific mechanism of induction is unclear. Furthermore, West Nile virus (WNV) NS3 has the ability to cleave caspase-8 and caspase-3 which triggers the apoptotic pathway (Ramanathan et al. 2006). Further, DENV-2 NS3 has been reported to interact with the host nuclear receptor binding protein (NRBP) that influences trafficking between the ER and trans-Golgi network, and involves in alteration of the cell membrane structures (Chua et al. 2004).

1.2.3.8 NS4A

NS4A is a small protein (~16 kDa) and is highly hydrophobic. There is limited information about the specific role of this protein. NS4A is found in reticular structures and cytoplasmic foci derived from the ER which suggests its involvement in virus replication (Miller et al. 2007). NS4A has also been shown to play a role in membrane rearrangements during virus replication, and this is supported by recent structural analysis showing that NS4A is capable of inducing membrane undulation (Lin et al. 2014; Roosendaal et al. 2006). Furthermore, NS4A has been shown to be involved in autophagy which facilitates virus replication and prevents host cell death (McLean et al. 2011). Along with NS2A and NS4B, expression of NS4A in human cells inhibits IFN signalling indicating its functional role as IFN-antagonistic (Muñoz-Jordán 2010; Muñoz-Jordan et al. 2003). NS4A has also been shown to interact with polypyrimidine tract binding protein (PTB) by modulating the viral negative strand RNA synthesis (Jiang et al. 2009). Further examination has shown that silencing of PTB in DENV-infected cells decreases virus production.

1.2.3.9 NS4B

NS4B (~27 kDa) is a highly hydrophobic protein, which is found residing at the ER lumen side of the membrane (Miller et al. 2006). NS4B colocalizes with NS3 in the perinuclear region of infected human cells which suggests its involvement in viral replication (Umareddy et al. 2007). Although the precise role of NS4B is still unclear, the protein is thought to be involved in suppression of IFNs. In IFN-induction experiments, NS4B has shown to be the strongest DENV IFN inhibitor compared to NS2A and NS4A (Muñoz-Jordan et al. 2003). Furthermore, NS4B is capable of interfering with signal transducer and activator of transcription 1 (STAT1) phosphorylation, therefore blocking the IFN-induced signal transduction cascade (Ho et al. 2005). Recent evidence also suggests NS4B plays an important role in suppression of the human RNAi pathway. NS4B is capable of inhibiting RNase Dicer, a key enzyme of the antiviral RNAi pathway, which consequently promotes DENV replication (Kakumani et al. 2013). Conversely, deletion mutants of NS4B particular regions involving the transmembrane domains (TMDs); TMD3 and TMD5, has shown to activate the RNAi pathway and induce antiviral activity (Kakumani et al. 2013).

1.2.3.10 NS5

NS5 is cytoplasmic and is the largest DENV protein (~103 kDa). This protein has a methyltransferase domain (MTase) at its N-terminus and an RNA-dependent RNA polymerase (RdRp) at its C-terminus (Kapoor et al. 1995). The N-terminal MTase domain is required for RNA capping while the C-terminal domain of RdRp is required for RNA replication (Egloff et al. 2002; Ackermann & Padmanabhan 2001). NS5 is therefore thought to contain the components of the RNA replicase complex in concert with NS3 helicase activity (Kapoor et al. 1995). Due to the functional enzymatic ability of NS5, the protein is a significant target for the development of anti-viral compounds. For example, the MTase activity of NS5 has been shown to be affected by ribavirin 5'-triphosphate *in vitro*, thus the drug has potential anti-dengue activity (Benarroch et al. 2004). NS5 is also characterised as an IFN-antagonistic, because it has the ability to bind and degrade STAT2, therefore inhibiting the host immune responses (Ashour et al. 2009; Mazzon et al. 2009).

1.3 Dengue virus-host factors

1.3.1 Cell surface receptors

Interaction between DENV and its mosquito or human host factors occurs through many stages of the virus life cycle. The initial entry of the virus to the host cell requires binding of the viral E protein to receptors present on the cell surface. The precise mechanism of viral entry however, has not been completely elucidated due to the diverse tropism whereby virus infects the mosquito and human hosts through different cell surface receptors. In mammalian cells, the C-type lectins, such as the dendritic-cell-specific ICAM3-grabbing non-integrin (DC-SIGN), mannose receptors and C-type lectin domain family 5 member A (CLEC5A) have been described (Chen et al. 2008; Miller et al. 2008; Tassaneetrithep et al. 2003). Crystal structures of DC-SIGN have shown that the carbohydrate recognition domain is capable of binding to the DENV E asparagine residue 67, which facilitates virus entry (Pokidysheva et al. 2006). CLEC5A however, lacks carbohydrate binding sites, its homodimeric structures on the cell surface have been suggested to mediate binding to DENV glycoprotein ligands (Watson et al. 2011). Glycosaminoglycans (GAGs) such as heparan sulphate, have been described as

putative DENV attachment factors (Chen et al. 1997). Site-directed mutagenesis analysis indicated that DENV interacts with GAGs through two lysine residues (K291 and K295) located on domain III of E protein (Watterson et al. 2012). Heat-shock proteins (HSPs) present on surfaces of U937 and neuroblastoma cells, such as HSP90 and HSP70 have also been suggested as components of DENV receptor complex. Both HSPs act as chaperones in facilitating structural re-arrangement of DENV E protein during membrane fusion (Reyes-Del Valle et al. 2005). A major component of high density lipoprotein, apolipoprotein A-I (ApoA-I) has been shown capable to associate with DENV particles and promote virus infection (Li et al. 2013). This occurs through interaction between DENV E protein and lipoprotein receptor, scavenger receptor class B type I (SR-BI), which resulted in increased virus infectivity.

Recent progress has discovered two phosphatidylserine (PS) receptors; TIM-1 and AXL proteins, as potential DENV entry factors (Meertens et al. 2012). Both proteins play a vital role in PS-dependent phagocytic removal of apoptotic cells. Interaction of TIM-1 and AXL with PS on DENV surface has been shown to facilitate infection through a mechanism similar to engulfment of apoptotic cells (Meertens et al. 2012). This mechanism is supported by subsequent identification of another receptor, CD300a on the surface of human macrophages (Carnec et al. 2015). CD300a acts as a DENV attachment factor which is capable of recognising PS- and phosphatidylethanolamine-associated viral particles of the four DENV serotypes.

In mosquito cells, a small number of host factors have been identified. These include prohibitin receptor (Kuadkitkan et al. 2010), tubulin or tubulin-like protein (Chee & AbuBakar 2004), and several proteins characterised by molecular weight sizes (Cao-Lormeau 2009; Mendoza et al. 2002).

1.3.2 Screening of DENV host factors

Viruses interact with the host cellular components to complete their life cycle and this requires manipulation of certain host cellular pathways to ensure virus survival (Fischl & Bartenschlager 2011). While viruses aim to survive in the host cells and synthesize more progeny virions, the host may initiate a cascade of events that leads to the elimination of the invading virus (Fernandez-Garcia et al. 2009). The study of virus and host factors is therefore essential to assess gene expression and map the protein interaction networks, and provide understanding of the mechanisms underlying disease. Various high throughput screening technologies have been developed in order to identify the host cellular factors contributing to virus infection such as proteomics, microarray-based genomics, genome-wide RNAi screen and the yeast-two hybrid (Y2H) assay (Peng et al. 2009). Each screening technique has a certain level of strengths and weaknesses which may produce a unique distribution of interactions and the discovery of various interacting genes or proteins.

1.3.2.1 Proteomics and microarray studies

Many studies utilise a proteomic approach to analyse the host response to DENV infection. This includes the use of two-dimensional gel electrophoresis (2DE) combined with mass spectrometry which identified many differentially expressed proteins in human and insect cells (Zhang et al. 2013; Higa et al. 2008; Pattanakitsakul et al. 2007). Using this technique, global changes of a cellular response in infected or treated samples could be analysed in a single run. These traditional proteomics approaches however have limited dynamic range and reproducibility due to the difficulty in resolving protein samples (Domon & Aebersold 2006). Highly acidic or basic proteins, low abundance, hydrophobic and high molecular weight proteins are known to resolve poorly by 2DE, which affects proteomic outcomes. Advanced proteomic approach based on non-gel based techniques and label-free liquid chromatography-mass spectrometry (LC-MS) has been further developed. The advantages of these techniques include the requirement of less protein samples and sample processing time, and production of higher peptide sequence coverage (Patel et al. 2009).

Analysis of Huh-7 cells infected with DENV-2 by label-free LC-MS technique revealed a decrease in the expression of enzymes involved in glycolytic pathway, citrate cycle, and pyruvate metabolism, also alterations in the expression of many proteins involved in mitochondrial function (Pando-Robles et al. 2014).

Microarray uses complementary DNA sequences as probes for gene expression studies (Miller & Tang 2009). This technology allows simultaneous comparison of numerous genes by identification of genes associated with certain biological changes. Differential gene expression profiling in response to DENV infection by microarray has shown the involvement of host genes in NF-κB immune response and the ubiquitin proteasome pathway (Hanley & Weaver 2010; Fink et al. 2007). Microarray technology however, is rather expensive, and data generated from this study requires substantial bioinformatic analysis.

1.3.2.2 Genome wide RNAi screen

Genome-wide RNAi screen is a powerful method for high throughput analysis of sequence-specific knockdown of target genes. The gene silencing technique is highly efficient and able to simultaneously interrogate thousands of genes. A genome-wide RNAi screen in *Drosophila melanogaster* library led to the discovery of 116 DENV host factors; in which 82 have human homologs (Sessions et al. 2009). Of these, 42 are verified as human host factors including FLJ20254, TAZ, CNOT2, EXDL2, NPR2 and SEC61B, and knockdown of these proteins decreased DENV titres in HuH-7 cells. It has also been suggested that several proteins are exploited by DENV in both human and mosquito, probably because they play crucial roles for virus replication in both hosts (Sessions et al. 2009). Another RNAi screen by Krishnan et al. (2008) performed in HeLa cells has reported the identification of host cellular factors potentially important in WNV and DENV infection. Silencing at least 36% of WNV host proviral factors including SUMO-protein ligase UBE2I and vATPase has shown to decrease DENV infection. This study also highlights the ubiquitin-ligase CBLL1 in WNV internalisation and several protein components of the endoplasmic reticulum-associated protein degradation (ERAD) pathway that play a key role during WNV and DENV infection. A major drawback of using siRNA is the possibility of RNA sequences binding to more than one target which produces off-target effects (Jackson & Linsley 2010).

1.3.2.3 Yeast-two hybrid screen

The Y2H is a well-established technique used for detection and identification of protein-protein interaction. This assay employs the GAL4 system that encodes for two hybrid proteins; a DNA-binding domain and an activation domain. This system is capable of activating a downstream reporter gene when both DNA-binding and activation domains are in close proximity (Section 2.5). Several advantages and disadvantages of this technique are outlined in Table 1.1.

Using the Y2H approach, analysis of protein-protein interactions has revealed potential DENV host factors. Khadka et al. (2011) has identified 105 proteins from a human liver cDNA library interacting with DENV-2, in which most proteins are related to the complement and coagulation system, centrosome and cytoskeleton. Of these, six proteins have been confirmed to interact with DENV including calreticulin (CALR), ATP-dependent RNA helicase (DDX3X), rab6-interacting protein 2 (ERC1), golgin-95 (GOLGA2), thyroid receptor-interacting protein 11 (TRIP11) and SUMO-protein ligase (UBE2I) (Khadka et al. 2011). CALR in particular, may have a potential role in the viral RNA synthesis as the protein has been shown to co-localize with the viral NS3 and NS5 proteins, and the viral dsRNA in DENV-infected cells (Khadka et al. 2011). Analysis of HCV-human protein-protein interactions by Dolan et al. (2013) identified 112 unique interactions representing 94 human proteins. Interestingly, five proteins, CUL7, PCM1, RILPL2, RNASET2, and TCF7L2, were shown to be HCV and DENV shared targets, and required for both HCV and DENV replication. The remaining Y2H studies on DENV-human interactions are described in Chapter 3 of this thesis.

There are fewer protein-protein interaction studies investigating DENV and its mosquito host. Mairiang et al. (2013) have revealed 102 interactions involving 93 unique mosquito proteins, of which 58 have human orthologs. Several proteins had been previously encountered including the E3 ubiquitin ligase seven in absentia and seven in absentia homolog (SIAH2) (Le Breton et al. 2011), and the paramyosin and human cingulin like-1 (CGNL1) (Khadka et al. 2011). Further to this, carboxypeptidase B1 (CPB1) has been identified from *Ae. aegypti* midgut cDNA library interacting with DENV E protein (Tham et al. 2014). Binding of CBP1 to E which was demonstrated by a protein structural model is speculated to be involved in the viral encapsulation activity.

Table 1.1: Advantages and disadvantages of yeast two-hybrid assay.

Advantage	Disadvantage
Experiments are performed in yeast which enables analysis of protein-protein interaction *in vivo*.	Lack of post-translational modifications in yeast.
High throughput screening and can be performed using an automated robotic platform.	Difficulty of transmembrane proteins to be expressed in the nucleus and activated transcription of the reporter gene.
Easy to perform and scaling up yeast cultures, inexpensive and quick.	Absence of optimal conditions for binding of proteins in the yeast nucleus.
Simple readout by detecting the growth of yeast diploids on amino acid dropout medium.	The expression and subcellular localisation of proteins may have been altered due to artificial expression.
Able to identify transient and weak protein-protein interactions.	

1.3.2.4 Protein structure prediction

Several studies have identified DENV host factors through protein structure prediction (Doolittle & Gomez 2011; Guo et al. 2010). Guo et al. (2010) have predicted a DENV-mosquito protein-protein interaction network using computational approach, annotating 4,214 *Ae. aegypti* proteins of which 714 are potential DENV host factors. These proteins are related to replication/transcription/translation (RTT), immunity, transport and metabolism. Further validation by RNAi gene silencing indicates five hypothetical proteins including AAEL012515, AEL001005, AAEL013989, AAEL005351 and AAEL013275, have shown a significant reduction of DENV titre in mosquito midguts. A similar structure prediction study predicted approximately 2,000 DENV-human interactions (reduced to 19 after data mining from literatures), while 18 interactions were obtained for *Ae. aegypti* (Doolittle & Gomez 2011). Although the results are promising, the accuracy of interactions can be questioned due to the different structures of proteins *in vivo*, rather than *in silico*.

1.4 Mosquito host

1.4.1 Life cycle and behaviour

DENV is transmitted to humans by *Aedes (Stegomyia)* mosquito vectors; particularly *Ae. aegypti* and *Ae. albopictus*. Other *Aedes* species are found in specific endemic areas such as *Ae. polynesiensis* in French Polynesia, *Ae. scutellaris* in the Pacific Islands and New Guinea, and *Ae. niveus* in Philippines. *Aedes* mosquitoes have four developmental stages: eggs, larvae, pupae and adults (Figure 1.5). Female *Aedes* mosquitoes lay eggs on the wet walls of water-filled containers or stagnant water. The eggs resist desiccation for several months and hatch into larvae when submerged in water. The larvae feed on particulate organic matter in the water and moult three times followed by metamorphosis into pupae. After 2-3 days, the pupae develop into adult mosquitoes and emerge from the pupae skin leaving the water. The entire mosquito life cycle lasts 8-10 days at ambient temperatures.

Male mosquitoes feed on flower nectar, whereas female mosquitoes feed on human blood to develop their eggs. Human dengue transmission cycle begins when a female *Aedes* mosquito ingests the virus through blood feeding from a viraemic

human host. The infection first occurs in the mosquito midgut epithelial cells, spreads through the haemolymph to other organs such as the fat body and trachea, and finally disseminates to the mosquito salivary glands (Salazar et al. 2007; Linthicum et al. 1996). Once in the saliva, DENV can be transmitted to another host when the mosquito acquires a blood meal, thus spreading the disease. Female mosquitoes carrying the virus remain infectious for life.

Aedes aegypti mosquitoes are domestic and prefer to rest in dark areas, frequently in bedrooms, bathrooms, and kitchens (Chadee 2013; Perich et al. 2000). They prefer vertical surfaces such as walls, furniture, hanging articles such as clothing, towels and curtains, and can be found on the ceiling and under furniture such as beds. Although they are mostly active during daylight hours, blood feeding and oviposition activities usually occur between 6-9 in the morning and at 4-6 in the afternoon (Chadee 2013).

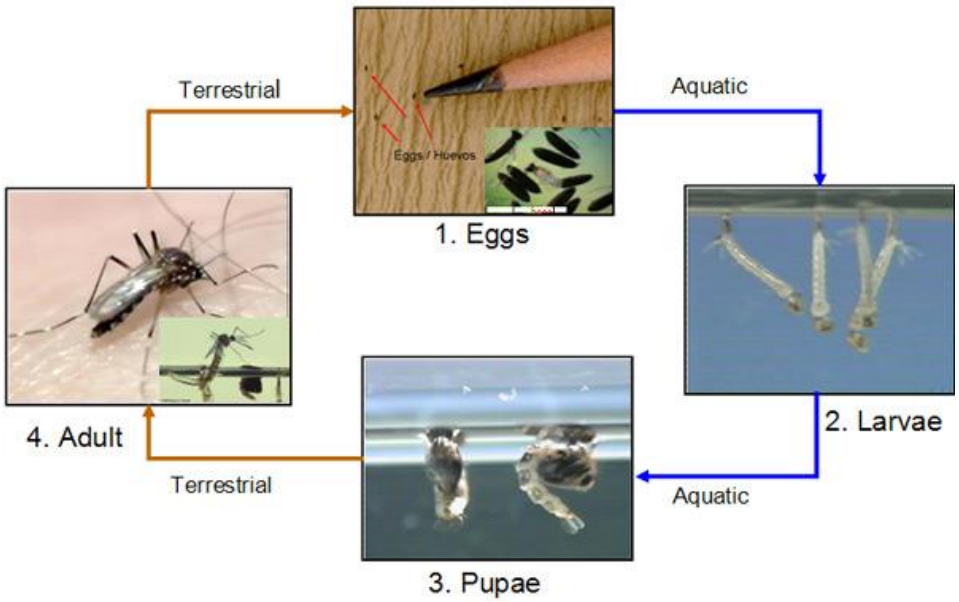

Figure 1.5: Mosquito life cycle.

Aedes mosquitoes have four life stages: egg, larva, pupae and adult, where the first three stages are aquatic. The entire life cycle, from an egg to an adult, takes approximately 8-10 days. The figure was adapted from CDC Dengue Homepage as link below:

http://www.cdc.gov/Dengue/entomologyEcology/m_lifecycle.html.

1.4.2 Routes of transmission

While DENV is transmitted horizontally from an infected person to another through bites of infected mosquitoes, the virus can also be transmitted vertically from infected female mosquitoes to their offspring. Experimental evidence demonstrated the persistence of DENV in successive generations of mosquitoes following intrathoracic inoculation with the virus (Joshi et al. 2002). In the wild, several studies have demonstrated the isolation of DENV from field-caught male *Aedes* mosquitoes indicating the occurrence of transovarial/vertical transmission (Espinosa et al. 2014; Arunachalam et al. 2008; Kow et al. 2001). Other studies on preimaginal stages of mosquitoes similarly detected the co-circulating DENV serotypes during an outbreak and during inter-epidemic periods (Martins et al. 2012; Thongrungkiat et al. 2011; Le Goff et al. 2011). Since transovarial transmission in *Aedes* populations seems to peak at certain periods in nature, it has been proposed as an important strategy for the virus to persist during adverse climate conditions which are unfavourable for transmission to humans (Angel & Joshi 2008; Pherez 2007; Guo et al. 2007). The importance of vertical transmission in maintaining DENV in nature is also supported by mathematical models, however the role of transmission in maintenance of the virus in nature is not clearly described (Esteva & Vargas 2000). In contrast to this, the low rate of vertical transmission is believed to dilute down the virus with every generation which subsequently causes the virus to disappear (Adams & Boots 2010). Thus, it is believed that virus maintenance in nature is more likely contributed to by dengue asymptomatic cases within human populations (Adams & Boots 2010).

Vertical transmission of dengue also occurs in humans where DENV is transmitted from an infected mother to the foetus. These cases however are rare and depend on the severity of disease and the stage of pregnancy during viral infection (Pouliot et al. 2010). Adverse outcomes have been suggested with symptomatic cases during the late stage of pregnancy including the risk of pre-term labour and low birth weight of infants (Friedman et al. 2014; Basurko et al. 2009). In a small number of cases, infection is associated with thrombocytopenia and even death in neonates (Chye et al. 1997; Thaithumyanon et al. 1994). There is also evidence that DENV can be transmitted through organ transplantation and blood transfusion (Tambyah et al. 2008; Tan et al. 2005). A recent case of blood transfusion contamination was encountered from a donor who had travelled to a dengue

endemic area and came down with dengue symptoms (Punzel et al. 2014), while other cases detected dengue from a high number of asymptomatic blood donors (Linnen et al. 2008; Mohammed et al. 2008). These scenarios imply a requirement of strict enforcements to forbid blood donations from donors four weeks after returning from disease endemic areas, and highlight the critical role of comprehensive screening prior to organs and blood transfusion.

1.4.3 Vector competence and control strategies

In addition to the use of biological and chemical control for dengue, other strategies including the use of genetically modified organisms have been established. One method was through the use of sterile insect technique (SIT), by releasing radiation-sterilised and chemosterilised male mosquitoes into the wild for mating with native females. Offspring produced from this mating are very few or non-viable, hence this technique can reduce mosquito populations (Dame et al. 2009). This technique however has several drawbacks including that irradiation induced random dominant lethal mutations in males which may reduce their fitness, hence are non-competitive to the wild populations (Dame et al. 2009; Alphey et al. 2000). Aside from this technique, the Release of Insects carrying a Dominant Lethal gene (RIDL) has been a promising tool by introducing a genetically engineered late-acting lethal gene into mosquitoes (Phuc et al. 2007). Progeny developed from this technique contain the lethal gene and will die before turning into an adult. A similar technique was developed to generate mosquito progenies carrying genes that impose a tetracycline-repressible flightless-female phenotype (Wise de Valdez et al. 2011). This decreases the capability of female offspring to avoid predators and seek animal hosts for probing, hence reduces their chances of survival.

Another efficient method involves inoculation of an insect parasitic bacterium, *Wolbachia* into mosquitoes which results in a reduction in their lifespan (McMeniman et al. 2009). Mosquitoes infected with *Wolbachia* will have high rates of cytoplasmic incompatibility, which kills the embryos produced by uninfected females after mating with infected males, thus preventing egg hatching (McMeniman et al. 2009). This has caused mosquito populations to decline, thereby reducing virus transmission.

1.5 Human host

1.5.1 Clinical manifestation

A person becomes infected when bitten by a DENV-infected mosquito. The onset of fever usually occurs after 4 to 12 days. During this period, dengue causes a highly infectious viremic phase that lasts 4-8 days (WHO 2011). Dengue illness ranges from asymptomatic and mild fever to the life-threatening forms; DHF and DSS. Both children and adults vary in clinical symptoms, depending on their age, immune status and genetic background. DF, also known as 'break-bone fever', is characterised by headache, retro orbital pain, severe muscle and joint pains, nausea, vomiting and maculopapular rash (WHO 2011). Patients with DHF/DSS may manifest a high fever, plasma leakage, thrombocytopenia or organ failure. Haemorrhagic signatures are bleeding into the skin, leakage of fluid into the interstitial space, elevated haematocrit and hypotension that result in shock and eventually death (WHO 2011).

All four DENV serotypes result in similar clinical symptoms in humans. Infection with one serotype confers a lifelong immunity, however, a secondary infection with a different DENV serotype does not confer protection, which can lead to antibody-dependent enhancement (ADE) (Guzman et al. 2013; Halstead 1977). ADE is an explanatory hypothesis whereby the pre-existing circulating antibodies generated from a previous infection bind to the newly infecting virus and facilitate the viral entry into monocytes or macrophages through Fc receptor recognition (Guzman et al. 2013; Halstead 1977). These antibody-virus complexes are not neutralised, but enhance the infection resulting in high level of viraemia, which can lead to DHF/DSS (Flipse et al. 2013; Sasaki et al. 2013).

1.5.2 Laboratory diagnostics

Accurate diagnostic tests for detection of dengue are essential for early preventive measures to control the spread of disease. Clinical diagnostics for dengue are performed by isolation of the virus, detection of the viral nucleic acid or antigen, and virus-specific antibodies in the serum of infected patients (Mungrue 2014; Peeling et al. 2010). Earlier method of confirming dengue infection is through isolation of the virus in cell culture (Henchal et al. 1983), however this is time-consuming. Rapid detection of the viral nucleic acids with

higher sensitivity is achieved by reverse-transcriptase polymerase chain reaction (RT-PCR) during the viraemic phase of illness, thus are suitable for early detection of dengue (Yong et al. 2007; Lanciotti et al. 1992).

Serological tests are less expensive and routinely performed in many laboratories after the fifth day of dengue illness (Mungrue 2014). IgM- and IgG-captured enzyme-linked immunosorbent assay (ELISA) have been successfully able to detect virus-specific antibodies from patient sera (Kuno et al. 1991). Detection of antibodies against the viral NS1 using commercial ELISA-based diagnostic kits is easy to perform but they are very expensive and have limited sensitivity particularly in dengue endemic regions (Hermann et al. 2014; Lima et al. 2010; Dussart et al. 2006). IgM assays are more useful for early detection of dengue, although the sensitivity and specificity varies with different commercial assays (Hunsperger et al. 2009). IgG assays correlate well with previously established hemagglutination assays but are limited in their ability to detect early infection. In this test, past or current dengue infections can be specifically identified through seroconversion of antibody titer between acute and convalescent sera of an individual (Peeling et al. 2010). Rapid NS1 IgM- and IgG-based diagnostic tests currently exist in various formats as a quick and easy method for use at point of care, including the dipstick ELISA, immunochromatographic card assay and antigen strips (Blacksell et al. 2011; Wu et al. 2000). Other diagnostic tests have been developed such as salivary IgA assays (Yap et al. 2011; Cuzzubbo et al. 1998), however all these tests have to be evaluated following WHO guidelines.

1.5.3 Prevention and treatment

Early diagnosis and optimal clinical management reduces the likelihood of severe dengue in patients. Due to the lack of commercially available antivirals or vaccines for dengue, treatment of patients is supportive. In the case of a mild or moderate illness, patients are usually treated with oral or intravenous rehydration (Gubler 1998; WHO 1997). In severe dengue cases, particularly for patients with thrombocytopenia and active bleeding, intravenous fluid-replacement or prophylactic platelet transfusions are given in order to prevent haemorrhagic complications (Kaur & Kaur 2014).

Dengue can also be controlled by reducing the mosquito breeding sites and preventing exposure to the mosquito bites. Given that mosquito breeding sites are in close proximity to human settlements and domestic behaviour, controlling these breeding sites can be done through the use of effective chemical controls such as larvicides in water containers and insecticides (WHO 1997). The large usage of chemical agents however has led to development of insecticide-resistant *Ae. aegypti* which becomes an environmental and health concern (Rodríguez et al. 2007). In contrast, the use of biological control agents, such as larvivorous fish and copepod crustaceans has shown to be environmentally safe and can effectively control *Ae. aegypti* populations (Nam et al. 2012; Nam et al. 2000). Self-protection methods including the application of skin repellent during outdoor activities, wearing protective clothing and using mosquito bed nets are recommended in order to prevent mosquito bites. An efficient environmental management and active surveillance play an important role in prevention and control strategies against dengue (Guzman et al. 2010; Gubler 1998).

1.5.4 Vaccination strategies

To date, there is a lack of vaccine commercially available for dengue. Although major efforts have been made to develop an effective vaccine, this has been hampered by difficulties in eliciting a protective immune response against the four DENV serotypes. In early attempts, several vaccines were developed through the production of purified inactivated virus and live-attenuated virus (LAV) (Robert Putnak et al. 2005; Innis & Eckels 2003; Eckels et al. 2003). These vaccines however, appeared to be reactogenic and were incapable of inducing a broad range protective immune response (Edelman 2007). In addition, the vaccines have been associated with higher adverse effect particularly among children. Several dengue vaccine candidates are currently at different stages of clinical studies. For example, the DENVax vaccine is developed based on previous DEN-2 PDK-53 vaccine, with an additional mutation in NS3 gene for attenuation (Osorio et al. 2011). The vaccine contains a mixture of the live-attenuated DENV-2 containing chimeric prM and E proteins of DENV-1, DENV-3, DENV-4 on the attenuated DENV-2 backbone. Clinical trials in adults receiving this vaccine have recently shown an acceptable tolerability and immunogenicity (Osorio et al. 2014). This warrants further evaluation of this vaccine under the phase II clinical trials (https://clinicaltrials.gov/ct2/show/NCT02302066).

Among others, the most advanced vaccine candidate is the live-attenuated tetravalent chimeric yellow-fever dengue (CYD), developed by Sanofi Pasteur which is under evaluation in phase III clinical trials (Lang 2012; Guy et al. 2011). This vaccine is composed of the recombinant prM and E proteins of four DENV serotypes, each has been introduced into the yellow fever (YF) 17D virus backbone (Guy et al. 2011). Very recently, this vaccine has shown to be promising, which demonstrated a reduction in dengue among 35,000 children in Asian-Pacific and Latin American countries (Hadinegoro et al. 2015).

1.5.5 Human innate immunity

1.5.5.1 Innate immune responses against dengue virus

The innate immune response plays an important role as the first defence mechanism against invading DENV. The initial cellular target upon infection is thought to be the interstitial dendritic cells followed by the lymphatic system and then distribution to monocytes and macrophages (Wong et al. 2012; Durbin et al. 2008). Upon acidification of endosome and internalisation of DENV, pattern recognition receptors, such as the Toll-like receptors (TLRs) and intracellular molecules such as the DExE/H box RNA helicases are responsible for recognition of the viral RNA (reviewed by Green et al. 2014). TLR3 (TLR7/TLR8) recognizes the DENV RNA and triggers the phosphorylation of TIR-domain-containing adapter-inducing interferon β (TRIF) (Figure 1.6) (Tsai et al. 2009). Interaction of TRIF with the TNF-receptor-associated factors (TRAF); TRAF3 and TRAF6, resulted in activation of two cascades: 1) TRAF3 interacts with TANK-binding kinase 1 (TBK1) and IkappaB kinase epsilon (IκKε) which activates the phosphorylation of interferon regulatory factor 3 (IRF3). Phosphorylated IRF3 translocates into the nucleus and induce the expression of type I IFNs. 2) TRAF6 recruits TAB2/3-TAK1 and NF-κB essential modulator protein (NEMO) to activate Iκα/β, leading to translocation of NF-κB transcription factors to the nucleus and activation of NF-κB targeted genes (Green et al. 2014).

Cytoplasmic helicases such as retinoic-acid-inducible gene I (RIG-I) and melanoma differentiation-associated gene 5 (MDA5) play an essential role in recognition of the viral RNA in the cytoplasm (Figure 1.6). RIG-I, MDA5 and TLR-3 have been reported to act synergistically inhibiting DENV replication *in vitro* (Nasirudeen et al. 2011). RIG-I recognizes short RNA ligands, whereas MDA5 recognizes long dsRNA and replication intermediates (Reikine et al. 2014). Upon recognition of these ligands, both RIG-I and MDA5 oligomerise, which subsequently activates the signalling partner mitochondrial antiviral signaling (MAVS) on the mitochondrial membranes. MAVS triggers an interaction with the ER protein stimulator of interferon genes (STING/MITA) and recruits TRAF3 and TRAF6 in order to activate the signaling cascades, hence the production of type I IFN (Liu et al. 2013).

Secreted IFN binds to the cell surface IFN-α/β receptor (IFNAR) and induces the Janus kinase-signal transducer and activator of transcription (JAK/STAT) signalling cascade (Green et al. 2014). This occurs through binding of the IFN on IFNAR which activates the adaptor molecules JAK1 and Tyk2 via tyrosine phosphorylation. This leads to the phosphorylation and dimerisation of STAT1 and STAT2, forming heterodimers that subsequently associate with IRF9. Association of these molecules generates an interferon-stimulated gene factor 3 (ISGF3) complex, which is translocated into the cell nucleus and binds to the interferon-stimulated response elements (ISREs) leading to the transcription of diverse IFN-stimulated genes (ISGs). This results in substantial production of pro-inflammatory cytokines and numerous effector proteins restricting virus infection, hence induction of an antiviral state (Fernandez-Garcia et al. 2009; Platanias 2005).

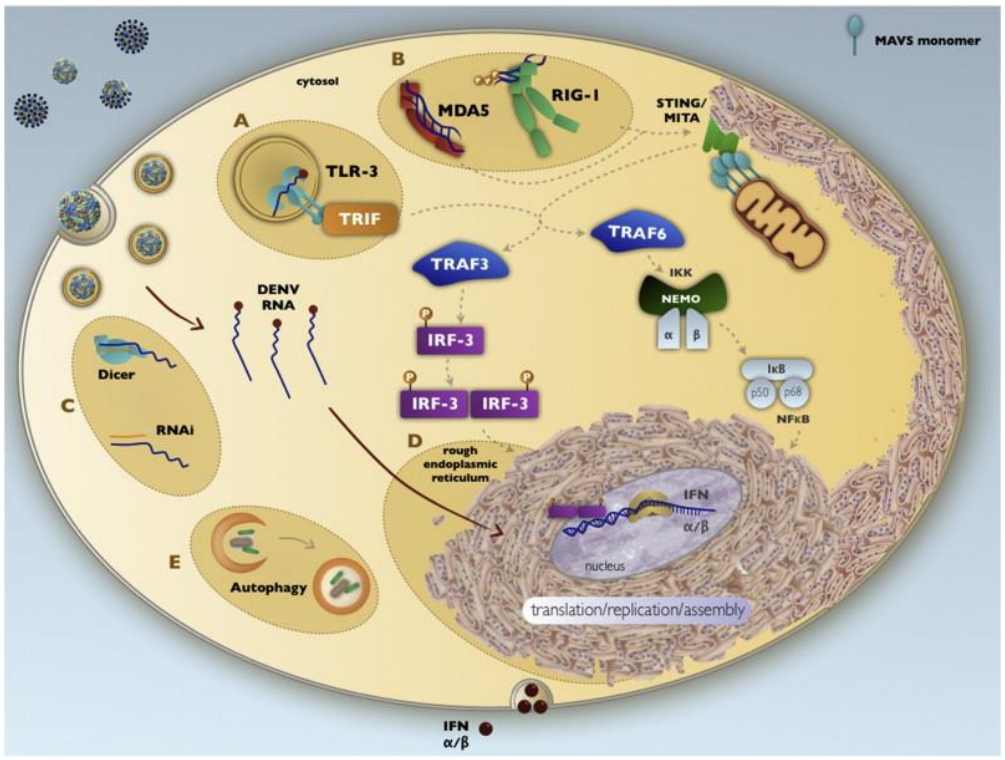

Figure 1.6: Host cellular innate immune responses during DENV infection.

A: Recognition of the viral RNA in endosome by TLR3, B: Recognition of the viral RNA in the cytoplasm by RIG-I and MDA5, C: Activation of the RNAi pathway, D: hypertrophy of endoplasmic reticulum, E: lysosomal degradation by autophagy. Figure adapted from Green et al. (2014).

1.5.5.2 Other immune responses

Humoral immunity usually develops ~6 days after an infection, in which antibodies target the E and prM proteins on the viral surface, as well as the secreted NS1 (Lai et al. 2008; Cardosa et al. 2002; Shu et al. 2000), resulting in either neutralisation or enhancement of dengue (Huang et al. 2006; Halstead 2003). It has been shown that the most potent neutralizing antibodies are strain-specific, which target the domain III of the E protein (Lisova et al. 2007; Oliphant et al. 2006). In the event of neutralisation, the antibodies are capable of preventing attachment of the virus to its receptor, thus inhibiting viral entry (Thompson et al. 2009). In contrast, the non-neutralizing antibodies are produced due to a secondary infection with a heterologous DENV serotype leading to ADE. It is believed that pre-existing antibodies bind to the virus particles and are engulfed by immune cells such as monocytes, macrophages and dendritic cells, through Fc receptors (Halstead 1977). This results in replication of the virus in target cells generating a higher viral load and enhancement of infection (Chareonsirisuthigul et al. 2007). In patients suffering from DHF/DSS, a cytokine storm occurs with a significant increase in the levels of cytokines and immune mediators such as IFN-α, IFN-γ, tumour necrosis factor-α (TNF-α) and interleukins (IL) which coincides with the severity of disease (Chakravarti & Kumaria 2006; Hober et al. 1993; Kurane et al. 1991a).

The precise role of the T cell response is debatable, either it contributes to the protection or enhancement of dengue (Malavige & Ogg 2013). It has been speculated that serotype-specific highly cross-reactive T cells may contribute to pathogenesis of dengue by producing high pro-inflammatory cytokines. However, this is difficult to define due to the lack of a suitable animal model for conducting such experiments. During a heterologous secondary infection, it is believed that the memory CD8+ T cells results in alteration of T cell function causing a marked increase in cytokines and immune modulators, which is a characteristic of DHF/DSS (Mathew & Rothman 2008). In contrast, a study by Yauch et al. (2009) using CD8+ T cell-depleted mice revealed that CD8+ T cells are important in defence mechanism against DENV (Yauch et al. 2009).

1.5.5.3 Subversion of host immune responses

DENV is capable of manipulating the host cellular machinery and developing immune evasion strategies to establish an infection (Fischl & Bartenschlager 2011). Recently published data suggests the virus is capable of antagonising cellular effects and blocking the host innate immune responses (Morrison et al. 2012; Muñoz-Jordán 2010). These include the role of NS5 as a potent IFN antagonist where the protein is capable of blocking the JAK/STAT tyrosine kinase 2 (Tyk2) phosphorylation (Ashour et al. 2009; Jones et al. 2005; Ho et al. 2005) (Figure 1.7). This causes an impairment of STAT2, followed by a subsequent degradation of STAT2. Further to this, DENV proteins NS2A, NS4A, and NS4B have been implicated in IFN inhibition (Rodriguez-Madoz et al. 2010; Muñoz-Jordán et al. 2005). Expression of these proteins in cell cultures has been shown to reduce STAT1 phosphorylation, which plays a key role in regulating type I IFN response pathway. Several reports show the inhibition of IFN production by NS2B/3 protease activity, in which the proteins directly cleaves STING, the downstream component of RIG-I/MDA5 (Angleró-Rodríguez et al. 2014; Rodriguez-Madoz et al. 2010).

DENV is able to subvert autophagy by manipulating cellular autophagic machinery. Other viruses including hepatitis C virus, poliovirus and coronaviruses are also capable of modulating autophagy for replication (Reggiori et al. 2010; Dreux et al. 2009; Taylor & Kirkegaard 2007). Increased formation of autophagosomes and higher expression of autophagy-related proteins have been shown to correlate with enhanced DENV replication (Lee et al. 2008). These are supported by co-localisation studies and detection of the virus translation/replication complex on immature autophagosomes (Panyasrivanit et al. 2009). Although the mechanism of DENV-induced autophagy is unclear, the role of ER stress response and suppression of the autophagic regulator, mammalian target of rapamycin (mTOR) have been suggested (Lee et al. 2008). DENV-induced autophagy has also been shown able to promote lipid metabolism for generation of energy which provides favourable conditions for virus replication (Heaton & Randall 2010).

Virus infection often interferes with cellular homeostasis and leads to ER stress. In order to cope with the stress, DENV is capable of manipulating the unfolded protein response (UPR) through induction of X box binding protein 1 (XBP1) (Yu et al. 2006). XBP1 is a key transcription factor of UPR and has been shown to increase

synthesis of membrane phospholipid and ER volume for cell survival (Sriburi et al. 2004). DENV NS proteins, such as NS2B/3 have been shown to activate XBP1, which resulted in prolong cell viability and thus, enhanced viral replication (Yu et al. 2006).

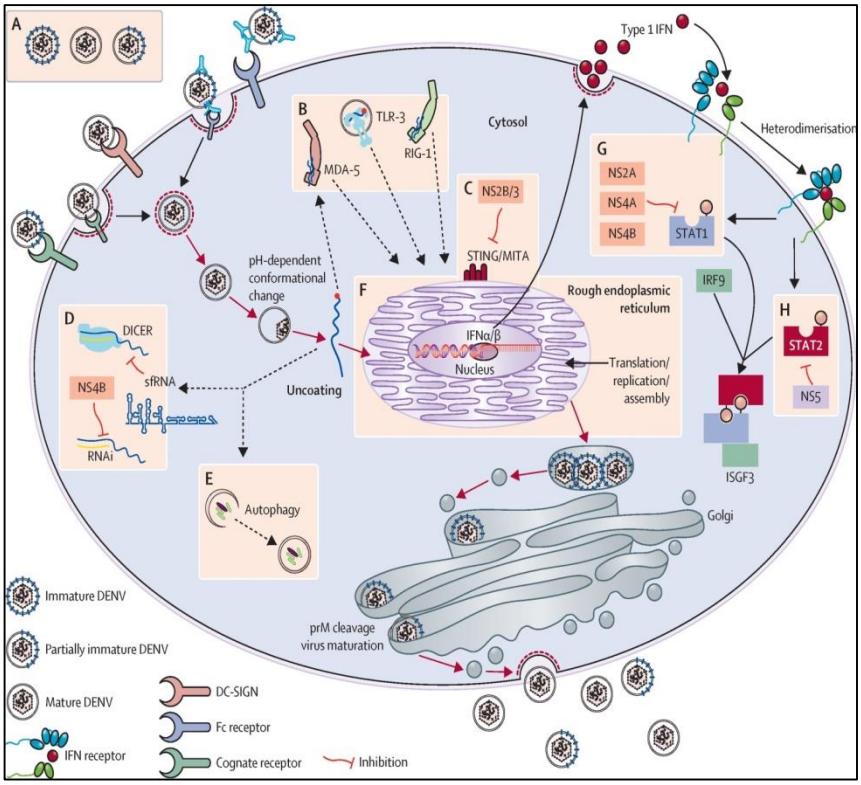

Figure 1.7: Subversion of antiviral responses during DENV infection.

Subversion of antiviral responses is shown in boxes labelled A–H. (A) Maturity of viruses that affects the outcome of viral infection. (B) Suppression of IFN response resulted from virus infection that disrupts RIG-I/MDA5 and TLR signalling cascades. (C) Suppression of antiviral response resulted from cleavage of MITA/STING by DENV NS2B/3. (D) Inhibition of RNAi antiviral pathway by subgenomic Flavivirus RNA (sfRNA) and NS4B. (E) Autophagy induced by DENV which is capable of enhancing viral replication. (F) DENV-induced endoplasmic reticulum hypertrophy and manipulation of the unfolded protein response to compensate ER stress. (G) Inhibition of STAT1 phosphorylation and suppression of the JAK-STAT pathway by NS2A, NS4A, and NS4B. (H) STAT2 degradation by NS5 which results in inhibition of the JAK-STAT pathway and IFN response. Entry and release of the mature DENV virions are shown by red arrows. Figure adapted from Guzman & Harris 2014.

1.6 Hypotheses and aims of study

Although DENV has been studied extensively, the molecular biology of the virus remains unclear. The hypothesis behind this research project was that a systematic analysis of virus-host protein-protein interaction would provide a greater understanding of the viral infection process. Identification of host factors interacting with the viral proteins indicates a putative physical association of DENV-host proteins during cellular processes which could reveal a specific mechanism or pathway contributing to the viral infection. Further, this interaction could be translated into a larger biological function, leading to the potential use of the identified proteins as candidates for diagnostics or drug discovery.

The aims of this study were as following:

1. To identify human host factors interacting with DENV-2 NS proteins through a yeast two-hybrid protein-protein interaction systematic analysis.

2. To validate and confirm the protein interaction between DENV-2 NS proteins and the human interactors in mammalian system.

3. To investigate the functional properties of the protein of interest and analyse its importance in DENV replication by siRNA gene silencing.

4. To identify mosquito host factors interacting with DENV-2 NS proteins and optimize the downstream innate immune signalling assays.

CHAPTER 2: MATERIALS AND METHODS

2.1 Cell culture techniques

2.1.1 Cell lines

2.1.1.1 Mammalian cells

Human embryonic kidney 293 (HEK293) and human lung adenocarcinoma epithelial cells (A549) were grown in Dulbecco's Modified Eagle's Medium (DMEM) (Gibco®) supplemented with 10% heat-inactivated fetal bovine serum (FBS) (Gibco®) and 100 U/ml penicillin/100 µg/ml streptomycin (Pen/Strep) (Gibco®). Baby hamster kidney-21 (BHK-21) cells were grown in Glasgow Minimum Essential Medium (GMEM) (Gibco®) supplemented with 5% newborn calf serum (NBCS) (Gibco®), 10% tryptose phosphate broth (TPB) (Gibco®) and Pen/Strep. Each cell line was propagated in a culture flask (Nunc) under sterile conditions in a Class II Biosafety Cabinet and incubated at 37 °C in a humidified incubation chamber with 5% carbon dioxide. All cell lines are listed in Table 2.1.

2.1.1.2 Mosquito cells

Aedes aegypti-derived Aag2 cells, *Aedes albopictus*-derived C6/36 and *Aedes albopictus*-derived U4.4 cells (Table 2.1) were maintained in L-15 (Leibovitz's) medium supplemented with 10% FBS, 10% TPB and 1% Pen/Strep. The cells were cultured under sterile conditions and incubated at 28 °C without carbon dioxide.

Table 2.1: Cell lines used in this study.

Cell name	Organism of origin	Reference
HEK293	*Homo sapiens*	(Graham et al. 1977). Received from Edward Dornan, University of Glasgow
A549	*Homo sapiens*	(Giard et al. 1973)
BHK-21	*Mesocricetus auratus*	(Macpherson & Stoker 1962)
Aag2	*Aedes aegypti*	(Peleg 1968)
C6/36	*Aedes albopictus*	(Condreay & Brown 1986)
U4.4	*Aedes albopictus*	(Condreay & Brown 1986)

2.1.2 Propagation of cells

2.1.2.1 Mammalian cells

Cells were sub-cultured once they reached approximately 80% confluence and continuously propagated up to 30 passages before replacing them with fresh stocks from liquid nitrogen. Prior to harvesting, the medium was removed and the cell monolayer rinsed with 5 ml versene in PBS (E&O Laboratories Ltd.). After decanting the solution, 1x Trypsin (Sigma-Aldrich)/Versene was added and incubated at 37 °C to allow detachment of cells. The trypsinisation reaction was halted by adding 5 ml of medium and the cell suspension was spun down at 1,500 rpm for 5 min. The cell pellet was re-suspended in fresh medium and the required volume was transferred to a new culture flask containing medium, followed by incubating at 37 °C for 4-5 days.

2.1.2.2 Mosquito cells

To allow propagation of mosquito cells, medium was removed from a culture flask of 80% confluent cells and 5 ml fresh L-15 medium was added. The cells were detached by gently scraping them off from the surface of flask using a cell scraper and transferred into 15 ml Falcon tube (Corning). The cells were re-suspended followed by adding an appropriate volume of L-15 medium and subsequently transferred into a fresh culture flask prior to incubation at 28 °C.

2.1.3 Seeding of cells

Cells were detached from the culture flasks as described in the above protocols (Section 2.1.2.1 and 2.1.2.2). After resuspension with medium, the total number of cells was counted using a haemocytometer under the microscope and the required number of cells (Table 2.2) was calculated as below:

Number of cells/ ml =	Average count per square x dilution factor x 10^4

An appropriate volume of pre-warmed growth medium was added to make up the required cell density and dispersed into 24-well plates (reduced by one-log when seeded in a 96-well plate) prior to incubation at their respective growth temperatures.

Table 2.2: Number of seeded cells used for experiments.

Cell name	Number of seeded cells (cells/ ml)	Growth conditions
HEK293	1.4×10^5	37 °C
A549	1.2×10^5	37 °C
BHK-21	1.2×10^5	37 °C
Aag2	1.7×10^5	28 °C
C6/36	1.2×10^5	28 °C
U4.4	1.2×10^5	28 °C

2.1.4 Cryopreservation of cells

To preserve the mammalian and mosquito cells for long-term storage, the cells were harvested following their respective protocols above and re-suspended in medium containing 10% dimethyl sulfoxide (DMSO) (BDH). Prior to freezing, the cells were gently mixed to achieve a homogeneous suspension and divided into 1 ml-aliquots in cryogenic storage vials (Greiner Bio-One). The vials were immediately placed in Mr. Frosty™ Freezing Container (Nalgene®) in the presence of isopropanol and kept at -80 °C overnight before storing them in liquid nitrogen the next day.

2.1.5 Recovery of frozen cells

A cryovial containing frozen cells was removed from liquid nitrogen and the content was thawed by placing the vial at 37 °C in a water bath with gentle agitation. The vial content was quickly transferred into 25 cm^2 culture flask containing 8 ml fresh medium prior to incubation at their respective growth temperature overnight. The culture medium was replaced with fresh medium the next day and the cells were incubated for 3-4 days before sub-culturing into a medium flask. All cell lines were reconstituted as mentioned above with the exception of HEK293 that required a complete removal of DMSO prior to growth. Once HEK293 cells were thawed, they were quickly transferred into a 15 ml tube containing 10 ml DMEM to dilute the DMSO and then immediately spun down at 800 rpm for 1 min. The cell pellet was gently re-suspended in 5 ml fresh medium and transferred into a 25 cm^2 culture flask followed by an incubation at 37 °C for 2 days until further sub-culture was required.

2.2 Nucleic acid techniques

2.2.1 RNA isolation

Total RNA was extracted from cultured cells using TRIzol® reagent (Invitrogen) according to the manufacturer's instruction. Briefly, the cells were washed with 1x phosphate buffered saline (PBS) and spun at 1,500 rpm for 5 min. To lyse the cells, 1 ml TRIzol® reagent was added and incubated for 5 min at room temperature. Chloroform (0.2 ml) was added to the suspension, vortexed and spun for 15 min at 12,000 rpm at 4 °C. The colourless upper phase containing RNA was precipitated by adding 0.5 µl RNase free glycogen (10 mg/ ml) and 0.5 ml isopropanol. The mixture was incubated for 10 min at room temperature and spun at 12,000 rpm for 10 min at 4 °C. The RNA pellet was washed with 70% ethanol, spun at 10,500 rpm for 5 min at 4 °C and air-dried for 5 min. The RNA was re-suspended in 20 µl nuclease free water and stored at -20 °C. All steps involving RNA procedures was performed in RNase free conditions.

2.2.2 RT-PCR

To generate the first-strand cDNA, 1-5 µg total RNA, 1 µl oligo dT or random primers (50 µM), 1 µl dNTP mix (10 mM) (Invitrogen) and water (adjusted to make up 13 µl) was added into a nuclease-free PCR tube. The mixture was incubated at 65 °C for 5 min in a thermal cycler followed by cooling on ice for 1 min. The reverse-transcriptase reaction was performed by adding 4 µl First-Strand buffer (5x), 1 µl DTT (0.1 M), 1 µl RNaseOUT™ Recombinant RNase Inhibitor (40 U/ µl), 1 µl SuperScript™ II reverse transcriptase (200 U/ µl) (Invitrogen). An additional step when using random primers was done by incubating the mixture at 25 °C for 5 min. The mixture was subsequently incubated at 50 °C for 1 hr in a thermal cycler and inactivated at 70 °C for 15 min. The resulting cDNA (2 µl) was used as a template for subsequent PCR amplification using the gene-specific primers.

2.2.3 Polymerase chain reaction

Standard PCR reactions were prepared in a master mix containing 10 µl 5x GoTaq® Flexi buffer, 4 µl MgCl2 (25 mM) (Promega), 1 µl dNTP mix (10 mM each), 1 µl Forward primer (10 µM), 1 µl Reverse primer (10 µM), 0.5 µl GoTaq® DNA Polymerase (5 U/ µl) (Promega) and nuclease-free water (to make the reaction up to 50 µl). The mixture was aliquoted into PCR tubes followed by addition of 10 ng template DNA. Amplification of the DNA was carried out in a thermal cycler GeneAmp® PCR System 9700 (Applied Biosystems). The PCR cycling parameters were as listed in Table 2.3. Amplified PCR fragments were visualised by agarose gel electrophoresis and stored in -20 °C.

Table 2.3: Standard PCR parameters.

Step	Temperature	PCR cycle	Time
Initial denaturation	95 °C		2 min
Denaturation	95 °C	25-30 cycles	30 sec
Annealing	50–65 °C		30 sec
Extension	72 °C		1 min/ kb
Final extension	72 °C		5 min

2.2.4 KOD PCR

KOD PCR (Toyobo) was used for amplification of genes prior to cloning into appropriate vectors. The reaction kit contains high fidelity KOD DNA polymerase for efficient proof reading activity. KOD PCR reactions were prepared in 50 µl reaction containing 5 µl KOD Hot Start DNA Polymerase Buffer (10x), 3 µl $MgSO_4$ (25 mM), 5 µl dNTPs (2 mM each), 1.5 µl Forward primer (10 µM), 1.5 µl Reverse primer (10 µM), 1 µl KOD Hot Start DNA Polymerase (1 U/ µl), nuclease-free water and 10 ng DNA template. The KOD-PCR cycling conditions were listed in Table 2.4.

Table 2.4: KOD PCR parameters.

Step	Temperature	PCR cycle	Time
Initial denaturation	95 °C		2 min
Denaturation	95 °C	20-30 cycles	20 sec
Annealing	Lowest primer melting temperature		10 sec
Extension	70 °C		15 sec/kb

2.2.5 Agarose gel electrophoresis

Agarose gels (0.8-1.2% depending on the size of DNA) were prepared by weighing agarose powder (Promega) to a desired percentage and adding the appropriate volume of 1x TAE (Tris-Acetate-EDTA) buffer (Severn Biotec, Ltd.). The agarose was dissolved by boiling in a microwave for 1-2 min, gently swirled and allowed to cool down for 5 min prior to addition of ethidium bromide (Promega) (final concentration 0.5-1 µg/ ml). The liquid agarose was immediately poured into a gel tray with the well comb in place and allowed to solidify for 20-30 min. DNA samples mixed with loading buffer were loaded into the wells of the gel and electrophoresed at 100 V until the dye front was approximately 75-80% of the way down the gel. The DNA bands were visualised and imaged under UV-transilluminator Gel Doc™ 2000 Gel Documentation Systems (Bio-Rad).

2.2.6 Purification of DNA from PCR products

PCR products were purified using the High Pure PCR Product Purification Kit (Roche) according to the manufacturer's protocol with some modifications. Briefly, 500 µl Binding buffer was mixed with the PCR product and spun down through a spin column at 12,000 x g for 1 min. To wash the DNA, 500 µl Washing buffer was added and the column was spun at 12,000 x g for 1 min. This step was repeated by adding 200 µl Washing buffer and the spin column was spun again twice at 12,000 x g. Pre-heated Elution buffer (50 µl) was added to the spin column and incubated at 65 °C for 2 min followed by centrifugation at 12,000 x g for 2 min. The purified DNA was stored at -20 °C.

2.2.7 Purification of DNA from agarose gels

DNA was extracted from agarose gels using illustra™ GFX™ PCR DNA and Gel Band Purification Kit (GE Healthcare) following the manufacturer's instructions. In brief, the DNA fragment was excised from an agarose gel and dissolved in Capture buffer type 3 by incubating at 60 °C for 15–30 min. The mixture was transferred into GFX MicroSpin column, spun down at 12,000 x g for 1 min followed by washing of the DNA with 500 µl Wash buffer type 1. The column was spun again at 12,000 x g for 1 min to remove excess buffer and the DNA was eluted using 50 µl Elution buffer type 6 (sterile nuclease-free water) prior to storage at -20 °C.

2.2.8 Quantitation of nucleic acids

Measurement of DNA and RNA concentrations was carried out using a NanoDrop™ 1000 spectrophotometer (Thermo Scientific) at UV wavelength 260-280 nm. The instrument was initialised by applying 2 µl deionised water on the optical surface. This was followed by a blank measurement using nuclease-free water or Tris-EDTA (TE) buffer (depending on which was used to dissolve the DNA/RNA). The nucleic acid concentration was measured by mixing the tube contents and loading 2 µl onto the optical surface. Pure preparations of DNA and RNA were indicated by optical density (OD) ratios OD_{260}/OD_{280} of 1.8 to 2.0, respectively.

2.2.9 Transformation of plasmids

Plasmid DNA (10-50 ng) was added to 50 µl Subcloning Efficiency™ DH5α™ *E. coli* competent cells (Invitrogen) in a microcentrifuge tube. For propagation of the Gateway donor and destination vectors harbouring the *ccd*B gene, One Shot® *ccd*B Survival™ 2T1^R *E. coli* competent cells (Invitrogen) were used. The cells were mixed gently and incubated on ice for 30 min. This was followed by a heat-shock at 42 °C for 30 sec to allow the uptake of the DNA before placing the tube on ice again for 2 min. The bacterial cells were allowed to recover by the addition of 950 µl pre-warmed Luria Bertani (LB) broth (E&O Laboratories Ltd.) and incubation at 37 °C for 1 hr with shaking at 225 rpm. The transformed cells (100 µl) were plated on LB agar plates containing the appropriate antibiotic (Table 2.6) and allowed to grow at 37 °C for 16-18 hr.

2.2.10 Mini-scale plasmid purification

Plasmids were purified in small-scale using ISOLATE Plasmid Mini Kit (Bioline) according to the manufacturer's instructions. An overnight propagation of bacterial cultures were harvested and re-suspended in 250 µl of Buffer P1. To lyse the cells, 250 µl of Lysis buffer P2 was added and the content was incubated at room temperature for 5 min. The reaction was halted by adding 300 µl Neutralisation buffer P3 followed by centrifugation at 12,000 rpm for 5 min. The supernatant was applied into the spin column and spun at 12,000 rpm for 1 min. The DNA was washed with 600 µl Wash buffer PW2 supplemented with ethanol and spun at 12,000 rpm for 1 min. To remove excess residual ethanol, the spin column was spun again at 12,000 rpm for 2 min. Prior to elution of the DNA, 50 µl nuclease-free water was added onto the membrane and allowed to incubate at room temperature for 1 min, followed by centrifugation at 12,000 rpm for 1 min. The DNA concentration was determined (as described in Section 2.2.8).

2.2.11 Large-scale plasmid purification

2.2.11.1 High-copy plasmids

High-copy number plasmids were purified using Plasmid Maxi Kit (QIAGEN) following the manufacturer's protocol with minor modifications. Briefly, the bacterial cells were harvested by centrifugation followed by re-suspension in 10 ml Buffer P1. To lyse the cells, 10 ml Buffer P2 was added and the suspension was mixed by inverting the tube followed by incubation at room temperature for 5 min. Next, Buffer P3 (10 ml) was added and the suspension was immediately mixed by inverting the tube resulting in white precipitation of materials. After an incubation on ice for 20 min, the precipitated materials were removed by filtration through a coffee filter (a modified protocol). The filtrate containing plasmid DNA was applied into a QIAGEN-tip 500 spin column equilibrated with Buffer QBT. The DNA was washed twice with 30 ml Buffer QC and eluted with 15 ml Buffer QF into a 50 ml Falcon tube. Precipitation of the DNA was carried out by adding 10.5 ml isopropanol followed by centrifugation at 5,000 rpm at 4 °C for 1 hr. The DNA pellet was washed in 70% ethanol, spun at 5,000 rpm at 4 °C for 1 hr and air-dried for 5-10 min. The DNA was resolved in 100-150 µl nuclease free water or TE buffer prior to storage at -20 °C.

2.2.11.2 Low-copy plasmids

Low-copy number plasmids were purified as above (Section 2.2.11.1) with an additional DNA precipitation step after alkaline lysis to reduce the volume of lysate. Following cell lysis and removal of the precipitated cell debris through a coffee filter, the DNA in the supernatant was precipitated with 0.7 volumes isopropanol. This was followed by centrifugation at 9,500 rpm at 4 °C for 30 min and the DNA pellet was re-dissolved in 500 µl TE buffer (pH 8) and 4.5 ml Buffer QBT. The DNA was applied into the spin column QIAGEN-tip 500 and washed with Buffer QC twice. The remaining steps were performed as described for purification of high-copy plasmids above (Section 2.2.11.1).

2.2.12 Plasmid restriction digestion

For analytical-scale enzymatic reactions, 1 µg plasmid DNA was digested in a total volume of 20 µl. A master mix containing nuclease-free water, 2 µl restriction enzyme buffer (10x) (New England Biolabs Inc.), 0.2 µl bovine serum albumin (BSA) (10 µg/ µl) and 0.2 µl of restriction enzyme (10 U/ µl) (New England Biolabs Inc.) was prepared followed by addition of the DNA. The reaction was mixed gently, briefly spun and allowed to incubate at 37 °C for 1-2 hr. The digestion reaction was halted by heat-inactivation at 65 °C for 20 min. For a large-scale restriction digestion in 40 µl reaction mix, 4-5 µg plasmid DNA was used along with 2 µl restriction enzyme and the reaction was incubated at 37 °C for 4-5 hr.

2.2.13 DNA Ligation

DNA ligations were set up in a sterile 1.5 ml microcentrifuge tube by adding 1 µl T4 DNA Ligase buffer (10x) (Promega), plasmid DNA, insert DNA (in a plasmid:vector of 1:3 ratio), nuclease-free water (up to 10 µl) and 1 µl T4 DNA ligase (1 Weiss unit/ µl) (Promega). The ligation reaction was gently mixed, spun briefly and allowed to incubate at room temperature for 3 hr or at 4 °C overnight. The reaction was halted by heat-inactivating at 65 °C for 10 min followed by cooling down on ice prior to transformation (5 µl of the ligation mix) into competent cells.

2.2.14 DNA sequencing

Cloned genes of interest were sequence-verified by sending the plasmid DNA or PCR product and their respective primers to the DNA Sequencing Service, University of Dundee (http://www.dnaseq.co.uk/home.html). Sequencing of the MGC human cDNA library was performed by GATC Biotech, Konstanz, Germany. The sequencing results were analysed using BioEdit Sequence Alignment Editor and identification of the genes was accomplished using BLAST: Basic Local Alignment Search Tool (http://blast.ncbi.nlm.nih.gov/Blast.cgi).

2.2.15 Bacterial glycerol stock

Glycerol stocks were prepared for long-term storage of plasmid clones. Glycerol stabilizes the frozen bacteria which prevents damage to the cell membrane. An overnight bacterial culture (250 µl) was added to 250 µl of 50% sterile glycerol in a 2 ml screw-cap vial (a final concentration of 25% glycerol). The suspension was mixed well by briefly vortexing and immediately stored at -80 °C. To recover bacteria from the glycerol stock, a sterile loop was used to scrape off the top part of the frozen culture and streaked onto LB agar plate containing the appropriate antibiotic, followed by incubating at 37 °C overnight.

2.3 Protein techniques

2.3.1 Protein sample preparation

Preparation of protein samples was carried out on ice unless stated otherwise. Transfected mammalian cells were harvested by centrifugation at 1,500 rpm for 5 min at 4 °C, washed in 1 ml ice-cold PBS and spun again at 1,500 rpm for 5 min at 4 °C. The cell pellet was lysed in Nonidet P-40 (NP40) cold lysis buffer containing protease inhibitor cocktail mix (Roche) and incubated on ice for 5 min with vigorous vortexing twice for 5-10 sec. The protein sample was allowed to incubate at 4 °C with constant agitation for 30 min and spun down at 10,000 rpm for 10 min at 4 °C prior to storage at -20 °C.

2.3.2 Protein quantification

Proteins were quantified using the BCA Protein Assay kit (Pierce) following the manufacturer's instructions. In brief, the BCA working reagent was prepared by mixing 50 parts of Reagent A to 1 part of Reagent B, made up to a required volume as below:

Vol. of working reagent =	No. of samples x replicates x working vol. per sample

Protein samples were thawed on ice and 25 µl was loaded into a 96-well plate. The BCA working reagent was added into each well (200 µl/ well) and the plate was covered with tin foil followed by incubation at 37 °C for 30 min. After cooling to room temperature, the protein absorbance was measured at 562 nm using GloMax® Multi Detection System (Promega) for Protein BCA Assay. The cell lysis buffer was used as a blank measurement to subtract the protein background absorbance and the resulting values were calculated against the BSA standard curve to determine the protein concentration.

2.3.3 Protein electrophoresis

A pre-cast Bolt® 4-12% Bis-Tris Plus Gel (Invitrogen) was set up by placing the gel in a Bolt® Mini Gel Tank electrophoresis unit filled with 1x Bolt® MES [2-(N-morpholino) ethane sulfonic acid] SDS Running buffer (Invitrogen) according to the manufacturer's instructions. Protein samples (10 µg) were mixed with 5 µl lithium dodecyl sulfate sample buffer (4x) (Invitrogen) and 2 µl sample reducing agent (10x) (Invitrogen) followed by heating at 95 °C for 10 min. The proteins (20 µl) were loaded into the wells of the pre-cast gel along with SeeBlue® Plus2 Pre-Stained Standard protein marker (Invitrogen) and resolved at 120 V for 1 hr.

2.3.4 Protein transfer

After separation, the proteins were transferred onto a nitrocellulose membrane (GE Healthcare) using the Trans-Blot® Semi-Dry Electrophoretic Transfer Cell (BioRad). Prior to the transfer, the protein gels were removed from cassettes, using a gel knife and equilibrated in 1x Transfer buffer for 5 min. The nitrocellulose membrane and Whatman blotting papers (GE Healthcare) were cut

to the dimension of the gel and soaked in 1x Transfer buffer for 3-5 min. The materials were assembled in a sandwich layer by placing the pre-soaked Whatman blotting paper on the Trans-Blot anode platform surface followed by the membrane, protein gel and another piece of Whatman paper on top. The cathode safety cover unit were put in place and the proteins were transferred at 15 V, 0.3 A for 30 min.

2.3.5 Immunoblotting

Following protein transfer, the membrane was blocked with 5% milk powder in PBS/Tween-20 (0.001% Tween-20) for 1 hr at room temperature to prevent non-specific binding of the antibodies to proteins on the membrane. After washing three times in PBS/Tween-20 for 5 min, an appropriate dilution of primary antibody (Table 2.5) was added and the membrane was incubated at 4 °C overnight with gentle shaking. After incubation, the membrane was washed in PBS/Tween-20 for 5 min three times followed by incubating in an appropriate dilution of secondary antibody (Table 2.5) at room temperature for 1-2 hr. The membrane was washed with PBS/Tween-20 for 5 min three times, followed by detection of the proteins using enhanced chemiluminescence (ECL) Western Blotting Substrate (Pierce). Lower expression of proteins was detected using Amersham ECL Select™ Western Blotting Detection Reagent (GE Healthcare).

Table 2.5: List of antibodies used for immunoblotting.

Antibody	Target	Host	Dilution	Distributor
Primary	BANP	Rabbit	1:10,000	Bethyl Lab, Inc.
Primary	Kv1.3	Rabbit	1:1000	LSBio
Primary	Myc-NS2A	Mouse	1:1000	Santa-Cruz
Primary	Human beta-Actin	Rabbit	1:1000	Sigma-Aldrich
Primary	V5 epitope	Mouse	1:3000	Pierce
Primary	EGFP	Rabbit	1:3000	Abcam
Secondary	Anti-rabbit IgG conjugated with horseradish peroxidase	Goat	1:3000	Abcam
Secondary	Anti-mouse IgG conjugated with horseradish peroxidase	Goat	1:3000	Abcam

2.4 Yeast two-hybrid interaction analysis

2.4.1 MGC cDNA library, plasmids and yeast strains

The mammalian gene collection (MGC) human cDNA library, Gateway vectors and yeast strains used in the yeast two-hybrid (Y2H) experiments were kindly provided by Juergen Haas, University of Edinburgh. pDEST40 was a kind gift from Esther Schnettler, University of Glasgow. The Gateway vectors and their respective antibiotic selection markers are shown in Table 2.6. All antibiotics were purchased from Sigma-Aldrich. The yeast vector pGBKT7 was used to express DENV bait protein as a fusion with the GAL4 DNA-binding domain (Figure 2.2). For prey, pGADT7 expressed the MGC human cDNA library proteins downstream of the GAL4 activation domain. Both bait and prey fusion proteins were highly expressed under the control of *ADH1* yeast promoter and tagged respectively by c-Myc and haemagglutinin. *Saccharomyces cerevisiae* haploid strains AH109 and Y187 were used as hosts for protein expression of the bait and prey, respectively.

Table 2.6: Gateway donor and destination vectors used in this study.

Plasmid vector	Clone	Host	Antibiotic selection	Antibiotic concentration (µg/ ml)
pDONR207	Entry	Bacteria	Gentamycin	10
pDONR223	Entry	Bacteria	Spectinomycin	50
pGBKT7	Destination	Yeast	Kanamycin sulfate	50
pGADT7	Destination	Yeast	Ampicillin	100
pTREX-DEST30-Protein A	Destination	Mammalian	Ampicillin	100
pcDNA3-RL-GW	Destination	Mammalian	Ampicillin	100
pDEST40	Destination	Mammalian	Ampicillin	100

2.4.2 Dengue virus replicons

Dengue virus type 2 New Guinea-C (NGC) sub-genomic replicon; pDVRepGP2A (Figure 2.1a), was used in this study as a template for amplification of DENV genes prior to Gateway cloning. The replicon contained DENV-2 non-structural genes and green fluorescent protein (GFP) as a fusion with a drug selectable marker puromycin N-acetyl-transferase (PAC) at the N-terminus. This is followed by small 2A peptides from the foot and mouth disease virus in place of the DENV C, prM and E genes. In order to study DENV replication, DENV-2 NGC sub-genomic replicons expressing Firefly luciferase (*FFLuc*); pDVPACLuc (Figure 2.1b) (Massé et al. 2010; Pryor et al. 2004) and its derived mutant pDVW87I were used. Both replicons contained DENV non-structural and PAC genes in place of the DENV C, prM and E. pDVW87I has a mutation in NS5 gene (W87I) that prevents translation of the viral transcripts and thus abolishes replication. All replicons were kindly provided by Andrew Davidson, University of Bristol. The replicons were propagated and purified using Plasmid Maxi Kit following the manufacturer's protocol for very low-copy plasmids (Section 2.2.11.2).

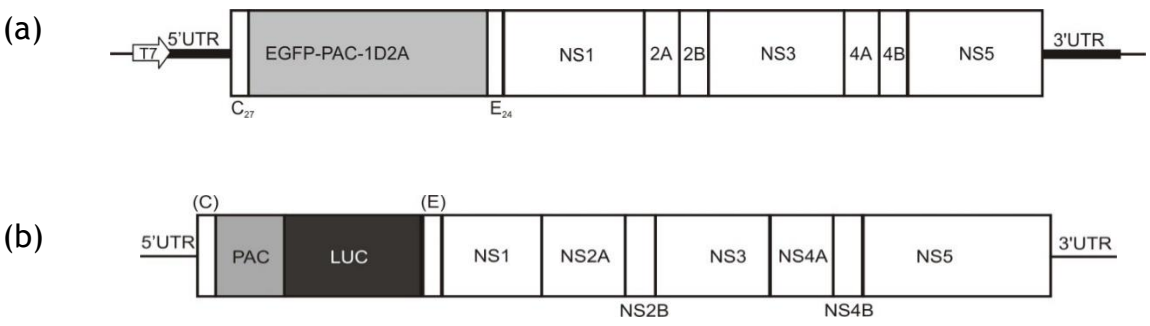

Figure 2.1: DENV-2 New Guinea C replicons used in this study.

(a) DENV-2 NGC replicon expressing GFP (pDVRepGP2A) and (b) DENV-2 NGC replicon expressing FFLuc (pDVPACLuc). Both replicons are fused to puromycin N-acetyl-transferase (PAC) at the N-terminus. pDVW87I (not shown) is a mutant version of pDVPACLuc, consisting similar replicon organisation, except a mutation was introduced in NS5 (amino acid position 87, tryptophan to isoleucine) (Massé et al. 2010; Pryor et al. 2004).

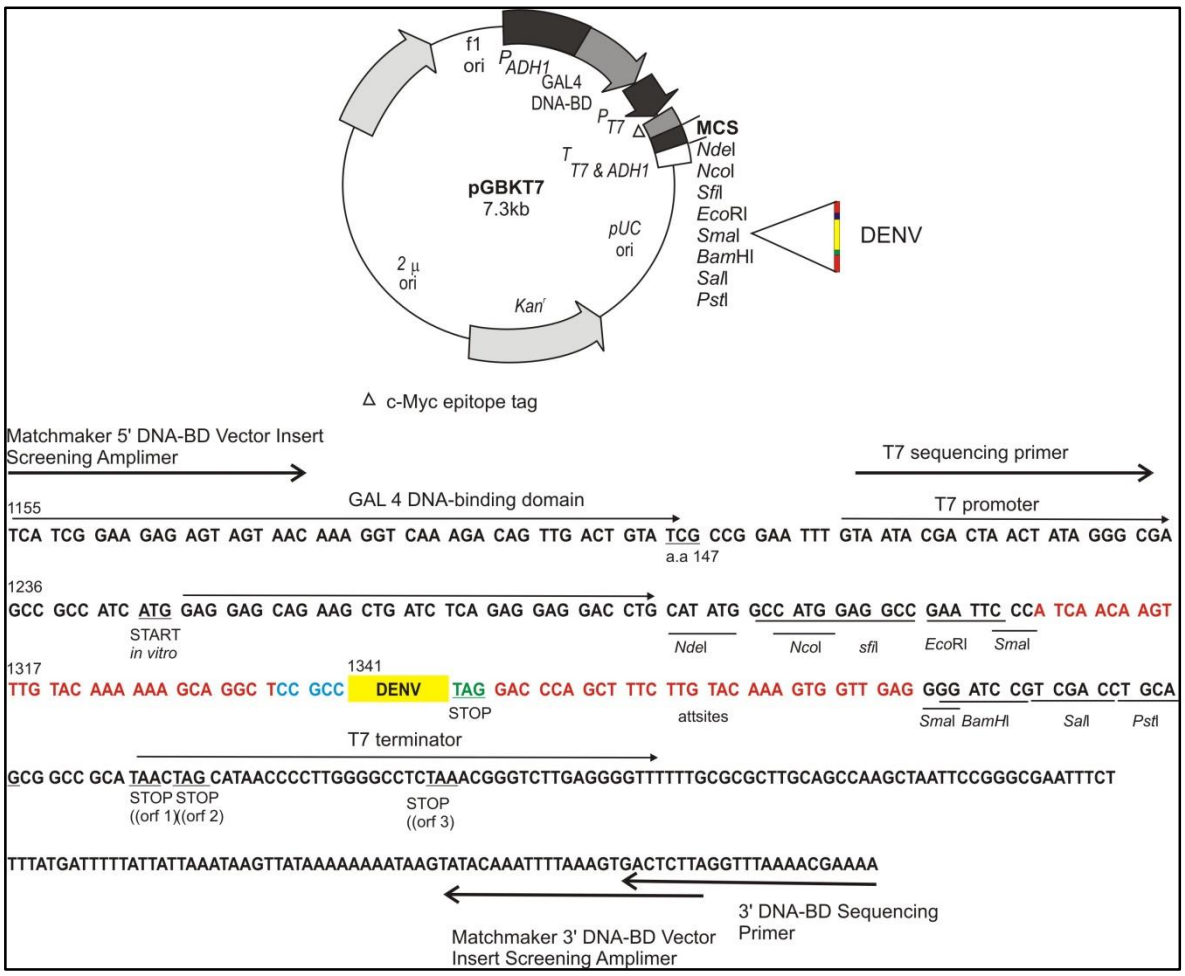

Figure 2.2: A schematic map of DENV bait construct in pGBKT7 yeast vector.

Below the plasmid map are sequences within the multiple cloning site (MCS). DENV genes were cloned into DNA Reading Frame Cassette B (RfB) within the *Sma*I restriction site of the vector MCS. The RfB contains *ccd*B and chloramphenicol resistance genes. Sequence in red is the Gateway attachment (*att*) sites for homologous recombination, blue is the Kozak sequence for expression of proteins in eukaryotic system, green is the stop codon. Highlighted in yellow is the DENV gene.

2.4.3 Determination of DENV transmembrane domains

Using structure prediction software available on the web (Table 2.7), DENV TMDs were identified based on the consistency of the predicted regions within NS2A, NS2B, NS4A and NS4B protein sequences. Removal of these regions resulted in the generation of nineteen intra/extracellular gene fragments. NS1, NS3 and NS5 were not included because they are cytoplasmic proteins, hence absent of TMDs.

Table 2.7: Transmembrane prediction software used in this study.

Software	Website link
TMPred	http://www.ch.embnet.org/software/TMPRED_form.html
TMHMM2	http://www.cbs.dtu.dk/services/TMHMM
HMMTOP	http://www.enzim.hu/hmmtop
Pred-TMR	http://www.enzim.hu/hmmtop
SPLIT4	http://split4.pmfst.hr/split/4
TopPred	http://bioweb.pasteur.fr/seqanal/interfaces/toppred.html
DAS	http://www.sbc.su.se/~miklos/DAS
SOSUI	http://bp.nuap.nagoya-u.ac.jp/sosui/sosui_submit.html

2.4.4 Gateway cloning technology

DENV bait constructs were generated using the Gateway technology (Invitrogen). This cloning technology was developed based on bacteriophage lambda site-specific recombination (Landy 1989), and subsequently improved (Hartley et al. 2000). The Gateway system provides an efficient way of cloning a gene of interest into multiple cloning vectors through DNA recombination at specific attachment sites (*att*). The recombination is mediated by proprietary enzymes mixes; BP clonase and LR clonase, which contains the necessary enzyme activities to excise and recombine the gene of interest. In order to express DENV proteins in yeast, entry clones containing DENV genes were generated through a BP reaction and subsequently transferred into the yeast expression vector through an LR reaction (Figure 2.3). BP clonase contains the phage lambda Integrase and the *E. coli* Integration Host Factor which catalyses recombination reaction between the DENV PCR-amplified fragment flanked by *att*B sequences and a donor vector containing *att*P sites, resulting in an entry clone (Figure 2.3). LR clonase has similar enzyme

components with additional lambda Excisionase, which catalyses the transfer of DENV fragments between *att*L of an entry clone and *att*R of a yeast destination vector, producing an expression clone (Figure 2.3).

For efficient selection of positive clones in *E. coli*, the DNA Reading Frame Cassette of Gateway vectors contain a *ccd*B lethal gene. During recombination, the DNA cassette with flanking *att* sites is swapped with the gene of interest resulting in two products; one carries the empty vector *ccd*B and the other carries the gene of interest. Bacteria cells that take up the empty vector carrying the *ccd*B gene fail to grow because the toxic protein CcdB interferes with the activity of *E. coli* DNA gyrase, thus killing the cells. On the other hand, the bacteria cells carrying the gene of interest will grow on antibiotic-selective medium (dependent on the selection marker which the vector carries) and this enables efficient recovery of the desired clones.

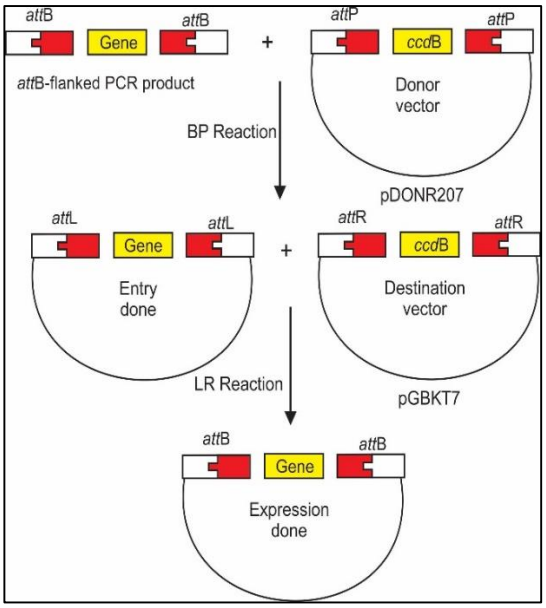

Figure 2.3: A schematic diagram of the Gateway cloning system.

BP reaction catalyses the recombination of an *att*B-flanking PCR product with a donor vector containing an *att*P site (*att*B x *att*P), producing an *att*L-entry clone. LR reaction facilitates the recombination of the *att*L-entry clone with a destination vector containing an *att*R site (*att*L x *att*R), producing an expression clone containing *att*B. The specific *att* recombination sites are shown in red and yellow. Figure was adapted from the Gateway Cloning Handbook (Invitrogen) (https://tools.thermofisher.com/content/sfs/manuals/gatewayman.pdf).

2.4.4.1 Amplification of DENV genes

Primer sets were designed to amplify DENV genes with specific attachment (att) sites for use in the Gateway cloning. The genes were amplified using the high fidelity KOD DNA polymerase by two rounds of PCR (Figure 2.4), using the gene-specific primers in the first round (Table 2.8), followed by the attB universal primers in the second PCR (Table 2.9). In the first PCR, the DENV genes were amplified from the DENV-2 NGC replicon, pDENRepGP2A, producing an amplified product containing Kozak consensus sequence (for initiation of translation in eukaryotic system), a DENV gene fragment with a stop codon and partial *att*B Gateway recombination sequence at both the 5' and 3' ends. The resulting PCR product (10 µl) was used as a template for the second PCR using the attB universal primers creating flanking *att*B sites (35 nucleotides) at both ends of the amplified products for insertion into the Gateway vector (Figure 2.4).

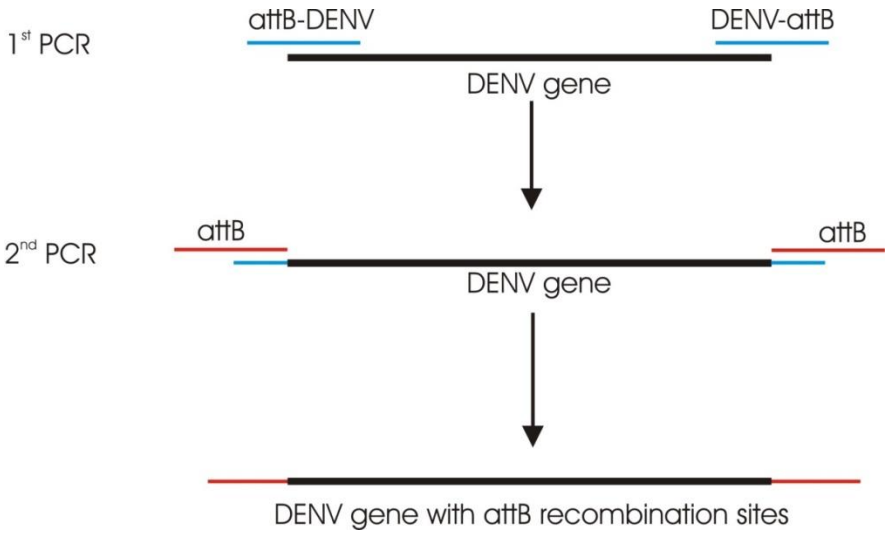

Figure 2.4: PCR amplification of DENV genes incorporating *att*B sites.

Table 2.8: DENV gene-specific primers for Gateway cloning.

Partial *att*B sequence overhangs (in blue), Kozak sequence (in red), DENV gene sequence (in black) and the stop codon (in bold black) are shown.

DENV	Size (bp)	Primer	Sequence 5' – 3'
NS1	1056	NS1-1F	AAAAAGCAGGCTCCGCCGATAGTGGTTGCGTTGTGAGC
		NS1-1056R	AGAAAGCTGGGTCCTAGGCTGTGACCAAGGAGTTG
NS2A	654	NS2A-1F	AAAAAGCAGGCTCCGCCGGACATGGGCAGATTGAC
		NS2A-218R	AGAAAGCTGGGTCCTACCTTTTCTTGTTGGTTCTTG
NS2B	390	NS2B-1F	AAAAAGCAGGCTCCGCCAGCTGGCCACTAAATGAGGC
		NS2B-130R	AGAAAGCTGGGTCCTACCGTTGTTTCTTCACTTCCCAC
NS3	1854	NS3-1F	AAAAAGCAGGCTCCGCCGCTGGAGTATTGTGGGATGTCC
		NS3-1854R	AGAAAGCTGGGTCCTACTTTCTTCCAGCTGCAAACTCC
NS4A	450	NS4A-1F	AAAAAGCAGGCTCCGCCTCCCTGACCCTGAACCTAATC
		NS4A-150R	AGAAAGCTGGGTCCTATGCCATGGTTGCGGC
NS4B	744	NS4B-1F	AAAAAGCAGGCTCCGCCAACGAGATGGGTTTCCTGG
		NS4B-248R	AGAAAGCTGGGTCCTACCTTCTCGTGTTGGTTGTG
NS5	2701	NS5-1F	AAAAAGCAGGCTCCGCCGGAACTGGCAACATAGGAGAG
		NS5-2700R	AGAAAGCTGGGTCCTACCACAGGACTCCTGCCTCTTC
NS2A1F	87	NS2A-1F	AAAAAGCAGGCTCCGCCGGACATGGGCAGATTGAC
		NS2A-29R	AGAAAGCTGGGTCCTACGTTCCTACTCGGGTC
NS2A58F	249	NS2A-58F	AAAAAGCAGGCTCCGCCAGAGACCTGGGAAGAGTGATG
		NS2A-140R	AGAAAGCTGGGTCCTACATTTTTCTCACCATTTTAAGGACC
NS2A187F	96	NS2A-187F	AAAAAGCAGGCTCCGCCCAGAAAGCGGATTGGATACC
		NS2A-218R	AGAAAGCTGGGTCCTACCTTTTCTTGTTGGTTCTTG
NS2B1F	75	NS2B-1F	AAAAAGCAGGCTCCGCCAGCTGGCCACTAAATGAGGC
		NS2B-25R	AGAAAGCTGGGTCCTAGTCATTCTTTAGGAGTGAACTGGC
NS2B49F	141	NS2B-49F	AAAAAGCAGGCTCCGCCGCCGATTTGGAACTGGAG
		NS2B-95R	AGAAAGCTGGGTCCTACAGTGTTTGTTCTTCCTCTTCG
NS4A1F	147	NS4A-1F	AAAAAGCAGGCTCCGCCTCCCTGACCCTGAACCTAATC
		NS4A-49R	AGAAAGCTGGGTCCTACGGCAGTTCACTGAGAG
NS4A122F	87	NS4A-122F	AAAAAGCAGGCTCCGCCGAACCAGAAAAGCAGAGAACACC
		NS4A-150R	AGAAAGCTGGGTCCTATGCCATGGTTGCGGC
NS4A101F	87	NS4A-101F	AAAAAGCAGGCTCCGCCCAGCCACACTGGATAGCAG
		NS4A-129R	AGAAAGCTGGGTCCTAGGGTGTTCTCTGCTTTTC
NS4B1F	96	NS4B-1F	AAAAAGCAGGCTCCGCCAACGAGATGGGTTTCCTGG
		NS4B-32R	AGAAAGCTGGGTCCTATAGATCTATGTCCAGGATGTTGC
NS4B58F	132	NS4B-58F	AAAAAGCAGGCTCCGCCAATTCCTCAGTGAACGTGTCC
		NS4B-101R	AGAAAGCTGGGTCCTATTGTGAGTAGCATCCAATGGC
NS4B129F	108	NS4B-129F	AAAAAGCAGGCTCCGCCGCAACCAGGGAAGCTCAGAAAAG
		NS4B-164R	AGAAAGCTGGGTCCTAAAACTTTGGATCATAGGGTATTGG
NS4B191F	174	NS4B-191F	AAAAAGCAGGCTCCGCCTGTGAGGCGTTAACCTTAGCG
		NS4B-248R	AGAAAGCTGGGTCCTACCTTCTCGTGTTGGTTGTG

Table 2.9: attB universal primers used in this study.

The *att*B sequences are shown in bold.

Primer	Sequence 5' – 3'
attB1-F	GGGG**ACAAGTTTGTACAAAAAAGCAGGCT**
attB2-R	GGGG**ACCACTTTGTACAAGAAAGCTGGGT**

2.4.4.2 BP reaction

Purified PCR products with flanking *att*B recombination sites were introduced into a donor vector in a Gateway BP reaction with BP® Clonase II enzyme mix (Invitrogen). The enzyme catalyzes a recombination reaction at the *att*B sites which results in insertion of the fragments into the donor vector creating an entry clone. The BP reaction was set up by adding 1 µl *att*B-PCR product (150 ng), 1 µl donor vector (150 ng), nuclease-free water (to 5 µl) and 1 µl BP Clonase™ II enzyme mix. The reaction was mixed gently, briefly spun down and allowed to incubate at room temperature for 18-24 hr. After this incubation, 2 µl of the reaction was transformed into DH5α competent cells and plated onto an LB plate containing 10 µg/ ml gentamycin (Section 2.2.9). The resulting entry clone was propagated and plasmid purified as described in Section 2.2.10. The gene insert was screened by PCR, enzymatic digested with *Eco*RI and *Bam*HI and sequence-verified (Section 2.2.12 and Section 2.2.14) using the primers listed in Table 2.10.

Table 2.10: Sequencing primers for gene insert in pDONR207 entry vector.

Primer	Sequence 5' – 3'
attL-F	TCGCGTTAACGCTAGCATGGATCTC
attL-R	GTAACATCAGAGATTTTGAGACAC

2.4.4.3 LR reaction

Genes within the entry clone were transferred into an appropriate destination vector in a Gateway LR reaction using LR® Clonase II enzyme mix (Invitrogen). The reaction was carried out in 1.5 ml tube by adding 1 µl plasmid-purified entry clone (150 ng), 1 µl destination vector (150 ng), nuclease-free water (added to 5 µl) and 1 µl LR® Clonase II enzyme mix. After mixing and briefly spinning down, the reaction was incubated at room temperature for 18-24 hr followed by transformation of 2 µl of the reaction into DH5α competent cells and plating on an LB plate containing 50 µg/ ml kanamycin (as described in Section 2.2.9). The expression clones were screened by PCR, sequence-verified using the primers listed in Table 2.11 and enzymatic digested with *Eco*RI and *Bam*HI as described in Section 2.2.12.

Table 2.11: Sequencing primers for gene insert in pGBKT7 yeast vector.

Primer	Sequence 5' – 3'
GBKT-F	TAATACGACTCACTATAGGGCGA
GBKT-R	TTTTCGTTTTAAAACCTAAGAGTC

2.4.4.4 BP/LR One Tube Format

Cloning of the DENV gene fragments (<200 bp) into the yeast destination vector was performed in a single tube reaction following the Gateway One Tube Format protocol (Invitrogen) with minor adjustments. This protocol eliminated the transformation and plasmid isolation step of the entry clone prior to the LR reaction. After an overnight BP reaction, the LR mixture was set up as described above (Section 2.4.4.3) by adding 2 µl BP reaction mixture instead of the purified plasmid entry clone. The reaction was mixed gently and incubated at room temperature for 18-24 hr followed by 2 µl transformation of the reaction into DH5α competent cells containing 50 µg/ ml kanamycin (as described in Section 2.2.9) and the expression clones were screened as described above (Section 2.4.4.3).

2.5 Yeast two-hybrid protein-protein interaction assay

Y2H is a powerful tool for investigation of protein-protein interactions within eukaryotic cells, rather than expression in bacterial systems or any *in vitro* techniques (Sobhanifar 2003). This method employs fully automated high-throughput screening which enables identification of large-scale global protein interactions. The Y2H employs a GAL4 yeast plasmid that encodes for two hybrid proteins; one has a DNA-binding domain (DBD) fused to a bait, whereas, the other has an activation domain (AD) fused to a prey (Figure 2.5). Successful interaction between the bait and the prey brings the DBD and AD in close proximity under the regulation of an upstream activation sequence (UAS), thus initiates an expression of the downstream reporter gene resulting in a change of the cell phenotype. The yeast cells can then be selected based on this new phenotype, for example the ability to grow on a specific minimal media.

The yeast host strain contains GAL4/UAS linked to the *HIS3* and *ADE2* reporter genes. These genes are responsible for histidine and adenine biosynthesis, respectively. By having these two reporters, the yeasts are capable to grow in the absence of histidine and adenine once the GAL4 promoter has been activated. Successful interaction between the bait and prey proteins that come in close proximity reconstituting the DBD and AD of the GAL4 system, thus activates the GAL4 promoter and synthesis of histidine and adenine (Figure 2.5).

In this study, DENV non-structural proteins were used as baits and tested for interactions with protein preys generated from a human cDNA library. The DENV bait constructs were generated using the Gateway cloning system as described in Section 2.4.4. The DENV gene was cloned into the bait expression vector (pGBKT7) harbouring *TRP1* gene, which allows the haploid yeast strain AH109 transformed with this plasmid to synthesise tryptophan. For expression of the human protein libraries, the haploid yeast strain Y187 was used. Human cDNA library was cloned into the prey expression vector (pGADT7) containing *LEU2* gene, which encodes for leucine biosynthesis. Mating of these haploid yeasts by mixing the yeast cultures allows co-expression of the bait and prey proteins, resulting in the formation of diploids that are able to grow on minimal media lacking tryptophan and leucine.

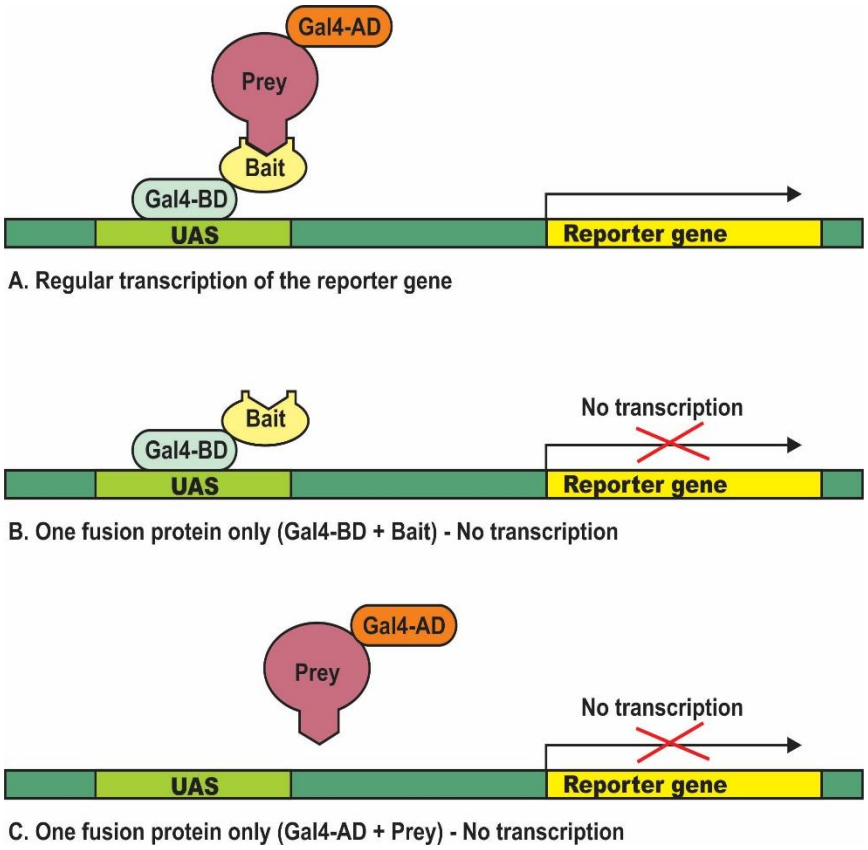

Figure 2.5: A schematic diagram of the yeast two-hybrid system.

The gene encoding the bait is cloned into the bait vector producing a protein fusion downstream of the GAL4 DNA-binding domain (DBD), while the gene encoding the prey is cloned into the prey vector, which fuses with GAL4 activation domain (AD). Both bait and prey are expressed in yeast. Interaction between the bait and the prey brings the two domains together and initiate the transcription of reporter genes (A). If the bait and prey are expressed alone (B and C), or they both are expressed but do not physically interact, the reporter genes are not expressed.

2.5.1 Production of competent yeast AH109

To make a starter culture, a single yeast AH109 colony was inoculated from a fresh agar plate into 50 ml yeast peptone dextrose (YPD) broth and incubated at 30 °C overnight with shaking at 250 rpm. Following this incubation, OD was measured at 600 nm (OD_{600}) followed by inoculation of the appropriate volume into 250 ml of fresh YPD and a further incubation at 30 °C with continuous shaking for approximately 3 hr. Once the OD_{600} reached 0.6, the cells were spun down at 2,000 rpm for 5 min, re-suspended gently in 125 ml of sorbitol/bicine/polyethylene glycol (SBEG) to make them competent and spun again at 2,000 rpm for 5 min. The cell pellet was re-suspended in 5 ml SBEG and immediately stored in 100 µl aliquots at -80 °C.

2.5.2 Transformation of DENV bait constructs

A bait plasmid harbouring a DENV NS gene fragment (1 µg) was added into 100 µl AH109 yeast competent cells and mixed gently. Transformation of the plasmid was carried out by adding 750 µl polyethylene glycol (PEG)/bicine solution followed by incubation at 30 °C for 1 hr on a thermomixer (Eppendorf) while shaking at 900 rpm. After a heat-shock at 45 °C for 5 min, the yeast cells were spun down at 3,500 rpm for 2 min, washed with 1 ml sodium chloride/bicine buffer and spun down again at 3,500 rpm for 5 min. The cell pellet was re-suspended in 200 µl sodium chloride/bicine buffer and plated on SD/-Tryptophan (SD/-Trp) prior to an incubation at 30 °C for 2-3 days.

2.5.3 Yeast two-hybrid screen

A bait AH109 yeast colony from a fresh plate was inoculated into 15 ml SD/-Trp broth and incubated at 30 °C overnight with shaking at 250 rpm. An appropriate volume of the starter culture was used to inoculate 15 ml SD/-Trp to an OD_{600} 0.1 and allowed to incubate at 30 °C overnight with shaking at 160 rpm. Inoculation of an appropriate volume of Y187 prey human cDNA library in 15 ml SD/-Leucine (SD/-Leu) followed by incubation at 30 °C overnight with shaking at 160 rpm was also carried out concurrently.

When the bait and prey cultures grew to an OD_{600} 0.9-1, an equal number of bait and prey cells (3.6×10^8) were mixed in a 50 ml tube following the formula below:

$$\text{X culture volume (ml)} = \frac{(3.6 \times 10^8 \text{ cells})}{(A \times 3 \times 10^7 \text{ cells})}$$

$$= \frac{12 \text{ ml}}{A}$$

A = Culture absorbance at OD_{600}

The mixed culture was spun down at 2,000 rpm for 2 min and the cell pellet was re-suspended in 25 ml yeast peptone dextrose adenine (YPDA) containing 20% PEG 6000. Mating of the yeast cells was performed at 30 °C with shaking at 100 rpm for exactly 3 hr, followed by centrifugation at 2,000 rpm for 3 min. The cell pellet was re-suspended in 10 ml SD medium lacking leucine, tryptophan and histidine (SD/-Leu-Trp-His) and added into 220 ml SD/-Leu-Trp-His medium with appropriate concentration of yeast inhibitor 3-amino-1,2,4-triazole (3-AT). Using a multichannel pipette, the whole suspension was dispersed into a 96-well plate (200 µl of suspension/ well) and incubated at 30 °C for 4-5 days. To confirm successful mating between the bait and prey, 10 µl of the yeast suspension in SD/-Leu-Trp-His was plated on SD/-Leu-Trp agar and incubated at 30 °C for 3 days to observe the growth of diploid cells.

2.5.4 Sequencing of human open reading frames

Diploid yeast colonies were picked and transferred into a round-bottom 96-well plate. Using a 96-point inoculator, the colonies were introduced onto an SD/-Leu-Trp-His agar plate containing 3-AT and the plate was incubated at 30 °C for 3 days. A single yeast colony grown on the plate was scraped off using a sterile tooth-pick and re-suspended in 20 µl 0.02 M sodium hydroxide in a 94-well PCR plate with strip caps (Greiner Bio-One). The suspension was heated up to 95 °C for 10 min in a PCR machine, allowed to cool down on ice and spun down at 1,000 rpm for 1 min. The supernatant (5 µl) was used as a template for amplification of the specific human gene using primers targeting the specific regions flanking the human cDNA insert in the prey vector. Two rounds of PCR were performed following the protocol in Section 2.2.3 with modified cycling conditions, using primers Oligo 136 and 137 (Table 2.12) in the first PCR followed by amplification using Oligo 80 and 81 primers (Table 2.12) in the second PCR. The PCR cycling

parameters were: initial denaturation at 95 °C for 5 min, followed by 20-25 cycles of denaturation at 95 °C for 30 sec, annealing at 55 °C for 1 min 30 sec, extension at 72 °C for 3 min 30 sec, and one cycle of final extension at 72 °C for 7 min. The final PCR products of the human transcripts were analysed by gel electrophoresis on 1% agarose and sent for sequencing in a 96-well PCR format to GATC Biotech, Germany (http://www.gatc-biotech.com/en/index.html) using the pAct2 primer (Table 2.12). The sequencing results were analysed as described in Section 2.2.14.

Table 2.12: Primer sequences for gene insert in yeast pGADT7.

Primer	**Sequence 5' – 3'**
PCR amplification	
Oligo 136	CTA GAG GGA TGT TTA ATA CCA CTA CAA TGG
Oligo 137	GGT TAC ATG GCC AAG ATT GAA ACT TAG AGG
Oligo 80	TGT TTA ATA CCA CTA CAA TGG ATG ATG
Oligo 81	CAT AAA AGA AGG CAA AAC GAT G
DNA sequencing	
pAct2	GAT GAT GAA GAT ACC CCA C

2.5.5 Protein-protein interaction analysis

The human interacting proteins identified from the Y2H screen were collated using the NCBI database of official gene name, gene ID and accession number, symbol and alias. Protein interaction network map was constructed using Cytoscape 3.0 (http://www.cytoscape.org/) and analysis of the enriched Gene Ontology annotation terms of the human proteins targeted by DENV was performed using the Database for Annotation, Visualisation and Integrated Discovery (DAVID) (http://david.abcc.ncifcrf.gov/). Literature mining was conducted from Medline using the PubMed interface to gather information describing binary interactions between DENV and human proteins.

2.5.6 Storage of yeast

To prepare a yeast stock for storage, a single yeast colony was picked using a sterile inoculation loop and suspended in 0.5 ml of YPD or YPDA medium containing 15–30% glycerol. The suspension was transferred into a 2-ml screw cap storage vial and the content was mixed well before immediate freezing at -80 °C. To recover, the top of the frozen stock was scraped off, streaked on YPD or YPDA agar and allowed to incubate at 30 °C for 4-5 days. For use in experiments, the yeast was sub-cultured fresh on agar plates or liquid media followed by a further incubation at 30 °C for 2-3 days.

2.6 Replication of DENV replicon

2.6.1 *In vitro* transcription

Prior to *in vitro* transcription, DENV replicon pDVPACLuc and its derived mutant pDVW87I were linearised using *Xba*I according to the large-scale restriction digestion protocol (Section 2.2.12), examined on 0.8% agarose gel and purified using High Pure PCR Product Purification Kit (Roche). *In vitro* transcription reaction was carried out using MEGAscript® T7 Transcription Kit (Ambion) according to the manufacturer's protocol. The reaction was assembled by adding nuclease-free water (made up to 30 µl), 2 µl each Ribonucleotide solutions (ATP, CTP, UTP and 1:5 diluted GTP), 3 µl Cap Analog (Ambion), 3 µl Reaction Buffer (10x), 1 µg linearised DENV replicon and 2 µl Enzyme Mix. The reaction was mixed gently, briefly spun down and incubated at 37 °C for 5 hr before stored at -70 °C.

2.6.2 Transfection of DNA and RNA

Cells were seeded in a 24-well plate (Section 2.1.3) in order to achieve 70-90% confluence on the day of transfection. For each transfection reaction, 1 µl Lipofectamine® 2000 transfection reagent (Invitrogen) or proprietary animal origin-free Lipofectamine® 2000 CD (Invitrogen) was diluted in Opti-MEM® I reduced serum media and allowed to incubate for 5 min. Plasmid DNA (50-100 ng) or 2.5 µl *in vitro*-transcribed DENV replicon RNA (per well) was diluted in 50 µl Opti-MEM® I reduced serum media. The reaction was scaled up or down depending

on the number of wells to be transfected. After 5 min, the diluted Lipofectamine reagent was added to the diluted DNA and incubated for 20 min at room temperature. The resulting Lipofectamine-DNA complex (100 µl) was added directly to each well and mixed gently by rocking the plate back and forth followed by incubation at the appropriate temperature for 18-24 hr.

2.6.3 Dual luciferase assay

Following transfection, medium from the transfected cells was removed and the cells were lysed in passive lysis buffer (100 µl/ well) followed by freezing at -20 °C. After thawing, the cell lysate was incubated for 15-20 min with shaking at room temperature and 25 µl was transferred into a 96-well white plate (Greiner CELLSTAR) for measurement of the luciferase activity using the dual-luciferase reporter® (DLR™) assay system (Promega). Prior to the measurement, luciferase assay reagent II (*FFLuc*) was prepared by re-suspension of lyophilised luciferase assay substrate in luciferase assay buffer II and stored in aliquots in -20 °C. Stop & Glo® reagent (*RLuc*) was prepared fresh to the required volume by diluting the Stop & Glo® substrate (50x) to a final 1x in Stop & Glo® buffer. Luciferase reagents were pre-warmed to room temperature prior to use, each diluted 1:10 with water (this was a minor adjustment) and fitted to the dual-injectors of the GloMax® multi detection system (Promega) luminometer. After priming both injectors, 70 µl of the diluted substrates was dispensed into the sample wells for measurement of luciferase activities. Once completed, the injector tubes were cleaned by flushing them through with water and 70% ethanol according to the recommended instructions. Data obtained from luciferase measurements was analysed using the Instinct® software (Promega) and Microsoft Excel.

2.7 Functional assays

2.7.1 LUMIER assay

The LUminiscence-based Mammalian IntERactome (LUMIER) assay was first introduced by Barrios-Rodiles et al. (2005) as a high-throughput method to map protein-protein interactions in mammalian cells. This assay is a variation of co-immunoprecipitation (co-IP) technique using luciferase readout. Although the LUMIER assay is not widely used, there are several advantages of this assay over the conventional co-IP. This includes its high sensitivity, high-throughput capability and requirement of small amounts of DNA for assessing protein interactions. In LUMIER assays, an interaction between two proteins X and Y is determined through transient co-expression of Protein A-tagged protein X and *RLuc*-tagged protein Y (Figure 2.6a). Upon cell lysis, Protein A fused to protein X immunoprecipitates with IgG-coated magnetic beads and pulls down protein Y in case of an interaction, which generates a luciferase signal. If X and Y proteins do not interact, there is no luciferase activity measured (Figure 2.6b and Figure 2.6c).

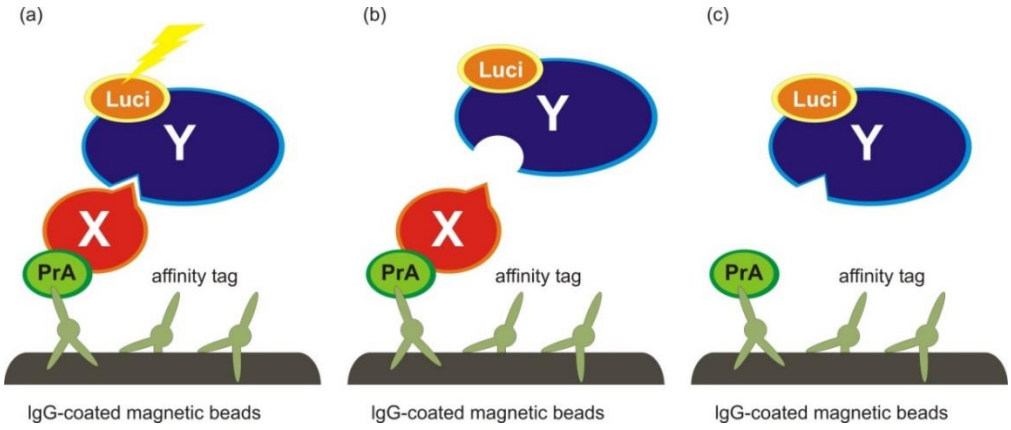

Figure 2.6: A schematic diagram of LUMIER assay.

Protein X is tagged with Protein A (PrA) and protein Y is tagged with *RLuc*. (a) If there is an interaction between X and Y, the protein complex is pulled down by immunoprecipitation of Pr A with IgG-coated beads. After extensive washing, *RLuc* readout shows a high luciferase activity indicating a positive X and Y interaction. In the case of (b) no interaction between X and Y, or (c) in the absence of X, no luciferase activity is measured. The diagram was adapted and re-drawn from reference (Blasche & Koegl 2013).

2.7.1.1 Mammalian cell expression cloning

LUminescence-based Mammalian IntERactome (LUMIER) assays were performed to confirm interactions between DENV and human proteins in HEK293 cells. Pre-cloned human cellular genes were obtained from the MGC cDNA library in pDONR223, which had been transformed into *E. coli* DH5α and sub-cultured on fresh LB agar plates containing 50 µg/ ml spectinomycin. Plasmids were harvested, sequence-verified using the appropriate primers (Section 2.2.14,Table 2.13) and cloned into a mammalian expression vector pTREX-DEST30-Protein A (N-terminal Protein A tag fusion) by LR reaction (Section 2.4.4.3). After transformation into *E. coli* DH5α, the resulting expression clones were purified and confirmed by digestion with *Xho*I and *Apa*I (Section 2.2.12). Corresponding DENV gene fragments interacting with the human proteins were sub-cloned from an entry vector pDONR207 into pcDNA3-RL-GW (N-terminal *RLuc* fusion) in a similar fashion. Both human and DENV expression plasmids (25 ng) were co-transfected into HEK293 cells in a 96-well plate and incubated at 37 °C for 48 hr. Two plasmid constructs expressing interacting proteins JUN and FOS were co-transfected in parallel and used as positive control.

Table 2.13: Primers sequences for MGC human insert in pDONR223.

Primer	**Sequence 5' – 3'**
DONR223-F	TCGCGTTAACGCTAGCATG
DONR223-R	TAATACGACTCACTATAGGG

2.7.1.2 Pull-down of interacting proteins

Prior to cell lysis, sheep anti-rabbit IgG-coated magnetic beads (Dynabeads M280, Invitrogen) were washed in washing buffer (containing 1x PBS and 1 mM DTT) and added into 1x passive lysis buffer (Promega) containing protease inhibitor cocktail mix (Roche). Medium was removed from transfected cells and the cells were lysed with lysis buffer containing beads (10 µl/ well) followed by incubation at 4 °C with shaking for 30 min. PBS (90 µl) was added into each well and the cell lysate was transferred into a 96-well white plate (Greiner CELLSTAR).

To measure the background luciferase activity of samples, 10 µl of lysate was removed into another 96-well plate containing 90 µl PBS/ well and placed on ice. From the remaining cell lysate, magnetic beads were pulled down to the bottom of the plate using a handheld magnetic separator block (Millipore) and 80 µl of the supernatant was gently removed by pipetting. The beads were washed by adding 200 µl washing buffer (containing 1x PBS and 1 mM DTT) and allowed to stand for 1 min off-magnet before applying the magnet again for removal of supernatant. The washing step was repeated four times before the addition of 80 µl PBS after the final wash, followed by measuring the luciferase activity in the initial cell lysate (unwashed beads) and the washed beads. The luciferase values were normalised against wells transfected with empty pTREX-DEST30-PrA. Signal-to-noise ratios and Z-scores were calculated for the lysate and washed beads as described previously (Tahoun et al. 2011).

2.7.2 Co-immunoprecipitation assay

Homo sapiens BTG3-associated nuclear protein (BANP) ORF was sub-cloned from the pDONR223 entry clone (obtained from Juergen Haas) into a Gateway destination vector pcDNA™-DEST40 by LR reaction (Section 2.4.4.3). This produced the pDEST40-BANP expression construct in which BANP was fused upstream of the His/V5-tag. For the potassium voltage-gated channel Kv1.3, a plasmid construct expressing GFP fused to the entire coding region of the protein Kv1.3 in the Emerald-C1 vector was provided by Jamel Mankouri, University of Leeds.

DENV NS2A was sub-cloned from the pDONR207 entry clone into the pTREX-DEST30-Protein A vector resulting in the expression of NS2A as a fusion with Protein A of *S. aureus*. The interaction of BANP and Kv1.3 proteins with DENV NS2A was tested independently by co-transfecting each construct with pTREX-DEST30-Protein A-NS2A in HEK293 cells. After 48 hr incubation, the cells were washed in ice-cold PBS and lysed in NP-40 lysis buffer containing protease inhibitor cocktail mix (Roche). Sheep anti-rabbit IgG-coated magnetic beads were added to cell lysate and incubated at 4 °C overnight with mixing on a tube rotator. After incubation, the beads were pulled down using a magnetic separator block and washed four times in washing buffer. Proteins bound to the washed beads were dissolved by adding 20 µl 1% SDS and heated up to 95 °C for 5 min, followed by Western blot analysis using the appropriate antibodies (see Table 2.5).

2.7.3 siRNA gene silencing

ON-TARGETplus SMART pool® small interfering (si) RNA BANP (Dharmacon) consisting a mixture of four individual siRNA (Table 2.14) was used to knockdown BANP protein. The lyophilised siRNA was dissolved in the siRNA buffer supplied to the required stock concentration. Transfection of the siRNA (100 nM) was carried out using Lipofectamine® 2000 CD as described in Section 2.6.2 in order to optimise knockdown conditions. Efficacy of the knockdown was evaluated by Western blot using anti-BANP and anti-V5 primary antibodies. β-Gal siRNA-1 targeting the human β-galactosidase was used as a negative control (Table 2.14).

Table 2.14: siRNA sequences of human BANP and β-galactosidase.

siRNA	Sequence 5' – 3'
BANP	CAAACCAGCAGUGUUGUUCUU UAACAGUAGACAGCUGACCUU UAUCUGUUAGGCGAGUUGCUU UAAAUAAUCAGCCAUCAGUUU
β-Gal	UAAGGCUAUGAAGAGAUAC

2.7.4 Immunostaining

Cells were seeded (Section 2.1.3) in a 24-well glass-bottom plate (Greiner Bio-One) for immunostaining. After performing the transfection and incubation as required, the cell monolayer was fixed in 4% paraformaldehyde for 10 min and washed with PBS for 5 min, three times. To allow antibody penetration of the cell membrane, the cells were permeabilised by adding 0.3% Triton X-100/PBS for 20 min and washed with PBS for 5 min, three times. The cells were then blocked with 5% FBS/PBS for 30 min, followed by washing with PBS for 12 min, three times. Primary antibodies (Table 2.5) were applied at the appropriate dilutions in 5% FBS/PBS and the cells were allowed to incubate at 4°C overnight. Cells were washed three times with PBS for 10 min followed by incubating with the corresponding secondary antibodies Alexa Fluor® 488 donkey anti-rabbit IgG (H+L) antibody or Alexa Fluor® 594 donkey anti-mouse IgG (H+L) antibody (Molecular Probes) for 1 hr at room temperature protected from light. After the incubation,

the cells were washed three times with PBS for 10 min and nuclear-stained using VECTASHIELD® Mounting Medium with DAPI (Vector Laboratories). A coverslip was immediately applied to the cell monolayer and the plate was viewed with a confocal laser scanning 710 microscope (Carl Zeiss). Scanned images were analysed using the ZEN software (Carl Zeiss) and Imaris image processing software (Carl Zeiss).

2.7.5 Interferon reporter assay

To test for the effect of over-expressed BANP in interferon (IFN) response, HEK293 cells were seeded in a 24-well plate as described in Section 2.1.3. The cells were transiently co-transfected using Lipofectamine® 2000 CD (as described in Section 2.6.2) with four plasmids; p125Luc (50 ng), pcDNA-mycNS2A (100 ng), pDEST40-BANP or pDEST-MBP (100 ng), and pRL-CMV vector (0.5 ng) (Promega) (Table 2.15). pDEST40-MBP expressing maltose-binding protein (MBP) was used as a negative control for IFN stimulation. pRL-CMV expressing constitutive *RLuc* was used as an internal control to which expression of the *FFLuc* reporter gene was calculated relative to. p55A2Luc contained the positive regulatory domain II (PRDII) of NF-κB elements which was used to test for regulation of NF-κB.

At 24 hr post-transfection (p.t), the transfected cells were stimulated by adding 5 µg polyinosinic-polycytidylic acid [Poly(I:C)] (LMW) (InvivoGen) per well according to the manufacturer's instructions to induce the production of IFN-β. 24 hr post-stimulation, the cells were lysed in passive lysis buffer and the luciferase activity was measured with the dual-luciferase reporter assay system as detailed in Section 2.6.3.

The effect of DENV proteins on the cellular IFN response was also tested with IFN-α-induced IFN-stimulated gene response element (ISRE) promoter activity. HEK293 cells was seeded as described in Section 2.1.3 and co-transfected with three plasmids; pGL4.17-ISREFluc (50 ng), plasmids expressing DENV proteins either pDEST40-NS2A, pDEST40-NS4B or pDEST40-NS5 (100 ng), and 0.5 ng pRL-CMV (Table 2.15). After 24 hr incubation at 37 °C, the cells were treated with 1000 IU/ml recombinant human Universal Type I IFN Alpha (PBL Interferon Source). At 24 hr post-treatment, the cells were lysed in passive lysis buffer and the luciferase activity was measured as described in Section 2.6.3.

Table 2.15: List of plasmids used in this study.

Plasmid	Features	Reference
p125Luc	murine IFN-beta promoter plasmid expressing *FFLuc*	a kind gift from Takashi Fujita, (Yoneyama et al. 1996)
p55A2Luc	multimerised PRDII element *FFluc* reporter	a kind gift from Takashi Fujita, (Yoneyama et al. 1998)
pcDNA-mycNS2A	DENV NS2A tagged with Myc epitope at the N-terminus in pcDNA3.1(+)	purchased from ShineGene Bio-Technologies, Inc.
pDEST40-BANP	BANP tagged with V5 epitope and 6x His	constructed in-house using Gateway system (Section 2.4.4)
pDEST40-MBP	MBP tagged with V5 epitope and 6x His	constructed in-house using Gateway system (Section 2.4.4)
pRL-CMV	constitutive *RLuc* driven by CMV promoter	Promega (Sherf et al., 1996)
pGL4.17-ISREFluc	ISRE promoter expressing *FFLuc*	a kind gift from Benjamin G Hale, University of Zurich
pDEST40-NS2A	DENV NS2A tagged with V5 epitope and 6x His	constructed in-house using Gateway system (Section 2.4.4)
pDEST40-NS4B	DENV NS4B tagged with V5 epitope and 6x His	constructed in-house using Gateway system (Section 2.4.4)
pDEST40-NS5	DENV NS5 tagged with V5 epitope and 6x His	constructed in-house using Gateway system (Section 2.4.4)

2.7.6 Cell proliferation assay

Cell proliferation assays were carried out using the CellTiter 96® non-radioactive cell proliferation assay (Promega) according to the manufacturer's instruction. This assay utilised the cellular conversion of tetrazolium salt into formazan product which reflected the number of viable cells. In brief, HEK293 cells were seeded (1.5 x 10^4 cells/ml) in a 96-well plate and transfected with varying concentrations of plasmid DNA or treated with potassium channel inhibitors (Table 2.16) followed by an incubation at 37 °C. After 6 hr, 15 µl dye solution was added into each well and the incubation prolonged for an additional 4 hr. Stop solution (100 µl/ well) was then added and the plate was allowed to stand overnight in a humidified chamber to solubilise the formazan crystals. Absorbance in cultures was recorded using the GloMax detection system the next day. Mock-transfected cell absorbance were used as blank and subtracted from the test sample values. Graphs plotting the absorbance versus concentration of plasmid DNA or potassium channel inhibitors were generated from the data.

2.7.7 BANP and Kv1.3 effect on dengue virus replication

2.7.7.1 Dengue virus infection

Experiments involving cell infection with infectious DENV were performed by Amjad Yousuf in a Containment Level 3 facility, University of Bristol. To determine the effect of BANP on DENV replication, HEK293 cells were transfected with either pDEST40-BANP or siRNA BANP (as described in 2.6.2 and 2.7.3). After an overnight incubation at 37 °C, the cells were infected with DENV-2 NGC strain at a multiplicity of infection (MOI) 10 for 1 hr and replaced with fresh medium, followed by an incubation at 37 °C. Transfection of the siRNA BANP was repeated in the designated wells the next day to ensure continuous BANP knockdown. All cells were incubated at 37 °C for 3-4 days post-infection followed by cell lysis in TRIzol® reagent and stored at -80 °C.

For Kv1.3 experiments, HEK293 cells were treated with the appropriate inhibitors (Table 2.16) to block the endogenous potassium channel Kv1.3 at concentrations pre-determined by the cell proliferation assay (Section 2.7.6) and incubated at 37 °C for 4 hr. Some wells were left untreated or individually treated with the diluent of inhibitors (either PBSA or water) as negative controls. After the incubation period, the inhibitors were removed and the cells were infected with DENV-2 NGC strain for 1 hr. The virus was replaced with fresh medium containing the appropriate inhibitors and incubated at 37 °C for 3-4 days before lysing the cells in TRIzol® reagent. All cell lysates were then sent to Glasgow for further analysis.

Table 2.16: Potassium channel inhibitors used in this study.

Channel inhibitor	Symbol	Stock diluent	Final concentration per well (diluted in DMEM)
Tetraethylammonium chloride	TEA	Water	10 mM
4-Aminopyridine	4-AP	Water	1 mM
Margatoxin	Mar	PBSA	10 nM

2.7.7.2 Quantitative real-time PCR

RNA was extracted from the DENV-infected cells as described in Section 2.2.1 and stored at -80 °C. The cDNA was synthesised using random primers as detailed in Section 2.2.2 and used as a template to measure the DENV gene expression by Taqman quantitative real-time PCR (qRT-PCR). Primers (Eurofins Genomics) amplifying partial DENV-2 capsid gene and the probe [labeled with 5' 6-carboxyfluoroscein (6-FAM) and 3' black hole quencher (BHQ-1)] fluorophores are listed in Table 2.17. Each reaction contained 12.5 µl Taqman Universal PCR master mix (2x) (Life Technologies), 1 µl forward and reverse primers (10 µM), 1 µl probe (5 µM) and 1 µl cDNA. The housekeeping human gene, hypoxanthine phosphoribosyltransferase 1 (HPRT1) was used as an internal control to which the expression of DENV capsid was normalised. The HPRT1 primer and probe (labeled

with FAM and minor groove binder (MGB) fluorophores) mixture was purchased from Life Technologies. Nuclease-free water was used as a negative control. qRT-PCR parameters were: 95 °C for 15 min (holding stage) followed by 40 cycles of 94 °C for 15 sec, 60 °C for 1 min.

Table 2.17: Primer and probe sequences used for qRT-PCR.

The primer and probe sequences were as established by Callahan et al. (2001).

Primer/probe	Sequence 5' – 3'
DENV-2-forward	CATGGCCCTKGTGGCG
DENV-2-reverse	CCCCATCTYTTCAGTATCCCTG
DENV-2-probe	TCCTTCGTTTCCTAACAATCC

2.8 Construction of *Ae. aegypti* cDNA library

Various techniques can be used to construct a cDNA library. In this study, a mosquito cDNA library was generated using the Make Your Own 'Mate and Plate™' Library System (Clontech). This method utilised a switching mechanism at the 5' end of the RNA transcript (SMART) oligonucleotides in the first-strand cDNA synthesis reaction which produced a pool of cDNA with SMART end sequences (Zhu et al. 2001) as described in Figure 2.7. The sequences are homologous to the linearised yeast expression vector pGADT7-Rec end sequences which allow *in vivo* recombination to occur between the vector and the mosquito cDNA following transformation into yeast (Figure 2.8). Colonies that have successful integration of the cDNA into the vector acquire the ability to synthesise leucine and thus are able to grow on a minimal media lacking leucine.

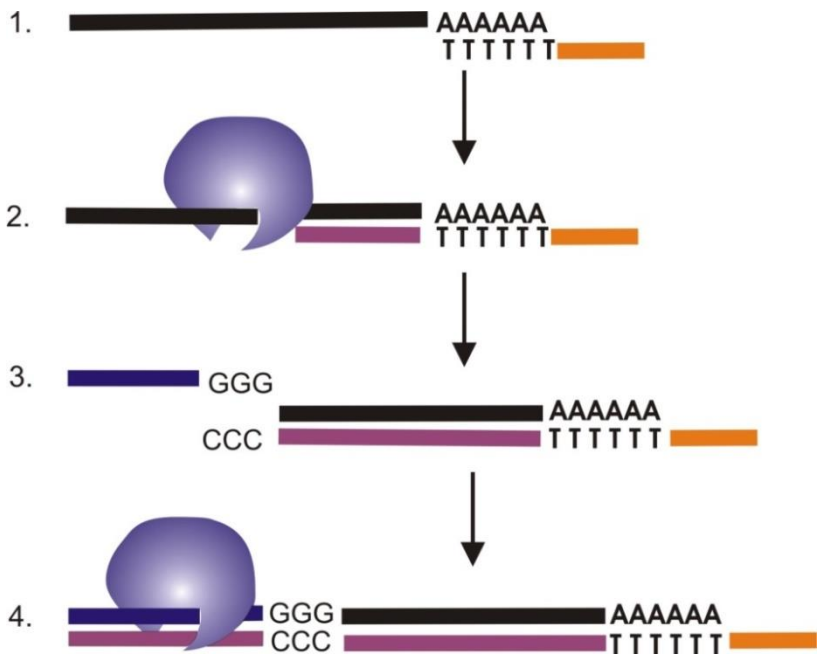

Figure 2.7: A schematic diagram of the SMART technology.

SMART is a switching mechanism at the 5' end of RNA transcript technology. Step 1: Oligo (dT) containing CDS III primer sequence binds to the poly(A) tail of the mRNA. Step 2: MMLV reverse transcriptase generates complementary DNA and adds additional deoxycytidine (CCC) nucleotides to the cDNA 3' end due to its terminal transferase activity. Step 3: SMART III oligonucleotides with guanine (GGG) sequence at 3' end binds to the CCC overhangs. Step 4: MMLV switches templates and continues incorporating nucleotides complementary to the SMART sequences to the 5' end. The SMART technology results in known sequences at both 3' and 5' ends of the cDNA which serves as priming sites for subsequent LD-PCR amplification. This diagram was adapted and re-drawn from the Make Your Own 'Mate and Plate™' Library System user manual (Clontech 2010).

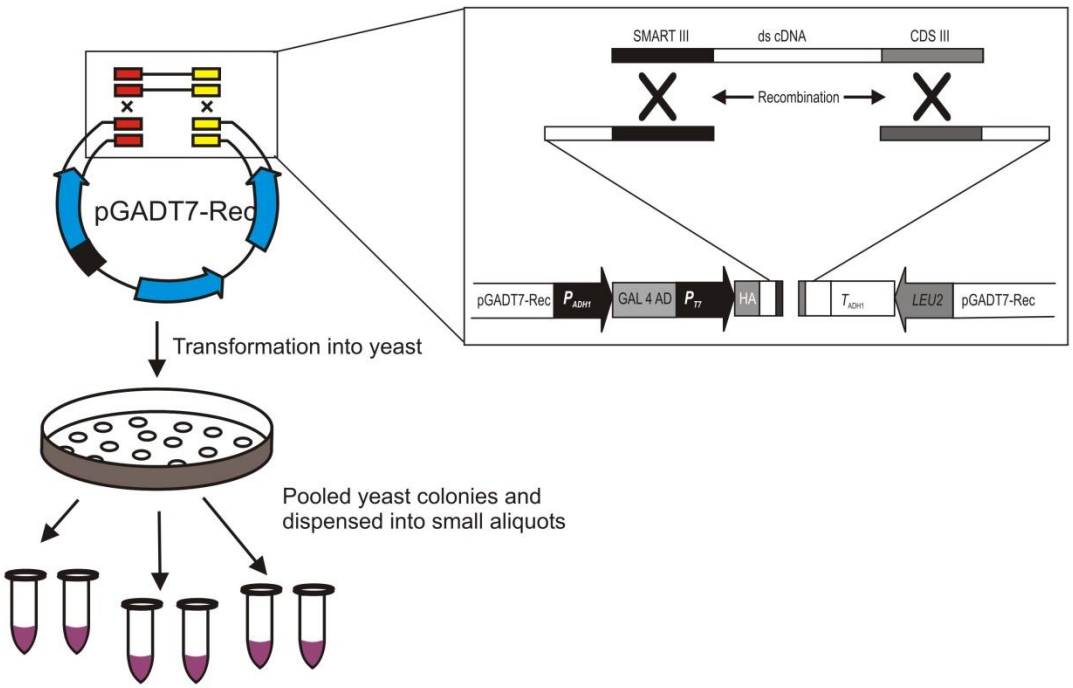

Figure 2.8: A schematic diagram of the homologous recombination in yeast.

The recombination reaction occurs between *SmaI*-linearised pGADT7-Rec vector and the mosquito cDNA in yeast. The linear pGADT7-Rec has sequence ends homologous to the SMART III and CDS III sequences of the Aag2 cDNA which allows integration of the cDNA into the vector through homologous recombination and gap repair (Fusco et al. 1999). In pGADT7-Rec, the gene of interest is expressed as a GAL4 activation domain (GAL4 AD) fusion under the constitutive ADH1 promoter (P_{ADH1}) and ends with the ADH1 termination signal (T_{ADH1}). P_{T7} is T7 RNA polymerase promoter, HA is hemagglutinin epitope tag, *LEU2* is yeast selection marker. This diagram was adapted and re-drawn from the Make Your Own 'Mate and Plate™' Library System user manual (Clontech, 2010).

2.8.1 Preparation of cDNA

A cDNA library obtained from *Ae. aegypti*-derived Aag2 cells was constructed using the "Mate and Plate™" library (Clontech) following the manufacturer's protocols.

2.8.1.1 RNA extraction

Total RNA was extracted from Aag2 cells using TRIzol® reagent following the manufacturer's instructions. Briefly, 80% confluent Aag2 cells from a medium flask were detached and spun at 1,500 rpm for 5 min. The protocol detailing the RNA extraction process was described in Section 2.2.1.

2.8.1.2 cDNA synthesis

To generate the first-strand cDNA, CDSIII primer (Table 2.18) containing the modified oligo (dT) was added to 2 µg Aag2 RNA and incubated at 72 °C for 2 min. After cooling down on ice, a reaction mix was added containing 2 µl First-strand buffer (5x), 1 µl DTT (100 mM), 1 µl dNTP mix (10 mM) and 1 µl SMART moloney murine leukemia virus reverse transcriptase. The mixture was incubated at 42 °C for 10 min followed by adding 1 µl SMART III Oligo (Table 2.18) and further incubated at 42 °C for 1 hr. The reaction was terminated by placing the tube at 75 °C for 10 min. After cooling down to room temperature, excess RNA was removed by incubating the reaction with 1 µl RNAse H (2 U/ µl) at 37 °C for 20 min and the resulting cDNA was stored at -20 °C. As a positive control, 1 µg mouse liver poly A^+ RNA (Clontech) was used in parallel to generate first-strand cDNA.

2.8.1.3 LD-PCR

The Aag2 first-strand cDNA was amplified by long-distance PCR (LD-PCR) using reagents purchased from Clontech according to the recommended protocol. Two PCR reactions (100 µl each) were set up as follows: 70 µl nuclease-free water, 10 µl Advantage® 2 PCR buffer (10x), 2 µl dNTP mix (50x), 2 µl 5' PCR primer (10 mM) (Table 2.18), 2 µl 3' PCR primer (10 mM) (Table 2.18), 10 µl melting solution (10x), 2 µl Advantage® 2 polymerase mix (50x) and 2 µl Aag2 first-strand cDNA. LD-PCR parameters are shown in Table 2.19. The PCR product (7 µl) was electrophoresed in a 1.2% agarose gel and stained with ethidium bromide. The first-strand cDNA of mouse liver poly A^+ RNA was PCR-amplified alongside and used as a positive control.

Table 2.18: Oligonucleotide sequences for construction of Aag2 cDNA library.

First-Strand cDNA Synthesis (Sequence 5' – 3')	
CDS III primer	ATTCTAGAGGCCGAGGCGGCCGACATG-d(T)30VN
SMART III Oligo	AAGCAGTGGTATCAACGCAGAGTGGCCATTATGGCCGGG
cDNA Amplification (Sequence 5' – 3')	
5' PCR primer	TTCCACCCAAGCAGTGGTATCAACGCAGAGTGG
3' PCR primer	GTATCGATGCCCACCCTCTAGAGGCCGAGGCGGCCGACA

Table 2.19: LD-PCR parameters.

Step	Temperature	PCR cycle	Time
Initial denaturation	95 °C		30 sec
Denaturation	95 °C	20-35 cycles	10 sec
Extension	68 °C		6 min; 5 sec increased for each cycle
Final extension	68 °C		5 min

2.8.1.4 cDNA size fractionation

PCR-amplified Aag2 cDNA (3 µg) was size-fractionated using CHROMA SPIN™ +TE-400 columns (Clontech). Prior to use, the spin column was inverted a few times to mix the gel matrix suspended in equilibration buffer. By holding the column upright, the break-away bottom of the column was snapped off followed by the top cap, before placing it into a 2 ml collection tube. The gel matrix was then spun down at 700 x g for 5 min to purge the equilibration buffer using a swing rotor centrifuge. This allowed liquid to pass through the gel matrix uniformly, leaving a semi-dry matrix bed in the column. The collection tube was then replaced with a nuclease-free 1.5 ml tube. PCR-amplified Aag2 cDNA (93 µl) was applied to the centre of the column and spun at 700 x g for 5 min. The flow-through samples containing amplified cDNA from two PCR reactions were pooled and purified by ethanol precipitation as described below.

2.8.1.5 Ethanol precipitation

To purify cDNA, sodium acetate (3M) (Clontech) (1/10th volume of cDNA) was added into the size-fractionated cDNA followed by the addition of 95% ice-cold ethanol (2.5 volume of cDNA) and the mixture was frozen at -20 °C. After 1 hr, the cDNA was spun down at 14,000 rpm for 20 min at room temperature and the supernatant was discarded. To remove excess liquid, the DNA pellet was spun down again at 14,000 rpm for 30 sec and air-dried for 10 min. The purified Aag2 cDNA was re-suspended in 20 µl nuclease-free water and stored at -20 °C.

2.8.2 Production of competent yeast Y187

Competent *S. cerevisiae* yeast Y187 (Clontech) strain cells were prepared following the yeastmaker yeast transformation system 2 protocol (Clontech). In brief, fresh yeast was recovered from glycerol stocks and a starter culture was prepared in 3 ml YPDA. This was incubated at 30 °C with shaking at 250 rpm for 8-12 hr. For larger volumes, 5 µl of the culture was inoculated into 50 ml YPDA in a conical flask and incubated at 30 °C with shaking at 250 rpm for 16-20 hr. Measurement of the culture absorbance was carried out using a spectrophotometer (Beckman) to obtain an OD_{600} 0.15-0.3 and the appropriate density of yeast cells were spun down at 700 x g for 5 min at room temperature.

The cell pellet was re-suspended in 100 ml YPDA broth and further incubated at 30 °C for 3-5 hr with shaking at 250 rpm. When the OD_{600} reached 0.4-0.5, the yeast culture was divided into two 50 ml sterile tubes, spun down at 700 x g for 5 min, followed by washing the cells in 30 ml sterile water. After centrifugation at 700 x g for 5 min, the cells were re-suspended in 1.5 ml 1.1x Tris-EDTA/Lithium acetate (TE/LiAc) to make them competent and then transferred into two 1.5 ml tubes. Centrifugation was carried out at high speed for 15 sec and the cell pellet was re-suspended again in 600 µl 1.1x TE/LiAc. The competent cells were immediately used for transformation with plasmid DNA.

2.8.3 Co-transformation and *in vivo* recombination in yeast

The Aag2 cDNA library was generated by co-transformation of Aag2 cDNA and *Sma*I-linearised pGADT7-Rec vector into the competent yeast strain Y187 using the "Mate and Plate™" Library (Clontech) following the manufacturer's protocol. Briefly, 3 µg Aag2 cDNA and 3 µg *Sma*I-linearised pGADT7-Rec vector (500 ng/ µl) were mixed in a pre-chilled sterile 15 ml tube. As a positive control, 3 µl plasmid SV40 large-T PCR fragment with flanking SMART sequences (25 ng/ µl) (supplied in the kit) was co-transformed with 1 µl *Sma*I-linearised pGADT7-Rec alongside with 1 µl *Sma*I-linearised pGADT7-Rec alone.

Prior to transformation, Yeastmaker™ carrier DNA (Clontech) (10 mg/ ml) was denatured by heating it up to 95 °C for 5 min followed by cooling down on ice and adding 20 µl into the reaction mixture. Next, 600 µl yeast competent cells were added, followed by 2.5 ml PEG/LiAc and the suspension was gently mixed. After incubating at 30 °C for 45 min with mixing every 15 min, 160 µl DMSO was added and the suspension was gently mixed. Transformation was carried out by placing the tube in a thermomixer and heat-shocked at 42 °C for 20 min with gentle mixing, followed by centrifugation at 700 x g for 5 min. The pellet was then re-suspended in 3 ml specially formulated YPD plus medium (Clontech). After incubating at 30 °C for 90 min with shaking at 250 rpm, the yeast cells were recovered by centrifugation at 700 x g for 5 min. The cell pellet was re-suspended in 15 ml 0.9% sodium chloride (Clontech), plated on 50 SD/-Leu square plates 150 mm x 150 mm (150 µl per plate) and allowed to incubate at 30 °C for 3-4 days.

2.8.4 Determination of cDNA library titre

In order to determine the Aag2 cDNA library titre, 100 µl cDNA-transformed yeast was vortexed vigorously and diluted in 0.9% sodium chloride (1:100, 1:1000 and 1:10,000). Each dilution (100 µl) was plated on SD/-Leu agar 100 mm diameter plates in triplicates and allowed to incubate at 30 °C for 3-4 days. Transformation of 1 µl pGBT9 (100 ng/ µl) was performed alongside as a positive control and 100 µl was plated on SD/-Trp agar. The cDNA library titre was determined by calculating the transformation efficiency and the number of independent clones following the formulas:

Transformation efficiency =	CFU x suspension volume (ml)
	volume plated (ml) x amount of DNA (µg)

No. of independent clones =	No. of CFU/ ml on SD/-Leu x resuspension volume (ml)

CFU = Colony Forming Units

2.8.5 Harvest of Aag2 cDNA library

SD/-Leu agar plates containing the Aag2 cDNA-transformed yeast colonies were chilled at 4 °C for 3-4 hr. Freezing medium (1 ml) containing YPDA and 75% glycerol was pipetted onto the agar surface. Under sterile conditions, the colonies were detached from the agar surface using a sterile spreader and pooled into a sterile tube. The cell density was estimated using a haemocytometer, divided into 1 ml aliquots and stored at -80 °C.

2.8.6 Mosquito innate immune signalling

Ae. aegypti-derived Aag2, *Ae. albopictus*-derived C6/36 and *Ae. albopictus*-derived U4.4 were seeded in 24-well plates (Section 2.1.3). Mosquito STAT, IMD and Toll immune signalling pathways were studied by transfecting individual reporter plasmids (Table 2.20) into each cell line (as described in 2.6.2). To study the STAT pathway, p6x2DRAF-Luc (50 ng) was transfected using 1 µl Lipofectamine™ 2000 as previously described (Fragkoudis et al. 2008). IMD was studied by transfecting pJL169 (50 ng) into the cells, whereas the Toll pathway was studied by co-transfection with pJM648 (500 ng) and pJL195 (400 ng). pAct-*Renilla* (12.5 ng) expressing constitutive *RLuc* was transfected into all wells which used as an internal control. The transfection mixture was removed 5 hr post-transfection, replaced with fresh medium and incubated at 28 °C overnight.

After the overnight incubation, the STAT and IMD pathways were stimulated by introducing the Gram-negative *E. coli* JM109 (approximately 3 x 10^9 CFU/ ml) into the mosquito cells, while the Toll pathway was activated using the Gram-positive *Bacillus* sp. To prepare the inoculum, an overnight bacteria culture was spun down at 2,500 rpm for 10 min at 4 °C and re-suspended in 500 µl PBS. The bacteria suspension was heat-inactivated at 80 °C for 10 min and 5 µl was inoculated into each well of the transfected mosquito cells. After 1 hr, the medium was replaced with fresh medium followed by incubation of the cells for an additional 11 hr at 28 °C. The cells were lysed in 100 µl passive lysis buffer (Promega) and luciferase activity was measured using GloMax luminometer (as described in Section 2.6.3).

Table 2.20: Reporter plasmids used in mosquito innate immune signalling.

Plasmid	Reporter	Immune pathway	Features	Reference
p6x2DRAF-Luc	*FFLuc*	STAT	multimerised *Drosophila* STAT-responsive element	(Müller et al. 2005), (Hombría et al. 2005)
pJL169	*FFLuc*	IMD	IMD-responsive *Drosophila Attacin A* promoter	(Fragkoudis et al. 2008)
pJM648	*FFLuc*	Toll	Toll-responsive *Drosophila Drosomycin* promoter	(Tauszig et al. 2000)
pJL195		Toll	Drosophila constitutively active Toll delta leucine-rich repeat (ΔLRR) mutant under control of *Drosophila* Actin 5C gene promoter	(Tauszig et al. 2000)
pAct-Renilla	*RLuc*	Internal control	*Drosophila* Actin 5C gene promoter	(Müller et al. 2005), (Karsten et al. 2006)

2.9 Commonly Used Solutions

Western blot

5x Transfer buffer

58.14 g Tris-base, 29.28 g glycine, 3.75 g SDS, water to 2 L

Nonidet-P40 buffer

150 mM sodium chloride, 1.0% NP-40, 50 mM Tris, pH 8.0

10x PBS

80 g sodium chloride NaCl, 2 g potassium chloride KCl, 14.4 g sodium hydrogen phosphate Na_2HPO_4, 2.4 g Potassium dihydrogen phosphate KH_2PO_4

Water was added to 800 ml, pH adjusted to 7.4 with hydrochloric acid. Water was added to 1L. 10x PBS was diluted to 1x before use.

1x PBS-Tween

100 ml 10x PBS, 1 ml Tween-20 (final conc 0.1%), Water was added to 1L

Yeast media/reagents

YPD

20 g peptone, 10 g yeast extract, 30 g agar (eliminated if making broth), water was added to make up 900 ml and autoclaved. After cooled down, 100 ml 20% filter-sterilised glucose was added (final conc 2%).

YPDA

YPD medium was prepared as above and autoclaved. After cooled down, 15 ml of 0.2% Adenine hemisulfate solution was added (final conc is 0.003%). Total volume was added to 1 L with sterile water.

SD Minimal Medium

26.7 g minimal SD base, 0.64 g -Leu-Trp drop-out supplement, 20 g agar

Water was added to 1L and autoclaved. After cooled down, 100 ml amino acid supplement (10x) was added (Trp for AH109 minus Leu, Leu for Y187 minus Trp)

10x Tryptophan

0.2 g Trp in 1 L water

10x Leucine

1 g Leu in 1L water

Sorbitol/ Bicine/ PEG

91.1 g sorbitol (final conc 1M), 5 ml 1M Bicine, pH 8.35 adjusted with sodium hydroxide (final conc 10 mM), 15 ml PEG. Water was added to 500 ml and filter-sterilised.

PEG/ Bicine

40 g PEG powder, 20 ml 1M Bicine adjusted pH 8.35 with sodium hydroxide (final conc 0.2 M), water was added to 100 ml and filter-sterilised

Sodium chloride/ Bicine buffer

0.88 g sodium chloride (final conc 0.15 M), 1 ml 1M Bicine (final conc 0.01 M), water was added to 100 ml and filter-sterilised

Mating medium

120 ml YPDA, 80 ml 50% PEG6000 (final conc 20%)

Freezing Medium

100 ml sterile YPDA, 50 ml 75% sterile glycerol

1.1XTE/LiAc

(Prepared fresh prior to transformation)

1.1 ml TE Buffer (10x), 1.1 ml 1 M LiAc (10x), 10 ml sterile water was added

PEG/LiAc

(Prepared 10 ml fresh solution prior to transformation)

8 ml 50% PEG 3350, 1 ml TE Buffer (10x), 1 ml 1 M LiAc (10x)

CHAPTER 3: DENGUE VIRUS-HUMAN PROTEIN-PROTEIN INTERACTIONS

3.1 Introduction

The study of protein-protein interactions is essential to understand the natural behaviour of proteins to form dynamic structures in order to become biologically functional. Physical interactions between proteins form the basis for diverse molecular processes, such as regulation of signalling networks, gene transcription or cell metabolism. In the context of viral infection of host cells, analysis of protein-protein interaction facilitates the identification of potential host cellular factors, leading to a better understanding of the mechanism of virus infection and thus progression of disease. Various techniques have been developed to systematically identify the host factors that underlie the various steps of the viral replicative processes and their functional role in virus replication. These include the genome-wide RNAi screens, proteomic profiling, gene expression microarrays and yeast two-hybrid (Y2H) screens. The Y2H assay in particular, is a powerful tool which has produced substantial quantities of interaction data in several model organisms (Li 2004; Giot et al. 2003; Uetz et al. 2000).

With regard to protein-protein interaction in virus infection of human cells, a large number of host proteins associated with virus infections have been identified by Y2H screens (Watanabe et al. 2010; Zhang et al. 2009). For example, the most extensively studied interactomes are those of the human immunodeficiency virus (HIV) and human, identified 8,024 protein-protein interactions in which 743 are unique human targets (Dyer et al. 2008). Identification of these interactors has elucidated various pathways known to be important in HIV. In contrast, the number of established DENV Y2H screens are very limited, in which only four studies have been reported (Mairiang et al. 2013; Silva et al. 2013; Khadka et al. 2011; Le Breton et al. 2011). The overlap between these protein datasets is relatively small with only a few proteins that have been functionally validated. Given this data constraint, additional Y2H screens are required in order to fill in the gaps of the DENV-human protein-protein interaction network. With these interaction data, the previously identified interactions can be supported with a higher confidence level and this can also increase the identification of potential new host factors.

The Y2H screen performed by Khadka et al. (2011) reported at least 105 human host proteins interacting with DENV-2 proteins, where the proteins identified were enriched in complement activation and coagulation cascade, centrosome and cytoskeleton. DENV have been reported interacting with six of the identified human proteins, and knockdown of these proteins has caused a significant decrease in DENV replicon replication (Khadka et al. 2011). These proteins include the calreticulin (CALR), DEAD (Asp-Glu-Ala-Asp) box polypeptide 3 X-linked (DDX3X), ELKS/RAB6-interacting/CAST family member 1 (ERC1), golgin subfamily a, 2 (GOLGA2) (GOLGA2), thyroid receptor-interacting protein 11 (TRIP11) and ubiquitin-conjugating enzyme E2I (UBE2I). CALR in particular, may have a potential role in DENV RNA synthesis as the protein has been shown to co-localize with the viral NS3 and NS5 proteins, as well as the viral dsRNA in DENV-infected cells. Additionally, 45 other human proteins that were shown to bind DENV proteins have been found associated with other virus infections including Hepatitis C virus (HCV), HIV and influenza virus (Khadka et al. 2011).

Due to the importance of NS1 during viral infection and its potential involvement in liver dysfunction (Chung et al. 2006), Silva et al. (2013) conducted a search for DENV-2 NS1 interacting partners from a human liver cDNA library. The screen putatively identified 50 host proteins. Mostly these are plasma-secreted and classified as acute-phase proteins, including the complement component 1 (C1q), plasminogen, haptoglobin, hemopexin, a-2-HS-glycoprotein, retinol binding protein 4, transferrin, and C4. C1q in particular, would appear promising. It is suggested to play an important role in the human complement response. NS1 interaction is thought to be important in immune evasion during DENV infection (Silva et al. 2013). Further to this, Mairiang et al. (2013) have identified 35 host factors from a cDNA library of human peripheral blood leukocytes screened against DENV proteins, C, NS3 and NS5. Of these, six proteins have been found to be similar to the previous DENV interactions including HBB and RPL5; NFκBIA, NRBP1, GOLGB1 and RILPL2 (Khadka et al. 2011; Doolittle & Gomez 2011; Le Breton et al. 2011; Chua et al. 2004).

Accumulating evidence indicates that identification of host proteins interacting among viruses within a family or genus may provide insights into the common interactors shared within the group (Dolan et al. 2013; Krishnan et al. 2008). In a

search of host proteins interacting with either NS3 or NS5 of Flaviviruses, Le Breton et al. (2011) have identified 108 proteins. The majority of these proteins are involved in RNA binding, transcription regulation, vesicular transport and regulation of innate immune responses. Of these, five proteins have been found interacting with both NS3 and NS5, including CAMTA2, CEP250, SSB, ENO1, and FAM184A. Several other proteins were found to overlap with findings from previous RNAi studies (Sessions et al. 2009; Krishnan et al. 2008), while some are novel involving intracellular trafficking such as kinesin family member and centrosomal components. Although numerous DENV-human host factors have been identified by several large-scale screens, only a limited number of proteins have been validated. While there is also a marked difference between independent studies, this suggests the DENV-human protein interaction networks are still incomplete and require further elucidation.

Overall, Y2H has been used in many large-scale protein-protein interaction studies. This technique has several advantages and has been selected as a screening method in this study because it is robust, cost-effective, and allows analysis of the protein interaction *in vivo*. This technology is easily scalable and can be performed using an automated robotic system for high throughput screening (Brückner et al. 2009). In addition, Y2H allows the use of various prey protein libraries derived from various tissues or cell types, thus serves as a flexible screening tool. This facilitates the study of various organisms by simply generating the yeast constructs expressing the protein of interest. Such constructs can be transformed into a suitable yeast host strain with specific reporter gene and growth selection marker.

In this study, a systematic protein-protein interaction analysis between DENV NS proteins and the human MGC cDNA library was performed using Y2H technique (Section 2.4). The interactions were further validated using LUMIER assay in mammalian cells (Section 2.7.1).

3.2 **Objectives**

1. Generation of DENV bait constructs for Y2H experiments.

2. Identification of human host proteins interacting with DENV NS proteins.

3. Bioinformatic analysis of DENV-human protein-protein interaction network.

4. Validation of the human interactors using LUMIER assay.

3.3 Results

3.3.1 Generation of DENV bait constructs

3.3.1.1 Amplification of DENV genes

DENV bait constructs generated for Y2H comprised of full length and fragments of DENV non-structural genes. The gene fragments were generated by eliminating the viral transmembrane domains (TMDs). This was performed on the basis that TMDs are unlikely to be translocated into the yeast nucleus for transcription and translation of functional proteins (Brückner et al. 2009; von Mering et al. 2002), and therefore may cause false negatives in Y2H screen. Using the available TMD prediction software (Table 2.7), the TMDs of DENV protein were mapped on NS2A, NS2B, NS4A and NS4B, and the corresponding gene sequences were removed, resulting in 12 intra/extracellular gene fragments (Table 3.1, Figure 3.1). DENV NS1, NS3 and NS5 are cytoplasmic proteins, thus they do not contain TMDs. While there was no absolute requirement regarding elimination of the TMDs, the full length gene constructs were also generated for comparative analysis. In total, 19 bait constructs, representing 7 full length NS genes and 12 gene fragments were generated (Table 3.1, Figure 3.1).

In order to generate these constructs, DENV NS genes were PCR-amplified from DENV-2 NGC replicon, pDVRepGP2A (Section 2.4.2, Figure 2.1) using specific primers containing *att*B sites (Table 2.8, Table 2.9). This is followed by separation of the amplified PCR products on a 1.2% agarose gels (Figure 3.2a lanes 2-8, Figure 3.2b lanes 2-13). As described above, the full length gene constructs encoded for the complete full length DENV NS proteins, while the fragment constructs encoded the viral protein fragments (without the TMDs).

Table 3.1: List of DENV bait gene constructs used in this study.

DENV bait	Description of gene	Size of insert (bp)
NS1	Full-length	1056
NS2A	Full-length	654
NS2A1F	Fragment	87
NS2A58F	Fragment	249
NS2A187F	Fragment	96
NS2B	Full-length	390
NS2B1F	Fragment	75
NS2B49F	Fragment	141
NS3	Full-length	1854
NS4A	Full-length	450
NS4A1F	Fragment	147
NS4A122F	Fragment	87
NS4A101F	Fragment	87
NS4B	Full-length	744
NS4B1F	Fragment	96
NS4B58F	Fragment	132
NS4B129F	Fragment	108
NS4B191F	Fragment	174
NS5	Full-length	2700

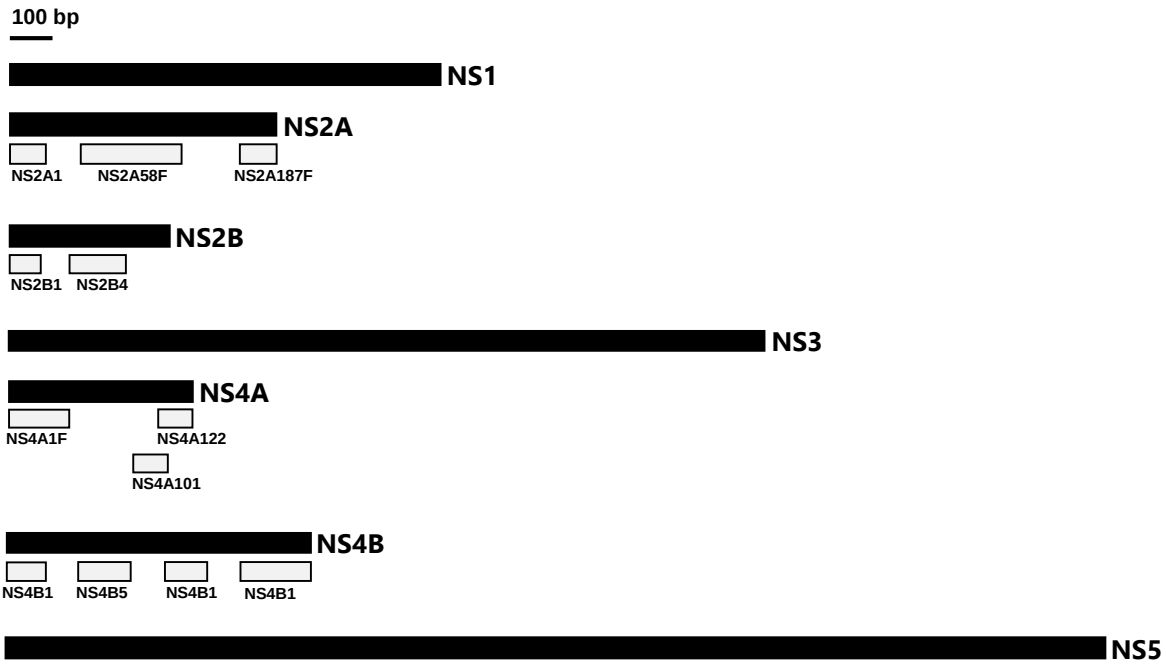

Figure 3.1: A schematic diagram of the DENV gene constructs.

Full length genes are shown in black and the gene fragments of NS2A, NS2B, NS4A and NS4B are indicated in gray. Scale denotes the size of the genes in basepairs.

(a)

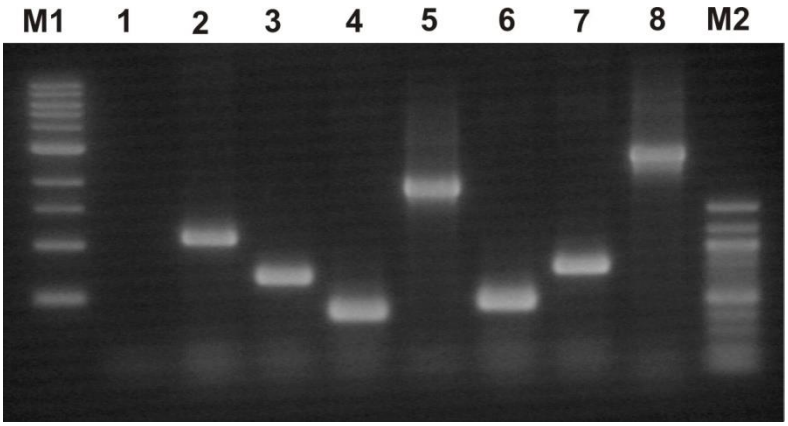

(b)

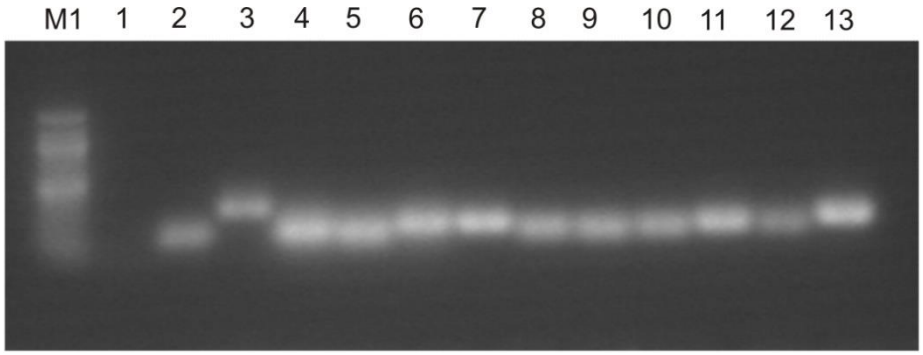

Figure 3.2: Amplification of DENV genes.

(a) Full length genes and (b) Gene fragments of DENV. Lanes 1 in both gels are water negative control. (a) Lanes 2-8 are NS1 (1056 bp), NS2A (654 bp), NS2B (390 bp), NS3 (1854 bp), NS4A (450 bp), NS4B (744 bp) and NS5 (2701 bp), respectively. (b) Lanes 2-13 are DENV fragments NS2A1F (87 bp), NS2A58F (249 bp), NS2A187F (96 bp), NS2B1F (75 bp), NS2B49F (141 bp), NS4A1F (147 bp), NS4A122F (87 bp), NS4A101F (87 bp), NS4B1F (96 bp), NS4B58F (132 bp), NS4B129F (108 bp) and NS4B191F (174 bp), respectively. Both lanes 1 in (a) and (b) are water negative control. Both lanes M1 and M2 are 1 kb DNA ladder (NEB) and 100 bp DNA ladder (NEB), respectively.

3.3.1.2 Cloning of DENV genes

Amplified products were sequence-verified and sub-cloned into a donor vector, pDONR207, according to the protocols described in the Gateway cloning (Section 2.4.4). The resulting DENV genes in the entry clones were then transferred into the yeast destination vector pGBKT7 to allow expression of the NS proteins. These proteins were fused to the yeast GAL4 DNA-binding domain and tagged with a c-Myc epitope at the N-terminus. While cloning of the full length DENV genes was done in independent BP and LR reactions, the smaller gene fragments were cloned in a combined single tube BP/LR reaction (Section 2.4.4.4) which was simpler, cost-effective and time-saving. To verify the clones, each construct was double-digested with *Eco*RI and *Bam*HI and sequence-verified (Figure 3.3a, lanes 2-8 and Figure 3.3b, lanes 2-13).

(a)

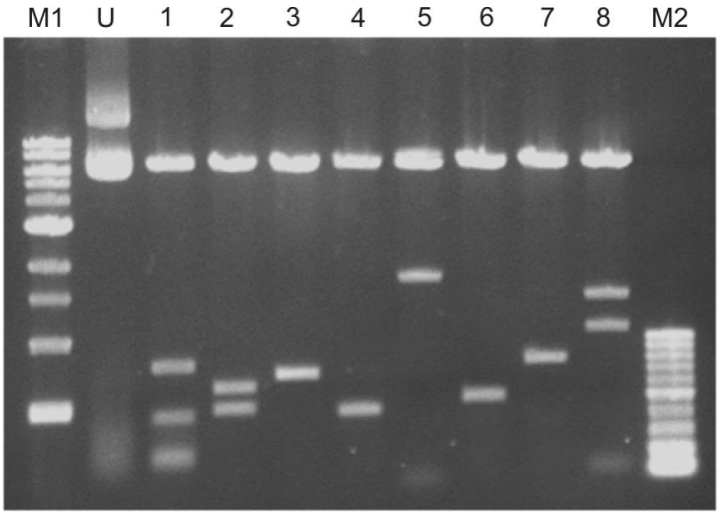

(b)

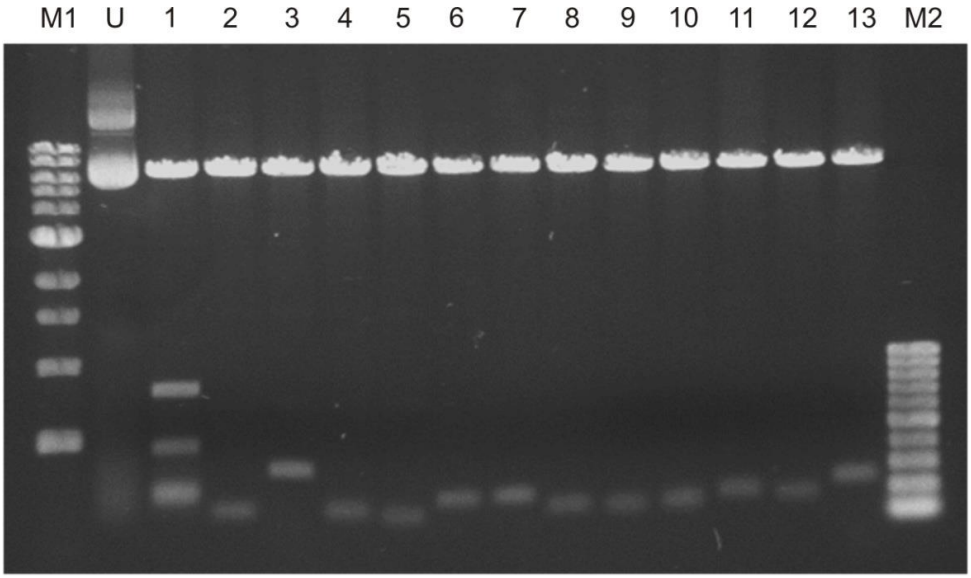

Figure 3.3: Enzymatic digestion of DENV bait constructs.

Digestion of DENV constructs using EcoRI and BamHI. (a) DENV full length gene constructs; NS1, NS2A, NS2B, NS3, NS4A, NS4B and NS5 (Lanes 2-8). (b) DENV gene fragments constructs; NS2A1F, NS2A58F, NS2A187F, NS2B1F, NS2B49F, NS4A1F, NS4A122F, NS4A101F, NS4B1F, NS4B58F, NS4B129F, NS4B191F (Lanes 2-13). Both U and 1 lanes, in each gel are undigested and digested empty pGBKT7 vector, respectively. Both lanes M1 and M2 are 1 kb DNA ladder (NEB) and 100 bp DNA ladder (NEB), respectively.

3.3.2 Yeast two-hybrid screen

In order to identify the human proteins targeted by DENV, the 19 DENV baits were screened against the human Mammalian Gene Collection (MGC) prey library. In brief, the bait constructs expressing DENV NS proteins were transformed into the haploid yeast strain AH109 (mating type a) and mated with the human cDNA library transformed into the haploid yeast strain Y187 expressing the prey. For each pairwise interaction, the two yeast haploids of the opposite mating types were allowed to mate by mixing the cultures together and the resulting diploid colonies were selected on media lacking histidine, supplemented with the yeast growth inhibitor 3-AT. To identify the human proteins responsible for this interaction, the diploid yeast were subjected to gene amplification by colony-PCR using the primers targeting a region flanking the human cDNA insert of the prey vector.

As the Y2H employs the GAL4 promoter and there is a chance of auto-activation during the screen. Auto-activation occurs despite the lack of interaction between the test proteins which wrongly activates the transcription of histidine reporter gene, and thus promotes the yeast growth on minimal media. To assay for auto-activation, all DENV baits were tested against the empty prey expressing GAL4 AD alone, and the prey library against the empty bait expressing GAL4 DBD alone. The interaction was tested by growth on drop-out media lacking amino acid histidine. From the assay, only one bait fragment (NS2A1F) resulted in an auto-activation activity, thus it was removed from further analysis (data not shown).

Analysis of the Y2H screen revealed 141 interactions between 94 human proteins and 16 of the 19 DENV baits as shown in the protein interaction map (Figure 3.4a). A complete list of the identified human proteins and a brief description of their functions is shown in Appendix A. Only one of the bait fragments (NS2A1F) was omitted due to auto-activation (as mentioned above), while two fragments (NS2A58F and NS4B58F) produced very limited number of diploid colonies with very poor sequence data. Thus, information of the human interactors was unavailable for these proteins. It was also noted that only one protein (VPS28), was found to interact with NS1.

A number of human proteins interacted with more than one viral protein, as seen in previous interactomes (Khadka et al. 2011; de Chassey et al. 2008; Calderwood et al. 2007). By grouping of DENV bait fragments into their respective full length proteins, the results indicate 78 (83%) of the human proteins interacted with one virus protein, while 8 (8.5%) interacted with 2 viral proteins and 8 (8.5%) interacted with 3 or more virus proteins as shown in the protein interaction map (Figure 3.4b, Appendix A).

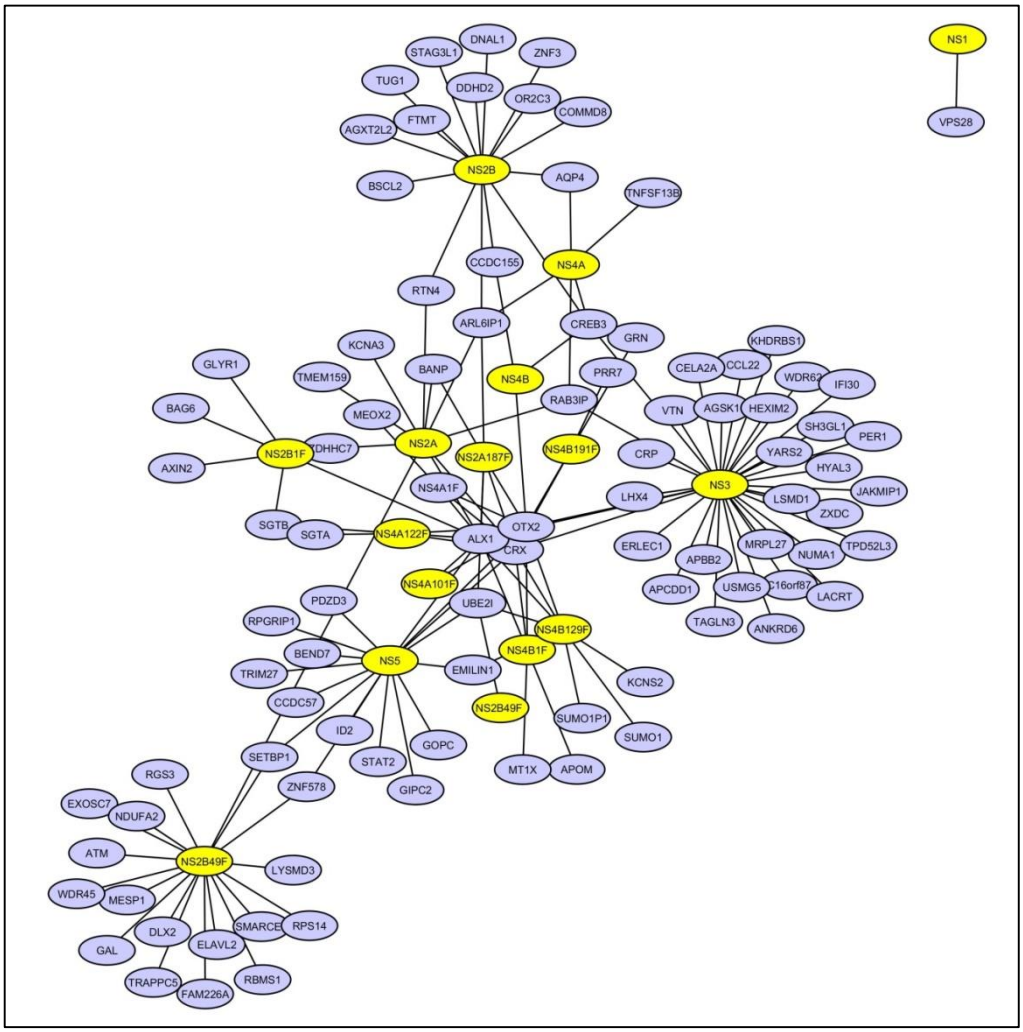

(a)

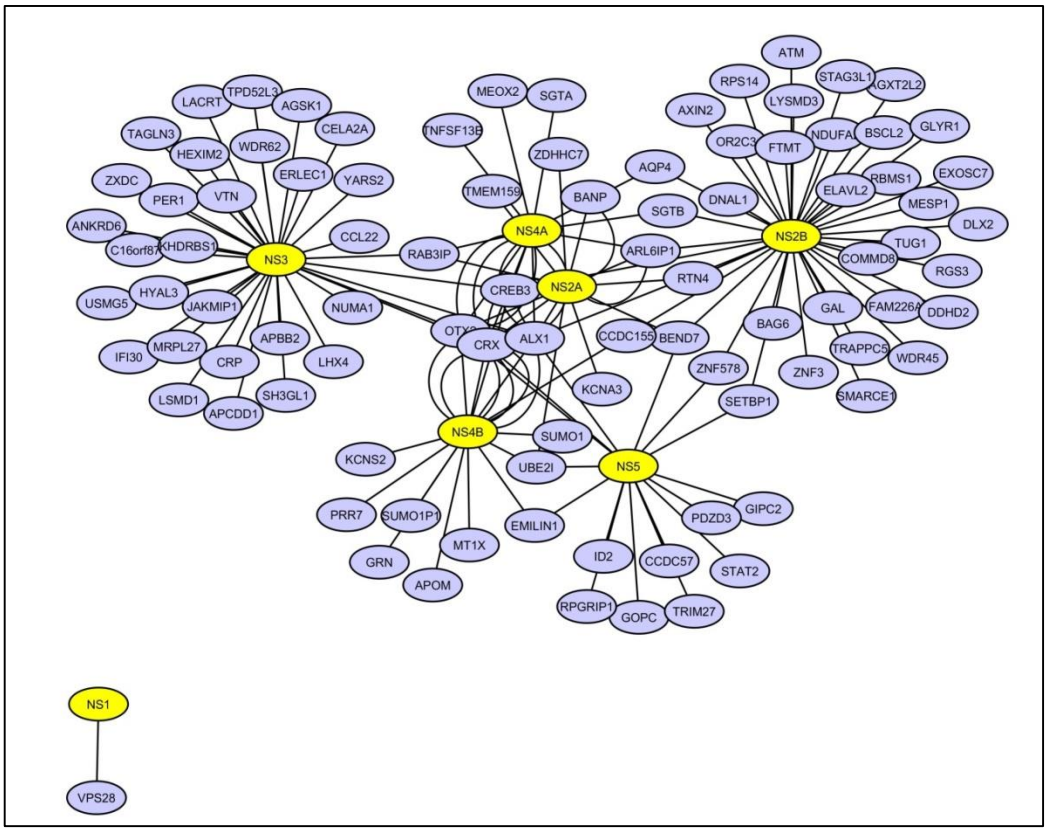

(b)

Figure 3.4: Graphical representation of the DENV-human protein-protein interaction network.

(a) This interaction map shows an interaction between DENV full length proteins or protein fragments and their corresponding human interactors. The DENV NS full length and proteins fragments are shown in yellow, whereas the human proteins are indicated in blue. (b) In this map, all protein fragments of DENV were grouped and displayed as their respective full length proteins on the same nodes. NS full length proteins are shown in yellow, whereas the human proteins are indicated in blue. All graphical assembly network and manipulations were performed on Cytoscape version 3.2.1.

Only four human proteins (4.3%) from this data set; STAT2, UBE2I, EMILIN1 and NUMA1 have been previously reported to specifically interact with DENV proteins, (Khadka et al. 2011; Le Breton et al. 2011) while two proteins (2.1%); GOPC and GRN have been reported to interact with other Flavivirus proteins (Le Breton et al. 2011) (Figure 3.5, Table 3.2). Interaction between STAT2 and NS5, and UBE2I with NS2B, NS4B and NS5, was in agreement to those observed by Khadka et al. (2011). It is noteworthy to detect STAT2 and NS5 interaction because STAT2 is a well-known NS5 targeted host cellular protein in the immune response pathway (Mazzon et al. 2009; Jones et al. 2005). This indicates that our methodology is validated.

Similarly, the ubiquitin-proteasome degradation pathway is an important pathway in DENV infection (Kanlaya et al. 2010a). Detection of the ubiquitin-conjugating enzyme UBE2I associated with more than one DENV NS protein in this study is not surprising. The protein has also been reported to interact with the viral envelope protein, E (Doolittle & Gomez 2011; Chiu et al. 2007). UBE2I interaction with multiple DENV proteins was also seen by Khadka et al. (2011) which signifies the importance of this protein in modulating many cellular processes. Silencing of this gene in particular, has been shown to reduce DENV replication (Khadka et al. 2011), and this is also true in WNV infection (Krishnan et al. 2008). UBE2I has also been detected in Influenza A (IAV) virus-host interactomes as well as in an Epstein-Barr virus (EBV) RNAi screen as shown in Table 3.3, indicating its significance in virus infection (de Chassey et al. 2013; Calderwood et al. 2007).

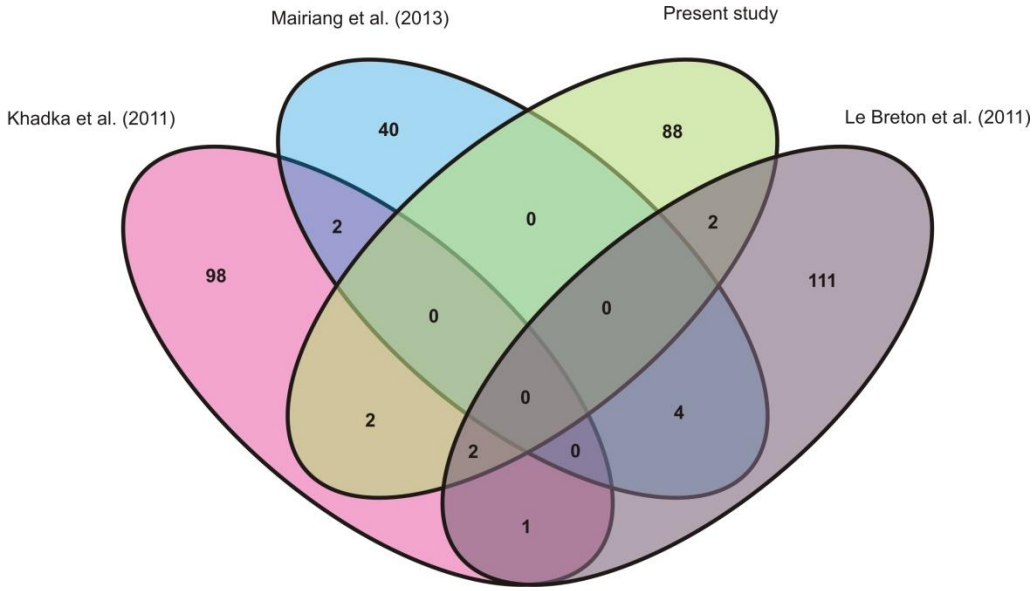

Figure 3.5: A Venn diagram representing the overlap DENV-human proteins.

Comparison between human proteins identified in the present study and the previous DENV/Flavivirus Y2H studies. DENV NS proteins in this study are shown in green, while the other three independent Y2H studies are performed by Khadka et al. (2011) (pink), Mairiang et al. (2013) (blue), and Le Breton et al. (2011) (gray). The overlap regions indicate similar proteins detected between the two or three screens. This diagram was generated using the SmartDraw software.

Table 3.2: List of the human proteins interacting with DENV or Flaviviruses.

DENV protein	Human protein	Gene ID	Description	Literature	Virus type	Virus protein	Method
NS5	STAT2	6773	Homo sapiens signal transducer and activator of transcription 2	(Khadka et al. 2011)	DENV-2	NS5	Y2H
				(Le Breton et al. 2011)	DENV-1	NS5	Y2H
NS2A, NS2B, NS4B, NS5	UBE2I	7329	Homo sapiens ubiquitin-conjugating enzyme E2I	(Khadka et al. 2011)	DENV-2	NS2B, NS4B, NS5	Y2H
				(Doolittle & Gomez 2011)	DENV-2	E	stuctural prediction
				(Krishnan et al. 2008)	DENV-2	whole virus	RNAi
NS4B, NS5	EMILIN1	11117	Homo sapiens elastin microfibril interfacer 1	(Khadka et al. 2011)	DENV-2	NS3	Y2H
				(Le Breton et al. 2011)	TBEV	NS5	Y2H
NS3	NUMA1	4926	Homo sapiens nuclear mitotic apparatus protein 1	(Khadka et al. 2011)	DENV-2	NS5	Y2H
NS5	GOPC	57120	Homo sapiens golgi-associated PDZ and coiled-coil motif	(Le Breton et al. 2011)	TBEV	NS5	Y2H
NS4B	GRN	2896	Homo sapiens granulin	(Le Breton et al. 2011)	ALKV, TBEV	NS5	Y2H
NS3	LACRT	90070	Homo sapiens lacritin	(Krishnan et al. 2008)	WNV	whole virus	RNAi

Table 3.3: List of the human proteins interacting with DENV or implicated in replication of other viruses.

DENV protein	Human protein	Description	Literature	Virus type	Virus protein	Method
NS5	STAT2	Homo sapiens signal transducer and activator of transcription 2	(Khadka et al. 2011)	DENV	NS5	Y2H
NS2A, NS2B, NS4B, NS5	UBE2I	Homo sapiens ubiquitin-conjugating enzyme E2I	(Khadka et al. 2011)	DENV	NS2B, NS4B, NS5	Y2H
			(Doolittle & Gomez 2011)	DENV	E	stuctural prediction
			(Krishnan et al. 2008)	WNV, DENV		RNAi
			(de Chassey et al. 2008)	IAV	NS1	Y2H
NS4B, NS5	EMILIN1	Homo sapiens elastin microfibril interfacer 1	(Khadka et al. 2011)	DENV	NS3	Y2H
			(Le Breton et al. 2011)	TBEV	NS5	Y2H
NS3	NUMA1	Homo sapiens nuclear mitotic apparatus protein 1	(Khadka et al. 2011)	DENV	NS5	Y2H
NS5	GOPC	Homo sapiens golgi-associated PDZ and coiled-coil motif	(Le Breton et al. 2011)	TBEV	NS5	Y2H
NS3	LACRT	Homo sapiens lacritin	(Krishnan et al. 2008)	WNV		RNAi

NS4B	GRN	Homo sapiens granulin	(Le Breton et al. 2011)	ALKV, TBEV	NS5	Y2H
			(Calderwood et al. 2007)	EBV		Y2H
			(de Chassey et al. 2008)	HCV	CORE	Y2H
			(Bouraï et al. 2012)	CHIKV	nsP2	Y2H
NS5	TRIM27	Homo sapiens tripartite motif containing 27	(Bouraï et al. 2012)	CHIKV	nsP2	Y2H
			(de Chassey et al. 2008)	IAV	NS1	Y2H
			(de Chassey et al. 2008)	HCV	NS2	Y2H
			(de Chassey et al. 2008)	HCV	NS3	Y2H
NS3	KHDRBS1	Homo sapiens KH domain containing, RNA binding, signal transduction associated 1	(de Chassey et al. 2008)	HCV	NS3	Y2H

While EMILIN1 and NUMA1 have been previously reported to specifically interact with DENV proteins (Khadka et al. 2011; Le Breton et al. 2011), these proteins were found interacting with a different DENV protein in this study. EMILIN1 interacts with DENV NS5, whereas NUMA1 with NS3 in this study, however Khadka et al. (2011) reported vice versa. While this is relatively predictable in the Y2H studies, and could be due to the interaction of host proteins with multiple DENV proteins (Dolan et al. 2013; Khadka et al. 2011), there is also a possibility of false-positive interactors. EMILIN1 is associated with elastic cell fibres and is expressed in lymphatic capillaries and is abundant in large blood vessels, lung, intestines and lymph nodes (Danussi et al. 2008; Bressan et al. 1993). NUMA1 plays an important role in organisation of mitotic spindles during cell division (Seo et al. 2014; Kotak et al. 2014). Although NUMA1 has not been reported to associate with DENV infection, the protein is prominent during virus-induced apoptosis (Taimen et al. 2004).

Aside from the additional testing required to confirm the interactions, literature curation from different experimental settings may also be useful to further support the findings. Le Breton et al. (2011) identified EMILIN1 and GOPC interacting with NS5 similar to this study, during TBEV infection. GOPC is associated with the host cellular Golgi apparatus and is expressed in all tissues, suggesting that it plays a housekeeping role and takes part in multiple functions such as in vesicular trafficking in secretory and endocytic pathways (Yao et al. 2001; Charest et al. 2001). This is interesting because processing of DENV occurs in the Golgi prior to production of new infectious virions (Kuhn et al. 2002), thus GOPC may have a potential role in viral maturation. In this study the human protein granulin, GRN interacted with DENV NS4B, however the protein was found interacting with NS5 in other Flavivirus infections (Le Breton et al. 2011). Although there is no study that has shown the association of GRN with DENV, this protein has been implicated in other virus interactions including Hepatitis C virus (HCV) and Chikungunya virus (CHIKV) (Bouraï et al. 2012; de Chassey et al. 2008). Of note, there was no overlap of the proteins identified in this study with those generated using the bacterial two-hybrid screen (Folly et al. 2011), neither with the host proteins interacting with DENV-2 NS1 identified by Silva et al. (2013).

Apart from EMILIN1, GOPC and GRN, three other human proteins; KHDRBS1, TRIM27 and LACRT, have been reported to associate with other viruses proteins. Similar to this study, KHDRBS1 (or the Src-associated substrate in mitosis of 68 kDa, Sam68) was found interacting with NS3, during a screen between HCV and human spleen and fetal brain cDNA libraries (de Chassey et al. 2008) however, its functional role in supporting HCV replication was unclear. This protein regulates alternative splicing by recognising specific RNA sequences in the cell nucleus (Matter et al. 2002). While alternative splicing can be regulated by host or viral proteins, this produces transcripts of different outcomes which are important during virus replication. For instance, herpesvirus has been shown to inhibit several host splicing factors, preventing the synthesis of antiviral proteins such as PML (Tavalai & Stamminger 2009; Nojima et al. 2009).

TRIM27 has been reported to be important for herpes simplex virus-1 (HSV-1) infection and known to target IkappaB kinases, thereby negatively regulating the pattern recognition receptor pathways (Conwell et al. 2015). This protein has been shown to interact with many different virus NS proteins (de Chassey et al. 2013; Bouraï et al. 2012; de Chassey et al. 2008) which suggests its potential role in viral infection, although additional testing is required for validation. LACRT has been identified as a host susceptibility factor in WNV infection by which silencing the gene reduced the viral infectivity (Krishnan et al. 2008). The protein however did not act in the same manner with regard to DENV as shown by Krishnan et al. (2008). Overall, although the mechanism of action of all the host proteins identified in this study with regard to DENV infection is not precisely known, their structural association with DENV or other viruses provides a strong basis for their possible involvement in the interaction, which requires validation by additional functional assays.

The human-DENV interactome obtained from this screen was further analysed for functional relationships between putative interactions using the Database for Annotation, Visualisation and Integrated Discovery (DAVID) ver. 6.7 (Huang et al. 2009). It was interesting to observe the DENV targeted human proteins are particularly enriched for components of the transcriptional process and negative regulation of transcriptional activity as shown in the Gene Ontology (GO) annotations (Table 3.4, Figure 3.6). This also includes down-regulation of cellular

biosynthetic processes of certain pathways (Table 3.4, Figure 3.6), which is in agreement with previous reports that down-regulation of processes may occur as a result of viral infection (Lee et al. 2013; Wang et al. 2012). The data also indicate the enrichment of the identified human proteins in cellular compartments including the ER membrane and intracellular organelle lumen. Identification of these proteins highlights their possible interaction or modulation during virus replication and assembly in the ER membranous compartments.

Table 3.4: Summary of the key functional description of enriched Gene Ontology terms.

The human proteins associated with the GO terms and the corresponding *P*-values are shown.

Functional description	*P*-value	Human proteins
Negative regulation of nucleobase-containing compound, transcription and cellular biosynthetic process	0.000033352	KHDRBS1, DLX2, SUMO1, ID2, HEXIM2, SMARCE1, RPS14, TRIM27, PER1, UBE2I, PDZD3, ALX1
DNA-binding region:Homeobox	0.00185233	DLX2, MEOX2, OTX2, LHX4, ALX1, CRX
Regulation of transcription and DNA-binding	0.002008	KHDRBS1, CREB3, OTX2, ZXDC, TRIM27, ELAVL2, BANP, UBE2I, ZNF3, CRX, STAT2, DLX2, SUMO1, SMARCE1, MEOX2, HEXIM2, ID2, RPS14, LHX4, ZNF578, PER1, MESP1, APBB2, ALX1
Somitogenesis, regionalisation and development protein	0.01189356	DLX2, ID2, MEOX2, OTX2, BANP, AXIN2, MESP1, ZNF3, ALX1, ATM
PDZ/DHR/GLGF domain	0.03171946	RGS3, GOPC, GIPC2, PDZD3

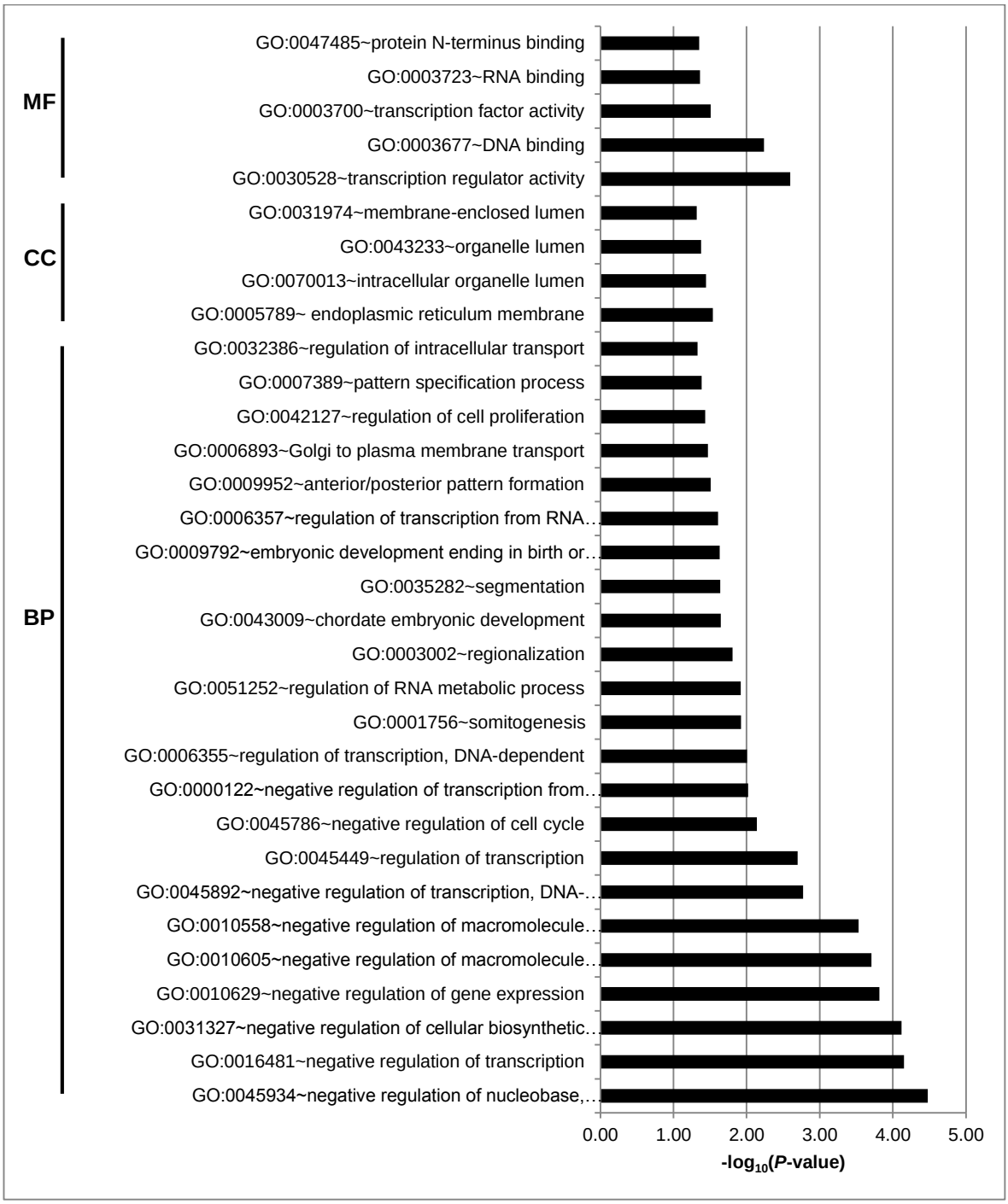

Figure 3.6: Enriched Gene Ontology annotation terms of the human proteins.

Data were analysed using DAVID Bioinformatics database. The graph displays -log10-transformed Benjamini-corrected P-values for each term. Analysis of the enrichment was set as the following, stringency = high, threshold of EASE score = 0.05 to obtain significant values. BP, MF and CC are biological process, molecular function and cellular compartment, respectively.

3.3.3 Confirmation of interactions

In order to validate the protein interaction in mammalian cells, LUMIER assays were performed. This assay uses luciferase-tags which are able to determine if two test proteins are interacting (Blasche & Koegl 2013) (as described in Section 2.7.1). HEK293 was the cell line used in this assay and for use in the downstream experiments because they are easily transfected, easy to grow and have been widely used as an excellent mammalian system for expression of recombinant proteins (Thomas & Smart 2005).

Data from the Y2H screen revealed 94 human proteins physically interacting with DENV NS proteins. Of these proteins, 15 were selected (Table 3.5), based on their potential involvement in virus infection. Aside from that, they were chosen considering the available tools in the lab to carry out the downstream experiments. cDNA clones expressing 15 of the 94 human proteins were obtained in pDONR223 (kindly provided by Juergen Hass, University of Edinburgh). The genes were cloned into the LUMIER vectors, pcDNA3-*RLuc*-GW and pTREX-dest30-Protein A as described in Section 2.7.1. Human proteins (tagged with *S. aureus* Protein A) and the corresponding DENV interacting partner (tagged with *RLuc*) were transiently co-expressed in HEK293 cells. Successful interaction between both test proteins formed a complex which then bound to the IgG-coated magnetic beads that have high binding affinity to the Protein A. This protein complex was separated from the non-interacting/unbound proteins by magnetic pull-down and the protein interaction was determined by the luciferase activity (as described in Section 2.6.3). Similarly, the interaction was also tested in the opposite orientation, in which the human proteins were tagged with *RLuc* and tested with DENV tagged with Protein A. This was expected to support the interaction data of the former pairwise orientation. A known protein interaction between JUN and FOS was used as positive control in this study. An interaction showing a z-score >1 was considered a weak interaction and >2 as a strong interaction.

Table 3.5: List of interactions tested by LUMIER assay.

A total of 15 human proteins were selected from Y2H data and tested for pairwise interaction with their corresponding DENV proteins. Interactions that occur with the protein fragments of DENV were also tested with the corresponding full length proteins.

Human protein	DENV protein
BANP	NS2A
KCNA3	NS2A
BANP	NS2A187F
UBE2I	NS2A187F
UBE2I	NS2A
UBE2I	NS2B
TRAPP	NS2B
JAKMIP1	NS3
IFI30	NS3
HEXIM2	NS3
TNFSF13B	NS4A
UBE2I	NS4B129F
KCNS2	NS4B129F
EMILIN1	NS4B129F
SUMO1	NS4B129F
PRR7	NS4B191F
UBE2I	NS4B
KCNS2	NS4B
EMILIN1	NS4B
SUMO1	NS4B
PRR7	NS4B
UBE2I	NS5
TRIM27	NS5
EMILIN1	NS5
STAT2	NS5

The first set of LUMIER experiments were performed to assess an interaction between the human proteins fused to Protein A, while the DENV NS proteins fused to *RLuc* reporter. At a z-score cut-off value >2, BANP, KCNA3, ARL6IP1, UBE2I, TRAPPC, HEXIM2, KCNS2, EMILIN1, PRR7 and TRIM27 were detected as strong interactors for DENV (Figure 3.7). However JAKMIP1 and IFI30 are weak interactors (z-score 1), and TNFSF13B has a z-score below 1 suggesting it does not interact with DENV NS proteins. It was interesting to observe that BANP interacted with both full length and truncated DENV NS2A and NS2A187F with strong z-scores. This suggests the potential association of BANP with NS2A and indicates the possible binding region of the interaction. Similarly, ARL6IP1 was also shown to interact with these proteins. Interaction between STAT2 and NS5 is well-established (Mazzon et al. 2009; Best et al. 2005), and was detected in our LUMIER assay. Human proteins interacting with DENV fragments, NS2A187F, NS4B129F and NS4B191F were also tested for interaction with the full length DENV proteins. In the majority of human proteins, interaction with the full length DENV proteins resulted in z-scores >1, indicating these interactions are well-supported. The interactions however, did not occur during Y2H screen which could be due to the TMDs that are present in the full length DENV proteins.

Further examination using the opposite orientation of the interacting proteins (human proteins fused to *RLuc* reporter, while the DENV NS proteins fused to the Protein A) however, was unable to give a significant interactions (Figure 3.8). Most interactions have z-scores <1 which indicates there was almost no interaction between the human and DENV proteins. Although JUN and FOS have shown to interact with a lower z-score, it was observed form this data set that the STAT2 and NS5 did not show an interaction. Thus, it was expected that there was a technical error with this set of experiments, which need further repetition. Nonetheless, interaction of human and DENV NS proteins using former orientation has shown promising results, which needs further validation by co-immunoprecipitation and co-localisation studies.

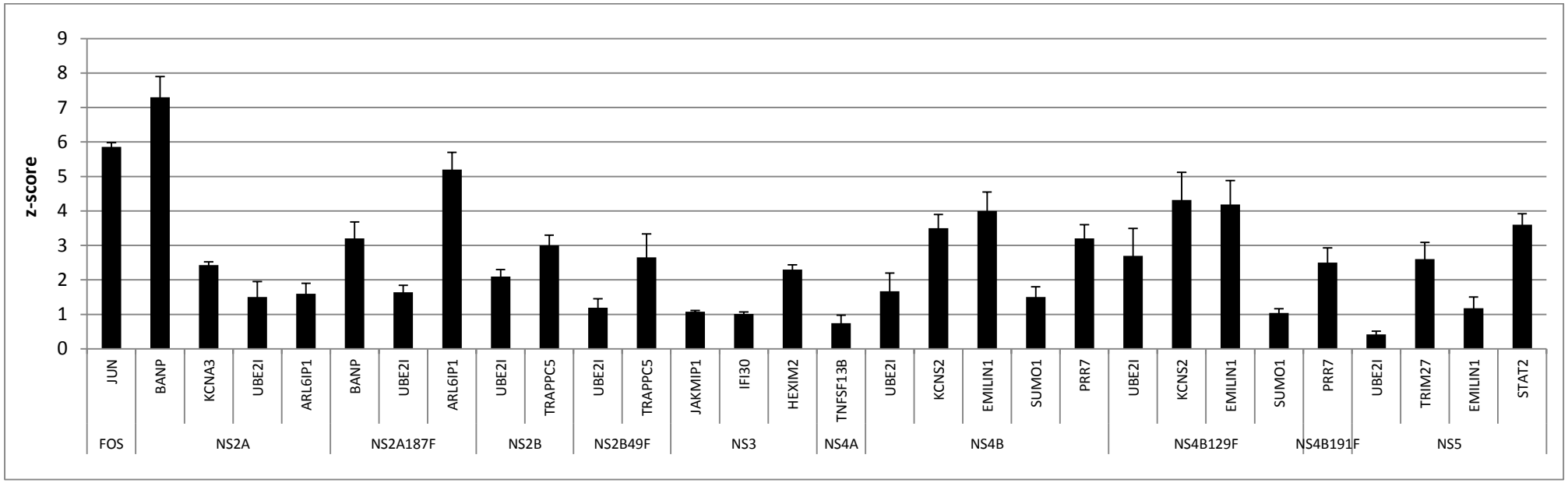

Figure 3.7: Interactions between Protein A-tagged human proteins and the *RLuc*-tagged DENV NS proteins by LUMIER assay.

Protein A-tagged human proteins and the *RLuc*-tagged DENV NS proteins were co-expressed in HEK293 cells and then pulled down by the IgG-coated magnetic beads. The cells were lysed and washed to remove unbound proteins. Luciferase activity was determined and the values were normalised to the negative control, Protein A. The bars indicate luciferase expression during an interaction between the human proteins and their DENV interacting partners (x-axis). Error bars represent a standard error of triplicates in three independent experiments. The z-zcores (y-axis) were calculated as described previously (Braun et al. 2009). A z-score cut-off value above 1 (one standard deviation higher than the mean) indicates the score is positive. Known interaction between the proto-oncogenes; c-FOS and c-JUN, were used as a positive control.

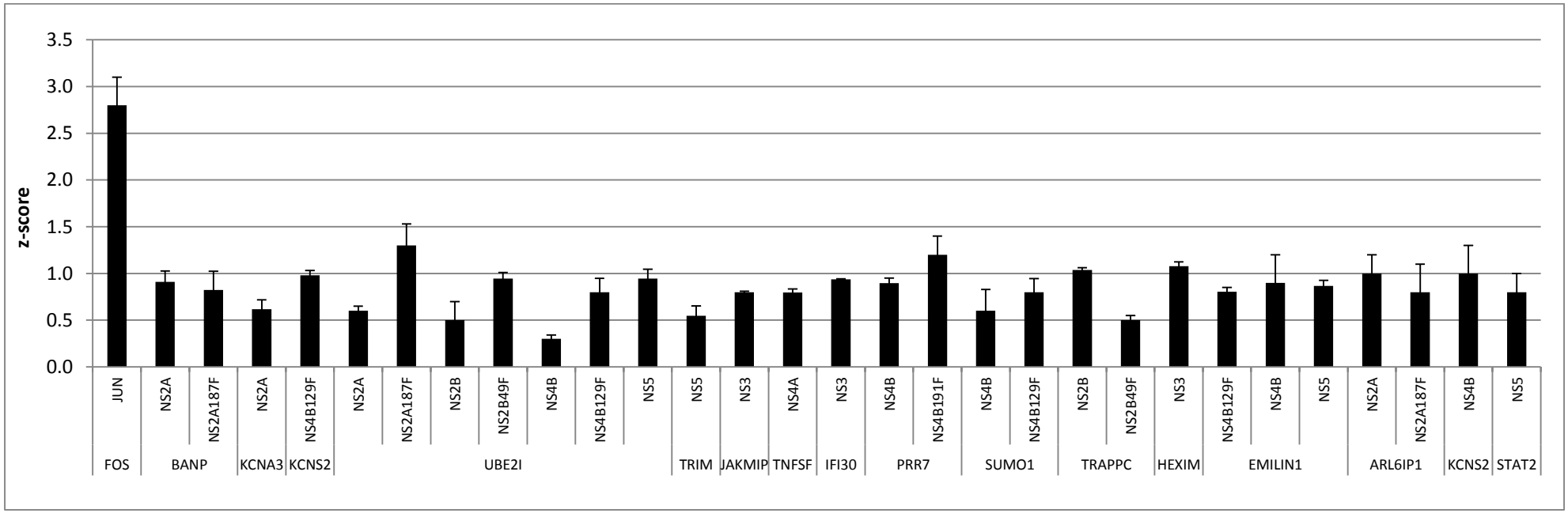

Figure 3.8: Interactions between *RLuc*-tagged human proteins and the Protein A-tagged DENV NS proteins by LUMIER assay.

RLuc-tagged human proteins and the Protein A-tagged DENV NS proteins using similar techniques as described above. Error bars represent a standard error of triplicates in three independent experiments. A z-score cut-off value above 1 (one standard deviation higher than the mean) indicates the score is positive. Known interaction between the proto-oncogenes; c-FOS and c-JUN, were used as a positive control.

3.4 Discussion

DENV-2 is the predominant dengue virus serotype causing infection in humans (Gubler 1998). It is known that the viral structural proteins, E, M and C proteins, play an important role during initiation of virus infection however, the roles of the NS proteins are less well-defined (Mukhopadhyay et al. 2005). Due to the importance of this serotype and in order to gain a better understanding of the roles of DENV NS proteins, analysis of their interacting partners in humans was carried out using Y2H.

In order to screen for protein-protein interaction between DENV-2 and human cDNA library, the DENV-2 bait constructs were first generated using the Gateway cloning technology (Invitrogen). It is believed that baits containing TMDs are unlikely to be translocated into the cell nucleus, where their presence may lead to transcription of the reporter gene (Brückner et al. 2009; von Mering et al. 2002). Therefore, the gene segments encoding for DENV TMDs were eliminated from the constructs, leaving the truncated segments encoding the intra/extracellular domains. Although the resulting protein fragments may cause some non-specific interactions due to improper folding, this is expected to be minimal as the fragments are generated based on their predicted specific intracellular domain boundaries. Previous studies have shown the use of protein fragments or polypeptides in many Y2H experiments (Dolan et al. 2013; Calderwood et al. 2007). This includes the shortest, 31 amino acids of DENV NS2A which were found interacting with 25 human proteins (Khadka et al. 2011). The use of well-defined smaller fragments may facilitate protein binding by making the polypeptides more accessible to interaction. Furthermore, the use of full length genes along with their overlapping fragments provides an additional support for a specific interaction which increases its confidence level.

At least four studies have been reported in which DENV-human interactions characterised by Y2H provided reliable data, hence these have been used as a comparison to this study (Mairiang et al. 2013; Silva et al. 2013; Khadka et al. 2011; Le Breton et al. 2011). Khadka et al. (2011) reported 105 human host proteins enriched in complement activation and coagulation cascade by which six have been previously reported interacting with DENV. The functional role of certain proteins, including STAT2 and ubiquitin-conjugating enzyme UBE2I was

confirmed by gene silencing (Khadka et al. 2011). This is consistent with the present study which detected similar interactions validated by the LUMIER assay. Interaction between STAT2 and NS5 during flavivirus infection is well-established (Shi 2014). NS5 binds to STAT2 and blocks its phosphorylation, hence inhibiting the downstream stimulation of the host IFN response (Mazzon et al. 2009). The role of UBE2I protein is known to be involved in conjugation of the small ubiquitin-like modifier (SUMO) to substrate proteins for alteration of subcellular functions including localisation, degradation and DNA repair (Mao et al. 2000; Müller & Dejean 1999). Such events are important in virus infection, thus interaction of the virus proteins with UBE2I and SUMO components may create a favourable environment for virus replication and survival in the host cells. Of note, SUMO1 was also detected interacting with one of NS4B fragment in this study, however the protein showed a marginal interaction by LUMIER assay.

There are several limitations to this study such as the difficulties in assessing the reliability of each DENV-human protein interactions. This is due to the fact that the yeast cells are dissimilar to the human cells, which makes it difficult to evaluate the reliability of DENV-human protein interactions in this setting. For example, there is no post-translational modification of proteins in yeast which may generate false-positive interactions while other interactions might not take place. It is also possible that both N- and C-terminal tagging resulted from fusion with the GAL4 may have altered the protein folding. This could be resolved by assessing the protein-protein interaction through both orientation of fusion tags that indicate any possible binding. The uncertain protein expression level and distribution of the bait and prey proteins, the lack of other binding partners to stabilise an interaction or protein misfolding may also contribute to the false-negatives or missed interactions in the Y2H screen. Therefore, it is imperative that results derived from the screen are confirmed by additional experiments to support the findings. Aside from that, the presence of TMDs may interfere with the nuclear translocation of proteins for activation of transcription. This however, can be resolved through the generation of truncated proteins as carried out in this study.

To make the Y2H test more stringent and prevent false-positives, the yeast inhibitor 3-AT was used in this study. 3-AT acts by inhibiting the histidine biosynthetic enzyme imidazoleglycerolphosphate dehydratase, which prevents the histidine biosynthesis in yeast thus, inhibits the yeast growth. While Y2H employs a HIS3 reporter encoding this enzyme, the 3-AT growth inhibition effect can be counteracted only in the case of a successful Y2H interaction. The addition of 3-AT in the medium therefore reduces the number of false-positives by giving a higher stringency to protein interactions. Overall, the Y2H system allows identification of putative DENV-human factors which may reveal cellular interactions and this could be translated into larger biological functions.

The limited overlap between data from this study and other data sets may be partly because of the different sources of the prey cDNA library used. Khadka et al. (2011) screened an interaction between DENV and the human library derived from liver, however other libraries such as peripheral blood leucocytes and mixed liver, brain, spleen and bronchial epithelia, have also been used (Mairiang et al. 2013; Le Breton et al. 2011). This resulted in a different level of interaction because the cellular host libraries contained different gene enrichments. Moreover, the different experimental conditions applied in independent large-scale screens may cause low reproducibility (Friedel & Haas 2011). Thus it is imperative to validate the human host factors identified from various Y2H screens by additional functional assays.

Results obtained from the Y2H screen revealed 94 human proteins interacting with DENV NS proteins. Of these proteins, 15 proteins including BANP, KCNA3, ARL6IP1, UBE2I, TRAPPC, HEXIM2, KCNS2, EMILIN1, PRR7 and TRIM27 have shown to be DENV interacting partners. This indicates the potential involvement of these proteins in viral infections, although further validation by functional tests is required. The importance of the remaining proteins in association with virus infection is unknown. However their specific roles such as vesicular transport from ER to Golgi (TRAPPC5), or in mediating DNA damage and repair (ATM) may imply their essential involvement in maintaining cellular conditions in response to viral infections.

Although little is known about human BANP, its mouse homolog SMAR1 (95% gene homology), has been reported to suppress NF-κB transactivation (Singh et al. 2009) in human cells. SMAR1 binds to the matrix attachment regions, and is able to form a complex with p53 which negatively regulates p53 transcription, and functions as a tumour suppressor and cell cycle regulator (Singh et al. 2009). It has also been shown that SMAR1 is involved in histone complexes and chromatin remodelling (Sinha et al. 2012; Malonia et al. 2011). Due to the capacity of SMAR1 to modulate NF-κB immune signaling, it is therefore important to investigate if BANP acts in a similar fashion, and is involved in any stage of the virus infection in humans, particularly in association with DENV NS2A. It was also observed that two human proteins; KCNA3 and KCNS2, interacted with NS2A and NS4B129F, respectively. Both proteins are potassium voltage-gated channels, which are responsive to the voltage changes of cell membrane potential. Potassium channels play a crucial role in the activation and proliferation of leukocytes. It has been shown there is an interaction between human immunodeficiency virus glycoprotein subunit and the cytoplasmic C-terminus of a voltage-gated potassium channel that represses the channel activity and prevents the release of virus (Herrmann et al. 2010). During virus infection, potassium channels are phosphorylated and translocated to the cell membrane, therefore mediating an outward potassium current resulting in the induction of apoptosis (Redman et al. 2007). This apoptotic response however, has been shown to be inhibited by HCV infection (Mankouri et al. 2009).

CHAPTER 4: FUNCTIONAL ANALYSIS OF BANP PROTEIN IN DENGUE VIRUS INFECTION

4.1 Introduction

4.1.1 MAR elements

The nuclear matrix is an extensive fibrogranular network within a cell nucleus, which functions as a dynamic support or scaffold for nuclear components. It maintains architectural features of the nucleus, hence it is involved in various nuclear events such as transcription, recombination, repair and splicing. Chromatin fibres are folded into DNA loops or highly structured DNA domains by tethering to this nuclear matrix. Such attachment occurs at specific non-coding regions on genomic DNA, termed matrix attachment regions (MARs) (Gasser & Laemmli 1987). MARs, also known as scaffold associated regions (SARs) or scaffold/matrix attachment regions (S/MARs), are unique *cis*-regulatory elements found on eukaryotic genomes (Pienta et al., 1991). Such sequences are AT-rich (>70%), representing 0.6-1 kb and have recognition sites for topoisomerase II (Gasser & Laemmli 1987). Although certain sequence characteristics have been suggested for MARs, many are highly polymorphic (Wang et al. 2010). MARs are mostly located upstream of various transcriptional promoters and enhancers, therefore, they act as platforms for the assembly of basal transcriptional factors complex controlling gene expression (Girod & Mermod 2003; Pienta et al., 1991). Interestingly, a recent report also suggests a role of MAR elements in viral integration, replication and transcription affecting the host immune system (Chakraborty et al. 2014; Sreenath et al. 2010).

MAR elements have also been used as epigenetic regulators responsible for enhancing transgene expression (Kim et al. 2004; Petersen et al. 2002), and stable cell line development (Zahn-Zabal et al. 2001). Although the functional role of MAR elements in transgene expression is not well understood, several models have been proposed. Spiker & Thompson (1996) suggested that integration of MAR allows formation of a transcriptionally active independent domain into an existing inactive DNA domain which makes binding sites accessible to transcriptional factors. Other findings described the formation of nucleation sites for displacement of histones to reduce DNA supercoiling (Käs et al. 1993), formation of nucleation points for DNA unwinding (Bode et al. 1992) and stabilisation of the

chromosomal structure resulted from hyperacetylation of histones (Schlake et al. 1994). Taken together, these findings indicate the significant role of MAR elements in mediating the topology of functional chromatin domains.

4.1.2 MAR-binding proteins

Matrix attachment region-binding proteins (MARBPs) which bind to the MAR elements are mostly found as components of the nuclear matrix (Wang et al. 2010). Several MARBPs have been characterised, such as the special AT-rich-binding protein 1 (SATB1), B cell regulator of IgH transcription (Bright), cut-like protein x/CCAAT displacement protein (Cux/CDP) in humans, and MAR binding filament-like protein 1 (MFP1) in plants (Goebel et al. 2002; Zong et al. 2000; Alvarez et al. 2000; Gindullis 1999). Most MARBPs are present as co-repressor/co-activator complexes which are involved in gene regulation (Chattopadhyay & Pavithra 2007). They play diverse roles in regulation of chromatin structure, gene transcription and progression of cell cycle (Chattopadhyay & Pavithra 2007). This means that any changes in the regulation or levels of MARBPs may directly contribute to the change in gene expression.

4.1.3 BANP/SMAR1

BTG3-associated nuclear protein (BANP) is a human MARBP and was identified from a protein-protein interaction study (Birot et al. 2000). The protein is ubiquitous and is commonly expressed in various organs and may act as a transcription factor or suppressor protein (Birot et al. 2000). Although the functional role of BANP is presently unknown, its mouse homolog, scaffold/matrix-associated region-binding protein 1 (SMAR1) has been extensively studied (Malonia et al. 2011). SMAR1 is a MARBP, first identified in murine thymocytes and multiple transcript variants encoding different protein isoforms have been found for this gene (Chattopadhyay et al. 2000a). The protein shares significant homology with other MARBPs such as SATB1, Bright and Cux/CDP in the MAR binding domains. SMAR1 contains a nuclear localisation signal, arginine-serine rich motifs which serve as a protein interaction domain, and C-terminal DNA binding domain (Chattopadhyay et al. 2000a). In addition, SMAR1 also contains the BEN domain mediating protein-DNA and protein-protein interactions during organisation of chromatin.

SMAR1 is a tumour suppressor, in which ectopic expression of SMAR1 in mouse melanoma cells leads to growth arrest (Kaul et al. 2003). SMAR1 expression is down-regulated in later stages of breast cancer cells, but can be induced upon treatment with the chemotherapeutic drug doxorubicin (Singh et al. 2007). Interestingly, SMAR1 has been shown interacting with the p53 tumour suppressor, which accounts for stabilisation in the nucleus by promoting serine phosphorylation and displacement of the p53 negative regulator mouse double minute 2 homolog (MDM2) (Jalota et al. 2005). Due to its association with p53, SMAR1 is induced during DNA damage in a p53 dependent manner (Singh et al. 2007), and is involved in modulation of the cell cycle by regulating cyclin D1 (Kaul et al. 2003). In regulation of cyclin D1, SMAR1 interacts with histone deacetylase complex 1 (HDAC1), SIN3 and pocket retinoblastoma protein (p130 and p107) forming a multiprotein repressor complex which is recruited to MAR site on cyclin D1 promoter (Rampalli et al. 2005). This results in deacetylation of chromatin and inhibition of gene transcription.

Apart from its role in tumorigenesis and cell cycle, SMAR1 has been reported to be involved in regulation of NF-κB signalling pathway and apoptosis. Molecular mechanisms revealed that SMAR1 binds to the MAR element present in IκBα promoter, recruits the HDAC1 dependent complex, together with p65/p50 to the locus and thus inhibits its transcription (Singh et al. 2009). Overall, given the diverse roles of SMAR1 and its ability to modulate the function of several genes, SMAR1 is a potential target for development of therapy for cancer or immune diseases.

4.1.4 Relevance of study

In the previous chapter describing a Y2H screen of DENV-host interactions, a total of 94 human proteins were found interacting with DENV NS proteins. Literature curation of the available data regarding these proteins, including the known host-virus interactions, roles in virus infections as well as potential tools to determine the importance of these interactions, was carried out in order to narrow down the interactions that are to be analysed further. In particular, the protein BANP interacting with DENV NS2A, was among the proteins of particular interest. BANP interacts with the full length NS2A and its fragment (NS2A187F) which indicates the potential NS2A binding region involved in the interaction.

BANP was first identified from a yeast two-hybrid approach in a search for a BTG3 interacting partner (Birot et al. 2000). *BANP* gene is located on the 16q24 region of the human chromosome and encodes for 509 amino acids (~55.4 kDa) (Birot et al. 2000). Further analysis of the amino acid composition suggests BANP is most probably a transcription factor (Birot et al. 2000). The knowledge about functional roles of BANP is very limited at present, however, its mouse homolog SMAR1 has been extensively studied (Malonia et al. 2011), as described earlier in this chapter.

Recent evidence indicates that SMAR1 can recruit HDAC1 and bind to a conserved MAR within the long terminal repeats (LTRs) promoter of proviral HIV-1, resulting in inhibition of viral transcription (Sreenath et al. 2010). Other small tumour viruses such as human papillomavirus (HPV16), simian virus 40 (SV40), HBV and human T-cell leukemia virus type 1 (HTLV-1) are also capable of integrating into the chromosomes through MAR (Kulkarni et al. 2004; Shera et al. 2001). In HIV-1, MAR elements account for 92.5% of the genome integration sites and many of these MAR sites have been documented (Kulkarni et al. 2004). Further to this, SMAR1 has been shown to repress *E6* oncogene expression by inhibiting the recruitment of tumour promoting factor c-Fos to the E6 promoter in HPV18-infected HeLa cells (Chakraborty et al. 2014). Binding of SMAR1 and HDAC1 to the HPV-18 E6 promoter results in deacetylation of chromatin, thus transcriptional repression of *E6* (Chakraborty et al. 2014).

Although SMAR1 is a multi-functional protein, this chapter particularly focused on SMAR1 capability in regulating NF-κB signalling. A previous study has shown that SMAR1 is capable of down-regulating IκBα and inhibit the NF-κB signalling pathway (Singh et al. 2009). A proposed mechanism suggesting this event is shown in Figure 4.1 This process occurs through the over-expression of SMAR1 which recruits the HDAC1 repressor complex and binds to the MAR elements located upstream of the NF-κB binding sites on the IκBα promoter. As a result, IκBα transcription is repressed and p65/p50 of NF-κB subunits in the cytoplasm are released to the cell nucleus forming a p65/p50-SMAR1-HDAC1 repressor complex. This complex is subsequently recruited to the MAR binding site of NF-κB target genes which inhibits transactivation of NF-κB. In addition, SMAR1 has been shown to repress numerous NF-κB target genes containing MAR elements through a similar fashion in MRC-7 cells (Singh et al. 2009). A decrease in expression of these genes including *IL-8, IL-10, CASP8, IκBKB, MAP3K1, NFκB1* and *CCL2* have been shown during NF-κB-mediated IFN stimulation (Singh et al. 2009).

With regard to the BANP potential involvement in DENV infection, it is therefore interesting to investigate if BANP mediates or regulates the human IFN response or other signalling pathways that may affect DENV replication. This chapter thus focused on investigation of BANP functional properties based on prior knowledge of SMAR1 and its potential involvement in DENV replication.

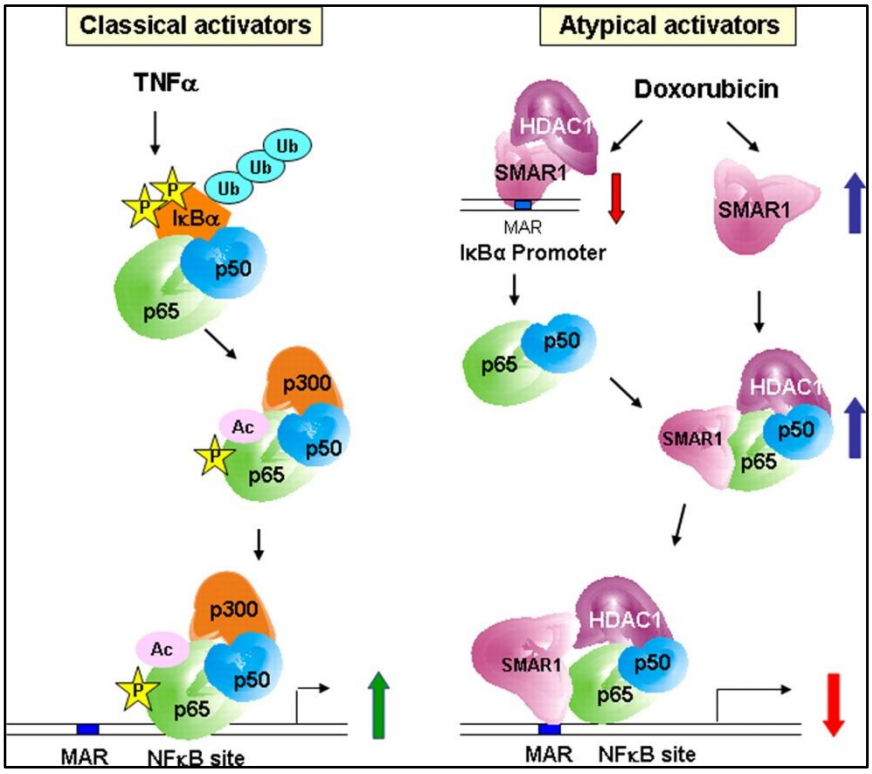

Figure 4.1: Regulation of NF-κB transactivation by SMAR1.

Left: In a classical NF-κB pathway, TNF-α mediates NF-κB activation through phosphorylation of IκBα by enzyme IκB kinase and subsequent ubiquitination (Ub), resulting in proteasome-mediated degradation. This allows nuclear translocation of p65/p50, which interacts with p300 co-activator and other proteins, leading to transcription of downstream IκB target genes. Right: In the atypical pathway, over-expression of SMAR1 (either by SMAR1 transfection or doxorubicin treatment) causes down-regulation of IκBα which subsequently allows translocation of p65/p50 NF-κB subunits into the cell nucleus. These subunits form an association with SMAR1-HDAC1 repressor complex and the complex is recruited to the MAR sites of κB target genes, resulting in repression of the NF-κB signalling pathway. The MAR site is shown in blue rectangles. Blue and red arrows indicate up-regulation and down-regulation of proteins, respectively. This figure was adapted from Singh et al. 2009.

4.2 Objectives

1. To confirm the interaction of BANP and NS2A.
2. To determine the cellular localisation of BANP and NS2A.
3. To determine the viability of cells during overexpression of BANP and NS2A.
4. To investigate the type I IFN-regulatory properties of BANP.
5. To analyse the effect and influence of BANP on DENV (replicon) replication.

4.3 Results

4.3.1 BANP amino acid sequences

There are seven variants of human BANP mRNA transcripts (namely transcript variant 1 to 7) documented on Genbank. These transcripts are translated into seven BANP isoforms, designated a to g, respectively. Aside from known amino acid sequence similarities (Figure 4.2), there is however a lack of knowledge describing functional capacity of each BANP isoform. The BANP identified as interacting with DENV NS2A belongs to the transcript variant 1 (isoform a) and has 81.3% sequence similarity with SMAR1. There are two stretches of BANP missing amino acids, position 131-169 (39 a.a) and position 443-484 (42 a.a) compared to SMAR1.

4.3.2 Confirmation of BANP-NS2A interaction

4.3.2.1 Construction and use of BANP expression construct

Previous results of the LUMIER assay showed a high luciferase activity following over-expression of Protein A-BANP and NS2A-*Rluc* indicating a strong interaction between the proteins (Section 3.3.3). The interaction was further validated in this study by a co-immunoprecipitation (co-IP)/pull-down assay. A BANP expression construct was initially generated using the Gateway cloning strategy (Section 2.4.4). The BANP ORF (1.4 kb) was cloned into the mammalian expression vector pDEST40 downstream of a CMV promoter and fused to a V5 epitope at the C-terminus. The resulting plasmid pDEST40-BANP was sequence-verified and used to transfect HEK293 cells for protein expression analysis. Results from Western blots detected the expression of BANP (~53-56 kDa) in the plasmid-transfected HEK293 cells and the presence of an endogenous BANP in the mock-transfected cells (Figure 4.3a). There were two bands in each sample indicating the BANP is present as isoforms, which is consistent with the previous study by Kaul et al. (2003). Given that BANP was fused to an epitope tag V5, the protein was also detected using anti-V5 antibody which was not seen in the mock-transfected cells (Figure 4.3b).

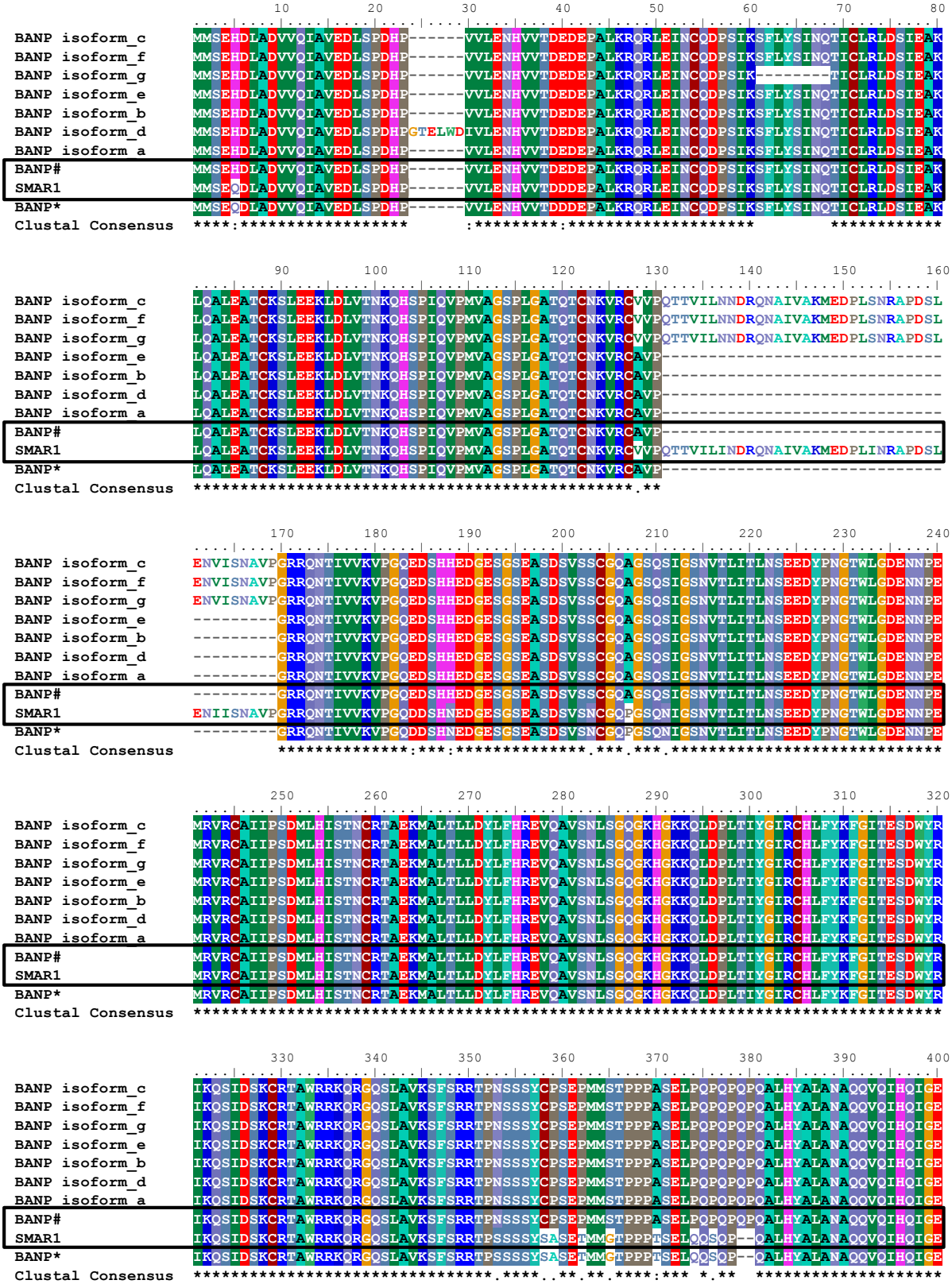
BANP isoform_c
BANP isoform_f
BANP isoform_g
BANP isoform_e
BANP isoform_b
BANP isoform_d
BANP isoform_a
BANP#
SMAR1
BANP*
Clustal Consensus

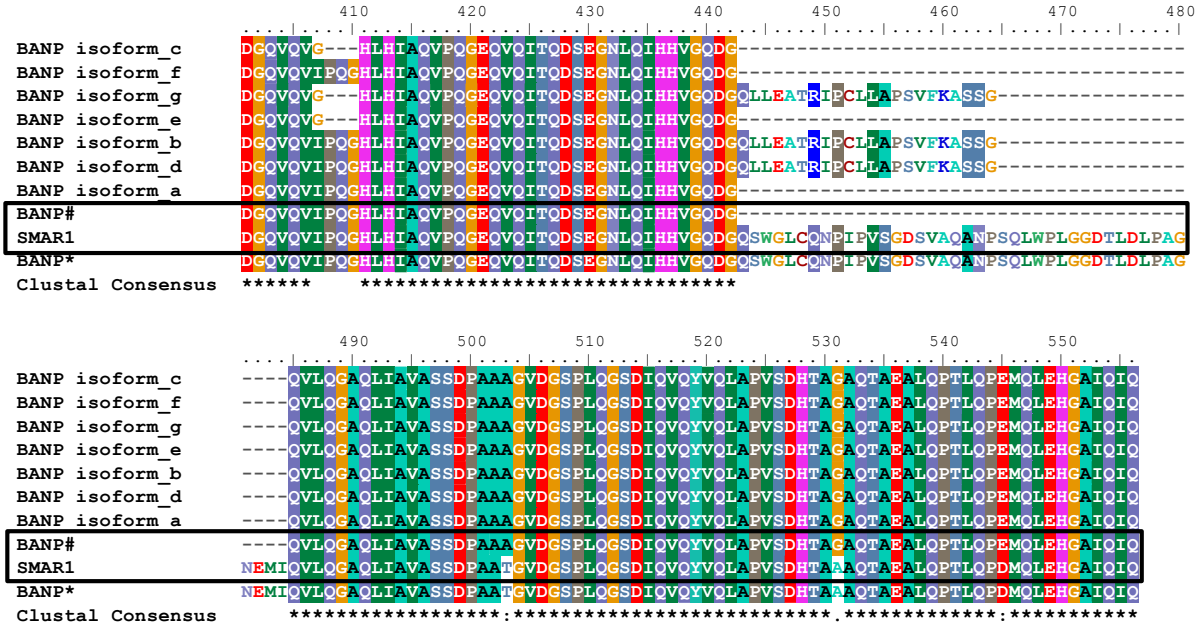

Figure 4.2: Sequence similarities of BANP isoforms and SMAR1.

Amino acid sequence alignment of BANP isoforms, a to g. Sequences derived from the Genbank and aligned using the ClustalX and BioEdit tools. Highlighted in rectangular boxes are sequence comparison between the human BANP in present study (BANP#) with the mouse SMAR1 from Chattopadhyay et al. 2000b. BANP* indicates sequences from Birot et al. 2000.

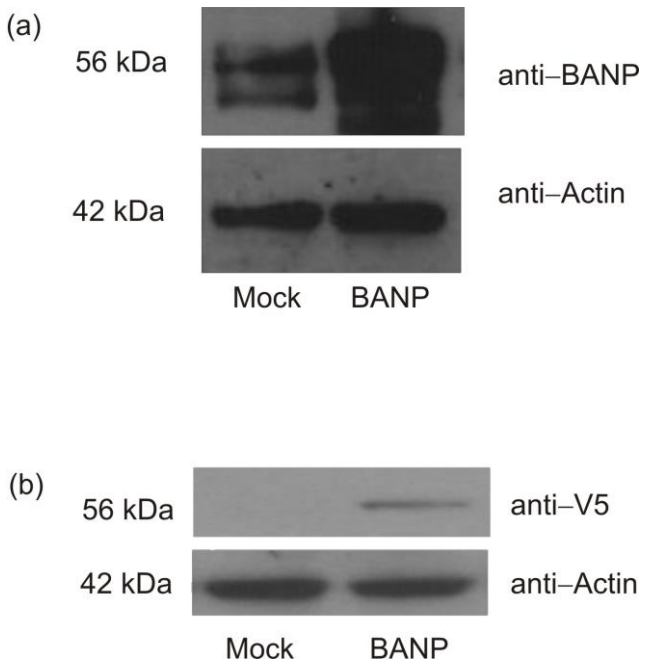

Figure 4.3: Over-expression of BANP and the endogenous BANP.

V5-tagged BANP was over-expressed in HEK293 cells and the proteins were detected by immunoblotting using (a) anti-BANP and (b) anti-V5 primary antibodies, followed by an anti-rabbit IgG conjugated with HRP. Actin was used as a loading control.

4.3.2.2 Co-immunoprecipitation of BANP and NS2A

In order to confirm the BANP and NS2A interaction in a mammalian system, pDEST40-BANP V5-tagged (from above) and the DENV NS2A construct (previously generated for LUMIER assays) pTREX-DEST30-Protein A-NS2A expressing Protein A-tagged NS2A were used for co-IP assays. In this assay, the IgG-coated magnetic beads have high affinity for Protein A which consequently pulls down NS2A. In brief, HEK293 cells were co-transfected with pTREX-DEST30-Protein A-NS2A and/or pDEST40-BANP. An empty pTREX-DEST30-Protein A expressing Protein A alone was used as a negative control. At 24 hr p.t, the proteins were harvested and pulled-down by incubation with IgG-coated magnetic beads. After several washing steps, proteins bound to the beads were eluted in SDS and analysed by Western blot. As shown in Figure 4.4(a) and Figure 4.4(b), overexpressed BANP was detected in the pull-down of NS2A co-expressed with BANP-V5 (lane 4). No endogenous BANP was detected in NS2A pull-down (lane 3); this is likely because its presence in the sample is insufficient to result in co-precipitation with the IgG-coated beads. In the absence of NS2A (lane 5), BANP did not react with Protein A which suggests its pull-down was only accomplished by the presence of NS2A. This data thus confirmed that physical interactions take place between BANP and NS2A.

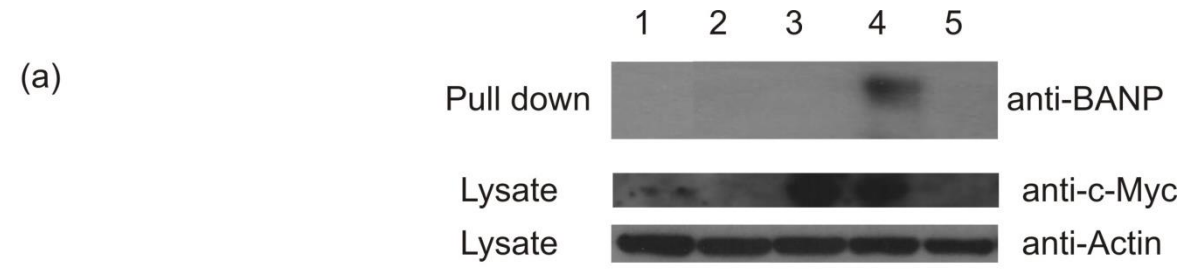

Empty pTREX-DEST30-ProteinA	-	+	-	-	+
pTREX-DEST30-ProteinA-NS2A	-	-	+	+	-
pDEST40-BANP	-	-	-	+	+

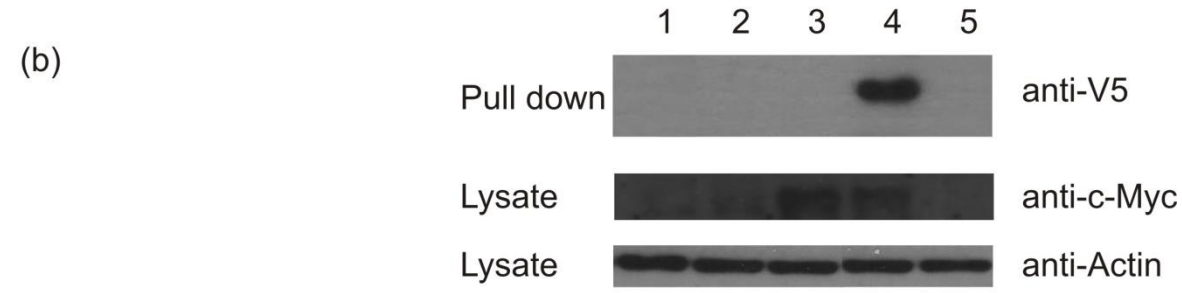

Empty pTREX-DEST30-ProteinA	-	+	-	-	+
pTREX-DEST30-ProteinA-NS2A	-	-	+	+	-
pDEST40-BANP	-	-	-	+	+

Figure 4.4: Validation of BANP and NS2A interaction by co-IP.

Proteins were harvested from transfected-cells and pulled down using IgG-coated magnetic beads. The bound proteins were subjected to immunoblotting and detected using (a) anti-BANP and (b) anti-V5 antibodies. The figure indicates pull-down protein samples from: mock (lane 1), Protein A alone (lane 2), Protein A-NS2A (lane 3), Protein A-NS2A and BANP-V5 (lane 4), Protein A and BANP-V5 (lane 5). Cell lysates probed with anti-c-Myc indicate the detection of NS2A. Actin was used as a loading control.

4.3.3 Localisation of BANP and NS2A

4.3.3.1 Expression of c-Myc-tagged NS2A

Initial experiments were carried out to test the DENV NS2A expression level and demonstrate its cellular co-localisation with BANP in HEK293 cells. The pcDNA-mycNS2A construct purchased from ShineGene Bio-Technologies, Inc. (Table 2.15) was used to express NS2A as a fusion with c-Myc epitope (N-EQKLISEEDL-C) at the N-terminus. From Western blot analysis, transiently transfected pcDNA-mycNS2A into HEK293 cells resulted in an expression of DENV NS2A, detected at 25 kDa using c-Myc antibody (Figure 4.5). The NS2A protein was expressed at a relatively low level and was detected using the hypersensitive chemiluminescent detection method (Section 2.3.5). pcDNA-EGFP expressing EGFP (constructed in-house) was used as a negative control for expression.

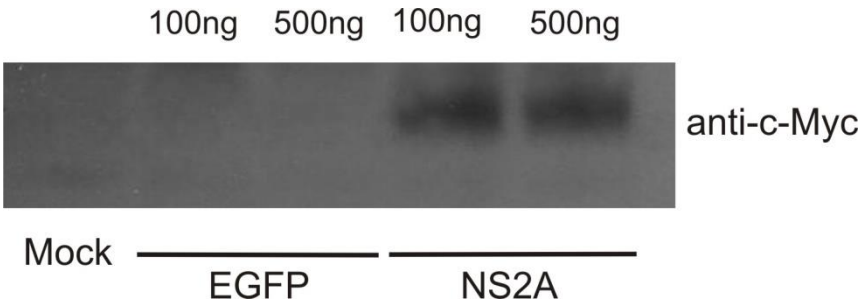

Figure 4.5: Expression of DENV NS2A in HEK293 cells.

The proteins were detected by immunoblotting using c-Myc antibody. pcDNA-mycNS2A and pcDNA-EGFP were individually transfected (100 ng, 500 ng) into HEK293 cells and the cells were lysed in NP-40 lysis buffer after 24 hr. The resulting proteins were subjected to immunoblotting and probed using c-Myc antibody, followed by an anti-mouse IgG conjugated HRP. pcDNA-EGFP was used as a negative control in this experiment.

4.3.3.2 Cellular localisation

In principal, two proteins can interact when both are located within the same cellular compartment. Although BANP and NS2A were successfully expressed in HEK293 cells (as seen in Section 4.3.2.1 for BANP and in the above Section for NS2A), it was important to know their sub-cellular localisation. This was studied by immunostaining using the protocols and primary antibodies as listed in Table 2.5 (Section 2.3.5). Transfected cells were fixed in 4% paraformaldehyde, probed with their corresponding antibodies and viewed with a confocal laser scanning microscope. Images were analysed using the ZEN software.

As shown in Figure 4.6a, endogenous BANP was found dispersed throughout the cell nucleus and cytoplasm. Overexpressed BANP was seen accumulated in the cell nucleus detected by the high signal intensity in the cell nucleus (Figure 4.6b), while a small amount of the protein was retained in the cytoplasm. This however is not surprising as BANP is nuclear-associated and therefore mainly localised in the cell nucleus (Jalota et al. 2005). In contrast, DENV NS2A was located exclusively in the cell cytoplasmic region (Figure 4.6c) which correlates with previous observations (Xie et al. 2013; Leung et al. 2008). In Figure 4.6d, it was noticeable that both endogenous BANP and NS2A are present in the cell cytoplasm. However, due to the narrow cytoplasmic region of HEK293 cells, their precise localisation within such limited space is difficult to be assessed. Additionally, NS2A remained in the cytoplasm during overexpression of BANP (Figure 4.6e), whereas most of BANP accumulates in the cell nucleus.

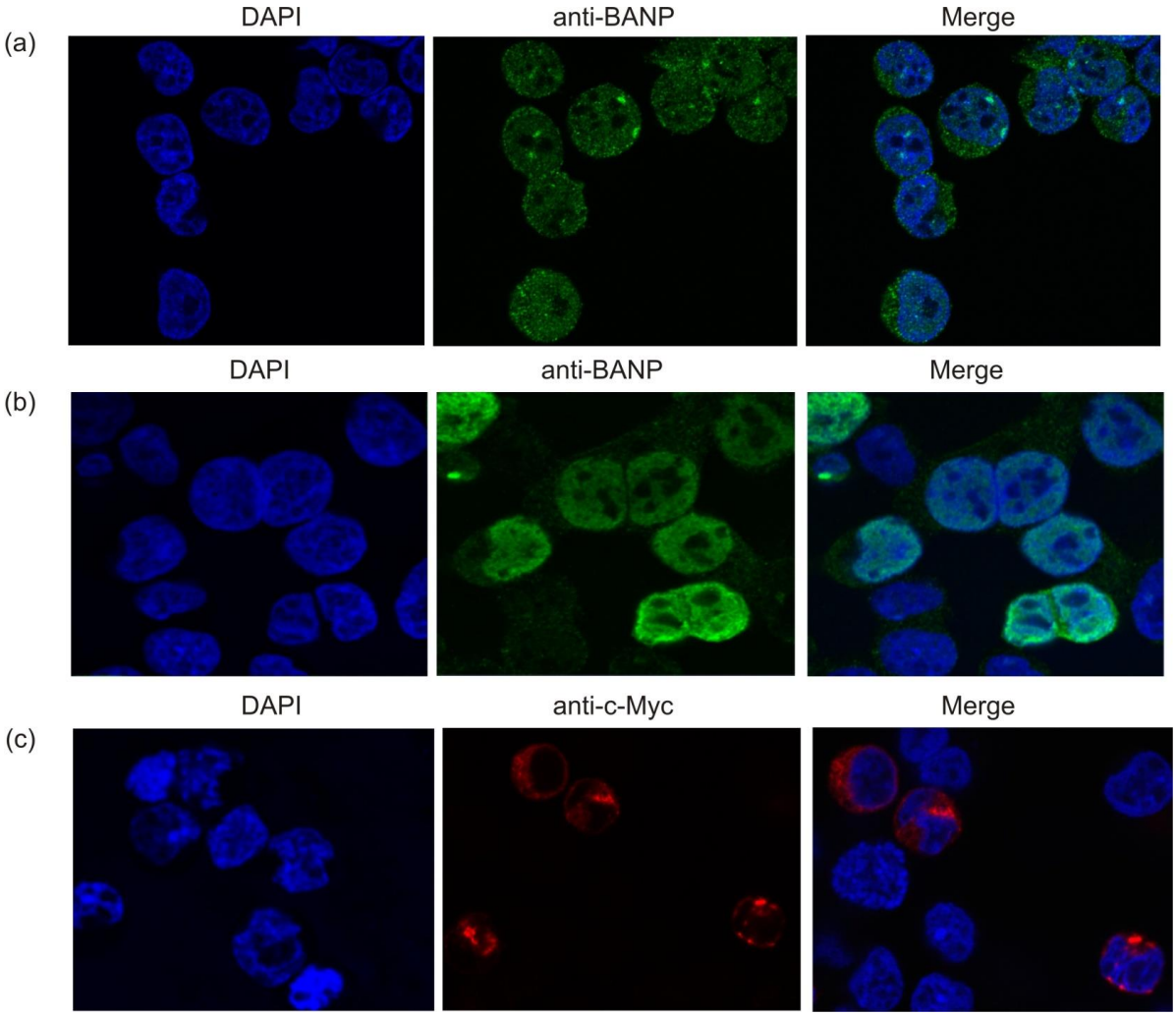
DAPI
anti-BANP
Merge
(a)
DAPI
anti-BANP
Merge
(b)
DAPI
anti-c-Myc
Merge
(c)

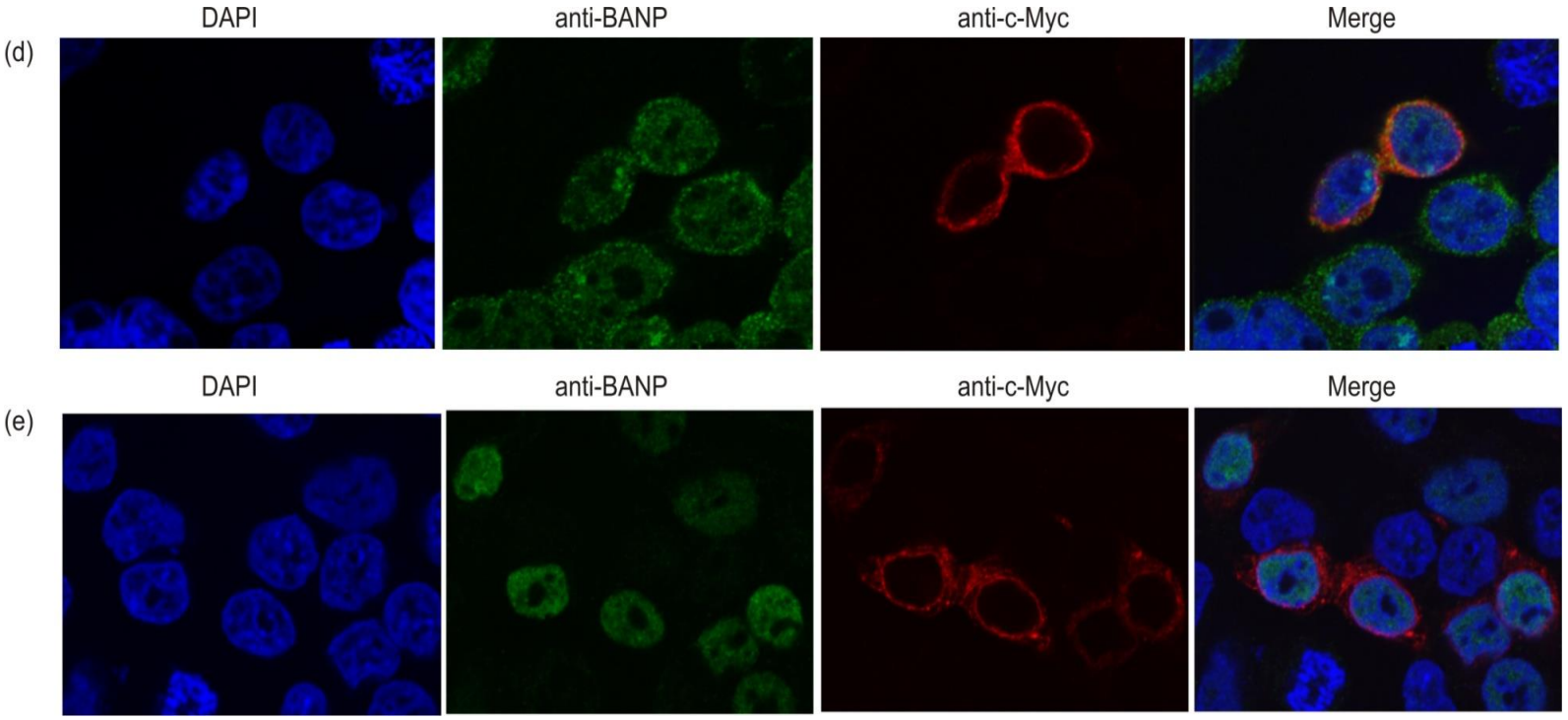

Figure 4.6: Cellular localisation of BANP and NS2A in HEK293 cells.

The cells were transfected and/or co-transfected with the following expression plasmids to examine the protein expression as follows: (a) endogenous BANP, (b) over-expressed BANP, (c) NS2A expression, (d) endogenous BANP during NS2A expression, and (e) co-expression of BANP and NS2A. The cells were fixed and stained with either anti-BANP or/and anti-c-Myc antibodies. Alexa Fluor® 488 anti-rabbit IgG (green) and Alexa Fluor® 594 anti-mouse IgG (red) were used to stain for BANP and NS2A, respectively. The cells were counterstained with DAPI to localise the nucleus.

4.3.4 Assessment of cell viability

It is important to determine the dose-response effect of BANP and NS2A on HEK293 cell viability. This ensures the over-expressed BANP and NS2A are not toxic to the cells which may affect the experimental outcome. This test was carried out using the CellTiter 96® Non-Radioactive Cell Proliferation Assay which measures the activity of NAD(P)H-dependent cellular oxidoreductase present in metabolically active cells. The enzyme reduces methyl-thiazolyl-tetrazolium (MTT) to its quantifiable formazan product (Mosmann 1983) which is directly proportional to the number of living cells (van Meerloo et al. 2011). Varying concentrations of pDEST40-BANP, pcDNA-mycNS2A or pDEST40-MBP (5 ng to 1 µg) were transiently transfected into the HEK293 cells followed by adding the tetrazolium solution at 24 hr p.t and incubated at 37 °C for 4 hr to allow cellular conversion of tetrazolium to formazan (Section 2.7.6). The reaction was halted by adding stop solution and the culture absorbance was recorded the next day. *E. coli* maltose-binding protein (MBP) was used as a positive control.

Results from the MTT assay (Figure 4.7) showed a concentration-dependent effect of BANP, NS2A and MBP expression on cell viability. Within the plasmid concentration range of 10-1000 ng/ ml, the expression of BANP resulted in at least 81% of the cells remaining viable, while 87% was observed with DENV NS2A. MBP expression revealed at least 80% of cell viability up to 250 ng/ ml of plasmid and subsequently reduced to 78% for higher plasmid concentration. This gives an overall number of viable cells: NS2A>BANP>MBP with all constructs and concentrations behaving very similar. While this data is useful to assess cell viability, it is a matter of considerable importance that all the cells remain above 80% viable at 100 ng/ ml plasmid concentration with the various constructs described here, as used in most experiments described herein.

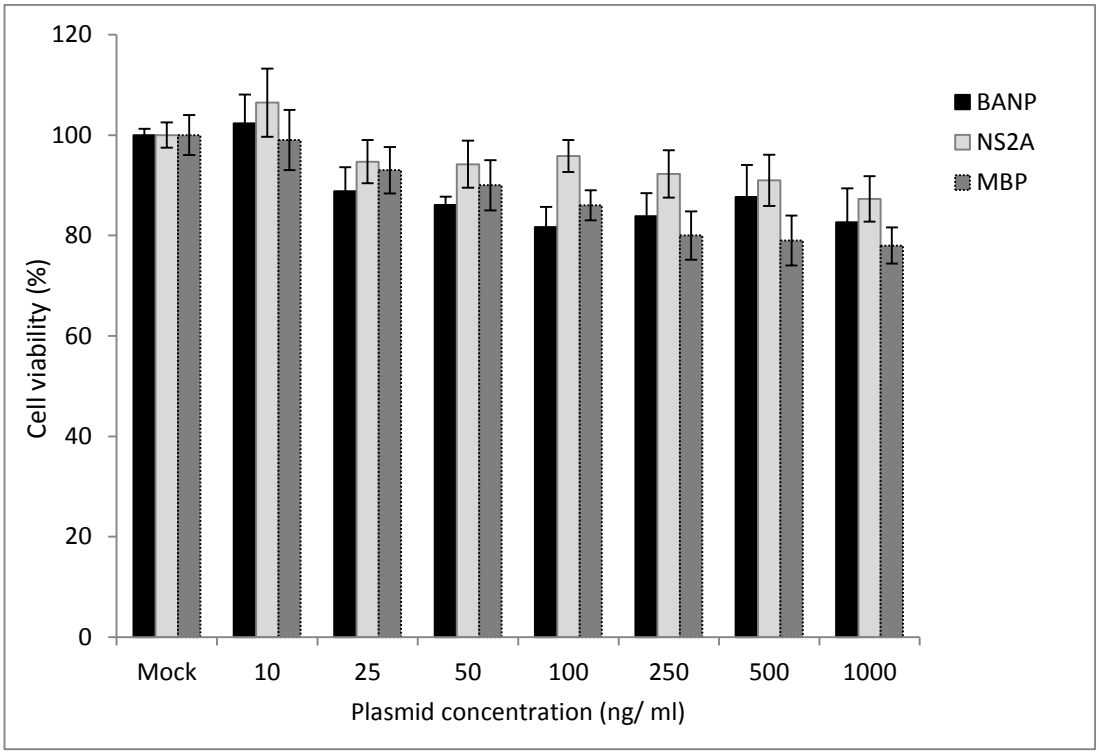

Figure 4.7: Effect of over-expressed BANP and NS2A on HEK293 cell viability.

This assay was carried out using the CellTiter 96® Non-Radioactive Cell Proliferation Assay (Promega) and the OD was measured at 570 nm using Glomax® Multi Detection System. The absorbance values of viable cells were calculated as a percentage relative to the mock (cells treated with Lipofectamine® 2000 CD alone). Data was expressed as the mean±standard deviation of triplicates from three independent experiments.

4.3.5 Effect of BANP on type I interferon response

The BANP mouse homolog, SMAR1, has been previously shown to inhibit NF-κB activation during its over-expression in cancer cell lines (Malonia et al. 2011). Due to the fact that BANP and SMAR1 has 81.3% amino acid sequence similarity (from our sequence data), initial experiments were carried out to investigate if human BANP caused a similar inhibitory effect on type I IFN signalling, which also depends on NF-κB (Yoneyama et al. 1998; Yoneyama et al. 1996).

4.3.5.1 Poly(I:C)-induced interferon responses

An initial experiment was performed to test the IFN production in HEK293 cells by stimulating with a synthetic dsRNA substrate, Poly(I:C). Poly(I:C) transfected into cells using a liposome-mediated procedure resembles intracellular dsRNA produced during viral infection and thus induces a strong type I IFN response (Matsumoto & Seya 2008; Kumar et al. 2006). In brief, HEK293 cells grown in 24-well plates were co-transfected with either p125Luc, a plasmid containing *FFLuc* expressed under the IFN-β promoter or p55A2Luc which contained repeated PRDII elements for NF-κB binding sites, and pRL-CMV a construct that constitutively expresses *Rluc* as an internal control (Section 2.7.5).

At 24 hr p.t of the plasmids, the cells were transfected with increasing concentrations of Poly(I:C) using Lipofectamine® 2000 CD and lysed 24 hr post-stimulation to determine the luciferase activity. Ratio of *FFLuc* values were calculated against the *RLuc* internal control and normalised to the mock-stimulated control. Treatment of HEK293 cells with Poly(I:C) resulted in an increase in *FFLuc* expression (Figure 4.8) which corresponded to the activation of the IFN-β promoter, in a concentration-dependent manner. The cells transfected with p125Luc were responsive to Poly(I:C) given as low as 0.1 µg/ ml concentration which resulted in an approximately 10-fold increase in *FFLuc* compared to the non-stimulated control. The production of IFN-β gradually increased to a maximum level (59-fold increase) at 5 µg/ ml, before decreasing thereafter. A similar trend of IFN induction was observed in cells transfected with p55A2Luc reporter construct upon Poly(I:C) stimulation. Although the overall luciferase signals were reduced compared to the cells transfected with p125Luc, results show an increase of IFN induction with increasing Poly(I:C). The maximum induction was

with 10 µg/ ml Poly(I:C) generating a 12-fold increase compared to the non-stimulated control. Similar observations have been made in different cell lines by others (Reimer et al. 2008; Zhang et al. 2012), thus indicating a successful IFN activation induced by Poly(I:C) in HEK293 cells.

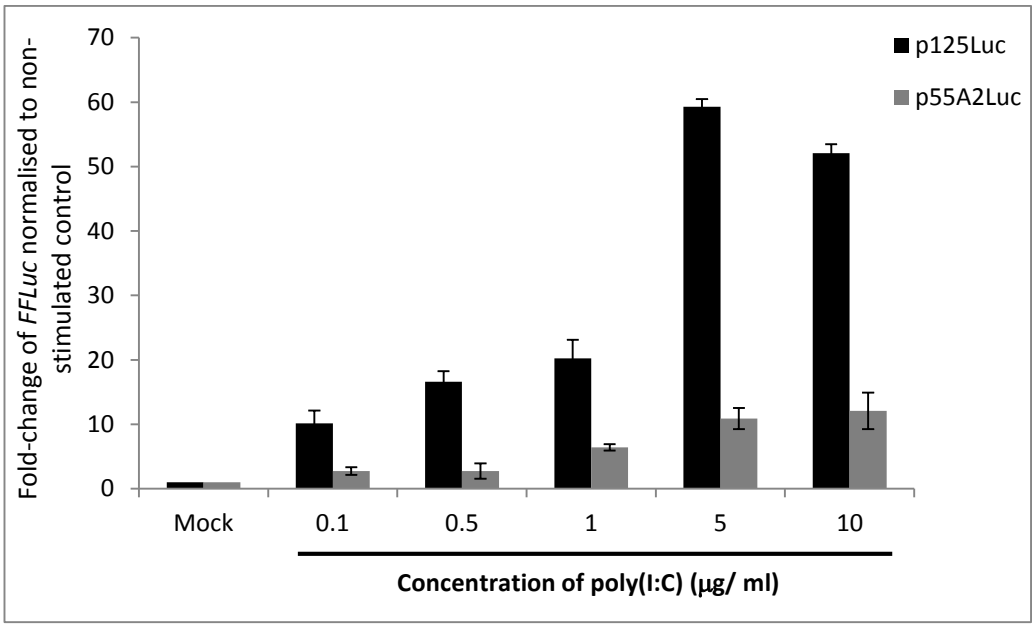

Figure 4.8: Poly(I:C)-induced interferon response in HEK293 cells.

Cells were co-transfected with either p125Luc (black bars) or p55A2Luc (gray bars), and pRL-CMV *RLuc* reporter (internal control) for 24 hr before transfection with increasing concentrations of Poly(I:C). The cells were lysed and luciferase activity was measured using the Dual-Luciferase Reporter Assay System. Ratio of IFN-β *FFLuc* was calculated against the *RLuc* internal control and normalised to the mock-stimulated negative control, which was cells treated with Lipofectamine® 2000 CD instead of Poly(I:C). Error bars indicate standard errors of triplicate wells from three independent experiments. Mock is Poly(I:C) non-stimulated cells.

4.3.5.2 BANP inhibits Poly(I:C)-induced IFN response

It is known from previous results that stimulation with Poly(I:C) in HEK293 cells was able to induce IFN-β. This effect was further analysed in cells expressing BANP. In brief, BANP or MBP were expressed in HEK293 cells transfected with either p125Luc IFN-β enhancer plasmid, or p55A2Luc containing repeated PRDII elements, and pRL-CMV *RLuc* reporter (as mentioned in the previous section). The total amount of transfected DNA was kept constant at 500 ng by adding empty vector backbone, pDEST40. This avoids concentration variables and prevents an IFN response resulting from unequal accumulation of plasmids. MBP served as a negative control to indicate a successful IFN stimulation. At 24 hr post-stimulation with 5 μg/ ml Poly(I:C), the cells were lysed and the luciferase activity was measured. The ratio of the over-expressed BANP *FFLuc* values were calculated against the *RLuc* internal control and normalised to MBP non-stimulated cells.

In Figure 4.9 (top panel), there was a decrease in *FFLuc* activity with increasing BANP expression. At least a 2.2-fold and 3.8-fold reduction of IFN induction was seen (relative to the stimulated MBP control) in cells transfected with 50 and 100 ng/ ml BANP plasmid, respectively (Student's *t*-test, *p*-values <0.05). A larger reduction, 5.3-fold and 6.4-fold was observed in 200 and 500 ng/ ml BANP plasmid, respectively (Student's *t*-test, *p*-values <0.05). A similar trend was also observed in cells transfected with p55A2Luc as shown in Figure 4.9 (bottom panel). The luciferase signals however, were significantly less. Overall, this indicates an inhibition of NF-κB response with increasing concentrations of BANP. It was also clear that there was a high level of IFN-β and NF-κB induction following stimulation with Poly(I:C) in MBP over-expressed samples (Figure 4.9, top and bottom panels). This indicates that MBP does not inhibit IFN and NF-κB responses, thus is a suitable negative control for inhibition. Overall, these findings show that overexpression of BANP leads to inhibition of IFN-β induction, which suggests BANP acts as an IFN-β negative regulator in stimulated HEK293 cells.

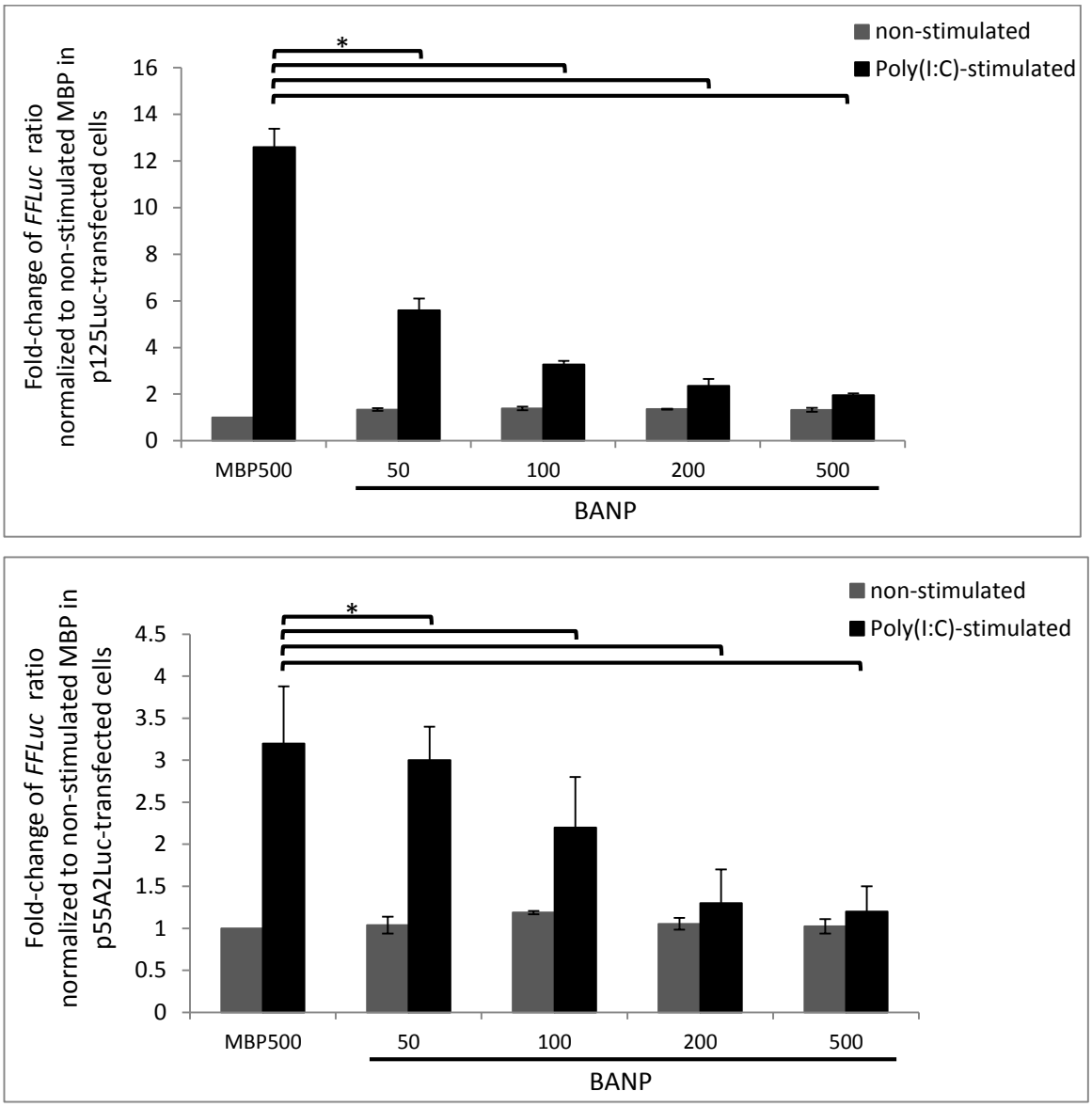

Figure 4.9: Overexpression of BANP inhibits IFN-β production.

Transfected HEK293 cells containing either p125Luc IFN-β promoter (top panel) or p55A2Luc PRDII elements (bottom panel), with increasing concentrations of BANP were stimulated with 5 µg/ ml Poly(I:C) and lysed at 24 hr post-stimulation. The luciferase activity was determined using Dual-Luciferase Reporter Assay System. Ratio of *FFLuc* values were calculated against the *RLuc* internal control and normalised by assigning a value of 1 to the level of non-stimulated MBP. Error bars indicate standard errors of triplicate wells in three independent experiments. Asterisk (*) indicates Student's *t*-test, *p*-value <0.05.

4.3.5.3 BANP-NS2A inhibits Poly(I:C)-induced IFN response

To observe an effect of IFN response in BANP and NS2A co-expression, a similar experiment was carried out as outlined above, but in the presence of NS2A. Similar to BANP and MBP, NS2A expression construct (pDEST40-NS2A without c-Myc tag) was generated in the same vector backbone pDEST40, using the Gateway cloning system (Section 2.4.4). Cells were transfected with either BANP and/or NS2A, along with the luciferase reporter plasmids p125Luc and pRL-CMV. Due to the low luciferase signals obtained from p55A2Luc PRDII plasmid, this construct was omitted from further analysis. At 24 hr post-transfection the cells were stimulated with 5 µg/ ml Poly(I:C) and lysed the next day, followed by measurement of the luciferase activities. The total amount of transfected DNA was kept constant at 200 ng by adding an empty vector pDEST40. MBP served as a negative control to indicate successful type I IFN pathway stimulation by the dsRNA RNA mimic.

At least a 3.5-fold decrease of *FFLuc* expression was observed in stimulated BANP over-expressing cells relative to its stimulated MBP control (Figure 4.10) (Student's *t*-test, *p*-values <0.05), indicating an inhibition of IFN-β activity. NS2A also showed a small reduction of IFN-β induction compared to MBP. NS2A has been reported to be an IFN-antagonist (Muñoz-Jordan et al. 2003), thus an inhibitory effect is expected. Interestingly, co-expression of both BANP and NS2A diminishes IFN-β induction though at least in this system no enhancement or additive effect is seen. To what effect BANP and NS2A interacts is thus presently not clear, and at least in this reporter system not obvious.

Data from the IFN-β experiments (Section 4.3.5.2 and 4.3.5.3) indicate that over-expression of BANP inhibits the IFN response, which correlates to a similar observation with mouse SMAR1 (Singh et al. 2009). Over-expression of SMAR1 results in a decrease in IκBα promoter activity upon TNFα stimulation, resulting in down-regulation of IκBα transcription. This effect however is reversible using siRNA SMAR1 knockdown. Furthermore, SMAR1 over-expression recruits histone deacetylase 1 (HDAC1) complex to the MAR-binding sites of NF-κB target genes and thus decreases gene expression (Singh et al. 2009). Taken together, data from this study provide evidence that both BANP-NS2A are responsible for inhibition of IFN induction in Poly(I:C)-stimulated cells.

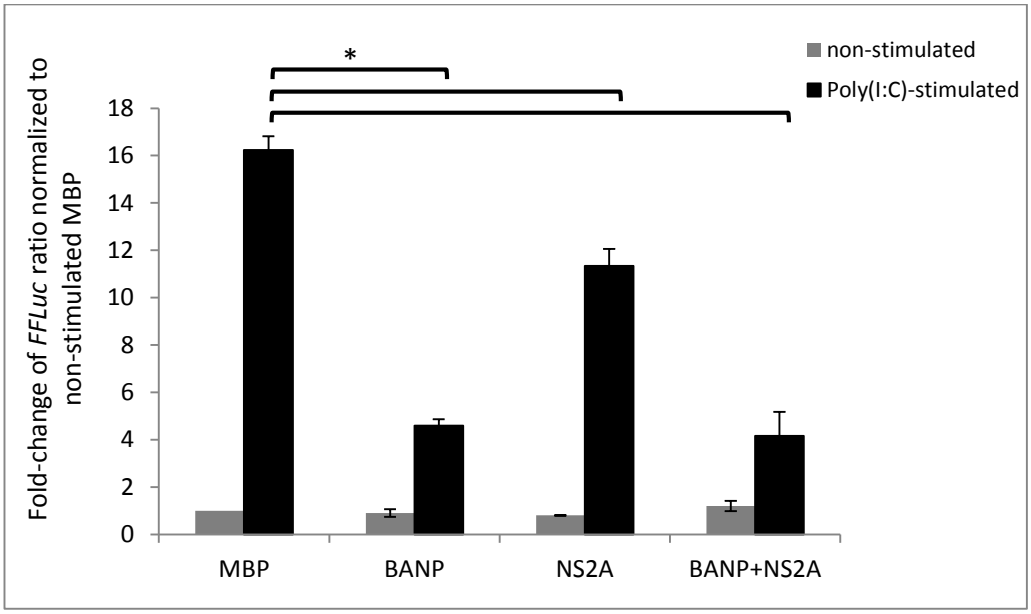

Figure 4.10: Co-expression of BANP-NS2A inhibits IFN-β.

Transfected cells were stimulated with 5 µg/ ml Poly(I:C), lysed at 24 hr post-stimulation and the luciferase activity was determined. Ratio of FFLuc values were calculated against the RLuc internal control and normalised by assigning a value of 1 to the level of non-stimulated MBP control. Error bars indicate standard errors of triplicate wells from three independent experiments. Asterisk (*) indicates Student's *t*-test, *p*-value <0.05.

4.3.5.4 BANP and NS2A inhibits IFN-induced IFN response

To examine whether a type I IFN response induced by interferons may be affected by this interaction or by the two proteins individually, an IFN response was induced by treatment with a high concentration of Universal Type I IFN protein units in HEK293 cells. This stimulates the IFN response through the JAK-STAT signaling cascade after activation of the IFNAR receptor (Ivashkiv & Donlin 2014; O'Neill & Bowie 2010).

DENV proteins NS4B and NS5 were also tested for their IFN inhibitory effect. NS5 in particular, was used as a control for the IFN stimulation as it should inhibit this pathway (Laurent-Rolle et al. 2014; Mazzon et al. 2009; Best et al. 2005). All DENV expression plasmids were generated in the same pDEST40 vector to minimise variability. The total amount of transfected DNA was kept constant at 200 ng by adding empty vector. A similar experiment was carried out as outlined in the previous section but pGL4.17-ISREFluc (Table 2.15) was used instead of p125Luc. pGL4.17-ISREFluc has an IFN-stimulated gene response element (ISRE) promoter expressing *FFLuc*. HEK293 cells were transfected with the expression plasmids (either BANP, MBP, NS2A, NS4B or NS5) along with the luciferase reporter plasmids pGL4.17-ISREFluc and pRL-CMV. The cells were treated with 1000 U/ ml Universal Type I IFN 24 hr p.t and lysed the next day.

As shown in Figure 4.11, either BANP alone or the combination of BANP and NS2A inhibited IFN-β induction (Student's *t*-test, *p*-values <0.05). This indicates regardless of the method of IFN-β induction (either through Poly(I:C) stimulation or IFN treatment), data show consistent inhibition of IFN induction. Again there was no combined or additive effect by expressing NS2A and BANP in this assay, as strong inhibition was observed. It was also observed that DENV protein NS5 has the most inhibitory effect (Student's *t*-test, *p*-values <0.05), followed by NS2A and NS4B. NS5 is a known Flavivirus IFN-antagonist and has been reported to inhibit JAK-STAT signaling by blocking STAT2 phosphorylation (Best et al. 2005; Mazzon et al. 2009). Besides NS5, DENV NS2A and NS4B have also been previously reported to inhibit IFN responses (Muñoz-Jordan et al. 2003; Muñoz-Jordán et al. 2005). Furthermore, JEV NS2A blocks IFN-induced dsRNA-activated protein kinase R (Tu et al. 2012), while KUNV NS2A has also shown to be IFN antagonist (Liu et al. 2006).

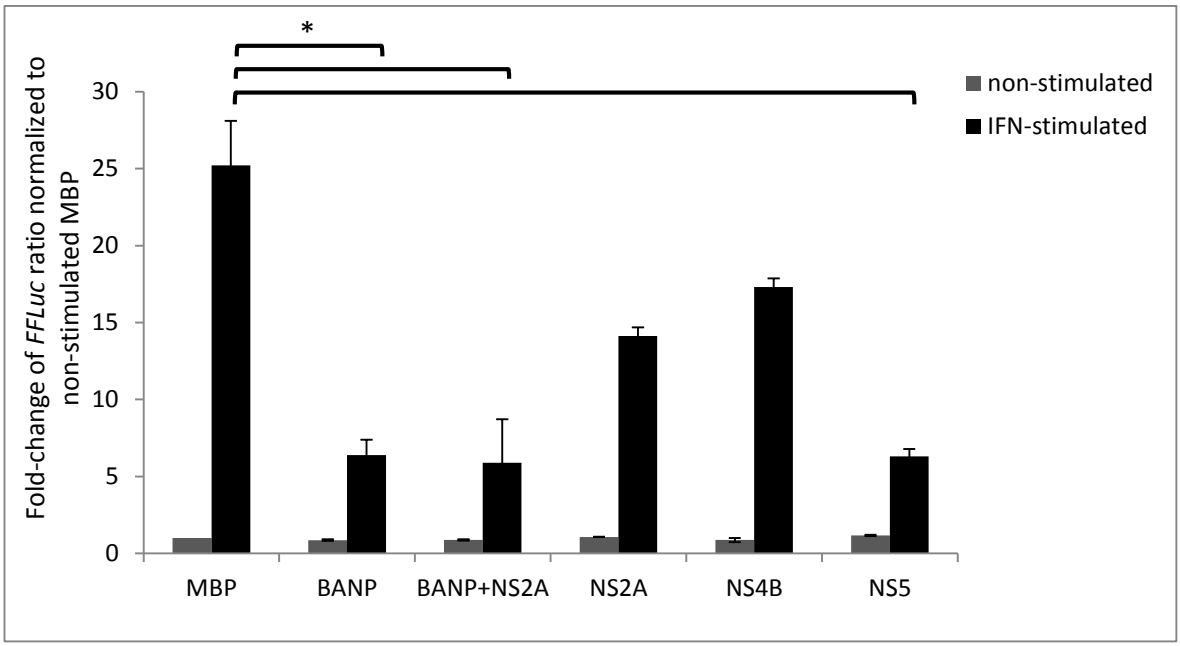

Figure 4.11: Inhibition of IFN-β-mediated gene expression.

Inhibition of IFN-β-mediated gene expression by BANP and/or NS2A, NS4B and NS5 during type I IFN-induced activation. HEK293 cells were co-transfected with pGL4.17-ISREFluc FFLuc reporter plasmid, pRL-CMV (RLuc internal control) and expression plasmids as follows: BANP, NS2A, NS4B or NS5. MBP was used as a negative control for IFN inhibition. The cells were stimulated with Universal Type I IFN (1000 U/ ml), lysed at 24 hr post-stimulation and the luciferase activity was determined. The ratio of luciferase was calculated and normalised to the level of non-stimulated MBP. Data reflects the mean±standard error of triplicates from three independent experiments. Asterisk (*) indicates Student's *t*-test, *p*-value <0.05.

4.3.6 Effect of BANP knockdown in DENV infection

Due to the difficulty in working with the live DENV strains which requires specific regulations and safety control measurements in a Containment Level 3 facility (not available at the CVR at the time of this work), cell culture-based experiments using a DENV sub-genomic replicon were carried out. This study aimed to investigate the effect of BANP silencing on translational DENV replicon which may indicate its importance in the viral life cycle. Initial experiments focused on testing whether the mammalian cell lines were suitable for DENV replicon replication. This was followed by optimising the concentration of siRNA BANP to achieve knockdown of this protein in the chosen cell line.

4.3.6.1 Dengue virus replicon

A sub-genomic DENV-2 NGC-derived replicon expressing *FFLuc*, pDVPACluc was initially tested for luciferase expression in mammalian cells (Section 2.6.3). The *in vitro* transcribed DENV replicon RNA was transfected into BHK-21, A549 and HEK293 cell lines using Lipofectamine® 2000 CD, followed by lysing the cells at 24 hr post-transfection and measuring the *FFLuc* activity. Although BHK-21 was a non-human cell line, it was included in this test because of its high transfection efficiency which enabled a significant *FFLuc* expression. As shown in Figure 4.12, all cell lines demonstrated higher *FFLuc* expression in the DENV replicon RNA-transfected cells compared to the mock-transfected control. BHK-21 gave the highest luciferase expression indicating the cells were permissive for replicon replication, followed by HEK293 and A549 cells. Due to the relatively higher *FFLuc* expression in HEK293 cells compared to A549 and their previous use in experiments, this cell line was therefore selected for subsequent experiments.

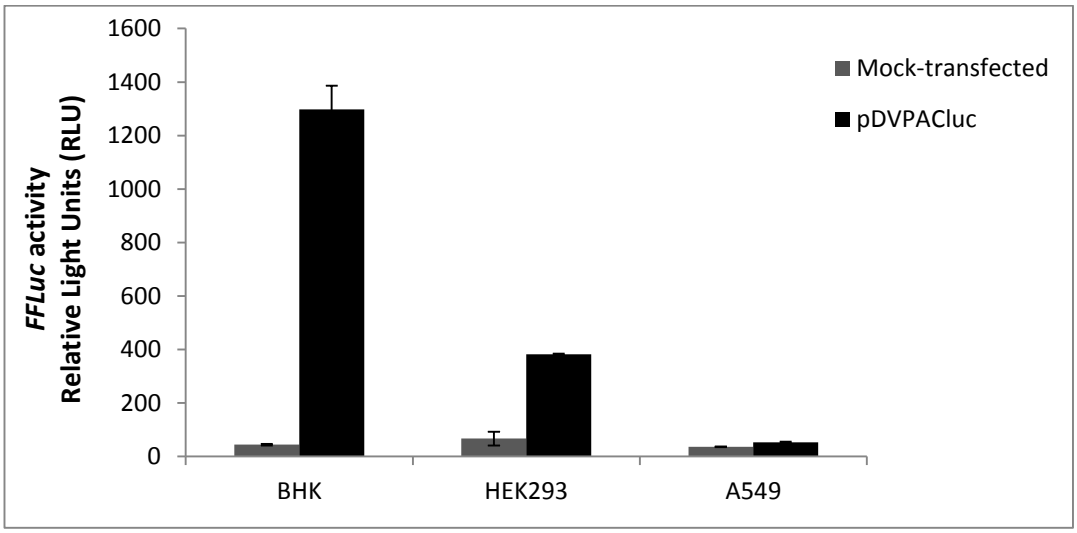

Figure 4.12: *FFLuc* expression of DENV replicon in mammalian cell lines.

The cells were lysed at 24 hr p.t and the luciferase activity was measured. Mock was cells transfected with Lipofectamine® 2000 CD alone. Data represent the average standard deviation of triplicate samples from three independent experiments.

4.3.6.2 Replication kinetics of the DENV replicon

Based on the above results, the replication kinetics of the DENV replicon was further tested in BHK-21 and HEK293 cells by a time-course study. Similar experiments were performed as detailed above, however the *FFLuc* activity was determined at various time-points; 6, 24, 48, 72, 96 and 120 hr post-transfection, which allowed detection of the initiation of replicon replication. In this experiment, pDVPACluc was used alongside its derived mutant, pDVW87I, as a negative control. pDVW87I has a mutation in NS5 gene (tryptophan to isoleucine at the amino acid position 87) that allows transcription, but prevents translation of the viral transcripts to NS proteins (Massé et al. 2010).

In both cell lines, *FFLuc* activity of wild-type pDVPACluc and the mutant pDVW87I was observed at its highest peak as early as 6 hour post-transfection (Figure 4.13, Figure 4.14). This corresponded to the direct translation of DENV NS proteins coming from the input *in vitro*-transcribed replicon RNA. At 96-120 hr post-transfection, a low level luciferase peak of the wild-type pDVPACluc replicon was detected in BHK-21, indicating a replication activity (Figure 4.13). This however, was not observed in HEK293 cells (Figure 4.14), which could be due to the ability of cells to induce immune responses against the replicon preventing its replication. In both cell lines, no *FFLuc* expression derived from replication was observed in the pDVW87I mutant at the given time-points, as expected (Figure 4.13, Figure 4.14).

The overall results from this study concluded an absence or very poor replication of the wild-type DENV replicon in HEK293 cells. Although it was possible to carry out the studies by examining the initial *FFLuc* expression level, the lack of suitable DENV construct for negative control (a failure in generating a DENV GDD mutant replicon in-house and inability to detect the DENV anti-genome), suggested that the experiment was not achievable as planned. A collaborative project was therefore set up with Dr. Andrew Davidson and his team at the University of Bristol to determine the effect BANP had on DENV replication using a live DENV strain, from which all our DENV proteins were derived. These subsequent experiments are described in Section 4.3.7.

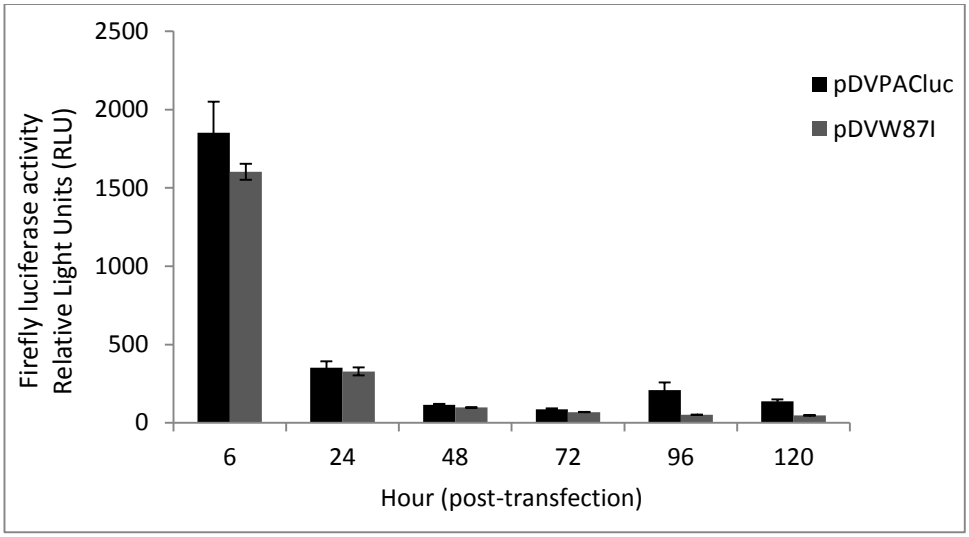

Figure 4.13: Expression of *FFLuc* in BHK-21 cells.

The cells were transfected with *in vitro* transcribed DENV replicon RNA (either the wild-type pDVPACluc or mutant pDVW87I), and cells were harvested at various time-points (6-120 hr p.t) and luciferase activity was measured. Data reflects the mean±standard error of triplicates from three independent experiments.

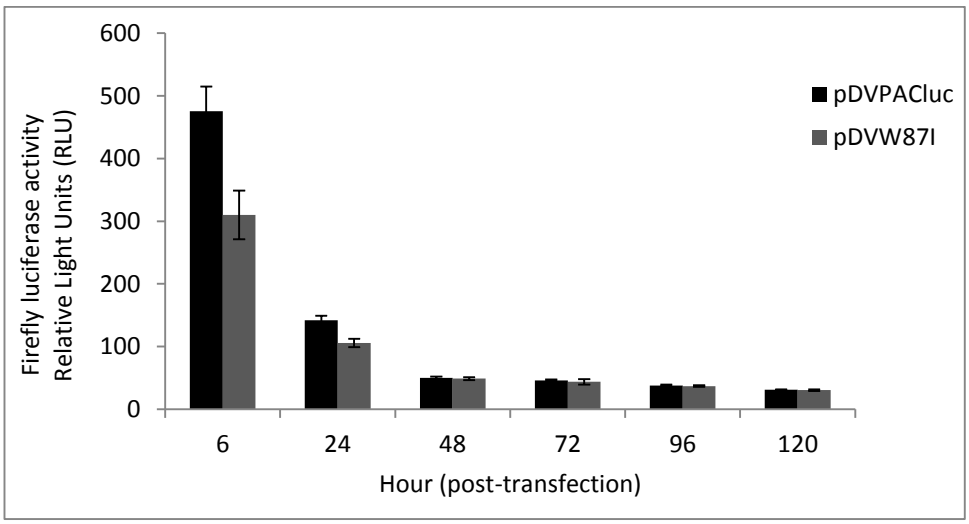

Figure 4.14: Expression of *FFLuc* in HEK293 cells.

The cells were transfected with *in-vitro* transcribed DENV replicon RNA (as above) and the luciferase activity was determined at time points as indicated. Data reflects the mean±standard error of triplicates from three independent experiments.

4.3.6.3 BANP knockdown

BANP knockdown in HEK293 cells was tested by transfecting a varying concentration of BANP siRNAs (ON-TARGETplus SMART pool® consisting a mixture of four individual siRNA) (Section 2.7.3). A non-targeting control siRNA for *E. coli* β-galactosidase (β-gal), was used in parallel as a negative control. At 24 hr p.t, the cells were lysed and protein levels analysed by immunoblotting.

Down-regulation of BANP was observed in BANP siRNA-transfected cells compared to mock-transfected and control β-gal siRNA-transfected cells (Figure 4.15). The signal intensity of BANP was quantified using the ImageJ software and the relative percentage of BANP was normalised to the housekeeping Actin protein level. The highest knockdown of the target protein was observed with 100 nM BANP siRNA (73.8% reduction) compared to control.

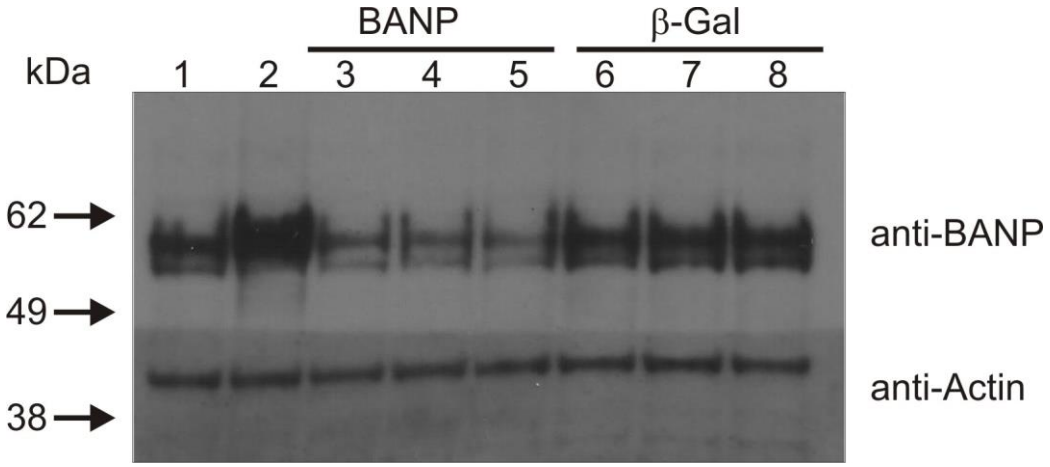

Figure 4.15: Validation of BANP knockdown in HEK293 cells.

Validation of BANP knockdown in HEK293 cells by using different concentration of BANP siRNA. Lane 1 is mock-transfected cells representing endogenous BANP, lane 2 is overexpressed BANP, lanes 3-5 are siRNA BANP; 10 nM, 50 nM and 100 nM, respectively. Lanes 6-8 are β-gal siRNA negative controls; 10 nM, 50 nM and 100 nM, respectively. Actin was used as a loading control.

4.3.7 Effect of BANP knockdown and overexpression in DENV production

4.3.7.1 Dengue virus infection and effect of BANP

This study aimed to determine the effect of BANP knockdown on DENV replication. Due to the poor replication of the DENV replicon in HEK293 cells (Section 4.3.6.2), these experiments were carried out using the live DENV-2 NGC strain. These experiments were performed by Amjad Yousuf in a Containment Level 3 facility, University of Bristol. In brief, HEK293 cells were transfected with BANP siRNA or expression plasmid. After an overnight incubation at 37 °C, the cells were infected with DENV-2 NGC at MOI 10 (Section 2.6.7). Transfection of the BANP siRNA was repeated in the knockdown cells the next day to ensure continuous BANP knockdown. Cells were lysed in TRIzol® reagent at 3 days post-infection. Each cell lysate was pooled from three-well replicates into a single tube and sent to Glasgow for further analysis.

4.3.7.2 Gene expression analysis

RNA was isolated from DENV-infected cell lysates (Section 2.2.1) and processed for gene expression studies as described (Section 2.7.7). Primers and fluorophore-labelled TaqMan probes targeting the DENV-2 capsid region (Callahan et al. 2001) were used. The human HPRT1 housekeeping gene was selected as an endogenous control as it has been previously validated for expression stability (Żyżyńska-Granica & Koziak 2012). The RNA samples were subjected to cDNA synthesis followed by qRT-PCR which was run in triplicates on a 96-well plate. As shown in Figure 4.16, DENV capsid gene expression was higher in BANP knockdown cells than the β-gal negative control knockdown. This indicated a 1.6-fold difference between the two samples. The expression of DENV in both the control knockdown and the mock DENV-infected cells was fairly consistent, given only a slight difference in their gene expression. DENV was detected at a very high level in BANP overexpressing cells, giving a 3-fold increase over mock DENV-infected cells. This finding was very interesting however it remained inconclusive as there was indeed no negative control (transfection with empty plasmid) for the overexpressed BANP. This experiment therefore needs repeated. Clearly at present, the results from BANP knockdown and overexpression experiments would appear to be contradictory and the experiment needs to be repeated under better conditions.

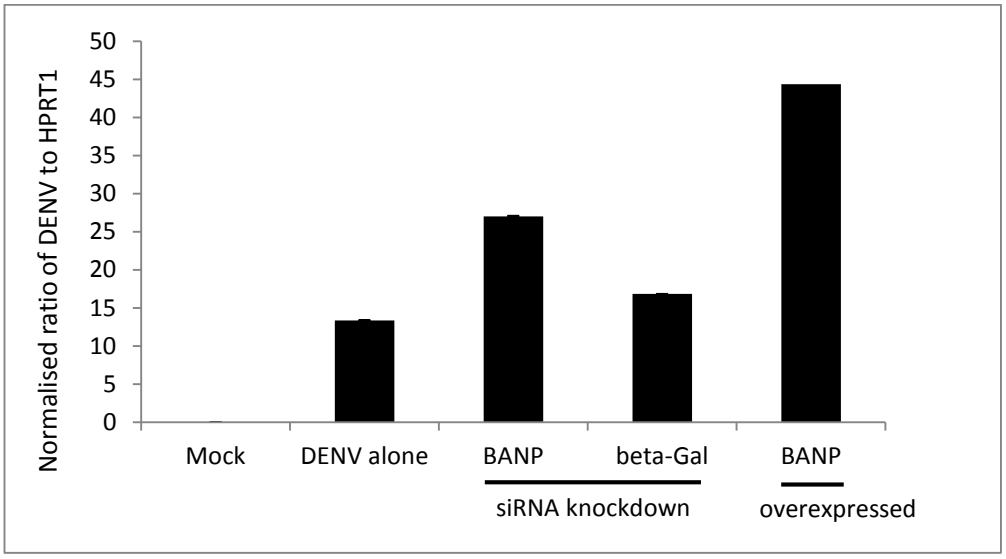

Figure 4.16: DENV replication in BANP overexpression and knockdown.

The data represents average viral copy numbers from triplicate wells of qRT-PCR reactions, with error bars showing standard errors. The viral copy numbers were generated from a standard curve based on cycle threshold (Ct) values and normalised to the human HPRT1 internal control. Data obtained in this study was derived from pooled samples in a single experiment.

4.3.7.3 mRNA expression of BANP

To investigate possible reasons for the inconclusive results, we sought to analyse the BANP knockdown efficiency. The protein cell lysates infected with DENV however, were unavailable due to the presence of infectious virus. BANP knockdown was therefore validated by analysing mRNA gene expression using the RNA samples obtained from Bristol. cDNA was synthesised from the RNA samples using oligo(dT) (Section 2.2.2) and subsequently amplified by standard PCR using the specific BANP primers. As shown in Figure 4.17 (lanes 1, 2, 4 and 5), the BANP fragment (501 bp) was not detected in all samples which made the analysis of knockdown inconclusive. Amplified BANP fragment was only detected in the cells transfected with BANP plasmid which results in a high mRNA expression (Figure 4.17, lane 3). The housekeeping human gene *Actin* (436 bp) was consistently observed in all samples.

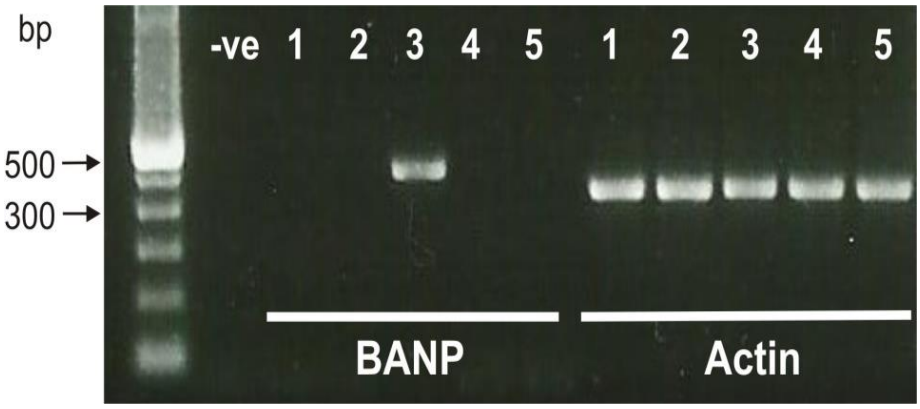

Figure 4.17: mRNA expression of BANP knockdown.

Amplified samples are: mock siRNA non-infected (lane 1), mock siRNA infected with DENV (lane 2), over-expressed BANP infected with DENV (lane 3), BANP knockdown infected with DENV (lane 4) and β-gal knockdown (BANP non-targeting) infected with DENV (lane 5). mRNA expression of the human *Actin* housekeeping gene corresponding to all samples are also shown (lanes 1-5 labelled Actin). –ve is a PCR water control.

4.4 Discussion

Identification of virus-targeted host proteins provides a better understanding of the mechanisms involved in regulating or fostering virus infection. Our previous Y2H study identified BANP as a potential DENV NS2A interacting partner. A smaller NS2A protein fragment (NS2A187F) has also been shown to interact with BANP and hence indicates a potential NS2A-BANP interaction binding site. Although BANP has 81.3% amino acid similarity with the mouse homolog SMAR1, the protein is not well-characterised and it is not known to possess similar functional properties as SMAR1. SMAR1 is a multi-functional protein and has been reported to modulate cell cycle, apoptosis, DNA damage and several pathways involving tumorigenesis (Malonia et al. 2011). As of yet, SMAR1 has not been implicated in any viral life cycle except that it can interfere with the LTR-mediated transcription of HIV-1 (Sreenath et al. 2010). SMAR1 has also been shown to down-regulate the NF-κB signalling through the proposed model described in Figure 4.1 (Singh et al. 2009). In this study, interaction between BANP and NS2A was further confirmed, and its potential role in regulating NF-κB pathway (as similar to SMAR1) was investigated (Malonia et al. 2011; Singh et al. 2009).

BANP was first tested for expression in HEK293 cells using a V5-tagged BANP construct. Two bands were detected by Western blot using anti-BANP antibody, which indicates the protein maybe present as isoforms.This could be explained by the fact that *BANP/SMAR1* gene is able to go through alternative splicing which produces transcript variants, and subsequently translated into different protein isoforms (Kaul et al. 2003; Chattopadhyay et al. 2000b). In the previous chapter, interaction between BANP and NS2A has been validated by LUMIER assay showing promising results. This interaction was further confirmed using similar co-IP pull down assay, an efficient technique to investigate protein interactions (Bonifacino et al. 2001), and the protein lysates were used for detection by Western blots. Results from this study demonstrated that BANP was indeed observed in the NS2A pull-down but not detected during the absence of NS2A. Although NS2A187F was not tested in this assay, this finding thus confirms a physical interaction exists between BANP-NS2A. There was however no pull down of the BANP native protein by NS2A, which could be due to its presence is insufficient for precipitation with IgG-coated beads or it binds weakly.

Observation by immunofluorescence staining revealed the native BANP was equally dispersed intracellularly, whereas overexpression of BANP causes accumulation of the protein in the cell nucleus. This is consistent with the expression of SMAR1 (Kaul et al. 2003; Chaudhary et al. 2014), suggesting BANP may be involved in a specific cell nuclear activity. It has also been shown that SMAR1 is found in the cytoplasmic fractions of various cancer cell lines, and able to interact with a member of Aldo-keto reductase family, AKR1a4 (S. Singh et al. 2010). Disruption of the SMAR1-AKR1a4 interaction by DNA damage results in nuclear translocation of SMAR1 and restoration of AKR1a4 function in scavenging free radical waste in the cytoplasm. Hence, this supports the findings that endogenous BANP is localised in both the cell nucleus and cytoplasm.

From the IF staining, DENV NS2A was exclusively localised in the cell cytoplasmic region. Although NS2A appears to be present in the cytoplasm where cytoplasmic BANP is localised, it is difficult to define if they co-localised, due to the narrow cytoplasmic space of HEK293 cells. In addition, there was no detection of native BANP in the NS2A pull down during co-IP, which indicates there may not have been a specific interaction, perhaps due to partitions in cellular compartments. Although there was no NS2A co-localisation with the over-expressed nuclear BANP, this does not necessarily indicate that interactions between BANP and NS2A are artefactual. Is it also possible that the interaction may have been affected by alteration in subcellular localisation. In Y2H, both proteins were directed to the nucleus via nuclear localisation signal on GAL4 system. However in subsequent expression by IF and co-IP, other signals may have directed the proteins to different cellular compartments where the proteins might never encounter each other. The properties of BANP clearly need further investigations to understand these observations. It is at present not clear why overexpression of BANP leads to re-distribution unless this is linked to transfected DNA of the expression vector itself. In the future, stable cell lines for example expressing BANP from retroviral constructs could be used to verify these processes.

While SMAR1 over-expression has an important role in the cellular transcriptional regulation (Malonia et al. 2011), the potential role of BANP and its involvement in DENV infection is unknown. Previous studies have indicated that SMAR1 plays a role in down-regulation of NF-κB in cancer cells (Singh et al. 2009). Although NF-κB is known to play a role in immune responses, it has many other roles in cellular processes including cancer (Hoesel & Schmid 2013; Tergaonkar 2006). In this study, the potential role of BANP in regulating type I IFN response and NF-κB was studied using a luciferase-based reporter gene assay. Plasmid-encoded luciferase gene controlled by the entire IFN-β promoter (p125Luc) or repeated PRDII elements responsive to NF-κB (p55A2Luc) were used.

IFN-ß expression has been shown to be induced by dsRNA or other products of virus infection (Jiajia Liu et al. 2012). A synthetic dsRNA mimic, Poly(I:C), known to induce a strong IFN-ß response was used in this study (Reimer et al. 2008; Matsumoto & Seya 2008; Kumar et al. 2006). Transfection of Poly(I:C) into cells resembles intracellular dsRNA generated during virus infection, which results in potent stimulation of the IFN-ß promoter (Li et al. 2005). Within the cell, Poly(I:C) is recognised by cytoplasmic receptors such as RIG-I and MDA-5. Upon recognition of viral components, both RIG-I and MDA5 activate MAVS on the mitochondrial membranes. MAVS interacts with STING/MITA and recruits TRAF3 and TRAF6 resulting in production of IFN response (Liu et al. 2013). Poly(I:C) is also recognised by TLR3 and activates IRF3 leading to the production of type I IFN, or through a second pathway involving TNF receptor-associated 6 (TRAF6) which activates the transcription factors NF-κB and activator protein-1 (AP-1) (Reimer et al. 2008; Kawai & Akira 2008; Yamamoto et al. 2003).

Expression of IFN is tightly controlled by transcription factors, which are activated upon recognition of viral components by cytoplasmic receptors. In typical NF-κB signalling pathway, NF-κB transcription factors translocate from the cytoplasm to the nucleus and bind to the PRDII elements within the IFN-β promoter, and subsequently activate the expression of IFN. Transcriptional activation of κB target genes which includes the IFN-β can lead to substantial production of IFN (Pahl 1999). Results from the assay indicate that expression of IFN-β and NF-κB is successfully induced by Poly(I:C) and is repressed in non-stimulated cells. Further tests in the presence of increasing BANP indicate that BANP is capable to inhibit

the IFN-β and NF-κB induction. The NF-κB luciferase signal is less compared to IFN-β as it detects a component of the IFN induction pathway. Nonetheless, the fact that NF-κB is inhibited during BANP over-expressed signifies the importance of BANP in NF-κB regulation. BANP inhibits IFN-β activation; the same is true for NS2A but the effect of the interaction of both is not clear. These observations were supported by previous findings, as it has been shown that SMAR1 interacts with HDAC1 and NF-κB subunits to repress transcription of NF-κB target genes (Singh et al. 2009). Furthermore, SMAR1 inhibits TNF-α mediated induction of IL-8 mRNA through NF-κB dependent, in which the knockdown of SMAR1 using shRNA resulted in an increase in IL-8 (Malonia et al. 2014).

Further studies with type I IFN-induced IFN responses show an inhibition of the type I IFN response, during expression of BANP and NS2A independently and during co-expression of both BANP-NS2A, which demonstrated this inhibition is independent of NF-κB signaling. Through type I IFN stimulation via the IFNAR receptor, the JAK/STAT signaling cascade was activated resulting in nuclear translocation and binding of phosphorylated STAT to the ISRE promoter and transcription of IFN-stimulated genes. While BANP is inhibiting this process, and NS2A also inhibits these signalling events, the interaction of both BANP-NS2A modulating this event is not clear. Perhaps other pathways are affected by this interaction or the signalling assay is not sensitive enough to pick up differences, which requires further experiments.

Poly(I:C)-mediated IFN response has been shown to induce IRF3 and NF-κB signalling which activates the NF-κB and IFN target genes leading to the production of type I IFN (Reimer et al. 2008). In this study, BANP could possibly repress the transcriptional activation of NF-κB target genes, which also include the IFN-β promoter genes. This mechanism is based on the recruitment of SMAR1-HDAC1-p65/p50 co-repressor complex that binds to the MAR elements, thus resulted in an inhibition of IFN as described previously (Singh et al. 2009). In the IFN-mediated IFN response, the ectopic IFN-α induction is recognised by IFNAR which subsequently activates the JAK/STAT pathway. Activation of this pathway triggers the ISRE activation, resulting in production of type I IFN and induction of an antiviral state. In this study however, an activation of the JAK/STAT pathway by treatment with the Universal Type I IFN Alpha in the presence of overexpressed

BANP resulted in an inhibition of IFN. The mechanism by which BANP governs this inhibition is unknown, which suggests other pathways or interacting molecules may be involved in this event. The inhibition of IFN response by DENV NS2A correlates to previous studies as the protein has been implicated in inhibition of IFN signalling (Muñoz-Jordán et al. 2005; Muñoz-Jordan et al. 2003). Furthermore, the role of NS2A as an IFN-antagonist has also been reported in WNV and KUNV (Liu et al. 2006; Liu et al. 2004).

Although BANP is capable of inhibiting an IFN response (through both NF-κB-mediated and JAK/STAT), the precise mechanism of inhibition and how its interaction with DENV might govern the inhibition is still unclear. Since SMAR1 is known as a tumour suppressor and all SMAR1 experiments have been carried out by researchers in tumour cell lines (which express less SMAR1), the precise role of BANP and how it regulates biological function in non-tumour cells is not known. Another possible explanation is that BANP could be involved in maintaining the intracellular conditions consequent to cellular stress. Similar to SMAR1, BANP is thought to be capable of regulating cell cycle arrest and DNA repair via a mechanism involving HDAC1 and p53 (Sinha et al. 2010). It has been shown that following a mild stress or DNA damage, SMAR1 is activated in association with HDAC1 and p53 tumour suppressor and recruited to the MAR sites upstream of promoter p53 apoptotic targets, *Bax* and *Puma*, leading to cell cycle arrest. This process inhibits apoptosis and favours cell cycle arrest for DNA repair. However, in a case of severe DNA damage, SMAR1 can activate *Bax* and *Puma* genes which leads to induction of apoptosis (Sinha et al. 2010). It is also possible that the use of a whole virus instead of a single NS2A protein might be informative as other NS proteins are likely to participate during viral infection and the effect can be assessed in the presence of BANP. Hence, this would be useful to evaluate the global IFN response as a result of BANP over-expression.

To further explore the role of BANP in DENV replication, an *in vitro*-transcribed RNA of sub-genomic DENV-2 NGC replicon with *FFLuc* reporter (pDVPACluc), was first tested in BHK-21, HEK293 and A549 cells. After 24 hr p.t, the replicon shows the highest *FFLuc* activity in BHK-21, followed by HEK293 and A549, corresponding to the translation of viral NS proteins. BHK-21 is recognised as having a defect in IFN production (Otsuki et al. 1979), which could be the reason why the cells exhibited the highest viral translational activity. In contrast, A549 cells are known to be highly IFN-α/β inducible (Tanabe et al. 2003). This may explain why they do not support translation. Given the aim of this study to assess the replication of a DENV replicon that mimics viral replication, further analysis was performed by transfecting the *in vitro*-transcribed replicon RNA into BHK-21 and HEK293, and measuring the *FFLuc* activities within an extended period. Although BHK-21 cells are known to be IFN-defective, the replicon was found to replicate very poorly. There was also no replication of the replicon in HEK293 which could be due to its capability of inducing an IFN response. As HEK293 are the required cells for use in the downstream experiments, it was decided to perform experiments using the live DENV NGC strain with collaborators at the University of Bristol.

In order to determine the importance of BANP in the DENV life cycle, experiments were carried out to test viral replication upon BANP gene silencing. Analysis of DENV replication was achieved by detecting the capsid gene expression and revealed a remarkably high level of virus replication during BANP overexpression (relative to DENV alone). This could be due to the down-regulation of IFN response regulated by BANP, as well as the existing IFN inhibition effect induced by the high virus MOI. However, the absence of a negative control (empty vector) within this experiment, makes the results at present inconclusive. It was also clear that the replication of DENV in BANP knockdown cells was higher (by 1.6-fold) compared to its knockdown control which has a basal level of native BANP. Results obtained from this study are therefore at present inconclusive. It is important to perform a more detailed study of the biology of BANP before these experiments can be redesigned. BANP seems to respond or react differently depending on conditions. Nonetheless its negative regulatory activity on type I IFN signalling makes it an interesting target for future experiments.

4.5 Conclusion

In this study, interaction between BANP and DENV NS2A was confirmed by co-IP pull-down assay. Further IF analysis has shown the cellular localisation of NS2A with BANP in the cytoplasm or ER/Golgi, however this is uncertain due to the small cytoplasmic space of HEK293 cells. It is clear that BANP is capable of inhibiting NF-κB and IFN response similar to NS2A, and this inhibition is retained during co-expression of both proteins within the cells, however the mechanism of BANP-NS2A interaction that contribute to the IFN inhibition requires further analysis. Besides IFN signalling, other cellular processes of BANP such as regulation of the cell cycle, DNA damage or apoptosis may be alternate explanations for the interaction with NS2A. Due to the fact that the DENV replicon did not replicate in HEK293 cells, further experiments using the infectious DENV were carried out. There were however inadequate controls which rendered the data inconclusive. Thus these experiments require redesign and repetition. Although the importance of BANP in DENV life cycle is as yet unknown, further experiments are called for to indicate its function in human cells.

CHAPTER 5: FUNCTIONAL ANALYSIS OF Kv1.3 IN DENGUE VIRUS INFECTION

5.1 Introduction

5.1.1 Voltage-gated potassium channel Kv1

Kv1 shaker-related delayed rectifier sub-family, comprising of at least six genes (Kv1.1, Kv1.2, Kv1.3, Kv1.4, Kv1.5 and Kv1.6) which exhibit distinct physiological roles (Pongs et al. 1988; Chandy 1991). This protein family shares a common pore-forming α-subunit comprising of six transmembrane segments (S1-S6) and a P loop region containing K^+ selectivity sequence (Miller 2000; Kreusch et al. 1998) (Figure 5.1). The fourth segment (S4) has positively charged amino acid residues at every third position which acts as an intrinsic voltage sensor that regulates protein conformational changes. Kv proteins consist of four α-subunits arranged as homo- or heterotetramers around a central pore that associates with different types of peripheral β-subunits (Sokolov 1997; Kreusch et al. 1998). Upon stimulation and membrane depolarisation, functional K^+ channels generate K^+ diffusion potentials across the cell membrane, which in turn facilitate the influx of calcium ions (Ca^{2+}) to maintain the cell resting membrane potential (Lin 1993). This leads to modulation of Ca^{2+} signalling and activation of lymphocytes in the antigen-driven activation of T lymphocytes (Nicolaou et al. 2009; Lewis & Cahalan 1995).

5.1.2 Potassium-gated channel Kv1.3

Screening of the DENV-2-targeted human proteins by Y2H identified two potassium ion (K^+) channel proteins; Kv1.3 and Kv9.2 (KCNA3 or KCNS2), as interacting partners for DENV-2 NS2A. Both proteins belong to the voltage-gated K^+ channel (Kv) family, which plays an important role in regulating passive flow of K^+ upon changes in cell transmembrane potential (Yellen 2002; Bezanilla 2000). Kv1.3 was first described in human T lymphocytes (Cahalan et al. 1985), whereas Kv9.2 was identified more recently and is known to act through co-assembly with the Kv2 channel subunit (Salinas et al. 1997). There is however limited knowledge of Kv9.2 function in modulating the Kv2 channel. Kv1.3 in contrast, has been a subject of many medical and scientific studies and is reported to be involved in T lymphocyte proliferation and functional Kv in platelets (Panyi et al. 2004; McCloskey et al. 2010). Previous studies have demonstrated the activation of T lymphocytes and

macrophages upon DENV infection and a significant decrease in the number of platelets in dengue patients (Kurane et al. 1991a). Since Kv1.3 channels are highly expressed in lymphocytes and platelets, which may contribute to the progression of the disease, further investigations are required to evaluate the channel association with DENV-2 infection.

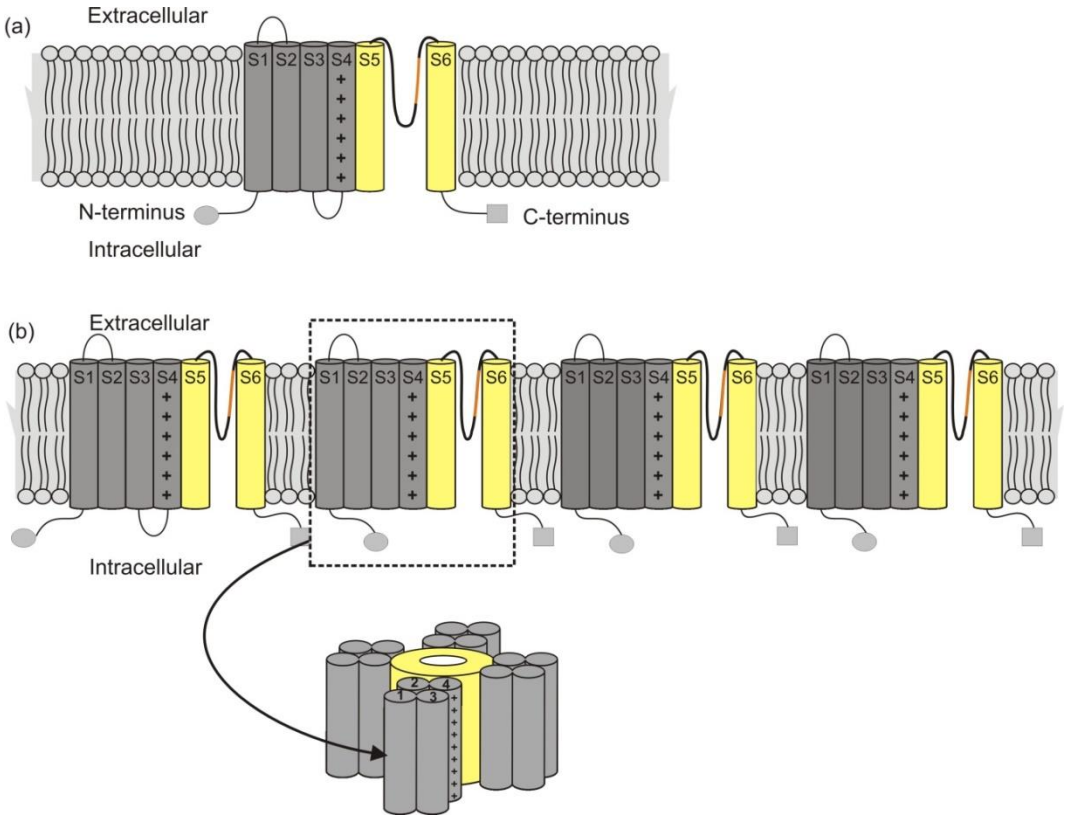

Figure 5.1: Schematic diagram of a voltage-gated K^+ channel.

Figure denotes: (a) an α-subunit of Kv, (b) a tetrameric structure comprising of four α-subunits forming Kv channel. Six transmembrane domains (S1-S6) and the P loop region (in red) are shown. This figure is adapted and re-drawn from Judge & Bever 2006.

Besides expression in T lymphocytes (Cahalan et al. 1985), Kv1.3 is also expressed in other immune cells, such as B-cells and macrophages (Vicente et al. 2006; Wulff et al. 2004), and other types of tissues including the brain, kidney and epithelia (Grunnet et al. 2003; Gazula et al. 2010; Yao et al. 1996). Enhanced expression of Kv1.3 has been previously reported in cancer cells, although the level of Kv1.3 expression does not correlate with the stage of tumour malignancy (Preußat et al. 2003). Notably, knockdown of Kv1.3 by gene silencing in many types of cancer cells resulted in inhibition of cell proliferation *in vitro* and *in vivo* and activation of the cellular caspase pathway, leading to apoptosis (Wu et al. 2013; Jang et al. 2011). Abolishment of Kv1.3 in gene knockout mice resulted in other interesting phenotypes including an increased metabolic rate and enhanced cellular anion currents to compensate for the Kv1.3 depletion (Xu 2003; Koni et al. 2003). Several K^+ channel blockers, such as those derived from scorpion toxins; Margatoxin (MgTx) and Charybdotoxin (Ctx), have been widely used to inhibit Kv1.3 expression (Hu et al. 2013; Sands 1989). Blockade of Kv1.3 by these toxins is able to suppress proliferation in cancer cell lines, suggesting the potential use of Kv1.3 as a target for cancer therapy (Comes et al. 2013; Jang et al. 2009; Felipe et al. 2012).

Although there is no known mechanism describing the specific involvement of Kv1.3 in DENV infection at present, several reports indicate its association with HIV-associated neurocognitive disorders. Data suggest an up-regulation of Kv1.3 and increase in K^+ current was induced by HIV type1 surface subunit glycoprotein 120 (gp 120) in microglia leading to neurotoxicity (Xu et al. 2011; J Liu et al. 2012). Similar observations in Kv1.3 using HIV-1 Tat (HIV *t*rans*a*ctivator of *t*ranscription) protein induced apoptosis via activation of the p38 mitogen activated protein kinase (MAPK) signaling (J. Liu et al. 2013). Further to this, other K^+ channels have been described participating with virus infection. For instance, the HIV-1 surface subunit glycoprotein 120 (gp 120) envelope protein has been shown to bind to the cytoplasmic C-terminus of a K^+ channel BEC1 (brain-specific ether-a-go-go-like channel 1) (Herrmann et al. 2010). As a result, the channel activity was suppressed which prevented the release of virus into the supernatant (Herrmann et al. 2010). It is also demonstrated that Kv2.1 has been a target for HCV replication. During virus infection, this channel is phosphorylated and translocated to the cell membrane which mediates an outward K^+ current, resulting in the induction of apoptosis (Redman et al. 2007). It is interesting

however, that HCV NS5A is capable of modulating the function of Kv2.1, inhibiting apoptosis through modulation of MAPK signaling (Mankouri et al. 2009).

Severe illnesses resulting from DENV infection are characterised by haemodynamic disturbances, increased vascular permeability, bleeding and shock (WHO, 1997). These clinical features are commonly associated with thrombocytopenia and platelet dysfunction which greatly impact progression of the disease (Schexneider & Reedy 2005; de Azeredo et al. 2015). The mechanisms underlying thrombocytopenia during DENV infection are poorly understood, however accumulating evidence suggests the suppression of bone marrow, destruction of platelets and alteration in platelet functions (Michels et al. 2014; Noisakran et al. 2012; Alonzo et al. 2012; Honda et al. 2009). More recently, gene expression and patch-clamp analysis revealed that Kv1.3 represents the Kv subunit in human platelet and megakaryocytes which are responsible for the K^+ conductance and resting potential of platelets (McCloskey et al. 2010). These findings are interesting which suggest that Kv1.3 is likely to contribute to the platelet dysfunction during DENV infection. This study aimed to validate the interaction between DENV-2 NS2A and Kv1.3, as detected in previous chapter by Y2H and LUMIER assay. The importance of Kv1.3 will be investigated in its involvement with DENV-2 infection.

5.2 Objectives

1. To confirm the interaction of Kv1.3 and NS2A.
2. To determine the cellular localisation of Kv1.3 and NS2A.
3. To determine the viability of cells during overexpression of Kv1.3.
4. To investigate the effect of Kv1.3 to DENV-2 replication.

5.3 Results

5.3.1 Confirmation of Kv1.3-NS2A interaction

5.3.1.1 Use of Kv1.3 expression construct

An interaction between Kv1.3 and NS2A has been shown by Y2H and LUMIER assay (Section 3.3.2 and 3.3.3). To further validate this interaction by co-immunoprecipitation/pull-down assay, an EGFP-tagged construct expressing Kv1.3 (a kind gift from Jamel Mankouri, University of Leeds), was used. This construct contained rat Kv1.3 full length coding region (GenBank accession no. M30312.1) fused to an EGFP reporter at the N-terminus. The gene encoded 525 amino acids resulting 89.1% protein similarity with the human Kv1.3 (NP_002223.3).

Kv1.3 expression was initially tested by transfecting the construct into HEK293 cells and immunoblotting using anti-Kv1.3 antibody (as described in Section 2.3.5). An empty vector pEGFP-C1 was used as an EGFP expression control. The western blot revealed Kv1.3 expression as a fusion with EGFP at 84 kDa (Figure 5.2a). A protein band at 58 kDa was also detected in all protein samples corresponding to a monomeric Kv1.3 subunit (lanes 1-3), suggesting the presence of endogenous Kv1.3 as previously reported (Holmes et al. 1996; Cai & Douglass 1993). A higher MW protein ~168 kDa was observed in Kv1.3-transfected cells which could be due to dimerisation of Kv1.3. Monomeric, dimeric and tetrameric forms of Kv1.3 have been previously demonstrated (Gulbins et al. 2010). Further analysis using anti-EGFP (Figure 5.2b) similarly detected the presence of Kv1.3-EGFP (84 kDa) (lane 3). Cells transfected with empty EGFP plasmid expressed EGFP (26 kDa) (lane 2) as expected, which was absent in mock (lane 1).

In order to confirm the presence of endogenous Kv1.3 in HEK293 cells, RNA was extracted from Kv1.3-transfected cells and subjected to mRNA expression analysis by semi-quantitative RT-PCR. The amplified PCR product show an expected 138 bp fragment (Figure 5.3, lane 1 to 3), indicating the endogenous Kv1.3. Although the expression of Kv1.3 genes at the mRNA level does not necessarily indicate translation of the corresponding protein, the data support the presence of endogenous Kv1.3 as shown by Western blot. The overall results conclude that Kv1.3 is successfully over-expressed, while the endogenous forms are present at detectable levels in HEK293 cells.

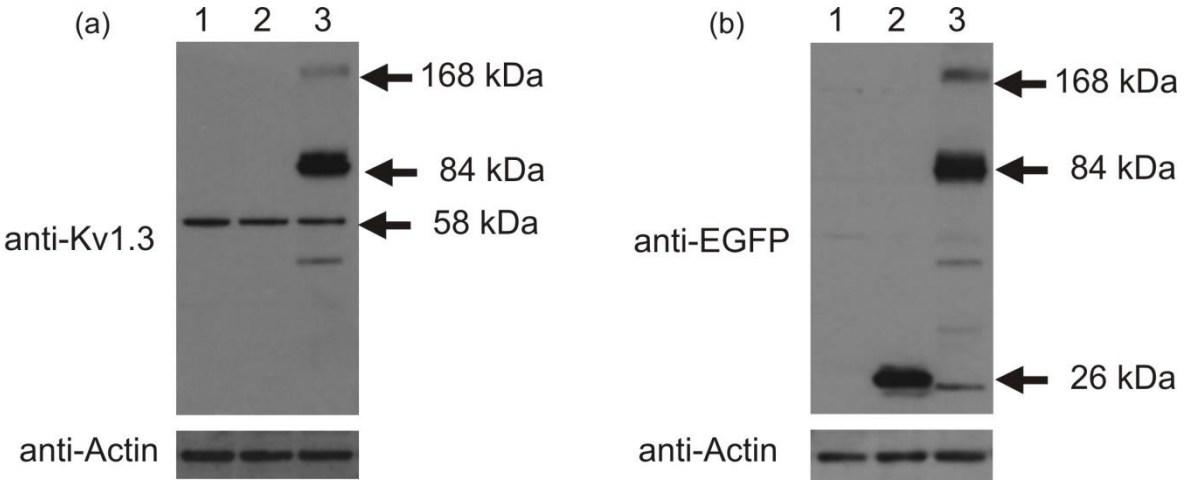

Figure 5.2: Expression of Kv1.3-EGFP and its native form in HEK293 cells.

Dimeric Kv1.3 is also shown. The proteins were detected by immunoblotting using (a) anti-Kv1.3 and (b) anti-EGFP antibodies. Each figure shows: mock (lane 1), EGFP (lane 2) and Kv1.3-EGFP (lane 3). Arrow indicates the MW size of proteins in kDa. Actin was used as a loading control.

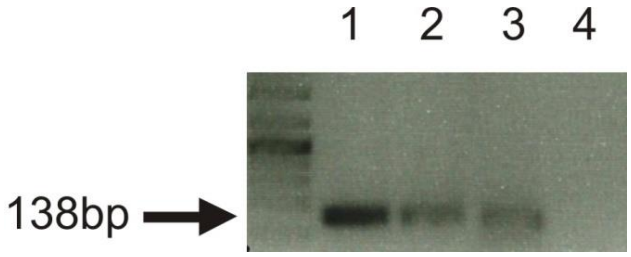

Figure 5.3: mRNA gene expression of endogenous Kv1.3 by RT-PCR.

Figure denotes cells transfected with the following plasmids: Kv1.3-EGFP (lane 1), empty EGFP (lane 2), mock-transfected endogenous Kv1.3 (lane 3), and mock-transfected (without SuperScript® II) as a negative control for RT-PCR (lane 4). A 100 bp DNA ladder (New England Biolabs) is shown. Arrow indicates the size of amplified products in basepair.

5.3.1.2 Co-immunoprecipitation of Kv1.3 and NS2A

Kv1.3 was further tested for interaction with DENV-2 NS2A by co-immunoprecipitation/pull-down assay as described in Section 2.7.2. EGFP-tagged Kv1.3 (as above) was co-expressed with Protein A-tagged NS2A and lysed 24 hour p.t. The cell lysates were immobilised on IgG-coated magnetic beads followed by several washing steps and subjected to immunoblotting using anti-EGFP. Empty EGFP co-expressed with Protein A-tagged NS2A was run as a negative control.

Based on the western blot probed with anti-EGFP, Kv1.3-EGFP was shown to co-precipitate with NS2A and was present in the NS2A pull-down lane at the expected size (84 kDa) (Figure 5.4, lane 4). There was no detection of EGFP in the NS2A pull down of co-expressed Protein A-NS2A and untagged EGFP (Figure 5.4, lane 3), which indicates NS2A does not co-precipitate with EGFP. This ruled out the possibility that EGFP binds to NS2A instead of Kv1.3.

While it has been shown that NS2A was capable to interact with the recombinant Kv1.3-EGFP, further analysis was performed to investigate if NS2A could interact with the native Kv1.3. Pull-down proteins and cell lysates were subjected to immunoblotting on the same membrane and probed using anti-Kv1.3 antibody. Interestingly, the native Kv1.3 (58 kDa) was captured by NS2A in all pull-down samples (Figure 5.5a, lane 2-4, second arrow). However, the band detection was very poor in lane 4 and there was no expression of the recombinant Kv1.3-EGFP (84 kDa) in either the pull-down or cell lysates (Figure 5.5b, lane 4, first arrow), which indicated the transfection did not work properly. It was also clear that the native Kv1.3 was not detected in the pull-down sample of mock (Figure 5.5a, lane 1, second arrow), due to the absence of NS2A to mediate the interaction. Taken together the results obtained from Y2H, LUMIER assay and current co-IP/pull-down assays using EGFP and Kv1.3 antibodies lead to the conclusion that NS2A interacts with Kv1.3.

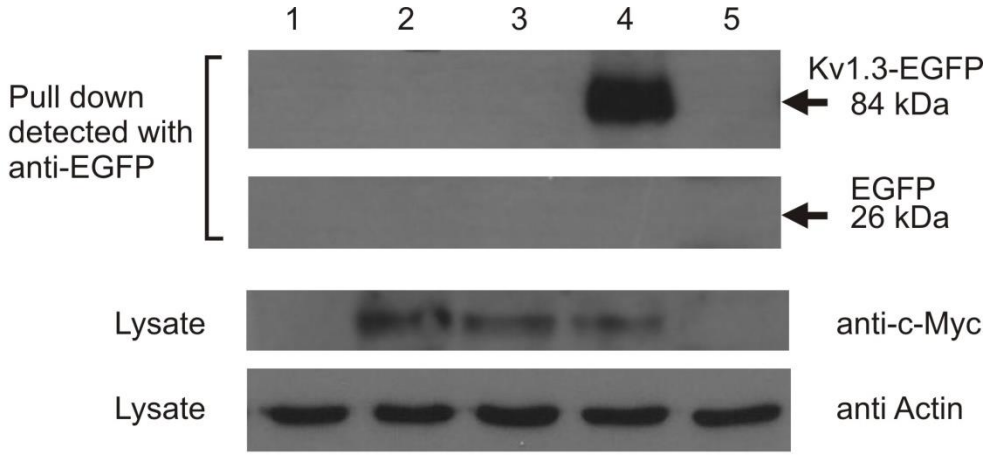

Protein A	-	-	-	-	+
EGFP	-	-	+	-	-
Protein A-NS2A	-	+	+	+	-
Kv1.3-EGFP	-	-	-	+	-

Figure 5.4: Interaction of Kv1.3-EGFP and NS2A by co-IP/pull-down assay.

Proteins were harvested from transfected-cells and captured by IgG-coated magnetic beads. Protein A-tagged NS2A was used to pull-down proteins and were detected with anti-EGFP, analysed by immunoblotting. Figure indicates: mock (lane 1), Protein A-NS2A (lane 2), co-expression of Protein A-NS2A and EGFP (lane 3), co-expression of Protein A-NS2A and Kv1.3-EGFP (lane 4), and empty Protein A (lane 5). Cell lysates probed with anti-c-Myc indicate the detection of NS2A. Actin was used as a loading control.

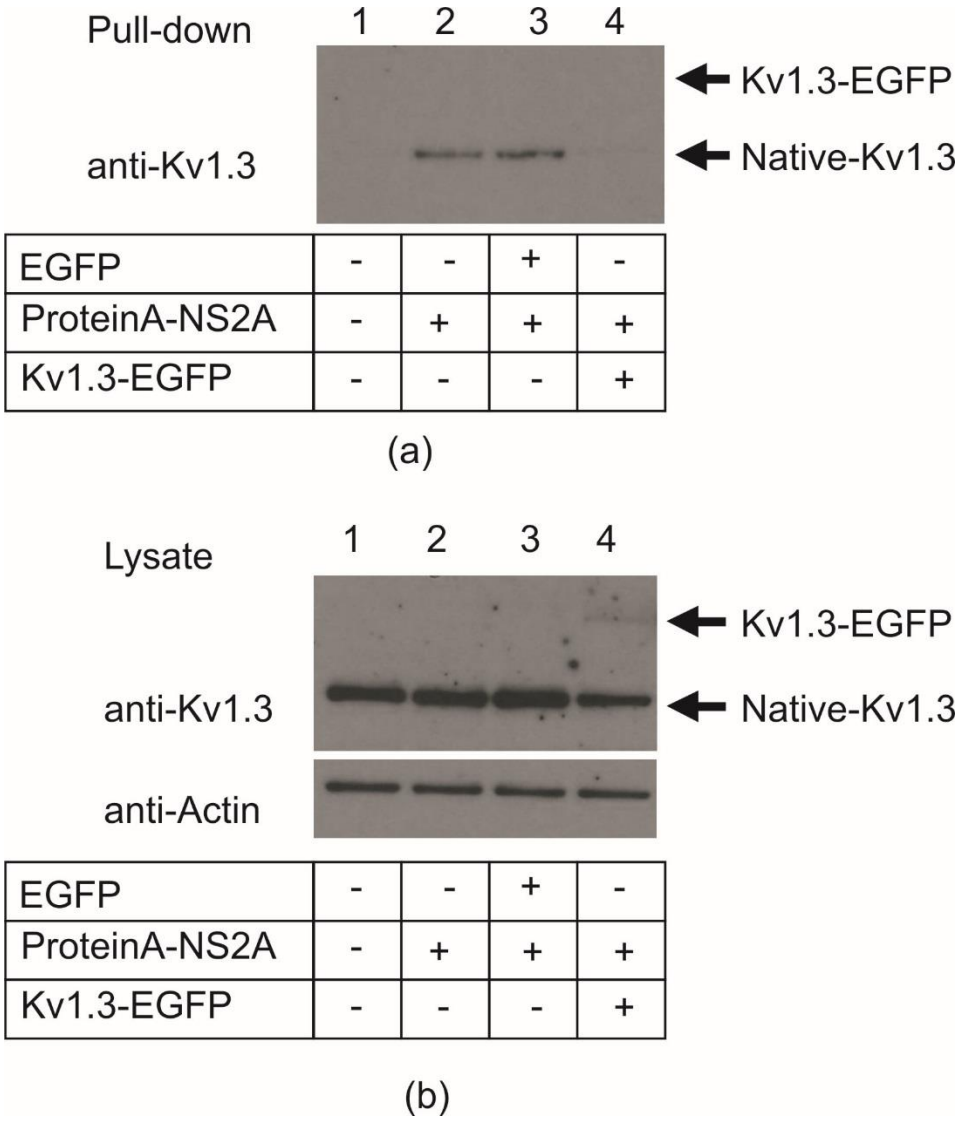

Figure 5.5: Interaction of Kv1.3 and NS2A detected with anti-Kv1.3 by co-immunoprecipitation/pull-down assay.

Proteins were harvested from transfected-cells and captured by IgG-coated magnetic beads. The pull-down proteins (a), and cell lysates (b), were subjected to immunoblotting and detected using anti-Kv1.3 antibody. Each figure indicates: mock (lane 1), Protein A-NS2A (lane 2), co-expression of Protein A-NS2A and EGFP (lane 3), co-expression of Protein A-NS2A and Kv1.3-EGFP (lane 4). Top arrows indicate overexpressed Kv1.3, bottom arrows indicates the native Kv1.3. Actin was used as a loading control.

5.3.2 Cellular localisation of Kv1.3 and NS2A

It is important to know where Kv1.3 resides within the cell as this may provide insights into the protein function. To determine the cellular localisation of Kv1.3, EGFP-tagged Kv1.3 was expressed in HEK293 cells and the protein localisation was examined through EGFP imaging by confocal microscopy.

Cells transfected with an EGFP plasmid construct (500 ng) showed a disperse intracellular distribution of EGFP across the cell cytoplasm (Figure 5.6a, left panel). In contrast, cells transfected with Kv1.3-EGFP plasmid (500 ng) demonstrated the expression of Kv1.3 mainly on the plasma membrane surrounding the cells (Figure 5.6a, right panel). Due to the fact that HEK293 cells contain a small cytoplasmic space, over-expression of proteins also led to patches of green spots resulting from accumulation of EGFP in the cell cytoplasm or ER/Golgi, which could also be due to cleavage of EGFP. The location of Kv1.3 surrounding the cell is consistent with previous observations on the presence of Kv1.3 on the plasma membrane (Szabò et al. 2005; Panyi et al. 2003). More recently, Kv1.3 was identified in the nuclear fraction of several types of cancer cells and in human brain tissues, which suggests its potential role in the regulation of the nuclear membrane potential and activation of transcription factors (Jang et al. 2015).

It was also clear in this study that endogenous Kv1.3 was expressed in the mock-transfected cells as shown in Figure 5.6c, which was consistent with the results from western blot. Mock-transfected cells probed with PBS (Figure 5.6b) was used as a negative control to indicate the Kv1.3 detection was not an artefact resulted from binding of antibody to non-specific proteins. Previous patch clamp analysis study has shown the presence of endogenous Kv1.3 in HEK293 cells which supports this finding (Yu & Kerchner 1998; Jiang et al. 2002). Notably, DENV-2 NS2A was localised exclusively in the cytoplasmic region (as shown in the previous chapter) (Figure 5.6d). Endogenous Kv1.3 co-expressed with NS2A was observed in Figure 5.6e, whereas overexpression of both Kv1.3 and NS2A (both transfected with 100 ng plasmid constructs) was observed in Figure 5.6f.

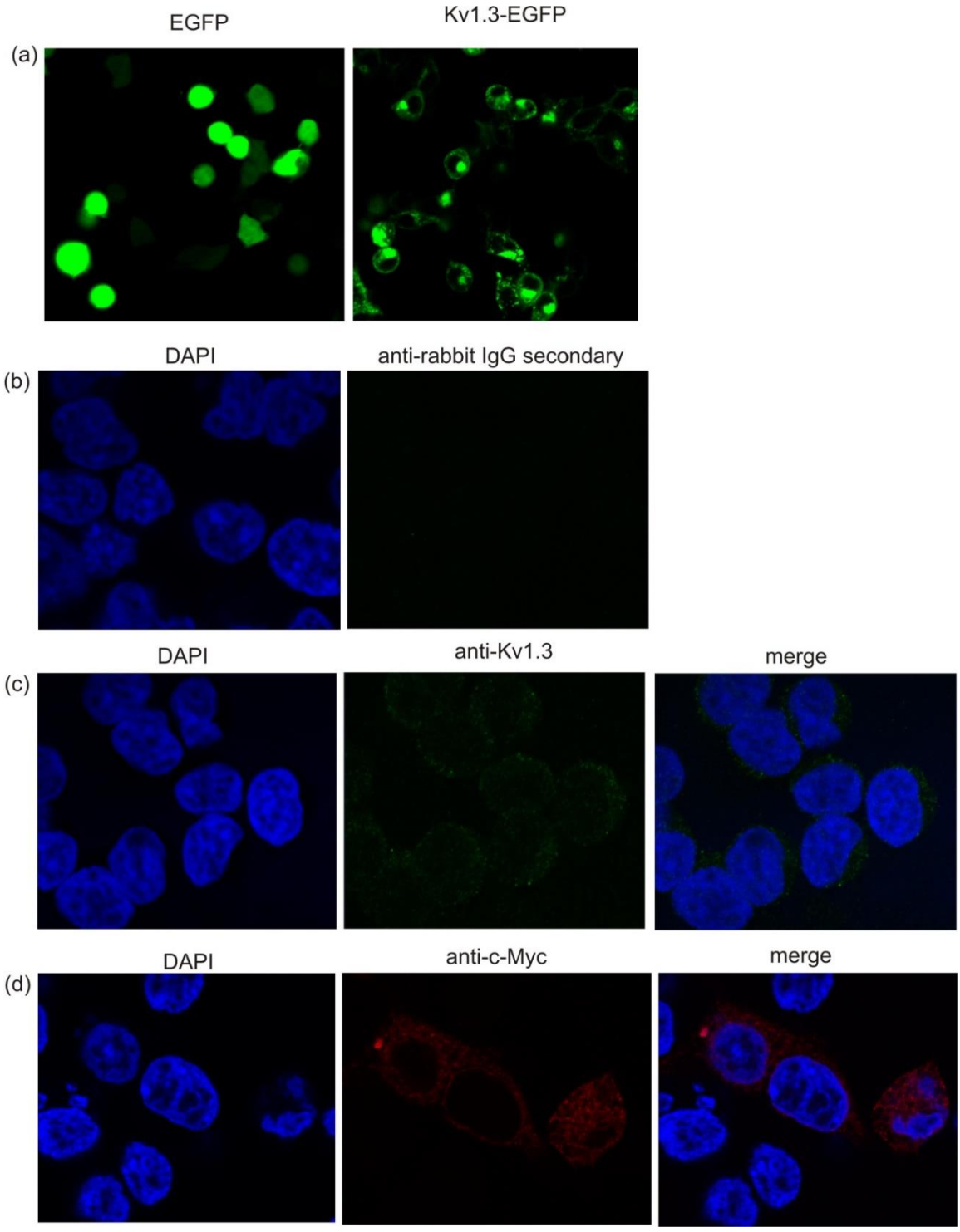
EGFP
Kv1.3-EGFP
(a)
DAPI
anti-rabbit IgG secondary
(b)
DAPI
anti-Kv1.3
merge
(c)
DAPI
anti-c-Myc
merge
(d)

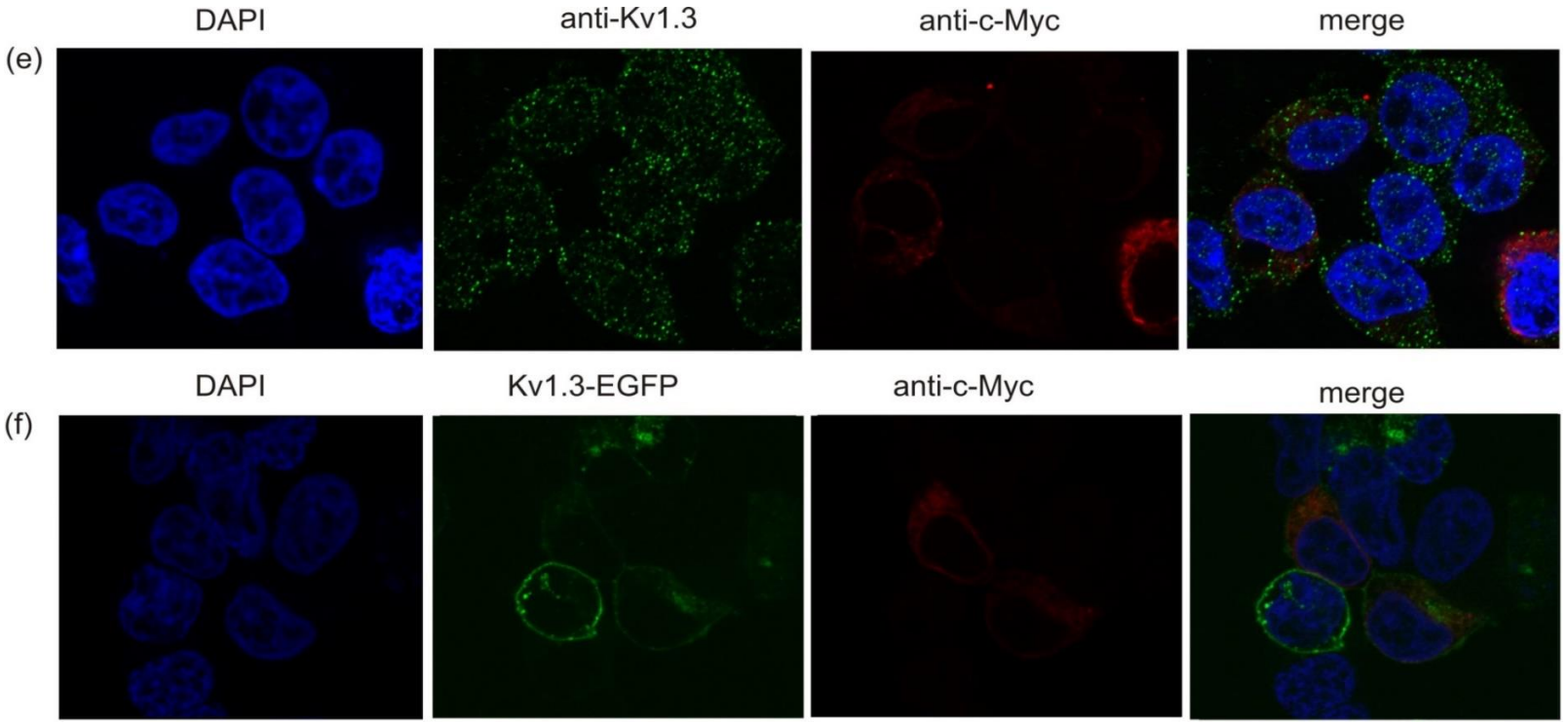

Figure 5.6: Cellular localisation of Kv1.3 and NS2A detected by immunofluorescence staining.

Proteins were co/expressed as follows: (a) EGFP (left panel) and Kv1.3-EGFP (right panel), (b) Mock-transfected cells detected with Alexa Fluor® 488 anti-rabbit IgG (green) secondary antibody (as a control for endogenous Kv1.3), (c) endogenous Kv1.3, (d) NS2A, (e) endogenous Kv1.3 and NS2A, (f) Kv1.3-EGFP and NS2A. Overexpressed Kv1.3 tagged with EGFP was determined by EGFP expression, endogenous Kv1.3 was detected using anti-Kv1.3 and Alexa Fluor® 488 anti-rabbit IgG (green). NS2A was detected using anti-c-Myc and Alexa Fluor® 594 anti-mouse IgG (red). The cells were nuclear-stained with DAPI (blue).

5.3.3 Kv1.3 effect on cell viability

Information derived from previous experiments indicates Kv1.3 is membrane-bound. Excessive amounts of this protein resulting from overexpression (driven by a CMV promoter) may cause improper cell function. It is therefore essential to determine the effective dose of DNA used for transfection that does not affect the overall cell viability. In brief, HEK293 cells were transfected with increasing concentrations of Kv1.3-EGFP plasmid and tested for cell viability 24 hr p.t (Section 2.7.6). As shown in Figure 5.7, the percentage of viable cells decreased to 85.5% during transfection with 25 ng/ ml plasmid and decreased further to 69.9-83.7% for transfection between 50-500 ng/ ml plasmid. Further increase of the plasmid to 1000 ng/ ml resulted in less than 50% of cells remaining viable. Overall, this indicates that Kv1.3 overexpression directly affects the cell proliferation and therefore should be used in concentrations of ≤100 ng/ ml during transfection.

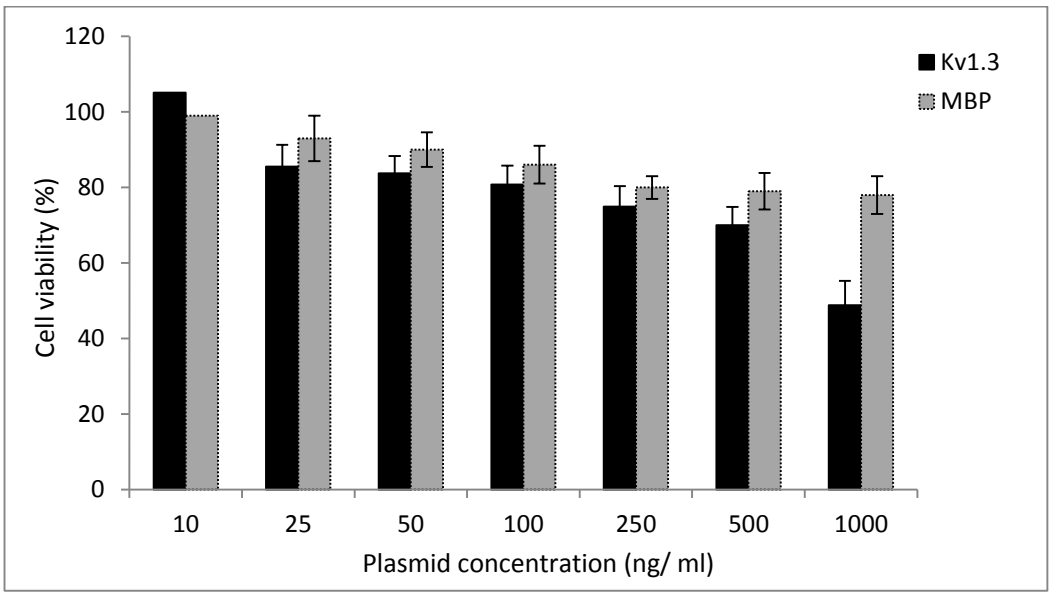

Figure 5.7: Effect of over-expressed Kv1.3 on HEK293 cell viability.

The cells were transfected with 10-1000 ng/ ml Kv1.3-EGFP plasmid and subjected to the cell viability test using CellTiter 96® Non-Radioactive Cell Proliferation Assay. The absorbance values of viable cells were calculated and shown as a percentage relative to the mock (cells treated with Lipofectamine® 2000 CD alone). Data reflects the mean ± standard error of triplicates from three independent experiments.

5.3.4 Effect of Kv1.3 blockade on DENV-2 infection

In order to investigate if Kv1.3 plays a significant role in DENV-2 infection, the channel function was inhibited and the effect was subsequently examined on DENV-2 *FFluc* expression replicon, pDVPACluc (Section 2.4.2). This study was performed by assessing endogenous Kv1.3 which are present at detectable levels in HEK293 cells and relatively mimicked natural cellular condition. Blocking of the Kv1.3 channels was induced through treatment with several K^+ channel blockers, TEA, 4-AP and MgTx.

5.3.4.1 Effect of potassium channel blockers on cell viability

The effect of K^+ channel blockers on cell viability was initially evaluated to select the suitable dose for K^+ channel inhibition before testing on the replicon. TEA, 4-AP and MgTx blockers were gifts from Dr Jamel Mankouri, the University of Leeds. Specific information regarding the blockers is listed in Table 5.1. Briefly, K^+ channel blockers were dissolved in suitable diluents (water for TEA and 4-AP, PBSA for MgTx) and further diluted with DMEM medium to achieve required concentrations (Section 2.7.7, Table 2.16). The effective concentration range varied among inhibitors due to their different inhibitory potency (Judge & Bever 2006). Cells were treated with the blockers for 4 hr, prior to adding the MTT dye for cell viability assay.

The percentage of cell viability was calculated relative to their respective negative controls, though there was no significant difference between the negative controls (water- and PBSA-treated cells) compared to the untreated cells. As shown in Figure 5.8, there was a clear dose-dependent effect of increasing concentration of blockers with a decrease in the percentage of viable cells. Given the low concentration range of MgTx (in nanomolar), MgTx was shown to be the most potent, followed by 4-AP and TEA, respectively. The percentage of viable cells decreased approximately to 80% (a cut-off value for *in-vitro* cytotoxicity) (Sambrook et al., 1989) for treatment with 50 mM, 2.5 mM and 250 nM of TEA, 4-AP and MgTx, accordingly. The suggested dose for use (based on personal communication with Jamel Mankouri), was found to be applicable only for MgTx, as TEA and 4-AP were quickly becoming more toxic at higher doses. Jiang et al. (2002) suggested that less TEA concentrations of 1-10 mM are sufficient

to efficiently inhibited Kv currents as shown by patch-clamp analysis. Overall, concentration of the Kv1.3 inhibitors were selected at 10 mM TEA, 1 mM 4-AP and 10 nM MgTx for use in subsequent experiments.

Table 5.1: List of relevant information describing the potassium channel blockers.

Blocker	Description	Specificity	Suggested dose for use*
Tetraethylammonium chloride (TEA)	Quaternary ammonium salt	Non-selective K+ channel blocker	10-100 mM
4-Aminopyridine (4-AP)	Drug prescribed for multiple sclerosis/ neuromuscular disorders	Non-selective voltage gated K+ channel blocker	0.5-2 mM
Margatoxin (MgTx)	Venom-derived peptide of scorpion *Centruroides margaritatus*	Kv1.3 blocker	20-100 nM

* personal communication with Jamel Mankouri

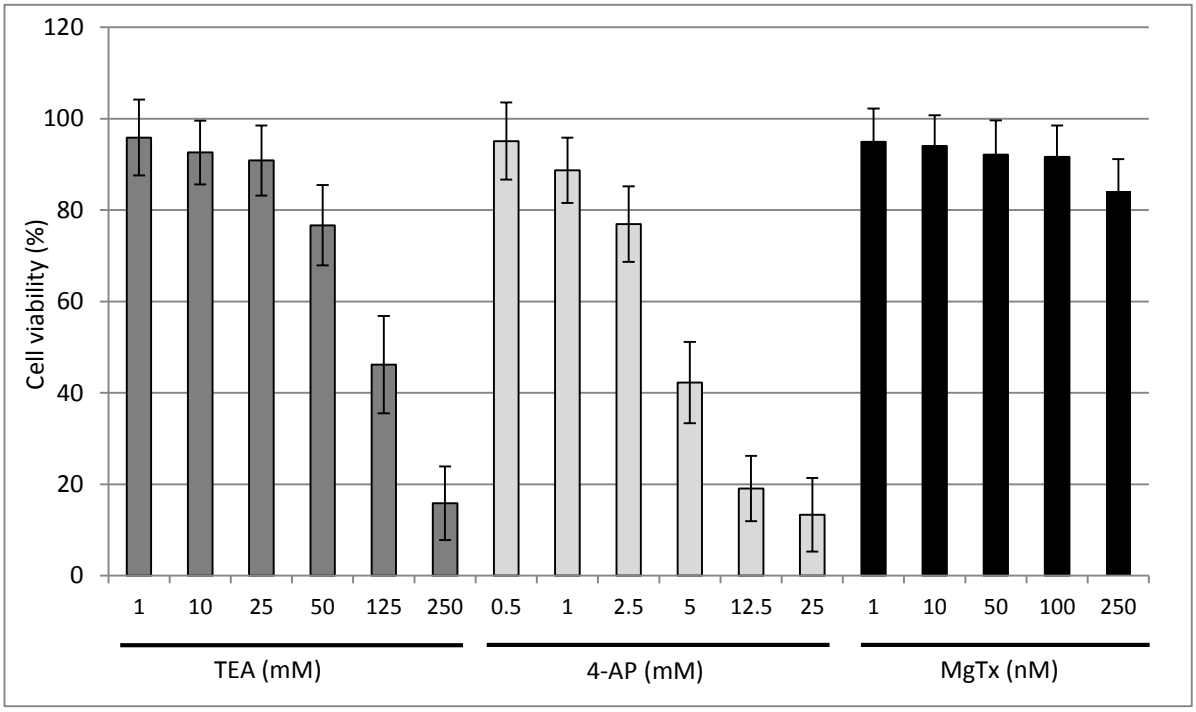

Figure 5.8: Effect of potassium channel blockers on cell viability.

The cells were treated with K^+ channel blockers; TEA, 4-AP and MgTx at various concentrations and subjected to the cell viability assay. The absorbance values were determined at 570 nm reference wavelength using the GloMax multi-detection system. The absorbance values were normalised against their respective negative controls (either PBSA or water) by assigning their values as 100% cell viability. Data reflects the mean±standard error of triplicates from three independent experiments.

5.3.4.2 Effect of MgTx-blocked Kv1.3 on DENV-2 infection

The effect of Kv1.3 blockade on DENV-2 replicon *FFluc* expression was tested using MgTx because of its specific inhibition of Kv1.3 (Helms et al. 1997; Knaus et al. 1995). As it is unclear how DENV-2 interacts with this channel and at which stage would the MgTx affect the replicon, these experiments were performed in two ways: 1) MgTx pre-treatment, by blocking the endogenous Kv1.3 and subsequently introducing DENV-2 NS proteins, and 2) MgTx post-treatment, by expressing DENV-2 NS proteins intracellularly for 6 hr and subsequently inhibiting the endogenous Kv1.3. DENV-2 replicon (pDVPACluc) was *in vitro* transcribed to produce RNA as described in Section 2.6.1 for use in this assay.

MgTx was dissolved in PBSA and diluted with DMEM to achieve required concentrations (0.1-100 nM). These concentrations were used where >80% cells were viable, to ensure the results were not affected by other cellular factors. The diluted MgTx was used to treat HEK293 cells for 4 hr (pre-treatment) followed by co-transfecting the cells with *in vitro* transcribed DENV-2 replicon RNA and pRL-CMV expressing *RLuc* (internal control). After 6 hr p.t (based on results in Section 4.3.6.2 which demonstrated a high *FFLuc* expression as early as 6 hr p.t), the cells were lysed and luciferase activities were measured. Similar experiments were performed but in the opposite sequence to test the replicon for MgTx post-treatment.

There was a slight increase (1.3-fold) in DENV-2 *FFLuc* expression resulting from Kv1.3 blockade using 1 nM MgTx (Figure 5.9, top panel) (Student's *t*-test, *p*-value <0.05). The expression remained constant at this level despite increasing concentrations of MgTx up to 100 nM. A small increase (1.3-fold) in *FFLuc* expression was observed in MgTx post-treatment using 1-10 nM MgTx (Figure 5.9, bottom panel), but the increase was not significant. Increasing doses of MgTx to 50-100 nM subsequently decreased the *FFLuc* expression to its initial basal level, similar to the PBSA negative control. Considering the small differences in *FFLuc* expression which resulted in non-significant statistical values (except as shown in the figure for MgTx pre-treatment), there was no clear or very minimal effect of Kv1.3 blockade on DENV-2 gene expression. This may require a longer incubation time as a result of MgTx treatment to observe a clearer effect. Furthermore, the efficiency of Kv1.3 blockade was not validated in this study. It is thus unknown if

the channel was completely inhibited which may give more reliable *FFLuc* expression. Further to this, the DENV-2 replicon has not been shown to replicate in HEK293 cells (as described in previous chapter), hence resulting in unconvincing *FFLuc* expression.

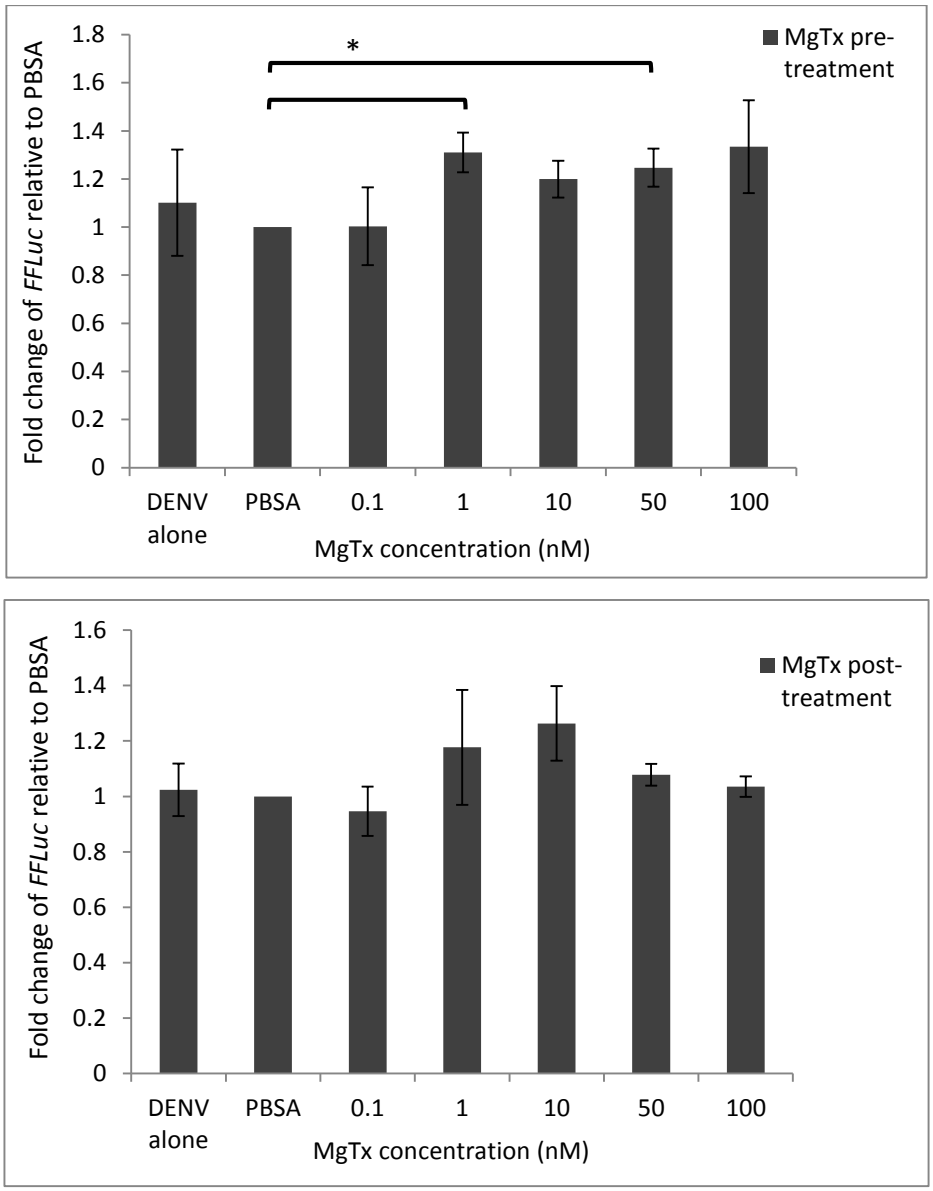

Figure 5.9: Effect of MgTx on *FFLuc* expression from DENV-2 replicon.

Top panel shows MgTx pre-treatment, in which Kv1.3 was inhibited prior to introducing the in vitro transcribed DENV-2 replicon RNA. Bottom panel shows MgTx post-treatment, where the replicon RNA was introduced into the cells followed by Kv1.3 inhibition. Data represents the fold change of FFLuc expression normalised to the PBSA negative control performed in triplicates from three independent experiments. Asterisk (*) indicates Student's t-test, p-value <0.05.

5.3.5 Effect of Kv1.3 on dengue virus replication

As experiments with DENV-2 replicon *FFLuc* expression were unable to produce reliable data, subsequent experiments were carried out by using infectious DENV-2. This study aimed to investigate the importance of K^+ channel in DENV-2 replication by inhibiting the functional Kv1.3 using K^+ inhibitors prior to virus infection. As mentioned in the previous chapter, work concerning the infectious DENV-2 was performed by Amjad Yousuf in a Containment Level 3 facility, University of Bristol. In brief, HEK293 cells were treated with K^+ channel blockers (Table 2.16) (10 mM TEA, 1 mM 4-AP and 10 nM MgTx) for 4 hr and subsequently infected with DENV-2 NGC strain. The infectious material was replaced by fresh medium containing the appropriate blockers to inhibit the K^+ channel. Isolated RNA samples were subjected to qRT-PCR with TaqMan probes and primers targeting the DENV-2 capsid region.

There was a clear decrease in DENV-2 gene expression as a result of the K^+ channel blockade (Figure 5.10). The most significant effect was caused by 4-AP (52%-decrease relative to PBSA), followed by MgTx and TEA giving approximately 30% and 26% decrease, respectively. Although there was no water control for TEA and 4-AP (as they were initially dissolved in water), these blockers have been diluted 100x in DMEM prior to the treatment, which greatly diluted the effect of water diluent. The overall data indicates blockade of Kv1.3 affects DENV-2 replication suggesting this channel may have a pro-viral activity that facilitates virus replication. Further biological replicates and assessment of potential mechanism (especially the role of NS2A) are required to support this finding.

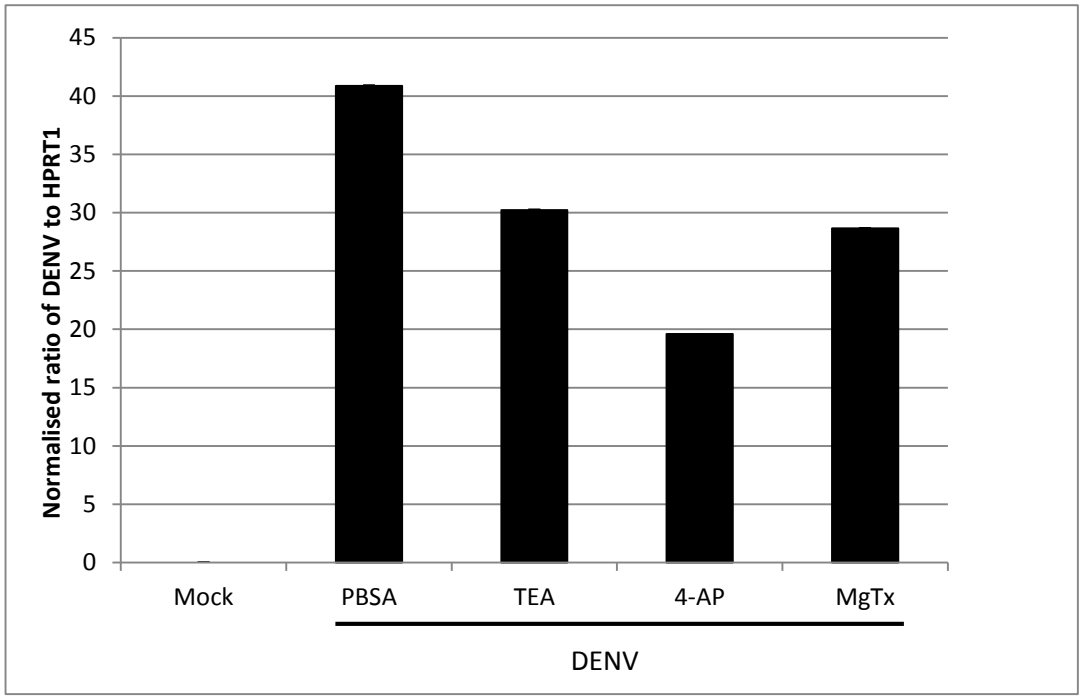

Figure 5.10: Gene expression of DENV-2 capsid region in HEK293 cells exhibiting Kv1.3 blockade.

The activity of K^+ channels was inhibited by TEA, 4-AP and MgTx. PBSA was used as a negative control for MgTx treatment. Data represents an average viral copy numbers from triplicate wells of qRT-PCR reactions. The viral copy numbers were generated from a standard curve based on cycle threshold (Ct) values and normalised to the human HPRT1 internal control. Error bars indicate standard error of triplicate wells. Data obtained in this study was derived from pooled of triplicate samples, generated in a single experiment.

5.4 Discussion

HEK293 cells were used in this study to assess the interaction between DENV-2 NS2A and Kv1.3. Although this cell line has been previously reported to be lacking the expression of endogenous Kv1.3 (Levitan & Barrantes 2012), the channel was successfully over-expressed and its endogenous form has been detected in this study by western blot and IF staining. This is supported by several patch-clamp studies which demonstrated endogenous Kv currents (Yu & Kerchner 1998; Jiang et al. 2002). Kv1.3 is a membrane-bound protein (Cahalan et al. 1985) and therefore is difficult to dissociate during cell lysis. The use of a lysis buffer such as 1% NP-40 is capable to efficiently disintegrate the cell membrane properties. It is noteworthy that Kv1.3 has been identified in the nucleus (Jang et al. 2015), mitochondrial inner membrane (Szabò et al. 2005; Bednarczyk et al. 2010) and is highly expressed in cancer cell lines (Jang et al. 2009; Wu et al. 2013; Preußat et al. 2003).

Further examinations by co-IP/pull-down assay using Protein A-tagged DENV-2 NS2A and EGFP-tagged Kv1.3 demonstrated both proteins co-precipitate and are detected in the pull-down samples. Moreover, it is interesting that NS2A was able to capture the endogenous Kv1.3 and detected in the pull-down samples which confirms interaction exists between both proteins. It is known that different cell lines express different types and different Kv channel expression level. HEK293 cells seem to have a detectable level of endogenous Kv1.3 as shown by western blot and IF. Based on these observations and the fact that endogenous Kv1.3 more likely resembles the natural condition, experiments analysing the effects of blocked endogenous Kv1.3 on DENV-2 infection were performed.

In order to determine the importance of Kv1.3, the effect of endogenous Kv1.3 blockade was evaluated using a DENV-2 replicon. While both experiments showed a small increase in translation of DENV-2 NS proteins resulting from Kv1.3 blockade at 1-10 nM MgTx, results from the experiments in general did not indicate a clear effect (based on statistical analysis) to derive a conclusion. It is known that MgTx has a reversible effect (Garcia-Calvo et al. 1993). Thus, removing MgTx from the culture cells during pre-treatment with MgTx may have restored the activity of Kv1.3 and the normal cellular functions, which allows DENV-2 translation to take place. This has led to a small increase in DENV-2 translation as seen with an

increase in *FFLuc* expression. Besides that, patch-clamp experiments were not performed in this study to confirm the channel blockade. It is therefore unknown if the Kv1.3 function was completely inhibited prior to testing with the DENV replicon assay. It is also possible that this assay would require the use of whole infectious virus particles to modulate specific host cellular interactions as naturally occuring virus infection. An alternative explanation would be that Kv1.3 is not necessarily involved in DENV replication but is needed for an earlier or later stage in the virus life cycle. This has been previously reported in K^+ (K_{2P}) channel during infection with Bunyamwera virus (BUNV) (Hover et al. 2016). Using specific K^+ channel modulating agent, the K^+ channel function has shown to be critical to events shortly after virus entry but prior to viral replication.

Further analysis was carried out to study the effect of Kv1.3 blockade on DENV-2 replication using the infectious DENV-2 NGC strain. Three blockers, TEA, 4-AP and MgTx, exhibiting different specificity towards K^+ channels (Table 5.1), were used to inhibit the channel function. TEA and 4-AP have been described to block the K^+ channels from the cytoplasmic side of the cell membrane, which occurs through modulation of conformational changes to these channels rendering them closed (Armstrong & Loboda 2001; Choquet & Korn 1992). MgTx in contrast, was proposed to act in either of two ways; through binding on the extracellular side of the channel pores therefore obstructing the pore, or by binding and modulating the voltage sensor region (S1-S4) of the K^+ channel (Judge & Bever 2006). Inhibition of K^+ channels by these blockers usually resulted in abrogated Kv currents analysed by patch-clamp (Kazama 2015; Hu et al. 2007; Gazula et al. 2010).

The effect of Kv1.3 blockade on DENV-2 replication was demonstrated by gene expression qRT-PCR analysis of the DENV-2 capsid gene. Data were normalised to the human housekeeping gene, hypoxanthine phosphoribosyltransferase 1 (HPRT1) which has removed any effect of blockers on the cells. It was interesting to observe a clear decrease in DENV replication as a result of the K^+ channel blockade in 4-AP, MgTx and TEA, accordingly. As TEA blocks all K^+ channels due to its capacity as a non-selective K^+ blocker, reduction of the virus replication signifies the importance these ion channels in regulating DENV-2 infection. The most prominent effect that decreased DENV-2 replication occurs during blockade of all voltage-gated channel including Kv1.3 by 4-AP, whereas blockade of Kv1.3 using

MgTx exhibited almost similar DENV-2 replication level to TEA. This suggests rather than Kv1.3, other Kv channels may be involved in DENV-2 replication. Therefore, although functional Kv1.3 is abrogated, other Kv channels are functional and able to facilitate infection.

While blocking the K^+ channels using chemical ion blockers or peptides represents a reliable assessment tool to develop potential pharmacological therapy, co-inhibition of other unspecific channels or the entire sub-family of the same channels makes it difficult to interpret the effect of a specific cellular response. Although MgTx has a high affinity to Kv1.3 (Helms et al. 1997; Garcia-Calvo et al. 1993), recent report suggests that the action was non-specific as the peptide concurrently inhibited Kv1.1 and Kv1.2 (Bartok et al. 2014). This complicates the findings, thus analysis by Kv1.3 gene silencing may be an effective way to ensure a specific target for inhibition. Apart from that, other highly-specific Kv blockers such as ShK derived from sea anemone *Stichodactyla helianthus* toxin (Kalman 1998), and non-peptide blocker PAP-1 (Schmitz et al. 2005) can be tested in parallel to block Kv1.3 activity. Reversal of the inhibitory effect of K^+ channel by removing the blockers from the test system may confirm the specific effect of this channel to DENV-2 infection.

Other relevant issues in this study include the fact that the native HEK293 cells are not homogenous in terms of the expression of Kv channels (Jiang et al. 2002). Besides Kv1.3, other Kv α-subunit genes are present including the Kv1.1, Kv1.2, Kv1.6, the transient outward Kv channels, Kv1.4, Kv3.3, Kv3.4, Kv4.1, and other Kvβ subunit genes (Jiang et al. 2002). This also creates diversity of functional Kv channels due to heterogeneous assembly of different Kv subunits rather than by assembly of four homogenous subunits. In particular, Kv1.3 can form heterotetrameric channel arrangements *in vivo* with other subunits from Kv1 sub-family including Kv.1.1, Kv1.2, and Kv1.6 (Gazula et al. 2010).

5.5 Conclusion

Interaction between DENV-2 NS2A and Kv1.3 was observed through co-IP/pull-down assay which confirms the previous findings from Y2H and LUMIER assay. K^+ channels, in particular the voltage-gated channels, seem to play a role in DENV-2 replication. Although it was difficult to conclude the importance of Kv1.3 due to its heterogenous native form in HEK293 cells, this channel, together with other Kv channels may contribute to the virus infection. It is also possible that Kv1.3 is not necessarily involved in DENV replication but is needed for an earlier or later stage in the virus life cycle. Further analysis including the experiments in mice model may extend our understanding of the role of Kv1.3 channels in DENV infection.

CHAPTER 6: ESTABLISHMENT OF *Ae. aegypti* cDNA LIBRARY

6.1 Introduction

Ae. aegypti and *Ae. albopictus* are primary vectors that transmit DENV (Gubler 1998). The virus is ingested during a mosquito blood meal, and infects the midgut epithelial cells and disseminates to the salivary glands (Salazar et al. 2007). During infection, the mosquito mounts innate immune responses, however the virus persists in the mosquito and is capable of being transmitted to the next vertebrate host (Sánchez-Vargas et al. 2009). It is therefore of particular interest to investigate the way mosquitoes control DENV infection, particularly through their antiviral defence mechanisms to ensure survival. This would also contribute to a greater understanding of protein-protein interactions between DENV-mosquito systems thus providing insights into the mechanism by which specific proteins and/or pathways play an important role during virus infection.

Several studies have predicted protein-protein interactions between DENV and its mosquito host (Mairiang et al. 2013; Doolittle & Gomez 2011; Guo et al. 2010). Although a large number of DENV-interacting mosquito proteins have been identified, very little has been validated to reveal their biological importance. This limits the knowledge of a precise mechanism contributing to successful virus replication in the mosquito. A genome-wide RNAi screen using DENV-2 strain adapted to *D. melanogaster* identified 116 host factors, including vacuolar ATPases and alpha-glucosidases that facilitate virus replication (Sessions et al. 2009). A number of cellular events occur in DENV-infected *Ae. albopictus* proteomes suggesting the involvement of oxido-reduction stress and activation of glycolysis pathways and cellular damage (Patramool et al. 2011). It has also been shown that alteration of protein expression in DENV-2 infected salivary glands of *Ae. aegypti*, including aegyptin, enhances virus replication (Chisenhall et al. 2014; Wasinpiyamongkol et al. 2012), and upregulation of cadherin on the surface of mosquito cells suggests a potential receptor for DENV (Colpitts et al. 2011). Using virus overlay protein binding assay (VOPBA), Cao-Lormeau (2009) identified several DENV-binding proteins between 37 and 77 kDa from *Ae. aegypti* salivary glands, however the protein identities were unknown.

Aside from various non-immune host proteins expressed as a result of virus infection, proteins involved in immune signalling pathways are equally important. This is due to the fact that innate immunity plays an important role in insects to counter microbial challenges (Kingsolver et al. 2013; Hoffmann 1995). Most studies of insect immunity have been conducted in *D. melanogaster* as an insect model. Innate immune pathways including the Janus kinase signal transducer and activator of transcription (JAK-STAT), immune deficiency (IMD), Toll pathways, are known to respond to microbial infection, which activates the transcription of genes involved in defense (Sim et al. 2014; Sabin et al. 2010). Activation of these genes triggers proteolytic cascades in the haemolymph that leads to melanisation of the invading microbe at the site of injury, cellular responses such as phagocytosis or encapsulation of foreign material, and production of effector molecules through the secretion of antimicrobial peptides from the fat body (Ferrandon et al. 2007; Agaisse & Perrimon 2004; Hoffmann 1995). Seven inducible antimicrobial peptides have been described in *Drosophila,* exhibiting defense against Gram-negative bacteria (attacins, cecropins, drosocin, diptericins), Gram-positive bacteria (defensin) and fungi (drosomycins, metchnikowin) (Bulet 1999).

The JAK-STAT pathway has been demonstrated to be involved in *Ae. aegypti* antiviral response against DENV (Souza-Neto et al. 2009), as well as in *Drosophila* against Drosophila C virus (Dostert et al. 2005). Knockdowns and mutations in JAK kinase have been shown to cause an increase in viral infection, indicating JAK/STAT plays a role in the antiviral response as a result of STAT-dependent expression of regulated effector molecules (Souza-Neto et al. 2009; Dostert et al. 2005). The IMD pathway in *Drosophila* produces antimicrobial peptides mainly to counteract Gram-negative bacteria (Lemaitre et al. 1995). This pathway is also involved in defence against viruses and has been shown to enhance Sindbis virus replication when pathway components were mutated (Avadhanula et al. 2009). The Toll pathway is activated against fungi, Gram-positive bacteria, and viruses (Zambon et al. 2005; Rutschmann et al. 2002; Lemaitre et al. 1996) and has been reported as an antiviral defence against DENV (Xi et al. 2008). Although the JAK-STAT, IMD and Toll pathways have been implicated in many virus infections, the exogenous RNAi pathway is thought to be the most significant antiviral response (Donald et al. 2012; Blair 2011). This type of defence pathway has been shown to

be induced by DENV and SFV in mosquitoes and their derived cell lines (Siu et al. 2011; Sánchez-Vargas et al. 2009).

A search for host factors or finding relevant genes involved in virus infection, can be achieved through screening of an appropriate host cDNA library. Construction of cDNA libraries derived from tissue specific organisms or cell cultures can be established for investigation of their functions as well as for protein-protein interaction analysis (Mayhew et al. 2007; Gomez et al. 2005). The available *Ae. aegypti* genome sequence has revealed 15,419 putative genes and 80% were protein coding regions (Nene et al. 2007). This data, in combination with the high-throughput gene expression and reverse genetic studies, provides opportunities to study the mosquito immune responses against DENV infection. Transcriptomic analysis has been able to identify specific genes potentially involved in xenobiotic response and insecticide tolerance (David et al. 2010). In this study, the use of an *Ae. aegypti* cDNA library is useful to screen for protein-protein interactions between DENV and its primary host. There is however, a lack of a commercially available *Ae. aegypti* cDNA library expressed in yeast, thus an attempt to construct the library was initiated. Although an *Ae. aegypti* cDNA library generated from tissue midguts has been successfully established in yeast (Tham et al. 2014), the present study was undertaken to construct a library from *Ae. aegypti*-derived Aag2 cells.

There are two techniques commonly used for construction of Y2H libraries, which include the ligation-assisted cloning and recombination-based cloning. The ligation-assisted technique has several limitations, such as an additional digestion-ligation step, the risk of enzymatic cleavage of cDNA clones containing the restriction enzyme sites and size bias in the ligation reaction (Ohara & Temple 2001). In contrast, the recombination-based technique is much simple and requires only a single step to incorporate cDNA inserts into the vector. The recombination technique has a higher transformation efficiency and has been shown to produce a high number of full-length cDNA clones (Ohara & Temple 2001; Zhu et al. 2001). In this study, the recombination-based strategy was adopted using the Make Your Own 'Mate and Plate™' Library System (Clontech). This technique uses the cap-switch mechanism to incorporate SMART sequences and allow enrichment of full-length cDNA (as described in Section 2.8)(Zhu et al. 2001;

Chenchik et al., 1998). Directional cloning occurs through homologous recombination of highly specific *att* sites between the cDNA and cloning vectors, which can take place either *in vitro* or *in vivo*. This study took advantage of the capability of yeast, *S. cerevisiae,* which is known to carry out homologous recombination efficiently *in vivo* through double-strand break repair mechanism (Oldenburg et al. 1997; Ma et al. 1987).

6.2 Objectives

1. To generate an *Ae. aegypti* cDNA library for Y2H screen against DENV NS proteins.

2. To establish mosquito immune signalling experiments.

3. To assess the expression of DENV non-structural proteins in mosquito cells.

6.3 Results

6.3.1 Construction of *Ae. aegypti* cDNA library

6.3.1.1 Isolation of Aag2 RNA

To construct a cDNA library, isolation of high integrity RNA is essential. A crude method to determine the RNA integrity is through analysis of the highly abundant 28S and 16S ribosomal RNA (rRNA). Prior to generating a mosquito cDNA pool, total RNA was harvested from *Ae. aegypti*-derived Aag2 mosquito cells using TRIzol® reagent (Section 2.2.1) and the RNA yield was determined using NanoDrop™ 1000 spectrophotometer (Section 2.2.8). The isolated RNA was estimated at 950 ng/µl and $A_{260/280}$ ratio 2.05, which complied with the recommended range for pure RNA (Sambrook et al., 1989). Further analysis of the Aag2 rRNA profiles on a non-denaturing agarose gel demonstrated two distinct bands approximately at 0.8 and 1.2 kb corresponding to the 28S and 18S rRNA (Figure 6.1), which indicated intact rRNA. There was an absence of a smear along the gel with no indication of RNA degradation. High integrity RNA isolated from *Anopheles* sp. tissues has been shown to produce similar rRNA profiles, which correlated to this study (Macharia et al. 2015).

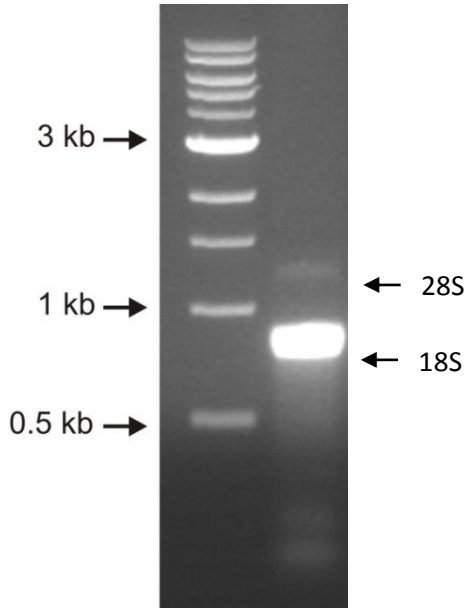

Figure 6.1: 28S and 18S ribosomal RNA profile analysis of Aag2 cells.

The RNA was harvested from Aag2 cells and separated on a 1.2% non-denaturing agarose gel. Marker is 1 kb DNA ladder (NEB).

6.3.1.2 Amplification of Aag2 cDNA

The RNA obtained from Aag2 cells (described above) was immediately used for construction of the *Ae. aegypti* cDNA library using the Make Your Own `Mate & Plate™' Library System (Clontech). In brief, the RNA was reverse-transcribed by MMLV reverse transcriptase using an oligo (dT) primer containing CDS III sequences followed by SMART oligonucleotides to generate cDNA. During this process, SMART sequences were introduced to both 5' and 3' ends of the cDNA. This was followed by LD-PCR amplification of the cDNA using Advantage® 2 Polymerase Mix (Clontech) for 20 and 25 cycles according to the manufacturer's instructions (Section 2.8.1.3). A mouse liver poly A^+ RNA was run in parallel as a positive control. In order to check the quality of ds cDNA, the amplified products were separated on agarose gel electrophoresis. As shown in Figure 6.2 (lane 3), *Ae. aegypti* cDNA had a size range of between 0.1-2 kb after 20 cycles of PCR amplification. Increasing the PCR cycles to 25 (the maximum number of cycles suggested by the manufacturer) produced cDNA between 0.3-2 kb (Figure 6.2, lane 4). As this has higher MW and generated a more uniform smear indicating good cDNA (Islam et al. 2012), the sample was selected for construction of the mosquito library. It was shown that the positive control mouse liver poly A^+ exhibited cDNA smear ranging between 0.3-6 kb (Figure 6.2, lane 2). A more intense smear covering a larger MW range was seen in this sample as it came from purified poly A^+, therefore produced a good amplification signal.

Prior to transformation into yeast, the cDNA was size-fractionated to obtain >200 bp transcripts followed by ethanol precipitation to purify the cDNA. This step removed the low MW ds cDNA or unincorporated nucleotides which allowed enrichment of the cDNA with full-length and larger inserts (Wellenreuther et al. 2004). Following resuspension of the cDNA in nuclease-free water, the total ds cDNA was 86.4 ng/ µl which gave 1.7 µg in total, $A_{260/280}$ ratio 1.7 and $A_{260/230}$ ratio 2.59. The cDNA yield was lower due to removal of lower MW cDNA, however the amount did not achieve the expected 2-5 µg, as suggested by Clontech. Due to the low cDNA yield, the above steps with regard to PCR amplification, size fractionation and purification of the cDNA were repeated using a fresh aliquot of the first-strand cDNA. The resulting ds cDNA ($A_{260/280}$ ratio 1.72 and $A_{260/230}$ ratio 2.3) was pooled and 3 µg was used for construction of the mosquito cDNA library.

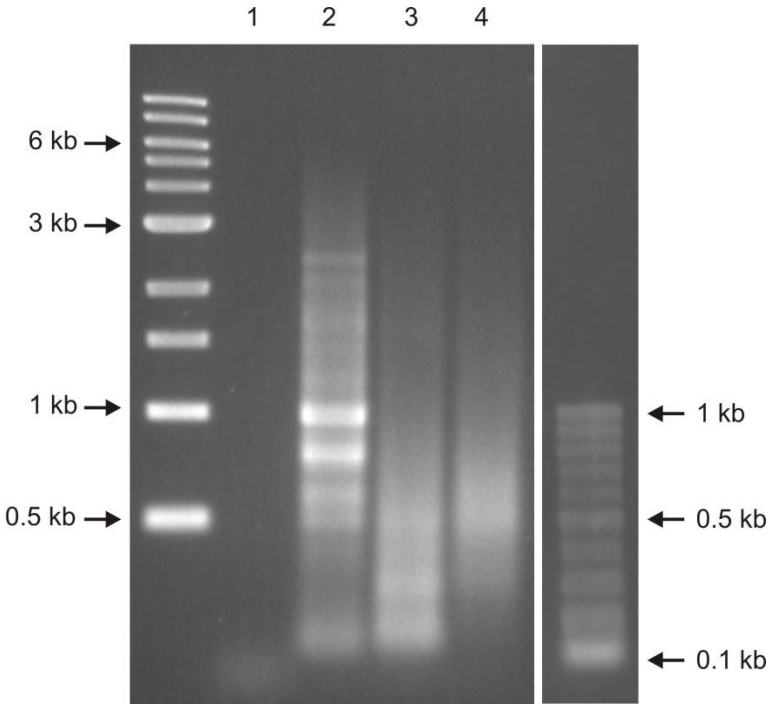

Figure 6.2: Amplification of Aag2 mosquito cDNA by LD-PCR.

The amplified products were separated on 1.2% agarose gel. Figure denotes: Lane 1: water negative control; Lane 2: cDNA of mouse liver poly A^+ positive control; Lane 3: cDNA of Aag2 amplified for 20 cycles; Lane 4: cDNA of Aag2 amplified for 25 cycles. Markers are 1 kb DNA ladder (NEB) and GeneRuler™ 100 bp DNA ladder (Thermo Scientific).

6.3.1.3 Complexity and titre of library

Prior to transformation into yeast, the Aag2 cDNA was further evaluated for complexity. This determined if the library was representative enough for comprehensive cDNA analysis. Three mosquito gene fragments; *Actin*, *Dicer-2* and *Argonaute-2*, were amplified by standard PCR using the cDNA as a template. *Actin* represents highly conserved housekeeping gene which is present in all stages of mosquito development (Salazar et al. 2007; Mounier et al. 1992), therefore should be picked up during PCR. *Dicer-2* and *Argonaute-2* are key factors responsible for mosquito RNAi immune pathway (Blair 2011), and should be present in Aag2 as the cells are RNAi competent (Scott et al. 2010). As shown in Figure 6.3, the gene fragments were detected at their corresponding sizes, indicating the cDNA library was likely to be satisfactory. Although only fragments of the genes were amplified, this would normally indicate a full length gene.

In order to allow the expression of mosquito proteins in yeast, the Aag2 cDNA was co-transformed with *Sma*I-linearised pGADT7-Rec into competent yeast strain Y187 (Section 2.8.3). As described in Figure 2.7, the linear pGADT7-Rec has compatible sequence ends to the SMART III and CDS III sequences of the Aag2 cDNA which allows homologous recombination in yeast. As a positive control, SV40 large-T PCR fragment with flanking SMART sequences was co-transformed with linear pGADT7-Rec, alongside transformation of the linear pGADT7-Rec alone. The resulting library titer was determined as described by Clontech. Based on the number of yeast colonies grown on the dilution plates, the Aag2 cDNA library titer was estimated at 2.3×10^3 cfu/ ml. The total number of independent clones which served as an indication of the library complexity was 3.45×10^4. This data however does not meet the standard number of independent clones suggested by Clontech ($>1 \times 10^6$).

Furthermore, co-transformation of the positive control SV40 large-T PCR and linear pGADT7-Rec was expected to obtain ten times more yeast colonies than those transformed with linear pGADT7-Rec alone (as suggested by Clontech). Results from this study however, failed to obtain any colonies on both transformation plates. As it was not known if yeast competency could be the reason of this failure, further assessment was performed by making a competent yeast strain AH109, using the same protocol and reagents that were used to make

competent Y187 yeast, and transformed with a positive control pGBT9 (supplied by Clontech). Although a different yeast host strain was used, a transformation efficiency of 3 x 10^5 cfu/ µg plasmid DNA was obtained as suggested by Clontech, which is also in agreement to previous study (Cao & Yan 2013). This indicates a satisfactory transformation efficiency, nearly equivalent to 1 x 10^6 cfu/ µg plasmid as required for transformation (Gietz & Schiestl 2007; Klickstein 2001).

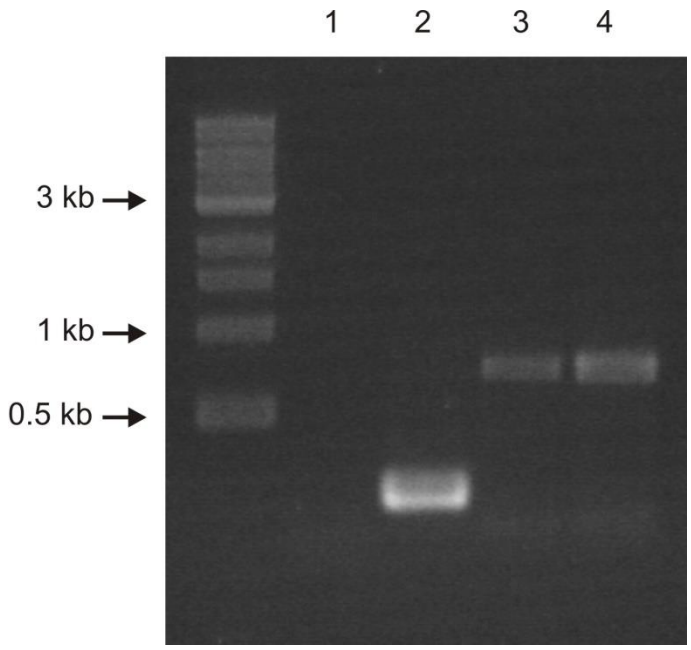

Figure 6.3: Amplification of mosquito gene fragments.

Standard PCR amplification was performed using Aag2 cDNA template. Amplification of *Actin* (250 bp), *Dicer-2* (800 bp) and *Argonaute-2* (780 bp) are shown in lane 2, 3 and 4, respectively. Lane 1 is a PCR water negative control. Markers are 1 kb DNA ladder (NEB).

6.3.2 Mosquito immune signaling pathways

The use of mosquito-derived cell lines to study innate immunity is important to reflect the natural host immune response restricting DENV infection in mosquitoes. Immune-competent Aag2 cells have been widely used to study immune signalling pathways in response to arbovirus infection (Barletta et al. 2012; Sim & Dimopoulos 2010a). *Ae. albopictus*-derived C6/36 cells have been previously shown to be permissive for a wide range of arboviruses and are able to promote DENV replication (White 1987). In order to test for an interaction or functional correlations between DENV and any mosquito interacting partners resulting from Y2H, downstream experiments involving the mosquito immune signalling pathways were initially optimised.

6.3.2.1 Activation of JAK/STAT, IMD and Toll pathways

The present study was carried out using Aag2 and C6/36 cells to assess activation of STAT, IMD and Toll pathways upon exogenous stimulation (as described in Section 2.8.6). Three *FFLuc* reporter constructs; p6x2DRAF-Luc containing multimerised *Drosophila* STAT-responsive element, pJL169 containing IMD-responsive *Drosophila Attacin A* promoter, and pJM648 containing Toll-responsive *Drosophila Drosomycin* promoter, were used to test for activation of JAK/STAT, IMD and Toll pathways, respectively. The JAK/STAT and IMD pathways were stimulated by introducing heat-inactivated *E. coli* as previously described (Fragkoudis et al. 2008), whereas Toll pathway was stimulated by co-transfecting pJL195, a constitutively active Toll ΔLRR mutant under control of *Drosophila* Actin 5C gene promoter (Tauszig et al. 2000). PBS was used as negative control for STAT and IMD stimulation, whereas for Toll, the negative control was cells not transfected with pJL195. pAct-*Renilla* expressing *RLuc* under the control of Drosophila *Actin* promoter was used as internal control for transfection.

There was a significant increase of *FFLuc* expression (Student's *t*-test, *p*-value <0.05) corresponding to JAK/STAT and IMD pathways of Aag2 cells upon stimulation with *E. coli* (Figure 6.4, top panel). Similarly, an increase of *FFLuc* expression (Student's *t*-test, *p*-value <0.05) was also seen in JAK/STAT and IMD pathways of C6/36 cells (Figure 6.4, bottom panel), suggesting the mosquitoes are responsive to the *E. coli* exogenous stimulus, therefore triggering the activation of JAK/STAT and IMD pathways. In contrast, there was no clear activation of Toll pathway in both Aag2 and C6/36 cell lines as a result of pJL195 stimulation. This was quite surprising as Toll activation has been previously demonstrated in *Ae. albopictus*-derived U4.4 cells (Fragkoudis et al. 2008).

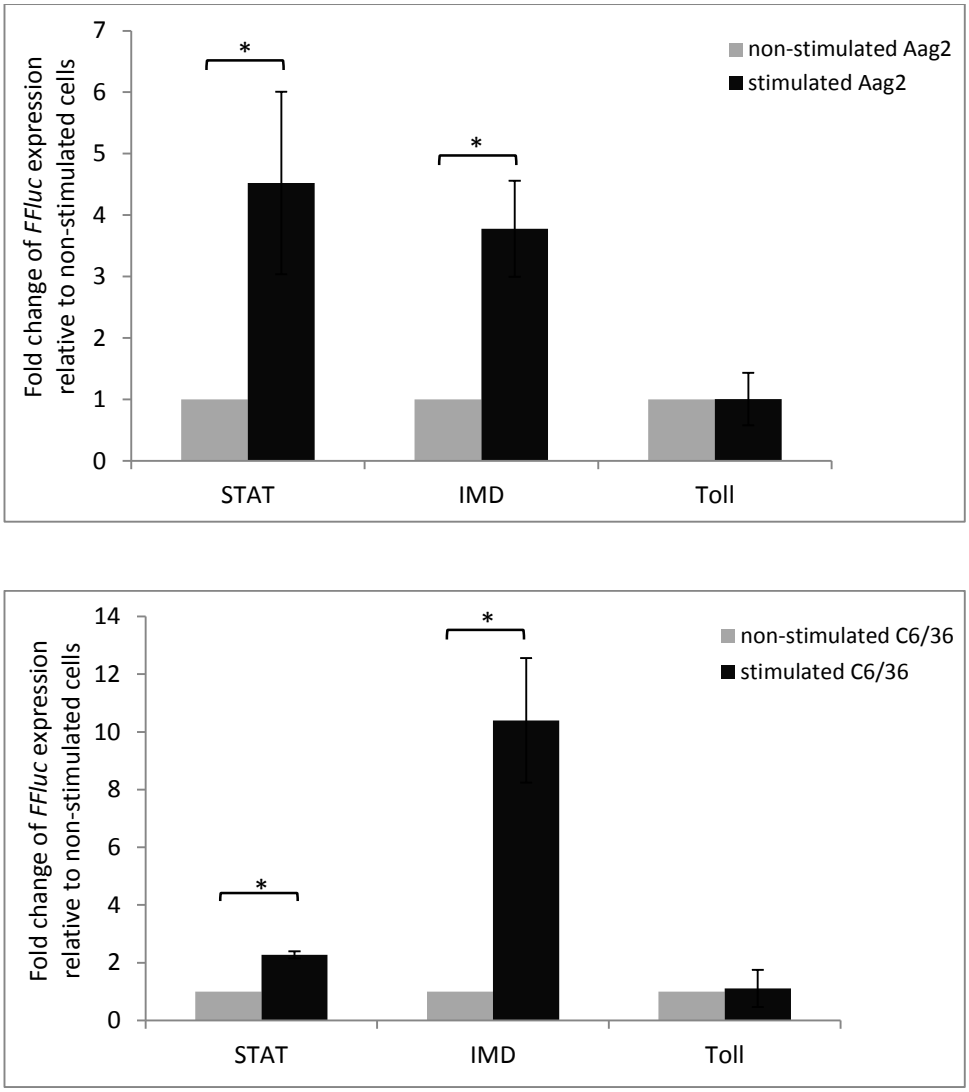

Figure 6.4: Activation of JAK/STAT, IMD and Toll immune signaling pathways.

Activation of JAK/STAT, IMD and Toll immune signaling pathways in Aag2 (top panel) and C6/36 cells (bottom panel). Both cell types were transfected with either p6x2DRAF-Luc, pJL169 or pJM648 expressing *FFLuc* corresponding to the JAK/STAT, IMD and Toll antimicrobial peptide promoters respectively. For JAK/STAT and IMD, the cells were stimulated with heat-inactivated *E. coli* or PBS (non-stimulated cells). For Toll pathway, the cells were either co-transfected with pJL195 for stimulation or without pJL195 (non-stimulated cells). Ratio of *FFLuc* values were calculated against the *RLuc* internal control and normalised by assigning a value of 1 to the level of the corresponding non-stimulated cells. Graph represents the average ratio of *FFLuc* to *RLuc* activities ± standard error of triplicates from three independent experiments. Statistical significance was determined by paired Student's *t*-test (*p*-value <0.05) indicated by an asterisk (*).

6.3.2.2 Activation of Toll pathway by pJL195-expressed Toll receptor mutant

Activation of the Toll pathway was further optimised in Aag2, C6/36 and *Ae. albopictus* U4.4 cells. U4.4 was tested in parallel because this cell line has previously shown an activation of the Toll pathway using similar experimental settings (Fragkoudis et al. 2008). In order to allow for comparable Toll stimulation, an empty insect expression vector pIB/V5 and pIB-MBP plasmid expressing MBP were used as negative controls for stimulation. Due to the fact that the efficiency of pJL195 in stimulating Toll pathway was unknown, two methods of Toll pathway activation were tested: 1) by co-transfecting Toll reporter plasmid pJM648 with either pIB/V5, pIB-MBP or pJL195 followed by cell lysis 24 hr p.t, and 2) by pre-stimulating cells with pIB/V5, pIB-MBP or pJL195, followed by transfecting pJM648 Toll reporter plasmid after 24 hr. Pre-stimulation of the Toll pathway prior to transfection with the Toll reporter pJM648 was expected to allow longer time for stimulation to be assessed. pAct-*Renilla* internal control was co-transfected with pJM648 in each set of experiments.

In the first co-stimulation test, a significant increase of *FFLuc* expression (8.8-fold, Student's *t*-test *p*-value <0.05) was seen in stimulated U4.4 cells compared to the negative controls pIB/V5 and pIB-MBP (Figure 6.5). This correlates with previous data reflecting the activation of Toll pathway upon stimulation with pJL195 (Fragkoudis et al. 2008). C6/36 cells showed a similar increase of *FFLuc* expression (Student's *t*-test, *p*-value <0.05) upon stimulation with pJL195, though with less expression level. In contrast, there was a suppression of Toll pathway in Aag2 cells as *FFLuc* significantly decreased in expression following the stimulation. In the second pre-stimulation test, the Toll pathway was pre-stimulated prior to adding the Toll reporter. This was done to allow sufficient stimulation of the cells because the efficiency of the pJL195 Toll stimulant was unknown. Data from this set of experiments revealed an activation of the Toll pathway in U4.4 cells, giving a two-fold increase of *FFLuc* expression (Figure 6.6, Student's *t*-test, *p*-value <0.05). This is consistent with the findings in the first test and correlates with previous data (Fragkoudis et al. 2008). The Toll immune pathway was also activated in Aag2 cells but not in C6/36 (Figure 6.6), which contrasts to the results of the first test. Taken together, Toll pathway is activated by pJL195, dependent on the mosquito cell types and manner of introduction of the stimulation.

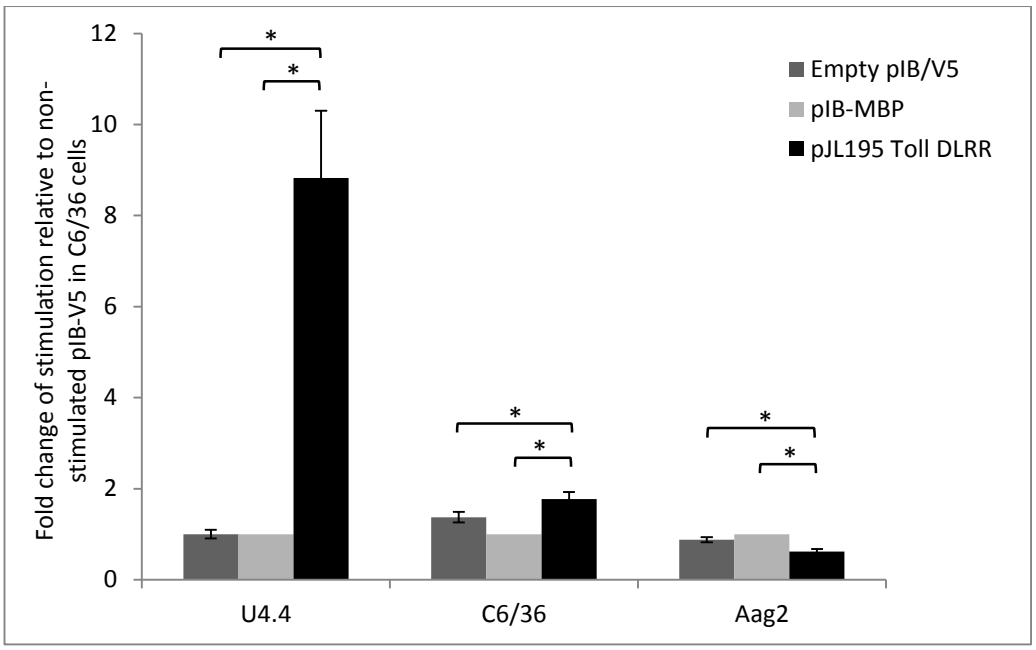

Figure 6.5: Activation of Toll through co-stimulation with pJL195.

Cells were co-transfected with Toll reporter pJM648 and either pIB/V5, pIB-MBP or pJL195 and lysed 24 hr p.t. Average ratios of *FFLuc* to *RLuc* internal control were calculated and normalised by assigning a value of 1 to the level of pIB-MBP of the corresponding cells (non-stimulated control). Error bars indicate standard error of triplicate wells from three independent experiments. Statistical significance was determined by paired Student's *t*-test (*p*-value <0.05) indicated by an asterisk (*).

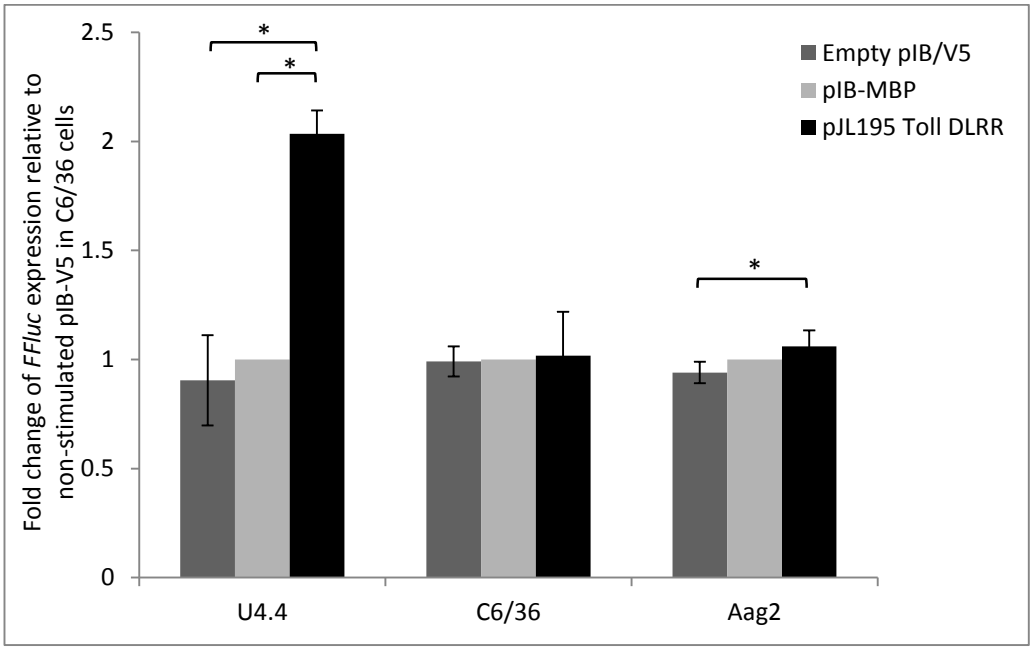

Figure 6.6: Activation of Toll through pre-stimulation with pJL195.

Cells were pre-stimulated with either pIB/V5, pIB-MBP or pJL195 prior to transfection with Toll reporter pJM648 at 24 hr post-stimulation and the cells were lysed 48 hr post-stimulation. Average ratios of *FFLuc* to *RLuc* internal control were calculated and normalised by assigning a value of 1 to the level of pIB-MBP of the corresponding cells (non-stimulated control). Error bars indicate standard error of triplicate wells from three independent experiments. Statistical significance was determined by paired Student's *t*-test (*p*-value <0.05) indicated by an asterisk (*).

6.3.2.3 Activation of Toll pathway by *Bacillus* sp.

Toll immune signalling pathway is known to be activated by Gram-positive bacteria (Rutschmann et al. 2002). Although this pathway could be stimulated by introduction of pJL195 particularly in U4.4 cells (as shown in previous section), the activation caused by Gram-positive *Bacillus* sp. was investigated due to the poor activation of the receptor plasmid in Aag2 cells. The experiments were performed in a similar fashion as described for JAK/STAT and IMD pathways, thus reducing experimental variables, allowing a more reliable comparison among the immune signalling pathways. Following transfection of pJM648 Toll reporter plasmid into mosquito cells, *Bacillus* sp. heat-inactivated and live cultures were used to stimulate the Toll pathway. The bacteria were introduced to the cells for 1 hr and subsequently removed and fresh medium added, or exposed to the cells for 12 hr stimulation. PBS was used as a negative control for stimulation. The cells were lysed 12 hr post-stimulation and luciferase activities were determined. The total number of bacteria cells in the suspension was calculated to be 10^8-10^9 cfu/ml (10^5-10^6 bacteria cells were used for stimulation on the mosquito cells).

There was a two-fold increase of *FFLuc* expression (Student's *t*-test, *p*-value <0.05) in U4.4 when exposed to heat-inactivated *Bacillus* sp. for 12 hr (Figure 6.7, top panel). Increased *FFLuc* expression was also seen after 1 hr stimulation with freshly grown culture, suggesting the Toll pathway was activated in response to *Bacillus* sp. It is noteworthy that 1 hr-stimulation with heat-inactivated *Bacillus* sp. did not significantly activate Toll, as seen by Fragkoudis et al. (2008) with *Staphylococcus aureus*. In C6/36 cells, the Toll pathway was mainly activated through stimulation with the live bacteria exhibiting a marked increase in Toll immune response (Figure 6.7, middle panel). This resulted in a nine-fold and seven-fold increase of *FFLuc* expression (Student's *t*-test, *p*-value <0.05) upon 1 hr and 12 hr exposure to the live bacteria, respectively. Toll activation was also seen by 12-hr stimulation with heat-inactivated bacteria but with less activity. It was clear that Aag2 cells responded efficiently to both forms of bacteria by activating the Toll pathway particularly within 1 hr exposure to the stimulant (Figure 6.7, bottom panel). Overall, exposure to *Bacillus* sp. particularly freshly grown bacteria activates the Toll pathway in mosquito cells. The use of heat-inactivated bacteria as a stimulant requires an extended exposure time in *Ae. albopictus* cells for activation of this pathway.

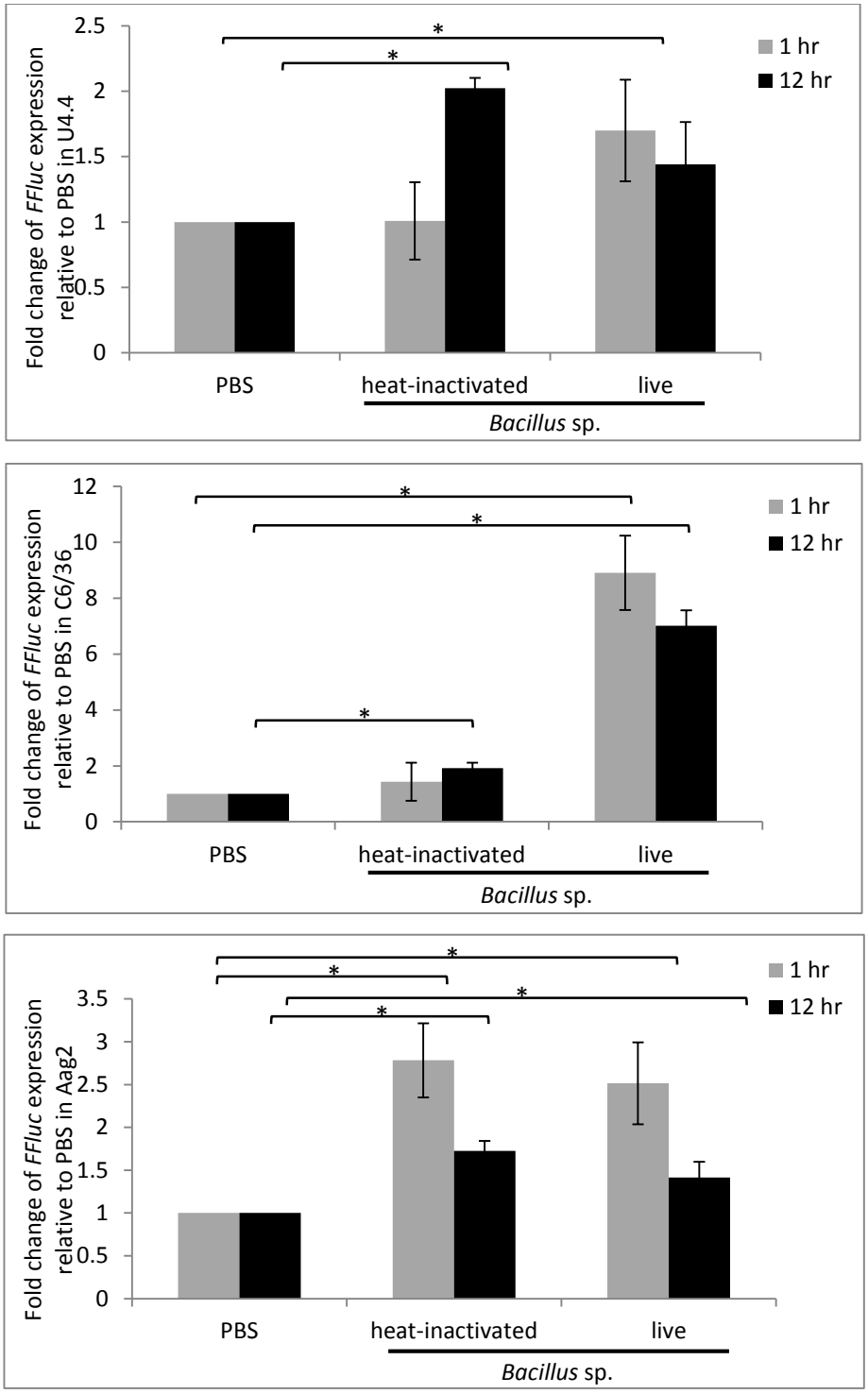

Figure 6.7: Toll activation through ectopic stimulation with *Bacillus* sp.

Activation of Toll pathway in U4.4 (top panel), C6/36 (middle panel) and Aag2 (bottom panel) mosquito cells upon exposure to heat-inactivated and live bacteria (for 1 or 12 hr where indicated), prior to cell lysis. Data represents the average fold change of *FFLuc* expression relative to PBS negative controls ± standard error of triplicate samples. Statistical significance was determined by paired Student's *t*-test (*p*-value <0.05) indicated by an asterisk (*).

6.3.3 Replication of DENV replicon in mosquito cells

6.3.3.1 Expression of DENV GFP

In order to investigate the mosquito host defence pathways in response to DENV, a sub-genomic DENV-2 NGC replicon pDENrepGP2A (a kind gift from Andrew Davidson, University of Bristol) encoding the virus non-structural proteins was used. The replicon contains a GFP-PAC-2A fusion protein under the control of T7 promoter replacing the C-prM-E genes at the N-terminus (Section 2.4.2) (Massé et al. 2010). This construct enabled the visualisation of DENV translation by examining GFP, without interfering with the luciferase reporter system used to test immune signalling. An initial study was firstly attempted to assess the replicon translation in mosquito cells by examining the GFP expression, followed by analysing the effect of DENV replication on mosquito host immune signalling. In brief, *in vitro* transcribed DENV replicon RNA was transfected into Aag2, C6/36 and BHK-21 cells, and continuously monitored for GFP expression. BHK-21 was included in this study because this cell line has been previously shown to allow DENV translation using DENV replicon, pDVPACLuc expressing *FFluc* (Section 4.3.6.1). A construct expressing EGFP in insect cells (provided by Margus Varjak, University of Glasgow) was used as a positive control.

EGFP expression was observed beginning at 24 hr p.t in Aag2, C6/36 and BHK-21 cells transfected with the positive control plasmid. Figure 6.8 shows the expression of EGFP at 48 hr p.t in positive control cells, but GFP was not seen in cells transfected with DENV replicon RNA. In BHK-21, the cells looked unhealthy (deterioration in cell numbers caused by cell death), which was similarly seen in the mosquito cells at 72 hr p.t onwards. Continuous examination up to 120 hr p.t was unable to detect the GFP expression, as most of the cells had died off whereas the EGFP in the positive control cells reduced in number due to proliferation of untransfected cells outnumbering the transiently transfected cells.

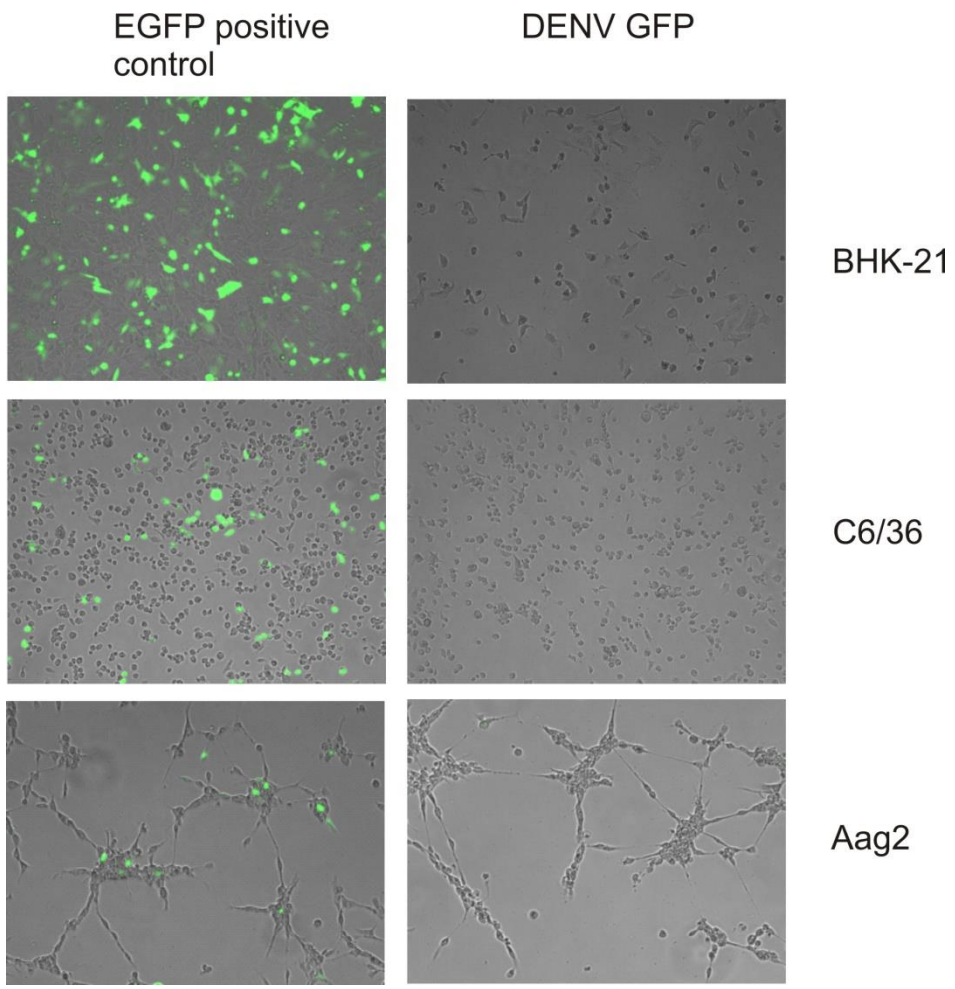

Figure 6.8: Expression of DENV NS proteins in Aag2 and C6/36 cells.

The cells were transfected with either positive control EGFP plasmid (left panels) or in vitro-transcribed DENV replicon RNA, pDVRepGP2A expressing GFP reporter (right panels) and continuously examined for 120 hr p.t. The live-cell images were captured at using EVOS f1 fluorescence digital microscope (Advanced Microscopy Group, USA). Only EGFP/GFP expression at 48 hr p.t is shown.

6.3.3.2 Expression of DENV luciferase

In order to assess the expression of DENV non-structural proteins in mosquito cells, the DENV-2 NGC replicon, pDVPACLuc expressing *FFLuc* (as described in Section 2.4.2) was used. *In vitro*-transcribed viral RNA was transfected into U4.4, C6/36 and Aag2 cells and expression of *FFLuc* was determined 24 hr p.t. There was a significant increase in *FFLuc* expression upon transfection with pDVPACluc compared to the mock-transfected cells (Figure 6.9). This corresponded to the expression of DENV non-structural proteins in the mosquito cell lines, while enhanced *FFLuc* expression was seen in C6/36 cells, followed by U4.4 and Aag2, respectively.

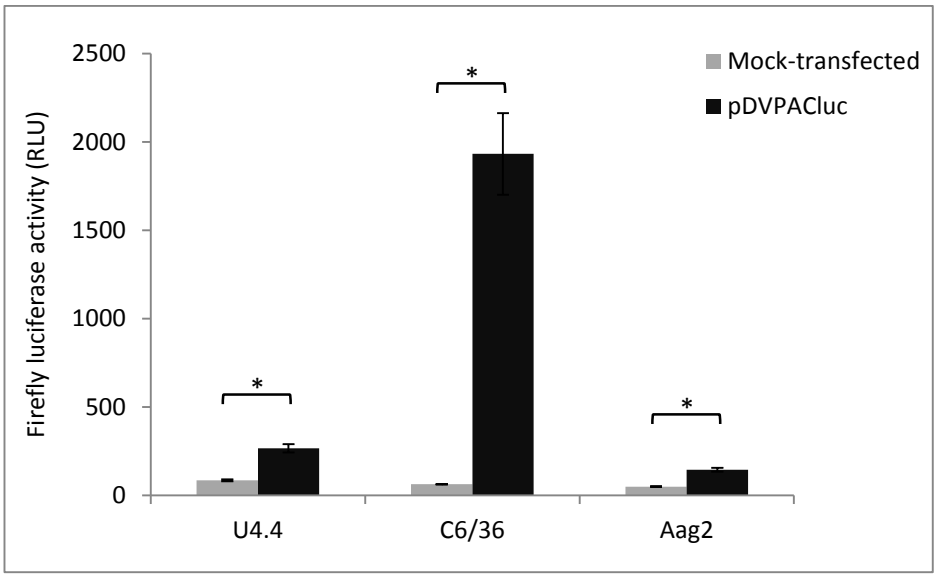

Figure 6.9: Expression of DENV NS proteins in mosquito cells.

The U4.4, C6/36 and Aag2 cells were transfected with *in vitro*-transcribed DENV replicon RNA pDVPACLuc, and lysed at 24 hr p.t, followed by determination of the luciferase activity. Negative control was cells transfected with Lipofectamine® 2000 CD alone. Data represent *FFLuc* relative light units (RLU) mean ± standard error of triplicate samples from a single experiment.

6.4 Discussion

An Aag2 cDNA library was constructed for use in Y2H screen to search for potential mosquito host factors (prey) interacting with DENV non-structural proteins (bait). Since construction of the library requires high quality RNA, a general assessment of the RNA quality was carried out by analysis of the mosquito 28S and 18S rRNA profiles. It is believed that a clear resolution of 28S and 18S rRNA profiles indicates a high integrity of the isolated RNA, which reflects the quality of other RNA fractions including the mRNA population. The $A_{260/280}$ ratio of RNA isolated from Aag2 cells was within the expected range (Sambrook et al., 1989) indicating a good RNA preparation. Further rRNA profile analysis demonstrated two clear bands corresponding to the 28S and 16S rRNA, visualised under non-denaturing conditions. Although a 2:1 ratio of 28S to 18S intensity has been suggested for mammalian total RNA (Sambrook and Russell., 2001), this was not the case for RNA samples of insects (Winnebeck et al. 2010). Insects may exhibit rRNA profiles as a single 18S rRNA band under denaturing conditions due to the presence of an endogenous 'hidden break' in the mid region of 28S rRNA (Fujiwara & Ishikawa 1986). It may also display both 16S and 28S rRNA together regardless of intensity under non-denaturing conditions (Matz 2002), as seen in this study. This finding is consistent with previous studies of high integrity RNA observed in insects (Macharia et al. 2015; Winnebeck et al. 2010).

In an attempt to generate a cDNA library derived from mRNA of Aag2 cells, the Make Your Own 'Mate and Plate™' Library System incorporating SMART technology was used according to the manufacturer's instructions (Clontech). LD-PCR has been reported to be suitable for low quantities of starting material of cDNA which was used to generate ds cDNA after first strand cDNA synthesis (Cheng et al. 1994). Following these procedures, a homogenous smear, which indicated a reasonably good cDNA library was observed (Islam et al. 2012). It is noteworthy that increasing LD-PCR cycles generated longer fragments of amplified cDNA because the extension time was increased by 5 sec of each additional cycle. It was however, not advisable to go above the recommended PCR cycles to avoid overcycling that may generate a smear at the high MW region (Bogdanov et al. 2010). cDNA with higher MW up to 2 kb (25 PCR cycles) was selected for use in the current library construction as a study reported an invertebrate cDNA library between 2-3 kb (Shcheglov et al. 2007). While the protocol used in this study most probably has

been optimised for mammalian libraries, for libraries derived from cells or tissues of different organisms such as mosquitoes, it is not known whether it is appropriate to use similar amplification cycles due to differences in gene composition. Optimisation of cycling parameters allows knowledge of when the reaction has reached an amplification plateau, thus giving better amplification products (Bogdanov et al. 2010).

In this study, size-fractionated cDNA using a CHROMA SPIN TE-400 column followed by ethanol precipitation has reduced the cDNA yield due to removal of low MW cDNA, however it also reduced the DNA purity. The yield of cDNA was 1.7 µg in total, lower than the expected 2-5 µg as suggested by Clontech. The DNA purity was $A_{260/280}$ 1.7, slightly lower than the standard range ($A_{260/280}$ 1.8-2.0) (Sambrook et al., 1989). This may suggest DNA degradation or possible contamination with proteins or organic solvents during purification step, such as ethanol (NanoDrop Technical Support Bulletin, 2007). Size-fractionation is known to eliminate low MW cDNA, resulting in enrichment of the cDNA with full length transcripts (Wellenreuther et al. 2004). It is however unknown if intervention by this step, followed by ethanol purification may increase the chances of DNA loss. This has been shown by Cao & Yan (2013) who obtained a larger cDNA library (~2.5×10^6 independent clones, with an average insert size of ~ 1.5 kb) via low-melting point gel fractionation. Consistent with this study, gel purification of human cDNA followed by PCR-amplification has been shown to produce 70% full length clones with an average insert of 7 kb (Wellenreuther et al. 2004). Besides fractionation, cDNA pellets resulting from ethanol purification are sometimes difficult to re-dissolve and the ethanol residues can remain in the samples, which affects both the DNA quantity and quality. Since the initial cDNA obtained from this preparation was not sufficient for library construction, the whole process was repeated to make more cDNA. However, even with the fact that subsequent steps including size-fractionation and ethanol precipitation were applied, this repetition was unable to improve the DNA quality.

There are several factors which may contribute to these difficulties. First, it is possible that partially transcribed cDNA occurs in most transcripts during first-strand cDNA synthesis, which is caused by mRNA degradation or the presence of high levels of secondary structures in mosquito mRNA. MMLV RT may thus be

unable to initiate terminal transferase activity and synthesize complementary SMART sequences at the 5' end. Given the switching mechanism occurs at the 5' end of template, partially transcribed cDNA lacks the SMART sequences thus are unavailable for amplification by LD-PCR using SMART primers, which contributes to a low yield of amplified cDNA. Second, it was difficult to assess the quality of amplified cDNA by visualisation of a cDNA smear. Hence, the success of LD-PCR through performing a specific number of cycles has not been accurately determined and may be misleading. Third, synthesis of cDNA using oligo(dT) primers have a strong bias towards having cDNA 3' fragments (Nam et al. 2002). In the event of incomplete PCR cycling conditions, this produces high percentage of 5'-truncated cDNA lacking the SMART sequences as mentioned above, which likely generates a smear.

Ideally, cDNA libraries have to be representative in which they should contain DNA copies for nearly all transcripts (Brown & Song 2005). Thus, a pre-assessment of complexity of the cDNA library was done by amplification of gene fragments; *Actin, Dicer-2* and *Argonaute-2*. It was shown that the gene fragments were successfully amplified, an early indication of a representative library. Given the time constraint however, only these genes were tested prior to transformation into yeast. Further analysis of full length cDNA clones would be achievable once they have been transformed into yeast which may also indicate the complexity of the library.

In order to allow expression of the mosquito proteins in yeast, the Aag2 cDNA was co-transformed with the yeast expression vector pGADT7-Rec into yeast strain Y187. The resulting Aag2 cDNA library however did not produce a sufficient number of independent clones as required. This outcome is contrary to other studies from mouse cDNA and *Ae. aegypti* midguts using the same SMART cloning strategy which produced 10^6-10^7 clones (Tham et al. 2014; Zhang et al. 2013). In addition, transformation of the positive control SV40 large-T PCR fragment with flanking SMART sequences failed to obtain any yeast transformants. All these difficulties may be accounted for by the following explanations:

1) Quality of cDNA used for transformation: There could be a low yield of first-strand cDNA to begin with, which produced cDNA with low quality. Although up to 5 µg was suggested by Clontech for transformation into yeast, only 3 µg was

obtained from pooled cDNA preparations and thus was entirely transformed. *Actin, Dicer-2* and *Argonaute-2* gene fragments have been shown to be present in the cDNA, but it was not tested if they were present as full length transcripts.

2) Linearisation of yeast vector pGADT7-Rec: The commercial yeast vector pGADT7-Rec harbouring recombination sites was supplied in a linearized form. The linearization however was not confirmed by gel electrophoresis in this study due to the limited supply of the vector in the library kit. Although re-circularization of pGADT7-Rec generated from *Sma*I blunt-end digestion is rare, this may still occur and might affect the vector's ability to perform a specific recombination with the cDNA. In the event of re-circularization, transformed pGADT7-Rec produces empty yeast colonies which were able to grow on selective media. There was no transformant however, resulting from the transformation of pGADT7-Rec alone, which indicates other factors may contribute to this failure.

3) Recombination strategy *in vivo:* Although many have shown a high yield of cDNA clones using a recombination strategy, subsequent recombination steps in the majority of studies were performed *in vitro* such as using *E. coli* or phage as host (Ohara & Temple 2001; Zhu et al. 2001). In this study, there was no transformant being produced as a result of co-transformation of the positive control SV40 large-T PCR fragment containing SMART sequences and pGADT7-Rec. It has been shown that at least 30 bp of a homologous sequence is sufficient for recombination (Fusco et al. 1999; Hua et al. 1997), thus a 40 bp overlap in SMART sequence should work. Other issues could be the condition of yeast where the recombination activity takes place involving the yeast repair enzymes (Fusco et al. 1999).

4) Transformation efficiency of yeast: We were unable to assess the transformation efficiency in yeast Y187 due to the lack of a suitable control plasmid for this strain. However, assessing the transformation efficiency of a yeast strain AH109 using similar reagents and experimental settings has produced transformants very close to the required standard efficiency. This indicates that the procedure used to generate competent yeast in this study was able to generate highly competent yeast suitable for transformation. Although this was achieved through a completely different yeast host strain, it is conceivable from this study that failure in generating a good cDNA library was not a consequence of issues with the method of producing competent yeast.

Each step throughout the construction of a cDNA library contributes greatly to the final product. It is likely that synthesis of the first-strand cDNA plays the most important role in obtaining full length molecules for downstream experiments. The limitation of making a full length cDNA from 3′ terminus produced partial lengths could be the main reason of failure which maybe subsequently intensified by the downstream experiments. In summary, it is clear that the Aag2 cDNA library generated from this study does not fulfil the required criteria of a standard library, this library is thus not suitable to be used for a comprehensive analysis by Y2H screen.

In parallel work, a cellular assay system involving mosquito immune signalling experiments was characterised for any subsequent analysis of DENV-targeted mosquito proteins identified from Y2H. While the pathways involved in regulating antiviral defense against DENV; the JAK/STAT, IMD, Toll and RNAi pathways have been reported (Sim et al. 2014), the specific mechanism underlying each pathway is still poorly understood. In an attempt to investigate the importance of these pathways against DENV infection, an initial study was carried out to explore the activation of these pathways through stimulation procedures described by Fragkoudis et al. (2008). It is important to mention that in their study, experiments were carried out only in *Ae. albopictus* U4.4 cells.

In the first set of experiments, plasmids expressing *FFLuc* (either p6x2DRAF-Luc, pJL169 or pJM648) driven by promoters responsive to the JAK/STAT, IMD and Toll pathways, respectively, were transiently transfected into Aag2 and C6/36 cells. Stimulation of both cells using *E. coli* was shown to successfully activate the JAK/STAT and IMD pathways which correlates to previous observations in U4.4 cells (Fragkoudis et al. 2008). This is also consistent with previous findings that both the JAK/STAT and IMD have been implicated in insect immune responses against Gram-negative bacteria (Costa et al. 2009; Hombría et al. 2005). Stimulation of the Toll pathway was carried out using an expression construct pJL195, containing a *Drosophila* Toll receptor mutant (Toll ΔLRR) under control of *Drosophila* Actin 5C gene promoter (Tauszig et al. 2000). This construct has a deletion of leucine-rich repeats in the Toll ectodomain, resulting in a constitutively active mutant Toll receptor. It has been previously reported that expression of this mutant receptor significantly enhanced the activation of the

Toll drosomycin promoter in *Drosophila* S2 cells by 5-10 fold (Tauszig et al. 2000). Furthermore, expression of the Toll ΔLRR receptor did not seem to stimulate the production of antimicrobial peptides other than drosomycin (Tauszig et al. 2000). In this study, stimulation of the Toll pathway with pJL195 however, was unable to activate the Toll pathway in both Aag2 and C6/36 cells. This could be due to the lack of proper negative control (un-transfected cells), which results in *FFLuc* data unsuitable for comparison.

Subsequent tests of the Toll pathway were performed by stimulation with pJL195, and the negative controls were transfected with either an empty insect expression vector (pIB/V5), or a plasmid expressing the *E. coli* protein MBP (pIB-MBP). It has been shown that pJL195 was capable of expressing the mutant Toll ΔLRR receptor and inducing the Toll pathway in U4.4 cells (Fragkoudis et al. 2008), however it's activity in both Aag2 and C6/36 cells is unknown. Thus, two sets of experiments (co-stimulation and pre-stimulation with pJL195) were performed, as described in Section 6.3.2.2. The procedure for the co-stimulation test (co-transfection of pJL195 and the drosomycin *FFluc* reporter pJM648), was similar to those performed by (Fragkoudis et al. 2008) in U4.4 cells and has been shown to work, therefore would give an indication of any response in Aag2 and C6/36 cells. The pre-stimulation test aimed to allow sufficient expression of the mutant Toll ΔLRR receptor with the hope of better stimulation, before transfecting the pJM648. Stimulation of Toll was clearly seen in U4.4 regardless of the way stimulation was being introduced, which correlates with previous observations (Fragkoudis et al. 2008). This however was not consistent in Aag2 and C6/36 cells in both stimulation tests, which suggests the stimulation by pJL195 is dependent on the mosquito cell types and the duration of stimulation. One possible reason could be that the *Drosophila* Toll receptor mutant although expressed constitutively in *Drosophila* S2 cells, may not be suitable or potent enough for stimulation in these mosquito cells. Besides, it is not known if the mutant Toll receptor was properly expressed in Aag2 and C6/36 cells. While C6/36 cells in general give a low Toll response almost similar to background, Aag2 cells show a suppression of Toll during co-stimulation. Aag2 cells are known to be efficient in mounting an immune response (Barletta et al. 2012), it is possible that over-stimulation of the cells causes a negative feedback reaction, which reduces the immune response in order to stabilize the mosquito cells (Gupta et al. 2009).

The Toll pathway is activated in response to Gram-positive bacteria (Rutschmann et al. 2002). This study therefore attempted to activate the Toll pathway using Gram-positive *Bacillus* sp. Additional parameters were determined by testing the stimulation exposure time (1 or 12 hr stimulation) and the nature of bacteria stimulants (live bacteria or heat-inactivated) used for stimulation. Various patterns of the Toll pathway activation following stimulation were observed. In general, the stimulation was optimal when exposed for 1 hr to live bacteria. This could be due to the fact that the live bacteria are capable of causing injury to the cells, therefore a stronger Toll immune response was produced to overcome this effect. It was also clear that the use of heat-inactivated bacteria as a stimulant was less potent, requiring longer exposure time particularly in *Ae. albopictus* U4.4 and C6/36 cells. While it is known that C6/36 cells are RNAi pathway deficient (Brackney et al. 2010), it is unknown whether these cells are less efficient in triggering the Toll pathway. This effect was also seen during pJL195 stimulation, where a low activation or almost no activation of Toll pathway was observed in C6/36, indicating inefficient Toll activation. In contrast, Aag2 cells are immune-competent (Scott et al. 2010), in most cases the Toll immune response was rapidly activated at 1 hr post-stimulation regardless of the nature of stimulant. The differential levels of Toll induction by *Bacillus* sp. in different mosquito cell lines, may suggest a degree of selectivity in the Toll response and indicates that the activation requires a specific induction exposure time and stimulant.

Procedures concerning the activation of JAK/STAT, IMD and Toll pathways have been optimised in this study, a further attempt was carried out in order to investigate the effect of DENV on these activation pathways. A DENV-2 replicon harbouring GFP reporter pDVRepGP2A (Section 2.4.1) (a kind gift from Andrew Davidson, University of Bristol) was used. The replicon contained DENV-2 non-structural genes and GFP as a fusion with a drug selectable marker PAC at the N-terminus (Massé et al. 2010). Previous studies demonstrated that the alphaviruses, chikungunya virus (CHIKV) and Semliki Forest virus (SFV) are able to inhibit the JAK/STAT, IMD and Toll pathways in mosquito cells (McFarlane et al. 2014; Fragkoudis et al. 2008). While the specific action of DENV on these pathways is unclear, the virus has been previously shown to suppress these pathways as a strategy for replication in *Ae. aegypti* (Sim & Dimopoulos 2010a).

GFP or *FFLuc* expression corresponding to DENV non-structural protein production was first tested in mosquito cells. An increase in the luciferase activity was shown in DENV replicon-transfected cells expressing *FFLuc*, with the highest luciferase activity in C6/36, U4.4 and Aag2, respectively. Since C6/36 cells are known to have a dysfunctional antiviral RNAi response (Brackney et al. 2010), it is however unknown if the cells were able to tolerate DENV translation, thus giving rise to elevated *FFLuc* activity. Overall, this set of experiments shows the ability of pDVPACLuc replicon to initiate translation in insect cells. This replicon however, was unable to be used because the *FFLuc* activity would interfere with the plasmid constructs encoding *FFLuc* under control of promoters activated in response to JAK/STAT, IMD and Toll stimulation. Hence, a DENV replicon harbouring a GFP reporter was used. EGFP expression was observed in positive control cells however the GFP was not seen in cells transfected with DENV replicon RNA up to 120 hr p.t. It was also seen that transfection of the DENV replicon in the mosquito cells resulted in deterioration of the cellular conditions, and cell death. Taken together, this reflects the unsuitability of the replicon to be used for the assay.

6.5 Conclusion

Although the quality of the mosquito library generated in this study is based on suggestions by Clontech and standard published literatures, the exact quality of the library remain unknown unless tested extensively. Further analysis of the library could be performed by amplification of the mosquito genes or enzymatic digestion of randomly-picked yeast colonies and sequencing of the cDNA clones. This gives information of the percentage of clones containing full-length cDNA, the average sizes of insert and gives a representative image of the library, which are important criteria in determining a cDNA library quality. Another important criteria is the normalization of the library, which is done by decreasing the highly abundant transcripts to increase the chances of discovering rare transcripts. Normalization is usually performed by treating ds cDNA with duplex-specific nuclease (DSN) before cloning into any host for plasmid propagation or protein expression (Shagin et al. 2002; Young & Anderson, 1985). In this process, ds cDNA is firstly denatured, followed by renaturation where most abundant transcript re-anneal efficiently than the rare transcripts, forming ds cDNA. Treatment with DSN subsequently degrades the ds cDNA and the remaining normalized ss DNA is PCR-amplified and used for library cloning (Bogdanov et al. 2010). Through this experience of generating a mosquito cDNA library, it was realized that many technical problems exist. Future improvements as to reverse-transcriptase conditions and cloning strategies might be possible to overcome these limitations.

Optimization of assays to test JAK/STAT, IMD and Toll immune pathways has been successfully achieved. It is clear that the Toll pathway can either be activated through the use of pJL195 Toll receptor mutant or *Bacillus* sp. dependent on the type of mosquito cells used. Further attempts were carried out in order to investigate the effect of these activation pathways on DENV, however failure of the DENV GFP replicon in the mosquito cells prevented us from achieving the aim of the study. Given more time, experiments such as RNAi-mediated silencing of the JAK/STAT, IMD and Toll immune pathway components and testing with the DENV *FFLuc* replicon may provide information on which pathway is affected in DENV replication in the mosquito cells.

CHAPTER 7: CONCLUDING REMARKS

Dengue is a global health threat and causes a burden in many countries. Although numerous attempts have been made to develop effective vaccines, most are hampered by an inability to provide significant protective immunity to all four DENV serotypes. Further to clinical efforts, many researchers have focused on identifying specific host determinants, known to be essential for DENV replication, which are potential targets for diagnostics or antiviral strategies. Systematic mapping of protein-protein interactions is essential for identification of host factors and for prediction of functional biological systems at the molecular level. To date, high throughput genome-wide interactions and global systematic analysis of large screen protein-protein interactions mapping have been reported. These include a large-screen of DENV-human protein-protein interactions established recently using the Y2H approach (Mairiang et al. 2013; Silva et al. 2013; Le Breton et al. 2011; Khadka et al. 2011). Although several potential DENV interacting proteins have been described, only a few of these proteins overlap between the independent screens and only a small number of proteins have been shown to be involved in DENV replication thus far.

In Chapter 3 of this study, analysis of protein-protein interaction between DENV-2 NS proteins and the MGC human cDNA library was performed using a Y2H assay. A total of 94 human proteins were identified, of which four have been reported in the previous DENV screens, these were STAT2, UBE2I, EMILIN1 and NUMA1 (Khadka et al. 2011; Le Breton et al. 2011). At least five proteins GOPC, GRN, LACRT, KHDRBS1 and TRIM27 have been implicated in other viral infections (Bouraï et al. 2012; Krishnan et al. 2008; Calderwood et al. 2007). The small number of overlap proteins with other studies, could be due to the different experimental conditions and also the different cDNA library used for screening that are enriched with different sets of genes (Friedel & Haas 2011). Data from this study indicate the enrichment of human proteins that are components of the ER membrane, and transcriptional processes including negative regulation of transcriptional activity which may occur during viral infections (Lee et al., 2013; Wang et al., 2012). Further validation of 15 selected human protein interactions in a human system was performed using the LUMIER pull-down assay. Of these, BANP, KCNA3, ARL6IP1, UBE2I, TRAPPC, HEXIM2, KCNS2, EMILIN1, PRR7 and TRIM27 have been detected as strong interactors for DENV. As BANP interacts with the full length

and a truncated DENV NS2A, and has been shown to be involved in NF-κB signalling, this strongly supports the potential interaction of BANP with NS2A thus, the interaction was tested further and described in Chapter 4 of this thesis. In addition, the voltage-gated K^+ channel, KCNA3 (or Kv1.3) was also selected for further analysis due to its potential role in virus life cycle, which was discussed further in Chapter 5 (Mankouri et al. 2009; Redman et al. 2007; Herrmann et al. 2010). Although only two proteins, BANP and Kv1.3 were investigated in this study, other human proteins identified from this screen require further elucidation of their specific roles and involvement in DENV infection.

In Chapter 4, a human protein BANP that was identified as interacting with DENV NS2A was further investigated. As previously mentioned, there was limited information about BANP, thus knowledge about this protein was inferred from its mouse homolog, SMAR1 (Malonia et al. 2011). BANP has been shown to be localised in the cell nucleus during its overexpression which may indicate its essential role in regulating cellular transcriptional activities (Birot et al. 2000; Chattopadhyay et al. 2000a). In this study, the potential role of BANP in regulating NF-κB and the type I IFN response was investigated. Both Poly(I:C)-mediated or the Universal Type I IFN-mediated stimulation in HEK293 cells clearly showed that NF-κB and the type I IFN response was inhibited in overexpressed BANP. This finding is consistent with prior knowledge of SMAR1 which is capable of inhibiting TNFα-mediated activation of NF-κB, hence repressing transcriptional activation of NF-κB target genes (Singh et al. 2009). The mechanism involves an interaction between SMAR1 with HDAC1 and other cofactors by forming a repressor complex which is recruited to the MAR elements present upstream of the NF-κB promoter, leading to deacetylation of histones and hence transcriptional repression of the NF-κB target genes (Malonia et al. 2011; Singh et al. 2009). Likewise, stimulation of these cells in the presence of DENV NS2A has been shown to inhibit the type I IFN response. The role of interaction between BANP and DENV NS2A in inhibiting the type I IFN however is unclear, as both proteins were found to be IFN-antagonist.

It could also be that BANP is involved in other cellular functions than the immune signalling given the diverse roles of SMAR1. BANP is thought to be capable of regulating the cell cycle arrest through DNA repair by a mechanism involving

HDAC1, p53 and other cofactors in order to maintain the cell survival during viral infection (Sinha et al. 2010; Kaul et al. 2003; Sinha et al. 2012). In cases of severe DNA damage, it has been shown that SMAR1 activates *Bax* and *Puma* genes which leads to induction of apoptosis (Sinha et al. 2010). SMAR1 has been shown to be capable of regulating the cell cycle and cellular stress by modulation of the cyclin D1 and the tumour suppressor p53 (Sinha et al. 2012; Rampalli et al. 2005; Kaul et al. 2003). Interaction between SMAR1 and p53 delays the cell cycle progression at G_2/M phase (Kaul et al. 2003), and the interaction of SMAR1 with Ku70 regulates the induction of cell death or repair (Chaudhary et al. 2014). It is possible that these mechanisms are useful to the cells in order to respond to viral infection. Further studies by overexpression or gene silencing of BANP during DENV infection incorporating the assessment of DNA damage, regulation of p53 and apoptotic pathway will be able to indicate the functional properties of BANP and whether it plays an important role in DENV life cycle.

In Chapter 5, the importance of voltage-gated protein channel Kv1.3 in DENV infection was studied. Kv1.3 is expressed mainly on the plasma membrane in many cell types and tissues particularly in T lymphocytes (Grunnet et al. 2003; Gazula et al. 2010; Yao et al. 1996). Kv1.3 is involved in T lymphocyte activation by expression of significantly higher levels, and has been reported as the major constituent of voltage-gated channel in platelets (Panyi et al. 2004; McCloskey et al. 2010; Wulff et al. 2003). Although there was no report of direct correlation of Kv1.3 to DENV infection, previous studies have demonstrated the activation of T lymphocytes and macrophages upon DENV infection and a significant decrease in the number of platelets in dengue patients (Alonzo et al. 2012; Kurane et al. 1991b). This seems very interesting as Kv1.3 has been identified in this study.

Further experimentation confirmed the physical interaction of Kv1.3 with DENV NS2A by LUMIER and co-IP/pull-down assay in this study. The effect of Kv1.3 blockade using MgTx on translation of a DENV-2 replicon containing *FFLuc* reporter was unable to produce significant results, as the replicon was not found to replicate in HEK293 cells. In order to improve the assay, the effect of Kv1.3 blockade should also be tested by patch-clamp analysis to indicate a complete inhibition of Kv1.3. Alternatively, the use of a fluorogenic indicator dye, such as the FluxOR™ potassium ion channel assay can be used to measure the K^+ ion flux.

Another explanation of the effect seen on DENV replicon during channel blockade would be that Kv1.3 is not involved in DENV replication. However the channel is needed for an earlier or later stage of the virus life cycle as previously observed in BUNV infection (Hover et al. 2016). Further analysis of DENV-2 replication by qRT-PCR shows a clear decrease in DENV replication as a result of the K^+ channel blockade in 4-AP, MgTx and TEA, accordingly which signifies the importance these K^+ channels in regulating DENV-2 infection. Although it is difficult to conclude the importance of Kv1.3 due to its heterogenous native form in HEK293 cells (Jiang et al. 2002), this channel, together with other Kv channels may contribute to the enhancement of DENV infection. Further analysis including experiments in mouse models may prove informative. Although further investigations are required to gather data on the specific contribution of Kv1.3, our data suggest that development of drugs that specifically inhibit Kv channels may provide a treatment for dengue.

In Chapter 6, an attempt at generating a mosquito cDNA library was described. The initial study was intended to analyse protein-protein interactions between DENV and its mosquito host by Y2H assay. *Ae. aegypti*-derived Aag2 cells were the chosen cell line due to the fact that the insect serves as a primary vector for DENV, possesses an efficient innate immune system and there is a complete genome annotation available (Barletta et al. 2012; Gubler 1998). Due to the lack of a commercial *Ae. aegypti* cDNA library in the yeast expression system, the construction of an in-house library using the Clontech library cloning kit was carried out. The resulting Aag2 cDNA library however, resulted in a poor number of cDNA clones unlike a previously reported cDNA library obtained from *Ae. aegypti* midgut using similar techniques (Tham et al. 2014), thus making it unsuitable for use in Y2H assay. There were several possible explanations for this, including the generation of truncated cDNA during the first-strand synthesis, sub-optimal PCR cycling conditions, yeast transformation efficiency and *in-vivo* recombination cloning (Shcheglov et al. 2007; Wellenreuther et al. 2004; Fusco et al. 1999). Nonetheless, the Aag2 cDNA library has not been fully evaluated, and further analysis is required to provide sufficient information of the quality of library with regard to its gene sequence composition and representation of the mosquito transcripts.

This chapter also described an optimisation of innate immune signalling experiments to test for potential DENV-mosquito interacting partners obtained from Y2H screen. In an assessment of these mosquito proteins for downstream experiments, one selection criteria would be that the candidate has a certain degree of involvement in the immune signalling pathways. This is because the related tools, expression constructs and knowledge of the innate immune responses are readily available in the lab. Innate immune responses play an important role as defense mechanisms in mosquitoes against viruses (Sim et al. 2014; Kingsolver et al. 2013; Sabin et al. 2010). Previous studies have indicated the involvement of JAK/STAT, IMD and Toll pathways in controlling DENV infections (Sim & Dimopoulos 2010b; Souza-Neto et al. 2009; Xi et al. 2008). Further attempts were carried out in order to investigate the effect of these activation pathways on DENV, however failure of getting the DENV GFP replicon to replicate in the mosquito cells hampered the aim of this study. Given more time, experiments such as RNAi-mediated silencing of the JAK/STAT, IMD and Toll immune pathway components and testing with the DENV *FFLuc* replicon may provide information on which immune pathway affects DENV replication in mosquito cells and their mechanism of action. Furthermore, establishment of a good Aag2 cDNA library would allow identification of mosquito host factors interacting with DENV by Y2H screen. These proteins can be used as a target for development of genetically-modified mosquitoes in order to control the spread of DENV in mosquito populations. In addition, these genes can also be manipulated for preventing DENV attachment or replication in mosquito, thus prevent the spread of dengue in the future.

Overall, the work presented in this thesis, in particular the Y2H screen provides a number of human factors potentially targeted by DENV during infection. Nonetheless, more work is required in order to validate these proteins and determine their functional properties, as well as testing them with infectious DENV to establish a biological significance. Additionally, it is also important to assess the quality of the mosquito cDNA library established in this study, which can then be considered for use in the future. In the long term, data from this study are useful to investigate potential human or mosquito target candidates for development of an antiviral strategy against dengue.

APPENDIX

DENV Full length/Fragment	DENV protein	MGC interactor	GeneID		Gene Details	3-AT conc	No. of clones
NS3	NS3	NUMA1	4926	NM_006185.2	Homo sapiens nuclear mitotic apparatus protein 1 (NUMA1), mRNA	0.25	1
NS5	NS5	STAT2	6773	NM_005419.3	Homo sapiens signal transducer and activator of transcription 2, 113kDa (STAT2), transcript variant 1, mRNA	0.25	1
NS4B129F	NS4B	EMILIN1	11117	NM_007046.3	Homo sapiens elastin microfibril interfacer 1 (EMILIN1), mRNA	1	1
NS5	NS5	EMILIN1				0.25	9
NS2A187F	NS2A	UBE2I	7329	NM_194261.2	Homo sapiens ubiquitin-conjugating enzyme E2I (UBE2I), transcript variant 4, mRNA	0.25	1
NS2B49F	NS2B	UBE2I				0.5	1
NS4B129F	NS4B	UBE2I				1	6
NS5	NS5	UBE2I				0.25	3
NS5	NS5	GOPC	57120	NM_001017408.2	Homo sapiens golgi-associated PDZ and coiled-coil motif containing (GOPC), transcript variant 2, mRNA	0.25	3
NS1	NS1	VPS28	51160	NM_183057.1	Homo sapiens vacuolar protein sorting 28 homolog (S. cerevisiae) (VPS28), transcript variant 2, mRNA	0	1
NS2A	NS2A	TMEM159	57146	NM_020422.4	Homo sapiens transmembrane protein 159 (TMEM159), mRNA	0.25	3
NS2B1F	NS2B	AXIN2	8313	NM_004655.3	Homo sapiens axin 2 (AXIN2), mRNA	0	1
NS5	NS5	TRIM27	5987	NM_006510.4	Homo sapiens tripartite motif containing 27 (TRIM27), mRNA	0.25	1
NS2B	NS2B	ZNF3	7551	NM_032924.3	Homo sapiens zinc finger protein 3 (ZNF3), transcript variant 2, mRNA	0.5	1
NS2B49F	NS2B	ZNF578	147660	NM_001099694.1	Homo sapiens zinc finger protein 578 (ZNF578), mRNA	0.5	4
NS5	NS5	ZNF578				0.25	2
NS3	NS3	ANKRD6	22881	NM_014942.4	Homo sapiens ankyrin repeat domain 6 (ANKRD6), transcript variant 3, mRNA	0.25	1
NS3	NS3	APBB2	323	NM_173075.4	Homo sapiens amyloid beta (A4) precursor protein-binding, family B, member 2 (APBB2), transcript variant 3, mRNA	0.25	1
NS2B49F	NS2B	FAM226A	203429	NR_026595.1	Homo sapiens family with sequence similarity 226, member A (non-protein coding) (FAM226A), non-coding RNA	0.5	1
NS4A	NS4A	TNFSF13B	10673	NM_006573.4	Homo sapiens tumour necrosis factor (ligand) superfamily, member 13b (TNFSF13B), transcript variant 1, mRNA	0.25	1
NS5	NS5	CCDC57	284001	NM_198082.2	Homo sapiens coiled-coil domain containing 57 (CCDC57), mRNA	0.25	1
NS2B	NS2B	CCDC155	147872	NM_144688.4	Homo sapiens coiled-coil domain containing 155 (CCDC155), mRNA	0.5	6
NS4B	NS4B	CCDC155				1	3
NS2B49F	NS2B	SMARCE1	6605	NM_003079.4	Homo sapiens SWI/SNF related, matrix associated, actin dependent regulator of chromatin, subfamily e, member 1 (SMARCE1), mRNA	0.5	1

NS2A	NS2A	RAB3IP	117177	NM_022456.3	Homo sapiens RAB3A interacting protein (rabin3) (RAB3IP), transcript variant alpha 1, mRNA	0.25	5
NS3	NS3	RAB3IP				0.25	1
NS4A	NS4A	RAB3IP				0.25	3
NS2A	NS2A	ARL6IP1	23204	NM_015161.1	Homo sapiens ADP-ribosylation factor-like 6 interacting protein 1 (ARL6IP1), mRNA	0.25	5
NS2A187F	NS2A	ARL6IP1				0.25	2
NS2B	NS2B	ARL6IP1				0.5	4
NS4A	NS4A	ARL6IP1				0.25	7
NS2A	NS2A	KCNA3	3738	NM_002232.3	Homo sapiens potassium voltage-gated channel, shaker-related subfamily, member 3 (KCNA3), mRNA	0.25	1
NS2A	NS2A	RTN4	57142	NM_207520.1	Homo sapiens reticulon 4 (RTN4), transcript variant 4, mRNA	0.25	1
NS2B	NS2B	RTN4				0.5	9
NS2A	NS2A	CRX	1406	NM_000554.4	Homo sapiens cone-rod homeobox (CRX), mRNA	0.25	3
NS2A187F	NS2A	CRX				0.25	1
NS3	NS3	CRX				0.25	6
NS4A1F	NS4A	CRX				0	2
NS4A122F	NS4A	CRX				0.25	1
NS4B1F	NS4B	CRX				0.5	4
NS4B129F	NS4B	CRX				1	2
NS4B191F	NS4B	CRX				0	2
NS5	NS5	CRX				0.25	4
NS2A	NS2A	BEND7	222389	NM_001100912.1	Homo sapiens BEN domain containing 7 (BEND7), transcript variant 2, mRNA	0.25	1
NS2B49F	NS2B	BEND7				0.5	1
NS5	NS5	BEND7				0.25	1
NS2A	NS2A	ALX1	8092	NM_006982.2	Homo sapiens ALX homeobox 1 (ALX1), mRNA	0.25	2
NS2A187F	NS2A	ALX1				0.25	1
NS2B1F	NS2B	ALX1				0	1
NS3	NS3	ALX1				0.25	8
NS4A1F	NS4A	ALX1				0	5
NS4A101F	NS4A	ALX1				0.25	1
NS4A122F	NS4A	ALX1				0.25	7
NS4B1F	NS4B	ALX1				0.5	1
NS4B129F	NS4B	ALX1				1	4
NS5	NS5	ALX1				0.25	8
NS2A	NS2A	BANP	54971	NM_001173541.1	Homo sapiens BTG3 associated nuclear protein (BANP), transcript variant 5, mRNA	0.25	3
NS2A187F	NS2A	BANP				0.25	2

NS2A187F	NS2A	OTX2	5015	NM_001270525.1	Homo sapiens orthodenticle homeobox 2 (OTX2), transcript variant 5, mRNA	0.25	1
NS3	NS3	OTX2	-	-		0.25	2
NS4A1F	NS4A	OTX2	-	-		0	1
NS4A101F	NS4A	OTX2	-	-		0.25	1
NS4A122F	NS4A	OTX2	-	-		0.25	1
NS4B	NS4B	OTX2	-	-		1	1
NS4B1F	NS4B	OTX2	-	-		0.5	3
NS4B129F	NS4B	OTX2	-	-		1	2
NS4B191F	NS4B	OTX2	-	-		0	1
NS5	NS5	OTX2	-	-		0.25	8
NS2A	NS2A	ZDHHC7	55625	NM_001145548.1	Homo sapiens zinc finger, DHHC-type containing 7 (ZDHHC7), transcript variant 1, mRNA	0.25	1
NS2B	NS2B	CREB3	10488	NM_006368.4	Homo sapiens cAMP responsive element binding protein 3 (CREB3), mRNA	0.5	10
NS3	NS3	CREB3	-	-		0.25	1
NS4A	NS4A	CREB3	-	-		0.25	5
NS4B	NS4B	CREB3	-	-		1	5
NS2B	NS2B	AQP4	361	NM_001650.4	Homo sapiens aquaporin 4 (AQP4), transcript variant a, mRNA	0.5	1
NS4A	NS4A	AQP4	-	-		0.25	1
NS2B	NS2B	BSCL2	26580	NR_037949.1	Homo sapiens Berardinelli-Seip congenital lipodystrophy 2 (seipin) (BSCL2), transcript variant 5, non-coding RNA	0.5	1
NS2B	NS2B	DDHD2	23259	NM_001164232.1	Homo sapiens DDHD domain containing 2 (DDHD2), transcript variant 2, mRNA	0.5	1
NS2B	NS2B	TUG1	55000	NR_002323.1	Homo sapiens taurine upregulated 1 (non-protein coding) (TUG1), non-coding RNA	0.5	1
NS2B	NS2B	OR2C3	81472	NM_198074.4	Homo sapiens olfactory receptor, family 2, subfamily C, member 3 (OR2C3), mRNA	0.5	1
NS2B	NS2B	COMMD8	54951	NM_017845.3	Homo sapiens COMM domain containing 8 (COMMD8), mRNA	0.5	1
NS2B	NS2B	FTMT	94033	NM_177478.1	Homo sapiens ferritin mitochondrial (FTMT), nuclear gene encoding mitochondrial protein, mRNA	0.5	1
NS2B	NS2B	AGXT2L2	85007	NM_153373.2	Homo sapiens alanine-glyoxylate aminotransferase 2-like 2 (AGXT2L2), mRNA	0.5	1
NS2B	NS2B	STAG3L1	54441	NR_040583.1	Homo sapiens stromal antigen 3-like 1 (STAG3L1), non-coding RNA	0.5	1
NS2B	NS2B	DNAL1	83544	NM_001201366.1	Homo sapiens dynein, axonemal, light chain 1 (DNAL1), transcript variant 2, mRNA	0.5	1
NS2B1F	NS2B	BAG6	7917	NM_001199698.1	Homo sapiens BCL2-associated athanogene 6 (BAG6), transcript variant 6, mRNA	0	1
NS2B1F	NS2B	SGTB	54557	NM_019072.2	Homo sapiens small glutamine-rich tetratricopeptide repeat (TPR)-containing, beta (SGTB), mRNA	0	1
NS4A122F	NS4A	SGTB	-	-		0.25	7
NS2B1F	NS2B	GLYR1	84656	NM_032569.3	Homo sapiens glyoxylate reductase 1 homolog (Arabidopsis) (GLYR1), mRNA	0	1
NS2B49F	NS2B	SETBP1	26040	NM_001130110.1	Homo sapiens SET binding protein 1 (SETBP1), transcript variant 2, mRNA	0.5	3
NS5	NS5	SETBP1	-	-		0.25	4
NS2B49F	NS2B	EXOSC7	23016	NM_015004.3	Homo sapiens exosome component 7 (EXOSC7), transcript variant 1, mRNA	0.5	3

NS2B49F	NS2B	ATM	472	NM_000051.3	Homo sapiens ataxia telangiectasia mutated (ATM), mRNA	0.5	1
NS2B49F	NS2B	GAL	51083	NM_015973.3	Homo sapiens galanin prepropeptide (GAL), mRNA	0.5	1
NS2B49F	NS2B	RPS14	6208	NM_001025071.1	Homo sapiens ribosomal protein S14 (RPS14), transcript variant 1, mRNA	0.5	1
NS2B49F	NS2B	RBMS1	5937	NM_016836.3	Homo sapiens RNA binding motif, single stranded interacting protein 1 (RBMS1), transcript variant 1, mRNA	0.5	1
NS2B49F	NS2B	ELAVL2	1993	NM_001171197.1	Homo sapiens ELAV (embryonic lethal, abnormal vision, Drosophila)-like 2 (Hu antigen B) (ELAVL2), transcript variant 3, mRNA	0.5	1
NS2B49F	NS2B	RGS3	5998	NM_144489.2	Homo sapiens regulator of G-protein signaling 3 (RGS3), transcript variant 5, mRNA	0.5	1
NS2B49F	NS2B	LYSMD3	116068	NM_198273.1	Homo sapiens LysM, putative peptidoglycan-binding, domain containing 3 (LYSMD3), mRNA	0.5	1
NS2B49F	NS2B	NDUFA2	4695	NM_002488.4	Homo sapiens NADH dehydrogenase (ubiquinone) 1 alpha subcomplex, 2, 8kDa (NDUFA2), nuclear gene encoding mitochondrial protein, transcript variant 1, mRNA	0.5	1
NS2B49F	NS2B	DLX2	1746	NM_004405.3	Homo sapiens distal-less homeobox 2 (DLX2), mRNA	0.5	1
NS2B49F	NS2B	TRAPPC5	126003	NM_174894.2	Homo sapiens trafficking protein particle complex 5 (TRAPPC5), transcript variant 1, mRNA	0.5	1
NS2B49F	NS2B	MESP1	55897	NM_018670.3	Homo sapiens mesoderm posterior 1 homolog (mouse) (MESP1), mRNA	0.5	1
NS2B49F	NS2B	WDR45	11152	NM_007075.3	Homo sapiens WD repeat domain 45 (WDR45), transcript variant 1, mRNA	0.5	1
NS3	NS3	TAGLN3	29114 TAGLN3	NM_001008273.1	Homo sapiens transgelin 3 (TAGLN3), transcript variant 3, mRNA	0.25	1
NS3	NS3	USMG5	84833 USMG5	NM_001206426.1	Homo sapiens up-regulated during skeletal muscle growth 5 homolog (mouse) (USMG5), transcript variant 1, mRNA	0.25	1
NS3	NS3	AGSK1	80154 AGSK1	NR_026811.1	Homo sapiens golgin subfamily A member 2-like (AGSK1), non-coding RNA	0.25	1
NS3	NS3	PER1	5187 PER1	NM_002616.2	Homo sapiens period homolog 1 (Drosophila) (PER1), mRNA	0.25	1
NS3	NS3	LSMD1	84316 LSMD1	NM_032356.3	Homo sapiens LSM domain containing 1 (LSMD1), mRNA	0.25	1
NS3	NS3	JAKMIP1	152789	NM_001099433.1	Homo sapiens janus kinase and microtubule interacting protein 1 (JAKMIP1), transcript variant 1, mRNA	0.25	1
NS3	NS3	ZXDC	79364	NM_025112.4	Homo sapiens ZXD family zinc finger C (ZXDC), transcript variant 1, mRNA	0.25	1
NS3	NS3	APCDD1	147495	NM_153000.4	Homo sapiens adenomatosis polyposis coli down-regulated 1 (APCDD1), mRNA	0.25	1
NS3	NS3	CCL22	6367	NM_002990.4	Homo sapiens chemokine (C-C motif) ligand 22 (CCL22), mRNA	0.25	1
NS3	NS3	HEXIM2	124790	NM_144608.1	Homo sapiens hexamethylene bis-acetamide inducible 2 (HEXIM2), mRNA	0.25	1
NS3	NS3	WDR62	284403	NM_173636.4	Homo sapiens WD repeat domain 62 (WDR62), transcript variant 2, mRNA	0.25	1
NS3	NS3	LHX4	89884	NM_033343.3	Homo sapiens LIM homeobox 4 (LHX4), mRNA	0.25	2
NS3	NS3	CRP	1401	NM_000567.2	Homo sapiens C-reactive protein, pentraxin-related (CRP), mRNA	0.25	1
NS3	NS3	ERLEC1	27248	NM_001127397.2	Homo sapiens endoplasmic reticulum lectin 1 (ERLEC1), transcript variant 2, mRNA	0.25	1
NS3	NS3	KHDRBS1	10657	NM_006559.1	Homo sapiens KH domain containing, RNA binding, signal transduction associated 1 (KHDRBS1), mRNA	0.25	1
NS3	NS3	VTN	7448	NM_000638.3	Homo sapiens vitronectin (VTN), mRNA	0.25	1
NS3	NS3	C16orf87	388272	NM_001001436.2	Homo sapiens chromosome 16 open reading frame 87 (C16orf87), mRNA	0.25	1
NS3	NS3	HYAL3	8372	NM_001200029.1	Homo sapiens hyaluronoglucosaminidase 3 (HYAL3), transcript variant 5, mRNA	0.25	1

NS3	NS3	LACRT	90070	NM_033277.1	Homo sapiens lacritin (LACRT), mRNA	0.25	1
NS3	NS3	CELA2A	63036	NM_033440.2	Homo sapiens chymotrypsin-like elastase family, member 2A (CELA2A), mRNA	0.25	1
NS3	NS3	IFI30	10437	NM_006332.3	Homo sapiens interferon, gamma-inducible protein 30 (IFI30), mRNA	0.25	1
NS3	NS3	SH3GL1	6455	NM_003025.3	Homo sapiens SH3-domain GRB2-like 1 (SH3GL1), transcript variant 1, mRNA	0.25	1
NS3	NS3	TPD52L3	89882	NM_001001875.3	Homo sapiens tumour protein D52-like 3 (TPD52L3), transcript variant 3, mRNA	0.25	1
NS3	NS3	MRPL27	51264	NM_016504.2	Homo sapiens mitochondrial ribosomal protein L27 (MRPL27), nuclear gene encoding mitochondrial protein, mRNA	0.25	1
NS3	NS3	YARS2	51067	NM_001040436.2	Homo sapiens tyrosyl-tRNA synthetase 2, mitochondrial (YARS2), nuclear gene encoding mitochondrial protein, mRNA	0.25	1
NS4A1F	NS4A	MEOX2	4223	NM_005924.4	Homo sapiens mesenchyme homeobox 2 (MEOX2), mRNA	0	1
NS4A122F	NS4A	SGTA	6449 SGTA	NM_003021.3	Homo sapiens small glutamine-rich tetratricopeptide repeat (TPR)-containing, alpha (SGTA), mRNA	0.25	1
NS4B1F	NS4B	MT1X	4501	NM_005952.3	Homo sapiens metallothionein 1X (MT1X), mRNA	0.5	1
NS4B1F	NS4B	APOM	55937	NM_019101.2	Homo sapiens apolipoprotein M (APOM), transcript variant 1, mRNA	0.5	1
NS4B129F	NS4B	SUMO1	7341	NM_001005781.1	Homo sapiens SMT3 suppressor of mif two 3 homolog 1 (S. cerevisiae) (SUMO1), transcript variant 2, mRNA	1	4
NS4B129F	NS4B	SUMO1P1	391257	NR_002189.3	Homo sapiens SUMO1 pseudogene 1 (SUMO1P1), non-coding RNA	1	3
NS4B129F	NS4B	KCNS2	3788	NM_020697.2	Homo sapiens potassium voltage-gated channel, delayed-rectifier, subfamily S, member 2 (KCNS2), mRNA	1	1
NS4B191F	NS4B	PRR7	80758	NM_001174102.1	Homo sapiens proline rich 7 (synaptic) (PRR7), transcript variant 3, mRNA	0	1
NS4B191F	NS4B	GRN	2896	NM_002087.2	Homo sapiens granulin (GRN), mRNA	0	1
NS5	NS5	RPGRIP1	57096 RPGRIP1	NM_020366.3	Homo sapiens retinitis pigmentosa GTPase regulator interacting protein 1 (RPGRIP1), mRNA	0.25	1
NS5	NS5	PDZD3	79849	NM_024791.3	Homo sapiens PDZ domain containing 3 (PDZD3), transcript variant 2, mRNA	0.25	1
NS5	NS5	ID2	3398	NM_002166.4	Homo sapiens inhibitor of DNA binding 2, dominant negative helix-loop-helix protein (ID2), mRNA	0.25	1
NS5	NS5	GIPC2	54810	NM_017655.4	Homo sapiens GIPC PDZ domain containing family, member 2 (GIPC2), mRNA	0.25	1

REFERENCES

Ackermann, M. & Padmanabhan, R., 2001. De novo synthesis of RNA by the dengue virus RNA-dependent RNA polymerase exhibits temperature dependence at the initiation but not elongation phase. *The Journal of biological chemistry*, 276(43), pp.39926–37. Available at: http://www.jbc.org/content/276/43/39926.long [Accessed November 2, 2015].

Adams, B. & Boots, M., 2010. How important is vertical transmission in mosquitoes for the persistence of dengue? Insights from a mathematical model. *Epidemics*, 2(1), pp.1–10. Available at: http://www.sciencedirect.com/science/article/pii/S1755436510000022 [Accessed August 20, 2015].

Agaisse, H. & Perrimon, N., 2004. The roles of JAK/STAT signaling in Drosophila immune responses. *Immunological reviews*, 198, pp.72–82. Available at: http://www.ncbi.nlm.nih.gov/pubmed/15199955 [Accessed November 8, 2015].

Alcon, S. et al., 2002. Enzyme-linked immunosorbent assay specific to Dengue virus type 1 nonstructural protein NS1 reveals circulation of the antigen in the blood during the acute phase of disease in patients experiencing primary or secondary infections. *Journal of clinical microbiology*, 40(2), pp.376–81. Available at: http://www.pubmedcentral.nih.gov/articlerender.fcgi?artid=153354&tool=pmcentrez&rendertype=abstract [Accessed October 26, 2015].

Allison, S. et al., 1995. Oligomeric rearrangement of tick-borne encephalitis virus envelope proteins induced by an acidic pH. *J. Virol.*, 69(2), pp.695–700. Available at: http://jvi.asm.org/content/69/2/695.abstract [Accessed October 20, 2015].

Alonzo, M.T.G. et al., 2012. Platelet apoptosis and apoptotic platelet clearance by macrophages in secondary dengue virus infections. *The Journal of infectious diseases*, 205(8), pp.1321–9. Available at: http://www.ncbi.nlm.nih.gov/pubmed/22383677 [Accessed August 31, 2015].

Alphey, L. et al., 2000. Insect Population Suppression Using Engineered Insects. Available at: http://www.ncbi.nlm.nih.gov/books/NBK6570/ [Accessed October 28, 2015].

Alvarez, J.D. et al., 2000. The MAR-binding protein SATB1 orchestrates temporal and spatial expression of multiple genes during T-cell development. *Genes & Dev.*, 14(5), pp.521–535. Available at: http://genesdev.cshlp.org/content/14/5/521.short [Accessed November 1, 2015].

Angel, B. & Joshi, V., 2008. Distribution and seasonality of vertically transmitted dengue viruses in Aedes mosquitoes in arid and semi-arid areas of Rajasthan, India. *Journal of vector borne diseases*, 45(1), pp.56–9. Available at: http://www.ncbi.nlm.nih.gov/pubmed/18399318 [Accessed October 23, 2015].

Angleró-Rodríguez, Y.I., Pantoja, P. & Sariol, C.A., 2014. Dengue virus subverts the interferon induction pathway via NS2B/3 protease-IκB kinase epsilon interaction. *Clinical and vaccine immunology : CVI*, 21(1), pp.29–38. Available at: http://www.pubmedcentral.nih.gov/articlerender.fcgi?artid=3910921&tool=pmcentrez&rendertype=abstract [Accessed November 13, 2015].

Arias, C.F., Preugschat, F. & Strauss, J.H., 1993. Dengue 2 virus NS2B and NS3 form a stable complex that can cleave NS3 within the helicase domain. *Virology*, 193(2), pp.888–99. Available at: http://www.sciencedirect.com/science/article/pii/S0042682283711980 [Accessed October 27, 2015].

Arima, Y. et al., 2013. Epidemiologic update on the dengue situation in the Western Pacific Region, 2011. *Western Pacific surveillance and response journal : WPSAR*, 4(2), pp.47–54. Available at: http://www.pubmedcentral.nih.gov/articlerender.fcgi?artid=3762964&tool=pmcentrez&rendertype=abstract [Accessed November 2, 2015].

Arima, Y. & Matsui, T., 2011. Epidemiologic update on the dengue situation in the Western Pacific Region, 2010. *Western Pacific Surveillance and Response Journal*, 2(2), pp.4–8. Available at: http://www.wpro.who.int/wpsar/volumes/02/2/2011_RA_Arima_Matsui/en/ [Accessed October 27, 2015].

Armstrong, C.M. & Loboda, A., 2001. A model for 4-aminopyridine action on K channels: similarities to tetraethylammonium ion action. *Biophysical journal*, 81(2), pp.895–904. Available at: http://www.sciencedirect.com/science/article/pii/S0006349501757499 [Accessed August 17, 2015].

Arunachalam, N. et al., 2008. Natural vertical transmission of dengue viruses by Aedes aegypti in Chennai, Tamil Nadu, India. *The Indian journal of medical research*, 127(4), pp.395–7. Available at: http://www.ncbi.nlm.nih.gov/pubmed/18577796 [Accessed October 23, 2015].

Ashour, J. et al., 2009. NS5 of dengue virus mediates STAT2 binding and degradation. *Journal of virology*, 83(11), pp.5408–18. Available at: http://www.pubmedcentral.nih.gov/articlerender.fcgi?artid=2681973&tool=pmcentrez&rendertype=abstract [Accessed June 13, 2015].

Avadhanula, V. et al., 2009. A novel system for the launch of alphavirus RNA synthesis reveals a role for the Imd pathway in arthropod antiviral response. *PLoS pathogens*, 5(9), p.e1000582. Available at: http://www.pubmedcentral.nih.gov/articlerender.fcgi?artid=2738967&tool=pmcentrez&rendertype=abstract [Accessed November 4, 2015].

Avirutnan, P. et al., 2007. Secreted NS1 of dengue virus attaches to the surface of cells via interactions with heparan sulfate and chondroitin sulfate E. *PLoS pathogens*, 3(11), p.e183. Available at: http://journals.plos.org/plospathogens/article?id=10.1371/journal.ppat.0030183 [Accessed October 24, 2015].

Avirutnan, P. et al., 2006. Vascular Leakage in Severe Dengue Virus Infections: A Potential Role for the Nonstructural Viral Protein NS1 and Complement. *The Journal of Infectious Diseases*, 193(8), pp.1078–1088. Available at: http://jid.oxfordjournals.org/content/193/8/1078.long [Accessed October 17, 2015].

de Azeredo, E.L., Monteiro, R.Q. & de-Oliveira Pinto, L.M., 2015. Thrombocytopenia in Dengue: Interrelationship between Virus and the Imbalance between Coagulation and Fibrinolysis and Inflammatory Mediators. *Mediators of inflammation*, 2015, p.313842. Available at: http://www.pubmedcentral.nih.gov/articlerender.fcgi?artid=4427128&tool=pmcentrez&rendertype=abstract [Accessed August 31, 2015].

Barletta, A.B.F., Silva, M.C.L.N. & Sorgine, M.H.F., 2012. *Validation of Aedes aegypti Aag-2 cells as a model for insect immune studies.*, Available at: http://www.pubmedcentral.nih.gov/articlerender.fcgi?artid=3419682&tool=pmcentrez&rendertype=abstract [Accessed September 14, 2015].

Barrios-Rodiles, M. et al., 2005. High-throughput mapping of a dynamic signaling network in mammalian cells. *Science (New York, N.Y.)*, 307(5715), pp.1621–5. Available at: http://www.sciencemag.org/content/307/5715/1621.abstract [Accessed September 18, 2015].

Bartelma, G. & Padmanabhan, R., 2002. Expression, Purification, and Characterization of the RNA 5′-Triphosphatase Activity of Dengue Virus Type 2 Nonstructural Protein 3. *Virology*, 299(1), pp.122–132. Available at: http://www.sciencedirect.com/science/article/pii/S0042682202915047 [Accessed October 27, 2015].

Bartholomeusz, A.I. & Wright, P.J., 1993. Synthesis of dengue virus RNA in vitro: initiation and the involvement of proteins NS3 and NS5. *Archives of Virology*, 128(1-2), pp.111–121. Available at: http://link.springer.com/10.1007/BF01309792 [Accessed October 30, 2015].

Bartok, A. et al., 2014. Margatoxin is a non-selective inhibitor of human Kv1.3 K+ channels. *Toxicon : official journal of the International Society on Toxinology*, 87, pp.6–16. Available at: http://www.sciencedirect.com/science/article/pii/S0041010114001287 [Accessed August 21, 2015].

Basurko, C. et al., 2009. Maternal and foetal consequences of dengue fever during pregnancy. *European Journal of Obstetrics & Gynecology and Reproductive Biology*, 147(1), pp.29–32. Available at: http://www.ejog.org/article/S0301211509004345/fulltext [Accessed September 23, 2015].

Bednarczyk, P. et al., 2010. Identification of a voltage-gated potassium channel in gerbil hippocampal mitochondria. *Biochemical and biophysical research communications*, 397(3), pp.614–20. Available at: http://www.sciencedirect.com/science/article/pii/S0006291X10011149 [Accessed September 4, 2015].

Benarroch, D. et al., 2004. A structural basis for the inhibition of the NS5 dengue virus mRNA 2'-O-methyltransferase domain by ribavirin 5'-triphosphate. *The Journal of biological chemistry*, 279(34), pp.35638–43. Available at: http://www.jbc.org/content/279/34/35638.long [Accessed November 2, 2015].

Best, S.M. et al., 2005. Inhibition of interferon-stimulated JAK-STAT signaling by a tick-borne flavivirus and identification of NS5 as an interferon antagonist. *Journal of virology*, 79(20), pp.12828–39. Available at: http://jvi.asm.org/content/79/20/12828.long [Accessed August 15, 2015].

Bezanilla, F., 2000. The Voltage Sensor in Voltage-Dependent Ion Channels. *Physiol Rev*, 80(2), pp.555–592. Available at: http://physrev.physiology.org/content/80/2/555 [Accessed August 31, 2015].

Bhatt, S. et al., 2013. The global distribution and burden of dengue. *Nature*, 496(7446), pp.504–7. Available at: http://dx.doi.org/10.1038/nature12060 [Accessed July 11, 2014].

Birot, A.-M. et al., 2000. Identification and molecular analysis of BANP. *Gene*, 253(2), pp.189–196. Available at: http://www.sciencedirect.com/science/article/pii/S0378111900002444 [Accessed October 29, 2015].

Blacksell, S.D. et al., 2011. Evaluation of six commercial point-of-care tests for diagnosis of acute dengue infections: the need for combining NS1 antigen and IgM/IgG antibody detection to achieve acceptable levels of accuracy. *Clinical and vaccine immunology : CVI*, 18(12), pp.2095–101. Available at: http://cvi.asm.org/content/18/12/2095 [Accessed October 29, 2015].

Blair, C.D., 2011. Mosquito RNAi is the major innate immune pathway controlling arbovirus infection and transmission. *Future microbiology*, 6(3), pp.265–77. Available at: http://www.futuremedicine.com/doi/abs/10.2217/fmb.11.11 [Accessed August 6, 2015].

Blasche, S. & Koegl, M., 2013. Analysis of protein-protein interactions using LUMIER assays. *Methods in molecular biology (Clifton, N.J.)*, 1064, pp.17–27. Available at: http://www.ncbi.nlm.nih.gov/pubmed/23996247 [Accessed June 22, 2015].

Bode, J. et al., 1992. Biological significance of unwinding capability of nuclear matrix-associating DNAs. *Science (New York, N.Y.)*, 255(5041), pp.195–7. Available at: http://www.ncbi.nlm.nih.gov/pubmed/1553545 [Accessed October 30, 2015].

Bogdanov, E.A. et al., 2010. Normalizing cDNA libraries. *Current protocols in molecular biology / edited by Frederick M. Ausubel ... [et al.]*, Chapter 5, p.Unit 5.12.1–27. Available at: http://www.ncbi.nlm.nih.gov/pubmed/20373503 [Accessed October 4, 2015].

Bonifacino, J.S., Dell'Angelica, E.C. & Springer, T.A., 2001. Immunoprecipitation. *Current protocols in molecular biology / edited by Frederick M. Ausubel ... [et al.]*, Chapter 10, p.Unit 10.16. Available at: http://www.ncbi.nlm.nih.gov/pubmed/18265056 [Accessed August 15, 2015].

Bouraï, M. et al., 2012. Mapping of Chikungunya virus interactions with host proteins identified nsP2 as a highly connected viral component. *Journal of virology*, 86(6), pp.3121–34. Available at: http://www.pubmedcentral.nih.gov/articlerender.fcgi?artid=3302312&tool=pmcentrez&rendertype=abstract [Accessed November 3, 2015].

Brabant, M. et al., 2009. A flavivirus protein M-derived peptide directly permeabilizes mitochondrial membranes, triggers cell death and reduces human tumor growth in nude mice. *Apoptosis : an international journal on programmed cell death*, 14(10), pp.1190–203. Available at: http://www.ncbi.nlm.nih.gov/pubmed/19693674 [Accessed September 30, 2015].

Brackney, D.E. et al., 2010. C6/36 Aedes albopictus cells have a dysfunctional antiviral RNA interference response. *PLoS neglected tropical diseases*, 4(10), p.e856. Available at: http://www.pubmedcentral.nih.gov/articlerender.fcgi?artid=2964293&tool=pmcentrez&rendertype=abstract [Accessed September 12, 2015].

Brault, J.-B. et al., 2011. The interaction of flavivirus M protein with light chain Tctex-1 of human dynein plays a role in late stages of virus replication. *Virology*, 417(2), pp.369–78. Available at: http://www.sciencedirect.com/science/article/pii/S0042682211002868 [Accessed September 9, 2015].

Braun, P. et al., 2009. An experimentally derived confidence score for binary protein-protein interactions. *Nature methods*, 6(1), pp.91–7. Available at: http://www.pubmedcentral.nih.gov/articlerender.fcgi?artid=2976677&tool=pmcentrez&rendertype=abstract [Accessed October 23, 2015].

Bray, M. & Lai, C.-J., 1991. Dengue virus premembrane and membrane proteins elicit a protective immune response. *Virology*, 185(1), pp.505–508. Available at: http://www.sciencedirect.com/science/article/pii/004268229190809P [Accessed October 26, 2015].

Bressan, G.M. et al., 1993. Emilin, a component of elastic fibers preferentially located at the elastin-microfibrils interface. *The Journal of cell biology*, 121(1), pp.201–12. Available at: http://www.pubmedcentral.nih.gov/articlerender.fcgi?artid=2119774&tool=pmcentrez&rendertype=abstract [Accessed November 3, 2015].

Le Breton, M. et al., 2011. Flavivirus NS3 and NS5 proteins interaction network: a high-throughput yeast two-hybrid screen. *BMC microbiology*, 11(1), p.234. Available at: http://www.biomedcentral.com/1471-2180/11/234 [Accessed May 2, 2015].

Brown, J.C. & Song, C., 2005. High quality cDNA libraries for discovery and validation of novel drug targets. *Emerging Therapeutic Targets*. Available at: http://www.tandfonline.com/doi/abs/10.1517/14728222.4.1.113 [Accessed September 29, 2015].

Brückner, A. et al., 2009. Yeast two-hybrid, a powerful tool for systems biology. *International journal of molecular sciences*, 10(6), pp.2763–88. Available at: http://www.pubmedcentral.nih.gov/articlerender.fcgi?artid=2705515&tool=pmcentrez&rendertype=abstract [Accessed August 27, 2015].

Bulet, P., 1999. Antimicrobial peptides in insects; structure and function. *Developmental & Comparative Immunology*, 23(4-5), pp.329–344. Available at: http://www.sciencedirect.com/science/article/pii/S0145305X99000154 [Accessed November 8, 2015].

Cahalan, M.D. et al., 1985. A voltage-gated potassium channel in human T lymphocytes. *The Journal of Physiology*, 358(1), pp.197–237. Available at: http://doi.wiley.com/10.1113/jphysiol.1985.sp015548 [Accessed August 29, 2015].

Cai, Y.C. & Douglass, J., 1993. In vivo and in vitro phosphorylation of the T lymphocyte type n (Kv1.3) potassium channel. *J. Biol. Chem.*, 268(31), pp.23720–23727. Available at: http://www.jbc.org/content/268/31/23720 [Accessed August 28, 2015].

Calderwood, M.A. et al., 2007. Epstein-Barr virus and virus human protein interaction maps. *Proceedings of the National Academy of Sciences of the United States of America*, 104(18), pp.7606–11. Available at: http://www.pnas.org/content/104/18/7606.long [Accessed June 16, 2015].

Callahan, J.D. et al., 2001. Development and evaluation of serotype- and group-specific fluorogenic reverse transcriptase PCR (TaqMan) assays for dengue virus. *Journal of clinical microbiology*, 39(11), pp.4119–24. Available at: http://jcm.asm.org/content/39/11/4119.long [Accessed August 3, 2015].

Cao, S. & Yan, L., 2013. Construction of a high-quality yeast two-hybrid (Y2H) library and its application in identification of interacting proteins with key vernalization regulator TaVRN-A1 in wheat. *BMC research notes*, 6(1), p.81. Available at: http://www.biomedcentral.com/1756-0500/6/81 [Accessed October 4, 2015].

Cao-Lormeau, V.-M., 2009. Dengue viruses binding proteins from Aedes aegypti and Aedes polynesiensis salivary glands. *Virology journal*, 6(1), p.35. Available at: http://www.virologyj.com/content/6/1/35 [Accessed October 22, 2015].

Cardosa, M.J. et al., 2002. Antibodies against prM protein distinguish between previous infection with dengue and Japanese encephalitis viruses. *BMC microbiology*, 2, p.9. Available at: http://www.pubmedcentral.nih.gov/articlerender.fcgi?artid=113253&tool=pmcentrez&rendertype=abstract [Accessed November 2, 2015].

Carnec, X. et al., 2015. The Phosphatidylserine and Phosphatidylethanolamine Receptor CD300a Binds Dengue Virus and Enhances Infection. *Journal of virology*, 90(1), pp.92–102. Available at: http://jvi.asm.org/content/90/1/92.long?hwshib2=authn%3A1460187267%3A20160408%253A1bd4e719-4a5f-4867-aba9-35c256d81831%3A0%3A0%3A0%3ARae0%2B5BeBmuqPE%2BM5j95eg%3D%3D [Accessed March 1, 2016].

Carvalho, F.A. et al., 2012. Dengue virus capsid protein binding to hepatic lipid droplets (LD) is potassium ion dependent and is mediated by LD surface proteins. *Journal of virology*, 86(4), pp.2096–108. Available at: http://jvi.asm.org/search?author1=Ivo+C.+Martins&sortspec=date&submit=Submit [Accessed October 27, 2015].

Catteau, A. et al., 2003. Dengue virus M protein contains a proapoptotic sequence referred to as ApoptoM. *The Journal of general virology*, 84(Pt 10), pp.2781–93. Available at: http://jgv.microbiologyresearch.org/content/journal/jgv/10.1099/vir.0.19163-0 [Accessed October 26, 2015].

Cervantes-Salazar, M. et al., 2015. Dengue virus NS1 protein interacts with the ribosomal protein RPL18: This interaction is required for viral translation and replication in Huh-7 cells. *Virology*, 484, pp.113–26. Available at: http://www.ncbi.nlm.nih.gov/pubmed/26092250 [Accessed November 2, 2015].

Chadee, D.D., 2013. Resting behaviour of Aedes aegypti in Trinidad: with evidence for the re-introduction of indoor residual spraying (IRS) for dengue control. *Parasites & vectors*, 6(1), p.255. Available at: http://www.parasitesandvectors.com/content/6/1/255 [Accessed October 22, 2015].

Chakraborty, S. et al., 2014. Nuclear matrix protein SMAR1 represses c-Fos-mediated HPV18 E6 transcription through alteration of chromatin histone deacetylation. *The Journal of biological chemistry*, 289(42), pp.29074–85. Available at: http://www.pubmedcentral.nih.gov/articlerender.fcgi?artid=4200262&tool=pmcentrez&rendertype=abstract [Accessed November 3, 2015].

Chakravarti, A. & Kumaria, R., 2006. Circulating levels of tumour necrosis factor-alpha & interferon-gamma in patients with dengue & dengue haemorrhagic fever during an outbreak. *The Indian journal of medical research*, 123(1), pp.25–30. Available at: http://www.ncbi.nlm.nih.gov/pubmed/16567864 [Accessed October 21, 2015].

Chandy, K.G., 1991. Simplified gene nomenclature. *Nature*, 352(6330), p.26. Available at: http://www.ncbi.nlm.nih.gov/pubmed/2062374 [Accessed August 31, 2015].

Chareonsirisuthigul, T., Kalayanarooj, S. & Ubol, S., 2007. Dengue virus (DENV) antibody-dependent enhancement of infection upregulates the production of anti-inflammatory cytokines, but suppresses anti-DENV free radical and pro-inflammatory cytokine production, in THP-1 cells. *The Journal of general virology*, 88(Pt 2), pp.365–75. Available at: http://jgv.microbiologyresearch.org/content/journal/jgv/10.1099/vir.0.82537-0 [Accessed October 2, 2015].

Charest, A. et al., 2001. Association of a novel PDZ domain-containing peripheral Golgi protein with the Q-SNARE (Q-soluble N-ethylmaleimide-sensitive fusion protein (NSF) attachment protein receptor) protein syntaxin 6. *The Journal of biological chemistry*, 276(31), pp.29456–65. Available at: http://www.ncbi.nlm.nih.gov/pubmed/11384996 [Accessed November 3, 2015].

de Chassey, B. et al., 2008. Hepatitis C virus infection protein network. *Molecular systems biology*, 4, p.230. Available at: /pmc/articles/PMC2600670/?report=abstract [Accessed June 17, 2015].

de Chassey, B. et al., 2013. The interactomes of influenza virus NS1 and NS2 proteins identify new host factors and provide insights for ADAR1 playing a supportive role in virus replication. *PLoS pathogens*, 9(7), p.e1003440. Available at: http://www.pubmedcentral.nih.gov/articlerender.fcgi?artid=3701712&tool=pmcentrez&rendert

ype=abstract [Accessed March 9, 2015].

Chattopadhyay, S. et al., 2000a. SMAR1, a novel, alternatively spliced gene product, binds the Scaffold/Matrix-associated region at the T cell receptor beta locus. *Genomics*, 68(1), pp.93–6. Available at: http://www.sciencedirect.com/science/article/pii/S0888754300962797 [Accessed August 15, 2015].

Chattopadhyay, S. et al., 2000b. SMAR1, a novel, alternatively spliced gene product, binds the Scaffold/Matrix-associated region at the T cell receptor beta locus. *Genomics*, 68(1), pp.93–6. Available at: http://www.ncbi.nlm.nih.gov/pubmed/10950932 [Accessed October 30, 2015].

Chattopadhyay, S. & Pavithra, L., 2007. MARs and MARBPs: key modulators of gene regulation and disease manifestation. *Sub-cellular biochemistry*, 41, pp.213–30. Available at: http://www.ncbi.nlm.nih.gov/pubmed/17484130 [Accessed November 1, 2015].

Chaudhary, N. et al., 2014. SMAR1 coordinates HDAC6-induced deacetylation of Ku70 and dictates cell fate upon irradiation. *Cell death & disease*, 5, p.e1447. Available at: http://www.pubmedcentral.nih.gov/articlerender.fcgi?artid=4237237&tool=pmcentrez&rendertype=abstract [Accessed August 15, 2015].

Chee, H.Y. & AbuBakar, S., 2004. Identification of a 48 kDa tubulin or tubulin-like C6/36 mosquito cells protein that binds dengue virus 2 using mass spectrometry. *Biochemical and Biophysical Research Communications*, 320(1), pp.11–17.

Chen, S.-T. et al., 2008. CLEC5A is critical for dengue-virus-induced lethal disease. *Nature*, 453(7195), pp.672–676. Available at: http://dx.doi.org/10.1038/nature07013 [Accessed October 21, 2015].

Chen, Y. et al., 1997. Dengue virus infectivity depends on envelope protein binding to target cell heparan sulfate. *Nature medicine*, 3(8), pp.866–71. Available at: http://www.ncbi.nlm.nih.gov/pubmed/9256277 [Accessed September 28, 2015].

Cheng, S. et al., 1994. Effective amplification of long targets from cloned inserts and human genomic DNA. *Proceedings of the National Academy of Sciences of the United States of America*, 91(12), pp.5695–9. Available at: http://www.pubmedcentral.nih.gov/articlerender.fcgi?artid=44063&tool=pmcentrez&rendertype=abstract [Accessed November 5, 2015].

Chisenhall, D.M. et al., 2014. Effect of dengue-2 virus infection on protein expression in the salivary glands of Aedes aegypti mosquitoes. *The American journal of tropical medicine and hygiene*, 90(3), pp.431–7. Available at: http://www.ajtmh.org/content/90/3/431.long [Accessed September 30, 2015].

Chiu, M.-W. et al., 2007. The type 2 dengue virus envelope protein interacts with small ubiquitin-like modifier-1 (SUMO-1) conjugating enzyme 9 (Ubc9). *Journal of biomedical science*, 14(3), pp.429–44. Available at: http://www.ncbi.nlm.nih.gov/pubmed/17265167 [Accessed November 3, 2015].

Choquet, D. & Korn, H., 1992. Mechanism of 4-aminopyridine action on voltage-gated potassium channels in lymphocytes. *The Journal of general physiology*, 99(2), pp.217–40. Available at: http://www.pubmedcentral.nih.gov/articlerender.fcgi?artid=2216608&tool=pmcentrez&rendertype=abstract [Accessed September 3, 2015].

Chua, J.J.E., Ng, M.M.L. & Chow, V.T.K., 2004. The non-structural 3 (NS3) protein of dengue virus type 2 interacts with human nuclear receptor binding protein and is associated with alterations in membrane structure. *Virus research*, 102(2), pp.151–63. Available at: http://www.sciencedirect.com/science/article/pii/S0168170204000437 [Accessed November 18, 2015].

Chung, K.M. et al., 2006. West Nile virus nonstructural protein NS1 inhibits complement activation by binding the regulatory protein factor H. *Proceedings of the National Academy of Sciences of the United States of America*, 103(50), pp.19111–6. Available at: http://www.pubmedcentral.nih.gov/articlerender.fcgi?artid=1664712&tool=pmcentrez&rendertype=abstract [Accessed November 18, 2015].

Chye, J.K. et al., 1997. Vertical transmission of dengue. *Clinical infectious diseases : an official publication of the Infectious Diseases Society of America*, 25(6), pp.1374–7. Available at: http://www.ncbi.nlm.nih.gov/pubmed/9431381 [Accessed October 22, 2015].

Clontech, 2010. *Make Your Own " Mate & Plate ™ " Library System User Manual*, Clontech Laboratories, Inc. Takara Bio Company [Accessed July 30, 2015].

Colpitts, T.M. et al., 2011. Use of a tandem affinity purification assay to detect interactions between West Nile and dengue viral proteins and proteins of the mosquito vector. *Virology*, 417(1), pp.179–87. Available at: http://www.pubmedcentral.nih.gov/articlerender.fcgi?artid=3166580&tool=pmcentrez&rendertype=abstract [Accessed September 30, 2015].

Comes, N. et al., 2013. The voltage-dependent K(+) channels Kv1.3 and Kv1.5 in human cancer. *Frontiers in physiology*, 4, p.283. Available at: http://journal.frontiersin.org/article/10.3389/fphys.2013.00283/abstract [Accessed August 29, 2015].

Condreay, L.D. & Brown, D.T., 1986. Exclusion of superinfecting homologous virus by Sindbis virus-infected Aedes albopictus (mosquito) cells. *J. Virol.*, 58(1), pp.81–86. Available at: http://jvi.asm.org/content/58/1/81.short [Accessed July 30, 2015].

Conwell, S.E. et al., 2015. Identification of TRIM27 as a novel degradation target of herpes simplex virus 1 ICP0. *Journal of virology*, 89(1), pp.220–9. Available at: http://jvi.asm.org/content/89/1/220.short [Accessed June 17, 2015].

Costa, A. et al., 2009. The Imd pathway is involved in antiviral immune responses in Drosophila. *PloS one*, 4(10), p.e7436. Available at: http://journals.plos.org/plosone/article?id=10.1371/journal.pone.0007436 [Accessed October 5, 2015].

Crill, W.D. & Roehrig, J.T., 2001. Monoclonal antibodies that bind to domain III of dengue virus E glycoprotein are the most efficient blockers of virus adsorption to Vero cells. *Journal of virology*, 75(16), pp.7769–73. Available at: http://jvi.asm.org/content/75/16/7769.long [Accessed October 29, 2015].

Cuzzubbo, A.J. et al., 1998. Detection of specific antibodies in saliva during dengue infection. *Journal of clinical microbiology*, 36(12), pp.3737–9. Available at: http://jcm.asm.org/content/36/12/3737.abstract [Accessed October 28, 2015].

Dame, D.A. et al., 2009. Historical applications of induced sterilisation in field populations of mosquitoes. *Malaria Journal*, 8(Suppl 2), p.S2. Available at: http://www.malariajournal.com/content/8/S2/S2 [Accessed October 22, 2015].

Danussi, C. et al., 2008. Emilin1 deficiency causes structural and functional defects of lymphatic vasculature. *Molecular and cellular biology*, 28(12), pp.4026–39. Available at: http://www.pubmedcentral.nih.gov/articlerender.fcgi?artid=2423131&tool=pmcentrez&rendertype=abstract [Accessed November 3, 2015].

David, J.-P. et al., 2010. Transcriptome response to pollutants and insecticides in the dengue vector Aedes aegypti using next-generation sequencing technology. *BMC genomics*, 11(1), p.216. Available at: http://www.biomedcentral.com/1471-2164/11/216.

Dolan, P.T. et al., 2013. Identification and comparative analysis of hepatitis C virus-host cell protein interactions. *Molecular bioSystems*, 9(12), pp.3199–209. Available at: http://www.pubmedcentral.nih.gov/articlerender.fcgi?artid=4171131&tool=pmcentrez&rendertype=abstract [Accessed May 20, 2015].

Domon, B. & Aebersold, R., 2006. Mass spectrometry and protein analysis. *Science (New York, N.Y.)*, 312(5771), pp.212–7. Available at: http://www.sciencemag.org/content/312/5771/212 [Accessed July 10, 2014].

Donald, C.L., Kohl, A. & Schnettler, E., 2012. New Insights into Control of Arbovirus Replication and Spread by Insect RNA Interference Pathways. *Insects*, 3(4), pp.511–531. Available at: http://www.mdpi.com/2075-4450/3/2/511/htm [Accessed August 17, 2015].

Doolittle, J.M. & Gomez, S.M., 2011. Mapping protein interactions between Dengue virus and its human and insect hosts. *PLoS neglected tropical diseases*, 5(2), p.e954. Available at: http://journals.plos.org/plosntds/article?id=10.1371/journal.pntd.0000954 [Accessed June 8, 2015].

Dostert, C. et al., 2005. The Jak-STAT signaling pathway is required but not sufficient for the antiviral response of drosophila. *Nature immunology*, 6(9), pp.946–53. Available at: http://www.ncbi.nlm.nih.gov/pubmed/16086017 [Accessed September 2, 2015].

Dreux, M. et al., 2009. The autophagy machinery is required to initiate hepatitis C virus replication. *Proceedings of the National Academy of Sciences of the United States of America*, 106(33), pp.14046–51. Available at: http://www.pubmedcentral.nih.gov/articlerender.fcgi?artid=2729017&tool=pmcentrez&rendertype=abstract [Accessed February 22, 2016].

Duan, X. et al., 2008. Novel binding between pre-membrane protein and vacuolar ATPase is required for efficient dengue virus secretion. *Biochemical and biophysical research communications*, 373(2), pp.319–24. Available at: http://www.sciencedirect.com/science/article/pii/S0006291X08011674 [Accessed October 26, 2015].

Durbin, A.P. et al., 2008. Phenotyping of peripheral blood mononuclear cells during acute dengue illness demonstrates infection and increased activation of monocytes in severe cases compared to classic dengue fever. *Virology*, 376(2), pp.429–35. Available at: /pmc/articles/PMC2546568/?report=abstract [Accessed November 2, 2015].

Dussart, P. et al., 2006. Evaluation of an enzyme immunoassay for detection of dengue virus NS1 antigen in human serum. *Clinical and vaccine immunology : CVI*, 13(11), pp.1185–9. Available at: http://cvi.asm.org/content/13/11/1185.abstract [Accessed October 28, 2015].

Dyer, M.D., Murali, T.M. & Sobral, B.W., 2008. The landscape of human proteins interacting with viruses and other pathogens. *PLoS pathogens*, 4(2), p.e32. Available at: http://www.pubmedcentral.nih.gov/articlerender.fcgi?artid=2242834&tool=pmcentrez&rendertype=abstract [Accessed June 8, 2015].

Eckels, K.H. et al., 2003. Modification of dengue virus strains by passage in primary dog kidney cells: preparation of candidate vaccines and immunization of monkeys. *The American journal of tropical medicine and hygiene*, 69(6 Suppl), pp.12–6. Available at: http://www.ncbi.nlm.nih.gov/pubmed/14740950 [Accessed November 2, 2015].

Edelman, R., 2007. Dengue vaccines approach the finish line. *Clinical infectious diseases : an official publication of the Infectious Diseases Society of America*, 45 Suppl 1(Supplement_1), pp.S56–60. Available at: http://cid.oxfordjournals.org/content/45/Supplement_1/S56.long [Accessed November 2, 2015].

Egloff, M.-P. et al., 2002. An RNA cap (nucleoside-2'-O-)-methyltransferase in the flavivirus RNA polymerase NS5: crystal structure and functional characterization. *The EMBO journal*, 21(11), pp.2757–68. Available at: http://www.pubmedcentral.nih.gov/articlerender.fcgi?artid=125380&tool=pmcentrez&rendertype=abstract [Accessed November 2, 2015].

Elshuber, S. et al., 2003. Cleavage of protein prM is necessary for infection of BHK-21 cells by tick-borne encephalitis virus. *The Journal of general virology*, 84(Pt 1), pp.183–91. Available at: http://jgv.microbiologyresearch.org/content/view.action?itemId=http%3A%2F%2Fsgm.metastore.ingenta.com%2Fcontent%2Fjournal%2Fjgv%2F10.1099%2Fvir.0.18723-0&view=&itemType=http%3A%2F%2Fpub2web.metastore.ingenta.com%2Fns%2FArticle [Accessed October 19, 2015].

Espinosa, M. et al., 2014. Vertical transmission of dengue virus in Aedes aegypti collected in Puerto Iguazú, Misiones, Argentina. *Revista do Instituto de Medicina Tropical de São Paulo*, 56(2), pp.165–7. Available at: http://www.pubmedcentral.nih.gov/articlerender.fcgi?artid=4085839&tool=pmcentrez&rendertype=abstract [Accessed October 23, 2015].

Esteva, L. & Vargas, C., 2000. Influence of vertical and mechanical transmission on the dynamics of

dengue disease. *Mathematical Biosciences*, 167(1), pp.51–64. Available at: http://www.sciencedirect.com/science/article/pii/S0025556400000249 [Accessed October 25, 2015].

Falgout, B. et al., 1991. Both nonstructural proteins NS2B and NS3 are required for the proteolytic processing of dengue virus nonstructural proteins. *Journal of virology*, 65(5), pp.2467–75. Available at: http://www.pubmedcentral.nih.gov/articlerender.fcgi?artid=240601&tool=pmcentrez&rendertype=abstract [Accessed October 27, 2015].

Fan, J., Liu, Y. & Yuan, Z., 2014. Critical role of Dengue Virus NS1 protein in viral replication. *Virologica Sinica*, 29(3), pp.162–9. Available at: http://www.ncbi.nlm.nih.gov/pubmed/24903593 [Accessed October 26, 2015].

Faustino, A.F. et al., 2014. Dengue virus capsid protein interacts specifically with very low-density lipoproteins. *Nanomedicine : nanotechnology, biology, and medicine*, 10(1), pp.247–55. Available at: http://www.sciencedirect.com/science/article/pii/S1549963413002724 [Accessed October 27, 2015].

Felipe, A. et al., 2012. Targeting the voltage-dependent K(+) channels Kv1.3 and Kv1.5 as tumor biomarkers for cancer detection and prevention. *Current medicinal chemistry*, 19(5), pp.661–74. Available at: http://www.ncbi.nlm.nih.gov/pubmed/22204339 [Accessed August 31, 2015].

Fernandez-Garcia, M.-D. et al., 2009. Pathogenesis of Flavivirus Infections: Using and Abusing the Host Cell. *Cell Host & Microbe*, 5(4), pp.318–328. Available at: http://www.sciencedirect.com/science/article/pii/S1931312809001024 [Accessed October 10, 2015].

Ferrandon, D. et al., 2007. The Drosophila systemic immune response: sensing and signalling during bacterial and fungal infections. *Nature reviews. Immunology*, 7(11), pp.862–74. Available at: http://dx.doi.org/10.1038/nri2194 [Accessed November 8, 2015].

Fink, J. et al., 2007. Host gene expression profiling of dengue virus infection in cell lines and patients. *PLoS neglected tropical diseases*, 1(2), p.e86. Available at: http://www.pubmedcentral.nih.gov/articlerender.fcgi?artid=2100376&tool=pmcentrez&rendertype=abstract [Accessed June 6, 2015].

Fischl, W. & Bartenschlager, R., 2011. Exploitation of cellular pathways by Dengue virus. *Current opinion in microbiology*, 14(4), pp.470–5. Available at: http://www.sciencedirect.com/science/article/pii/S1369527411000968 [Accessed June 28, 2015].

Flamand, M. et al., 1999. Dengue virus type 1 nonstructural glycoprotein NS1 is secreted from mammalian cells as a soluble hexamer in a glycosylation-dependent fashion. *Journal of virology*, 73(7), pp.6104–10. Available at: http://www.pubmedcentral.nih.gov/articlerender.fcgi?artid=112675&tool=pmcentrez&rendertype=abstract [Accessed October 26, 2015].

Flipse, J., Wilschut, J. & Smit, J.M., 2013. Molecular mechanisms involved in antibody-dependent enhancement of dengue virus infection in humans. *Traffic (Copenhagen, Denmark)*, 14(1), pp.25–35. Available at: http://www.ncbi.nlm.nih.gov/pubmed/22998156 [Accessed October 28, 2015].

Folly, B.B. et al., 2011. Dengue-2 structural proteins associate with human proteins to produce a coagulation and innate immune response biased interactome. *BMC infectious diseases*, 11(1), p.34. Available at: http://www.biomedcentral.com/1471-2334/11/34 [Accessed June 2, 2015].

Fragkoudis, R. et al., 2008. Semliki Forest virus strongly reduces mosquito host defence signaling. *Insect molecular biology*, 17(6), pp.647–56. Available at: http://www.pubmedcentral.nih.gov/articlerender.fcgi?artid=2710796&tool=pmcentrez&rendertype=abstract [Accessed July 31, 2015].

Friedel, C.C. & Haas, J., 2011. Virus-host interactomes and global models of virus-infected cells. *Trends in microbiology*, 19(10), pp.501–8. Available at: http://www.ncbi.nlm.nih.gov/pubmed/21855347 [Accessed October 28, 2015].

Friedman, E.E. et al., 2014. Symptomatic Dengue infection during pregnancy and infant outcomes: a retrospective cohort study. *PLoS neglected tropical diseases*, 8(10), p.e3226. Available at: http://journals.plos.org/plosntds/article?id=10.1371/journal.pntd.0003226 [Accessed October 25, 2015].

Fritz, R., Stiasny, K. & Heinz, F.X., 2008. Identification of specific histidines as pH sensors in flavivirus membrane fusion. *The Journal of cell biology*, 183(2), pp.353–61. Available at: http://jcb.rupress.org/content/183/2/353 [Accessed October 21, 2015].

Fujiwara, H. & Ishikawa, H., 1986. Molecular mechanism of introduction of the hidden break into the 28S rRNA of insects: implication based on structural studies. *Nucleic acids research*, 14(16), pp.6393–401. Available at: http://www.pubmedcentral.nih.gov/articlerender.fcgi?artid=311653&tool=pmcentrez&rendertype=abstract [Accessed October 3, 2015].

Fusco, C., Guidotti, E. & Zervos, A.S., 1999. In vivo construction of cDNA libraries for use in the yeast two-hybrid system. *Yeast (Chichester, England)*, 15(8), pp.715–20. Available at: http://www.ncbi.nlm.nih.gov/pubmed/10392448 [Accessed September 12, 2015].

Gao, F. et al., 2010. Novel binding between pre-membrane protein and claudin-1 is required for efficient dengue virus entry. *Biochemical and biophysical research communications*, 391(1), pp.952–7. Available at: http://www.sciencedirect.com/science/article/pii/S0006291X09023687 [Accessed October 26, 2015].

Garcia-Calvo, M. et al., 1993. Purification, characterization, and biosynthesis of margatoxin, a component of Centruroides margaritatus venom that selectively inhibits voltage-dependent potassium channels. *J. Biol. Chem.*, 268(25), pp.18866–18874. Available at: http://www.jbc.org/content/268/25/18866 [Accessed August 28, 2015].

Gasser, S.M. & Laemmli, U.K., 1987. A glimpse at chromosomal order. *Trends in Genetics*, 3, pp.16–22. Available at: http://www.sciencedirect.com/science/article/pii/0168952587901569 [Accessed November 1, 2015].

Gazula, V.-R. et al., 2010. Localization of Kv1.3 channels in presynaptic terminals of brainstem auditory neurons. *The Journal of comparative neurology*, 518(16), pp.3205–20. Available at: http://www.pubmedcentral.nih.gov/articlerender.fcgi?artid=2894291&tool=pmcentrez&rendertype=abstract [Accessed August 29, 2015].

Giard, D.J. et al., 1973. In vitro cultivation of human tumors: establishment of cell lines derived from a series of solid tumors. *Journal of the National Cancer Institute*, 51(5), pp.1417–23. Available at: http://www.ncbi.nlm.nih.gov/pubmed/4357758 [Accessed April 14, 2015].

Gietz, R.D. & Schiestl, R.H., 2007. High-efficiency yeast transformation using the LiAc/SS carrier DNA/PEG method. *Nature protocols*, 2(1), pp.31–4. Available at: http://dx.doi.org/10.1038/nprot.2007.13 [Accessed July 10, 2014].

Gindullis, F., 1999. Matrix Attachment Region Binding Protein MFP1 Is Localized in Discrete Domains at the Nuclear Envelope. *The Plant Cell Online*, 11(6), pp.1117–1128. Available at: http://www.plantcell.org/content/11/6/1117.full [Accessed November 1, 2015].

Giot, L. et al., 2003. A protein interaction map of Drosophila melanogaster. *Science (New York, N.Y.)*, 302(5651), pp.1727–36. Available at: http://www.sciencemag.org/content/302/5651/1727.abstract [Accessed October 25, 2015].

Girod, P.-A. & Mermod, N., 2003. *Gene Transfer and Expression in Mammalian Cells*, Elsevier. Available at: http://www.sciencedirect.com/science/article/pii/S0167730603380226 [Accessed October 30, 2015].

Goebel, P. et al., 2002. High frequency of matrix attachment regions and cut-like protein x/CCAAT-displacement protein and B cell regulator of IgH transcription binding sites flanking Ig V region genes. *Journal of immunology (Baltimore, Md. : 1950)*, 169(5), pp.2477–87. Available at: http://www.ncbi.nlm.nih.gov/pubmed/12193717 [Accessed November 1, 2015].

Le Goff, G. et al., 2011. Natural vertical transmission of dengue viruses by Aedes aegypti in Bolivia. *Parasite (Paris, France)*, 18(3), pp.277–80. Available at:

http://www.pubmedcentral.nih.gov/articlerender.fcgi?artid=3671471&tool=pmcentrez&rendertype=abstract [Accessed October 23, 2015].

Gomez, S.M. et al., 2005. Pilot Anopheles gambiae full-length cDNA study: sequencing and initial characterization of 35,575 clones. *Genome biology*, 6(4), p.R39. Available at: http://www.pubmedcentral.nih.gov/articlerender.fcgi?artid=1088967&tool=pmcentrez&rendertype=abstract [Accessed September 5, 2015].

Graham, F.L. et al., 1977. Characteristics of a Human Cell Line Transformed by DNA from Human Adenovirus Type 5. *Journal of General Virology*, 36(1), pp.59–72. Available at: http://jgv.microbiologyresearch.org/content/journal/jgv/10.1099/0022-1317-36-1-59 [Accessed May 4, 2015].

Green, A.M. et al., 2014. Innate immunity to dengue virus infection and subversion of antiviral responses. *Journal of molecular biology*, 426(6), pp.1148–60. Available at: http://www.sciencedirect.com/science/article/pii/S0022283613007341 [Accessed February 28, 2015].

Grunnet, M. et al., 2003. The voltage-gated potassium channel subunit, Kv1.3, is expressed in epithelia. *Biochimica et Biophysica Acta (BBA) - Biomembranes*, 1616(1), pp.85–94. Available at: http://www.sciencedirect.com/science/article/pii/S0005273603001986 [Accessed August 29, 2015].

Gubler, D., 1998. Dengue and Dengue Hemorrhagic Fever. *Clin. Microbiol. Rev.*, 11(3), pp.480–496. Available at: http://cmr.asm.org/content/11/3/480.full [Accessed October 15, 2015].

Gubler, D., 1997. Epidemic Dengue/Dengue Haemorrhagic Fever: a global public health problem in the 21st century. *Dengue Bulletin*, 21, pp.1–19. Available at: http://repository.searo.who.int/handle/123456789/16283 [Accessed October 28, 2015].

Gubler, D., 2002. Epidemic dengue/dengue hemorrhagic fever as a public health, social and economic problem in the 21st century. *Trends in Microbiology*, 10(2), pp.100–103. Available at: http://www.sciencedirect.com/science/article/pii/S0966842X01022880 [Accessed October 1, 2015].

Gubler, D. & Clark, G., 1995. Dengue/dengue hemorrhagic fever: the emergence of a global health problem. *Emerging infectious diseases*, 1(2), pp.55–7. Available at: http://www.pubmedcentral.nih.gov/articlerender.fcgi?artid=2626838&tool=pmcentrez&rendertype=abstract [Accessed October 16, 2015].

Gubler, D.J., 2006. Dengue/dengue haemorrhagic fever: history and current status. *Novartis Foundation symposium*, 277, pp.3–16; discussion 16–22, 71–3, 251–3. Available at: http://www.ncbi.nlm.nih.gov/pubmed/17319151 [Accessed October 27, 2015].

Guirakhoo, F., Bolin, R.A. & Roehrig, J.T., 1992. The Murray Valley encephalitis virus prM protein confers acid resistance to virus particles and alters the expression of epitopes within the R2 domain of E glycoprotein. *Virology*, 191(2), pp.921–31. Available at: http://www.ncbi.nlm.nih.gov/pubmed/1280384 [Accessed October 25, 2015].

Gulbins, E. et al., 2010. Role of Kv1.3 mitochondrial potassium channel in apoptotic signalling in lymphocytes. *Biochimica et Biophysica Acta (BBA) - Bioenergetics*, 1797(6-7), pp.1251–1259. Available at: http://www.sciencedirect.com/science/article/pii/S0005272810000198 [Accessed July 1, 2015].

Guo, X. et al., 2010. Response of the mosquito protein interaction network to dengue infection. *BMC genomics*, 11, p.380. Available at: http://www.pubmedcentral.nih.gov/articlerender.fcgi?artid=3091628&tool=pmcentrez&rendertype=abstract [Accessed September 30, 2015].

Guo, X. et al., 2007. Survival and Replication of Dengue-2 Virus in Diapausing Eggs of Aedes albopictus (Diptera: Culicidae). *Journal of Medical Entomology*, 44(3), pp.492–497. Available at: http://jme.oxfordjournals.org/content/44/3/492.abstract [Accessed September 23, 2015].

Gupta, L. et al., 2009. The STAT pathway mediates late-phase immunity against Plasmodium in the mosquito Anopheles gambiae. *Cell host & microbe*, 5(5), pp.498–507. Available at:

http://www.sciencedirect.com/science/article/pii/S1931312809001048 [Accessed November 22, 2015].

Gutsche, I. et al., 2011. Secreted dengue virus nonstructural protein NS1 is an atypical barrel-shaped high-density lipoprotein. *Proceedings of the National Academy of Sciences of the United States of America*, 108(19), pp.8003–8. Available at: http://www.pubmedcentral.nih.gov/articlerender.fcgi?artid=3093454&tool=pmcentrez&rendertype=abstract [Accessed October 21, 2015].

Guy, B. et al., 2011. From research to phase III: preclinical, industrial and clinical development of the Sanofi Pasteur tetravalent dengue vaccine. *Vaccine*, 29(42), pp.7229–41. Available at: http://www.ncbi.nlm.nih.gov/pubmed/21745521 [Accessed July 23, 2015].

Guzman, M.G. et al., 2010. Dengue: a continuing global threat. *Nature Reviews Microbiology*, pp.S7–S16.

Guzman, M.G., Alvarez, M. & Halstead, S.B., 2013. Secondary infection as a risk factor for dengue hemorrhagic fever/dengue shock syndrome: an historical perspective and role of antibody-dependent enhancement of infection. *Archives of virology*, 158(7), pp.1445–59. Available at: http://www.ncbi.nlm.nih.gov/pubmed/23471635 [Accessed November 2, 2015].

Guzman, M.G. & Harris, E., 2014. Dengue. *The Lancet*, 385(9966), pp.453–465. Available at: http://www.sciencedirect.com/science/article/pii/S0140673614605729.

Hadinegoro, S.R. et al., 2015. Efficacy and Long-Term Safety of a Dengue Vaccine in Regions of Endemic Disease. *The New England journal of medicine*, 373(13), pp.1195–206. Available at: http://www.ncbi.nlm.nih.gov/pubmed/26214039 [Accessed July 28, 2015].

Halstead, S., 1977. Dengue viruses and mononuclear phagocytes. I. Infection enhancement by non-neutralizing antibody. *Journal of Experimental Medicine*, 146(1), pp.201–217. Available at: http://jem.rupress.org/content/146/1/201 [Accessed October 29, 2015].

Halstead, S.B., 2008. Dengue virus-mosquito interactions. *Annual review of entomology*, 53, pp.273–91. Available at: http://www.annualreviews.org/doi/abs/10.1146/annurev.ento.53.103106.093326?url_ver=Z39.88-2003&rfr_dat=cr_pub%3Dpubmed&rfr_id=ori%3Arid%3Acrossref.org&journalCode=ento [Accessed October 6, 2015].

Halstead, S.B., 2007. Dengue. *Lancet (London, England)*, 370(9599), pp.1644–52. Available at: http://www.ncbi.nlm.nih.gov/pubmed/17993365.

Halstead, S.B., 2003. Neutralization and antibody-dependent enhancement of dengue viruses. *Advances in virus research*, 60, pp.421–67. Available at: http://www.ncbi.nlm.nih.gov/pubmed/14689700 [Accessed September 23, 2015].

Hanley, K.A. & Weaver, S.C., 2010. *Frontiers in Dengue Virus Research*, Horizon Scientific Press. Available at: https://books.google.com/books?hl=en&lr=&id=Z4o4zZ4vqbEC&pgis=1 [Accessed November 22, 2015].

Hartley, J.L., Temple, G.F. & Brasch, M.A., 2000. DNA Cloning Using In Vitro Site-Specific Recombination. *Genome Research*, 10(11), pp.1788–1795.

Heaton, N.S. & Randall, G., 2010. Dengue virus-induced autophagy regulates lipid metabolism. *Cell host & microbe*, 8(5), pp.422–32. Available at: http://www.pubmedcentral.nih.gov/articlerender.fcgi?artid=3026642&tool=pmcentrez&rendertype=abstract [Accessed February 3, 2016].

Helms, L.M. et al., 1997. Margatoxin binds to a homomultimer of K(V)1.3 channels in Jurkat cells. Comparison with K(V)1.3 expressed in CHO cells. *Biochemistry*, 36(12), pp.3737–44. Available at: http://www.ncbi.nlm.nih.gov/pubmed/9132027 [Accessed August 27, 2015].

Henchal, E.A. et al., 1983. Rapid identification of dengue virus isolates by using monoclonal antibodies in an indirect immunofluorescence assay. *The American journal of tropical medicine and hygiene*, 32(1), pp.164–9. Available at: http://www.ncbi.nlm.nih.gov/pubmed/6401944 [Accessed October 28, 2015].

Hermann, L.L. et al., 2014. Evaluation of a dengue NS1 antigen detection assay sensitivity and specificity for the diagnosis of acute dengue virus infection. *PLoS neglected tropical diseases*, 8(10), p.e3193. Available at: http://www.pubmedcentral.nih.gov/articlerender.fcgi?artid=4183466&tool=pmcentrez&rendertype=abstract [Accessed August 23, 2015].

Herrmann, M. et al., 2010. Interaction of human immunodeficiency virus gp120 with the voltage-gated potassium channel BEC1. *FEBS letters*, 584(16), pp.3513–8. Available at: http://www.sciencedirect.com/science/article/pii/S0014579310005715 [Accessed June 22, 2015].

Higa, L.M. et al., 2008. Secretome of HepG2 cells infected with dengue virus: implications for pathogenesis. *Biochimica et biophysica acta*, 1784(11), pp.1607–16. Available at: http://www.ncbi.nlm.nih.gov/pubmed/18639654 [Accessed November 22, 2015].

Ho, L.-J. et al., 2005. Dengue Virus Type 2 Antagonizes IFN- but Not IFN- Antiviral Effect via Down-Regulating Tyk2-STAT Signaling in the Human Dendritic Cell. *The Journal of Immunology*, 174(12), pp.8163–8172. Available at: http://www.jimmunol.org/content/174/12/8163.full [Accessed August 16, 2015].

Hober, D. et al., 1993. Serum levels of tumor necrosis factor-alpha (TNF-alpha), interleukin-6 (IL-6), and interleukin-1 beta (IL-1 beta) in dengue-infected patients. *The American journal of tropical medicine and hygiene*, 48(3), pp.324–31. Available at: http://www.ncbi.nlm.nih.gov/pubmed/8470771 [Accessed October 2, 2015].

Hoesel, B. & Schmid, J.A., 2013. The complexity of NF-κB signaling in inflammation and cancer. *Molecular cancer*, 12(1), p.86. Available at: http://www.molecular-cancer.com/content/12/1/86 [Accessed July 10, 2014].

Hoffmann, J.A., 1995. Innate immunity of insects. *Current Opinion in Immunology*, 7(1), pp.4–10. Available at: http://www.sciencedirect.com/science/article/pii/0952791595800220 [Accessed September 15, 2015].

Holmes, E. & Twiddy, S., 2003. The origin, emergence and evolutionary genetics of dengue virus. *Infection, Genetics and Evolution*, 3(1), pp.19–28. Available at: http://www.sciencedirect.com/science/article/pii/S1567134803000042 [Accessed November 24, 2014].

Holmes, T.C., Fadool, D.A. & Levitan, I.B., 1996. Tyrosine phosphorylation of the Kv1.3 potassium channel. *The Journal of neuroscience : the official journal of the Society for Neuroscience*, 16(5), pp.1581–90. Available at: http://www.ncbi.nlm.nih.gov/pubmed/8774427 [Accessed August 28, 2015].

Hombría, J.C.-G. et al., 2005. Characterisation of Upd2, a Drosophila JAK/STAT pathway ligand. *Developmental biology*, 288(2), pp.420–33. Available at: http://www.ncbi.nlm.nih.gov/pubmed/16277982 [Accessed July 31, 2015].

Honda, S. et al., 2009. Increased Phagocytosis of Platelets from Patients with Secondary Dengue Virus Infection by Human Macrophages. *Am J Trop Med Hyg*, 80(5), pp.841–845. Available at: http://www.ajtmh.org/content/80/5/841.long [Accessed August 31, 2015].

Hotta, S., 1952. Experimental studies on dengue. I. Isolation, identification and modification of the virus. *The Journal of infectious diseases*, 90(1), pp.1–9. Available at: http://www.ncbi.nlm.nih.gov/pubmed/14888958 [Accessed October 27, 2015].

Hover, S. et al., 2016. Modulation of Potassium Channels Inhibits Bunyavirus Infection. *The Journal of biological chemistry*, 291(7), pp.3411–22. Available at: http://www.jbc.org/content/early/2015/12/16/jbc.M115.692673.abstract [Accessed April 13, 2016].

Hu, L. et al., 2013. Blockade of Kv1.3 potassium channels inhibits differentiation and granzyme B secretion of human CD8+ T effector memory lymphocytes. *PloS one*, 8(1), p.e54267. Available at: http://journals.plos.org/plosone/article?id=10.1371/journal.pone.0054267#pone.0054267-Koo1 [Accessed July 27, 2015].

Hu, L. et al., 2007. Characterization of the Functional Properties of the Voltage-Gated Potassium Channel Kv1.3 in Human CD4+ T Lymphocytes. *The Journal of Immunology*, 179(7), pp.4563–4570. Available at: http://www.jimmunol.org/content/179/7/4563.full [Accessed August 29, 2015].

Hua, S.B. et al., 1997. Minimum length of sequence homology required for in vivo cloning by homologous recombination in yeast. *Plasmid*, 38(2), pp.91–96.

Huang, D.W., Sherman, B.T. & Lempicki, R.A., 2009. Systematic and integrative analysis of large gene lists using DAVID bioinformatics resources. *Nature protocols*, 4(1), pp.44–57. Available at: http://www.nature.com/nprot/journal/v4/n1/pdf/nprot.2008.211.pdf [Accessed July 9, 2014].

Huang, K.-J. et al., 2006. The dual-specific binding of dengue virus and target cells for the antibody-dependent enhancement of dengue virus infection. *Journal of immunology (Baltimore, Md. : 1950)*, 176(5), pp.2825–32. Available at: http://www.ncbi.nlm.nih.gov/pubmed/16493039 [Accessed November 2, 2015].

Hunsperger, E.A. et al., 2009. Evaluation of commercially available anti-dengue virus immunoglobulin M tests. *Emerging infectious diseases*, 15(3), pp.436–40. Available at: http://www.pubmedcentral.nih.gov/articlerender.fcgi?artid=2681117&tool=pmcentrez&rendertype=abstract [Accessed October 28, 2015].

Innis, B. & Eckels, K., 2003. Progress in development of a live-attenuated, tetravalent dengue virus vaccine by the United States Army Medical Research and Materiel Command. *Am J Trop Med Hyg*, 69(90060), pp.1–4. Available at: http://www.ajtmh.org/content/69/6_suppl/1.long [Accessed November 2, 2015].

Islam, S. et al., 2012. Highly multiplexed and strand-specific single-cell RNA 5' end sequencing. *Nature protocols*, 7(5), pp.813–28. Available at: http://dx.doi.org/10.1038/nprot.2012.022 [Accessed September 13, 2015].

Ivashkiv, L.B. & Donlin, L.T., 2014. Regulation of type I interferon responses. *Nature reviews. Immunology*, 14(1), pp.36–49. Available at: http://dx.doi.org/10.1038/nri3581 [Accessed July 10, 2014].

Jackson, A.L. & Linsley, P.S., 2010. Recognizing and avoiding siRNA off-target effects for target identification and therapeutic application. *Nature reviews. Drug discovery*, 9(1), pp.57–67. Available at: http://dx.doi.org/10.1038/nrd3010 [Accessed September 22, 2015].

Jalota, A. et al., 2005. Tumor suppressor SMAR1 activates and stabilizes p53 through its arginine-serine-rich motif. *The Journal of biological chemistry*, 280(16), pp.16019–29. Available at: http://www.jbc.org/content/280/16/16019.long [Accessed August 14, 2015].

Jang, S.H. et al., 2011. Anti-proliferative effect of Kv1.3 blockers in A549 human lung adenocarcinoma in vitro and in vivo. *European journal of pharmacology*, 651(1-3), pp.26–32. Available at: http://www.sciencedirect.com/science/article/pii/S0014299910010939 [Accessed August 28, 2015].

Jang, S.H. et al., 2015. Nuclear localization and functional characteristics of voltage-gated potassium channel Kv1.3. *The Journal of biological chemistry*, 290(20), pp.12547–57. Available at: http://www.ncbi.nlm.nih.gov/pubmed/25829491 [Accessed August 21, 2015].

Jang, S.-H. et al., 2009. Kv1.3 voltage-gated K + channel subunit as a potential diagnostic marker and therapeutic target for breast cancer. *BMB Reports*, 42(8), pp.535–539. Available at: http://www.researchgate.net/publication/26772513_Kv1.3_voltage-gated_K_channel_subunit_as_a_potential_diagnostic_marker_and_therapeutic_target_for_breast_cancer [Accessed August 31, 2015].

Jiang, B. et al., 2002. Endogenous KV channels in human embryonic kidney (HEK-293) cells. *Molecular and Cellular Biochemistry*, 238(1-2), pp.69–79. Available at: http://link.springer.com/article/10.1023/A%3A1019907104763 [Accessed August 27, 2015].

Jiang, L. et al., 2009. Polypyrimidine tract-binding protein influences negative strand RNA synthesis of dengue virus. *Biochemical and biophysical research communications*, 385(2), pp.187–92. Available at: http://www.sciencedirect.com/science/article/pii/S0006291X09009577 [Accessed

November 2, 2015].

Jones, M. et al., 2005. Dengue virus inhibits alpha interferon signaling by reducing STAT2 expression. *Journal of virology*, 79(9), pp.5414–20. Available at: http://jvi.asm.org/content/79/9/5414.long [Accessed August 14, 2015].

Joshi, V., Mourya, D.T. & Sharma, R.C., 2002. Persistence of dengue-3 virus through transovarial transmission passage in successive generations of Aedes aegypti mosquitoes. *The American journal of tropical medicine and hygiene*, 67(2), pp.158–61. Available at: http://www.ajtmh.org/content/67/2/158.abstract [Accessed October 23, 2015].

Judge, S.I. V & Bever, C.T., 2006. Potassium channel blockers in multiple sclerosis: neuronal Kv channels and effects of symptomatic treatment. *Pharmacology & therapeutics*, 111(1), pp.224–59. Available at: http://www.sciencedirect.com/science/article/pii/S0163725805002287 [Accessed August 1, 2015].

Kakumani, P.K. et al., 2013. Role of RNA interference (RNAi) in dengue virus replication and identification of NS4B as an RNAi suppressor. *Journal of virology*, 87(16), pp.8870–83. Available at: http://www.pubmedcentral.nih.gov/articlerender.fcgi?artid=3754049&tool=pmcentrez&rendertype=abstract [Accessed November 2, 2015].

Kalman, K., 1998. ShK-Dap22, a Potent Kv1.3-specific Immunosuppressive Polypeptide. *Journal of Biological Chemistry*, 273(49), pp.32697–32707. Available at: http://www.jbc.org/content/273/49/32697.full [Accessed September 4, 2015].

Kanlaya, R. et al., 2010a. The ubiquitin-proteasome pathway is important for dengue virus infection in primary human endothelial cells. *Journal of proteome research*, 9(10), pp.4960–71. Available at: http://dx.doi.org/10.1021/pr100219y [Accessed June 16, 2015].

Kanlaya, R. et al., 2010b. Vimentin interacts with heterogeneous nuclear ribonucleoproteins and dengue nonstructural protein 1 and is important for viral replication and release. *Molecular bioSystems*, 6(5), pp.795–806. Available at: http://pubs.rsc.org/en/content/articlehtml/2010/mb/b923864f [Accessed November 22, 2015].

Kapoor, M. et al., 1995. Association between NS3 and NS5 Proteins of Dengue Virus Type 2 in the Putative RNA Replicase Is Linked to Differential Phosphorylation of NS5. *Journal of Biological Chemistry*, 270(32), pp.19100–19106. Available at: http://www.jbc.org/content/270/32/19100.long [Accessed November 2, 2015].

Kaptein, S.J.F. et al., 2010. A derivate of the antibiotic doxorubicin is a selective inhibitor of dengue and yellow fever virus replication in vitro. *Antimicrobial agents and chemotherapy*, 54(12), pp.5269–80. Available at: http://www.pubmedcentral.nih.gov/articlerender.fcgi?artid=2981273&tool=pmcentrez&rendertype=abstract [Accessed July 8, 2015].

Karsten, P. et al., 2006. Mutational analysis reveals separable DNA binding and trans-activation of Drosophila STAT92E. *Cellular signalling*, 18(6), pp.819–29. Available at: http://www.ncbi.nlm.nih.gov/pubmed/16129580 [Accessed July 31, 2015].

Käs, E. et al., 1993. A model for chromatin opening: stimulation of topoisomerase II and restriction enzyme cleavage of chromatin by distamycin. *The EMBO journal*, 12(1), pp.115–26. Available at: http://www.pubmedcentral.nih.gov/articlerender.fcgi?artid=413181&tool=pmcentrez&rendertype=abstract [Accessed October 30, 2015].

Kassim, F.M. et al., 2011. Use of dengue NS1 antigen for early diagnosis of dengue virus infection. *The Southeast Asian journal of tropical medicine and public health*, 42(3), pp.562–9. Available at: http://www.ncbi.nlm.nih.gov/pubmed/21706934 [Accessed October 26, 2015].

Kaul, R. et al., 2003. Direct interaction with and activation of p53 by SMAR1 retards cell-cycle progression at G2/M phase and delays tumor growth in mice. *International journal of cancer. Journal international du cancer*, 103(5), pp.606–15. Available at: http://www.ncbi.nlm.nih.gov/pubmed/12494467 [Accessed August 15, 2015].

Kaur, P. & Kaur, G., 2014. Transfusion support in patients with dengue fever. *International journal of*

applied & basic medical research, 4(Suppl 1), pp.S8–S12. Available at: http://www.pubmedcentral.nih.gov/articlerender.fcgi?artid=4181139&tool=pmcentrez&rendertype=abstract [Accessed October 28, 2015].

Kawai, T. & Akira, S., 2008. Toll-like receptor and RIG-I-like receptor signaling. *Annals of the New York Academy of Sciences*, 1143, pp.1–20. Available at: http://www.ncbi.nlm.nih.gov/pubmed/19076341 [Accessed November 13, 2015].

Kazama, I., 2015. Physiological significance of delayed rectifier K(+) channels (Kv1.3) expressed in T lymphocytes and their pathological significance in chronic kidney disease. *The journal of physiological sciences : JPS*, 65(1), pp.25–35. Available at: http://www.ncbi.nlm.nih.gov/pubmed/25096892 [Accessed August 29, 2015].

Khadka, S. et al., 2011. A physical interaction network of dengue virus and human proteins. *Molecular & cellular proteomics : MCP*, 10(12), p.M111.012187. Available at: http://www.pubmedcentral.nih.gov/articlerender.fcgi?artid=3237087&tool=pmcentrez&rendertype=abstract [Accessed November 3, 2015].

Kim, J.-M. et al., 2004. Improved recombinant gene expression in CHO cells using matrix attachment regions. *Journal of Biotechnology*, 107(2), pp.95–105. Available at: http://www.sciencedirect.com/science/article/pii/S0168165603002670 [Accessed October 30, 2015].

Kingsolver, M.B., Huang, Z. & Hardy, R.W., 2013. Insect antiviral innate immunity: pathways, effectors, and connections. *Journal of molecular biology*, 425(24), pp.4921–36. Available at: http://www.sciencedirect.com/science/article/pii/S0022283613006323 [Accessed October 1, 2015].

Klickstein, L.B., 2001. Production of a complete cDNA library. *Current protocols in molecular biology / edited by Frederick M. Ausubel ... [et al.]*, Chapter 5, p.Unit5.8A.

Knaus, H.-G. et al., 1995. [125I]Margatoxin, an Extraordinarily High Affinity Ligand for Voltage-Gated Potassium Channels in Mammalian Brain. *Biochemistry*, 34(41), pp.13627–13634. Available at: http://dx.doi.org/10.1021/bi00041a043 [Accessed August 27, 2015].

Koni, P.A. et al., 2003. Compensatory anion currents in Kv1.3 channel-deficient thymocytes. *The Journal of biological chemistry*, 278(41), pp.39443–51. Available at: http://www.jbc.org/content/278/41/39443.long [Accessed August 29, 2015].

Kotak, S., Busso, C. & Gönczy, P., 2014. NuMA interacts with phosphoinositides and links the mitotic spindle with the plasma membrane. *The EMBO journal*, 33(16), pp.1815–30. Available at: http://www.pubmedcentral.nih.gov/articlerender.fcgi?artid=4195763&tool=pmcentrez&rendertype=abstract [Accessed November 23, 2015].

Kow, C.Y., Koon, L.L. & Yin, P.F., 2001. Detection of Dengue Viruses in Field Caught Male Aedes aegypti and Aedes albopictus (Diptera: Culicidae) in Singapore by Type-Specific PCR. *Journal of Medical Entomology*, 38(4), pp.475–479. Available at: http://dx.doi.org/10.1603/0022-2585-38.4.475 [Accessed October 23, 2015].

Kreusch, A. et al., 1998. Crystal structure of the tetramerization domain of the Shaker potassium channel. *Nature*, 392(6679), pp.945–8. Available at: http://dx.doi.org/10.1038/31978 [Accessed August 31, 2015].

Krishnan, M.N. et al., 2008. RNA interference screen for human genes associated with West Nile virus infection. *Nature*, 455(7210), pp.242–5. Available at: http://dx.doi.org/10.1038/nature07207 [Accessed August 4, 2015].

Kuadkitkan, A. et al., 2010. Identification and characterization of prohibitin as a receptor protein mediating DENV-2 entry into insect cells. *Virology*, 406(1), pp.149–161. Available at: http://dx.doi.org/10.1016/j.virol.2010.07.015.

Kuhn, R.J. et al., 2002. Structure of dengue virus: implications for flavivirus organization, maturation, and fusion. *Cell*, 108(5), pp.717–25. Available at: http://www.pubmedcentral.nih.gov/articlerender.fcgi?artid=4152842&tool=pmcentrez&rendertype=abstract [Accessed October 19, 2015].

Kulkarni, A. et al., 2004. HIV-1 integration sites are flanked by potential MARs that alone can act as promoters. *Biochemical and biophysical research communications*, 322(2), pp.672–7. Available at: http://www.ncbi.nlm.nih.gov/pubmed/15325282 [Accessed November 10, 2015].

Kumar, A., Zhang, J. & Yu, F.-S.X., 2006. Toll-like receptor 3 agonist poly(I:C)-induced antiviral response in human corneal epithelial cells. *Immunology*, 117(1), pp.11–21. Available at: http://www.pubmedcentral.nih.gov/articlerender.fcgi?artid=1782193&tool=pmcentrez&rendertype=abstract [Accessed August 6, 2015].

Kummerer, B.M. & Rice, C.M., 2002. Mutations in the Yellow Fever Virus Nonstructural Protein NS2A Selectively Block Production of Infectious Particles. *Journal of Virology*, 76(10), pp.4773–4784. Available at: http://jvi.asm.org/content/76/10/4773.long [Accessed October 27, 2015].

Kuno, G., Gómez, I. & Gubler, D.J., 1991. An ELISA procedure for the diagnosis of dengue infections. *Journal of virological methods*, 33(1-2), pp.101–13. Available at: http://www.ncbi.nlm.nih.gov/pubmed/1939502 [Accessed October 28, 2015].

Kurane, I. et al., 1991a. Activation of T lymphocytes in dengue virus infections. High levels of soluble interleukin 2 receptor, soluble CD4, soluble CD8, interleukin 2, and interferon-gamma in sera of children with dengue. *The Journal of clinical investigation*, 88(5), pp.1473–80. Available at: http://www.jci.org/articles/view/115457 [Accessed August 31, 2015].

Kurane, I. et al., 1991b. Activation of T lymphocytes in dengue virus infections. High levels of soluble interleukin 2 receptor, soluble CD4, soluble CD8, interleukin 2, and interferon-gamma in sera of children with dengue. *The Journal of clinical investigation*, 88(5), pp.1473–80. Available at: http://www.pubmedcentral.nih.gov/articlerender.fcgi?artid=295652&tool=pmcentrez&rendertype=abstract [Accessed October 27, 2015].

Lahiri, M., Fisher, D. & Tambyah, P.A., 2008. Dengue mortality: reassessing the risks in transition countries. *Transactions of the Royal Society of Tropical Medicine and Hygiene*, 102(10), pp.1011–6. Available at: http://trstmh.oxfordjournals.org/content/102/10/1011.short [Accessed November 18, 2015].

Lai, C.-Y. et al., 2008. Antibodies to envelope glycoprotein of dengue virus during the natural course of infection are predominantly cross-reactive and recognize epitopes containing highly conserved residues at the fusion loop of domain II. *Journal of virology*, 82(13), pp.6631–43. Available at: http://www.pubmedcentral.nih.gov/articlerender.fcgi?artid=2447043&tool=pmcentrez&rendertype=abstract [Accessed October 7, 2015].

Lanciotti, R.S. et al., 1992. Rapid detection and typing of dengue viruses from clinical samples by using reverse transcriptase-polymerase chain reaction. *Journal of clinical microbiology*, 30(3), pp.545–51. Available at: http://www.pubmedcentral.nih.gov/articlerender.fcgi?artid=265106&tool=pmcentrez&rendertype=abstract [Accessed October 28, 2015].

Landy, A. (1989) Dynamic, Structural, and Regulatory Aspects of Lambda Site-specific Recombination. Ann. Rev. Biochem. 58, 913-949 [Accessed July 7, 2015].

Lang, J., 2012. Development of Sanofi Pasteur tetravalent dengue vaccine. *Revista do Instituto de Medicina Tropical de São Paulo*, 54, pp.15–17. Available at: http://www.scielo.br/scielo.php?script=sci_arttext&pid=S0036-46652012000700007&lng=en&nrm=iso&tlng=en [Accessed November 21, 2015].

Laurent-Rolle, M. et al., 2014. The interferon signaling antagonist function of yellow fever virus NS5 protein is activated by type I interferon. *Cell host & microbe*, 16(3), pp.314–27. Available at: http://www.sciencedirect.com/science/article/pii/S1931312814002947 [Accessed November 4, 2015].

Lee, M.S. et al., 2013. Negative regulation of type I IFN expression by OASL1 permits chronic viral infection and $CD8^+$ T-cell exhaustion. *PLoS pathogens*, 9(7), p.e1003478. Available at: http://journals.plos.org/plospathogens/article?id=10.1371/journal.ppat.1003478 [Accessed June 11, 2015].

Lee, Y.-R. et al., 2008. Autophagic machinery activated by dengue virus enhances virus replication.

Virology, 374(2), pp.240–8. Available at: http://www.ncbi.nlm.nih.gov/pubmed/18353420 [Accessed October 28, 2015].

Lemaitre, B. et al., 1995. A recessive mutation, immune deficiency (imd), defines two distinct control pathways in the Drosophila host defense. *Proceedings of the National Academy of Sciences of the United States of America*, 92(21), pp.9465–9. Available at: http://www.pubmedcentral.nih.gov/articlerender.fcgi?artid=40822&tool=pmcentrez&rendertype=abstract [Accessed September 4, 2015].

Lemaitre, B. et al., 1996. The dorsoventral regulatory gene cassette spätzle/Toll/cactus controls the potent antifungal response in Drosophila adults. *Cell*, 86(6), pp.973–83. Available at: http://www.ncbi.nlm.nih.gov/pubmed/8808632 [Accessed January 16, 2015].

Leung, J.Y. et al., 2008. Role of nonstructural protein NS2A in flavivirus assembly. *Journal of virology*, 82(10), pp.4731–41. Available at: http://www.pubmedcentral.nih.gov/articlerender.fcgi?artid=2346727&tool=pmcentrez&rendertype=abstract [Accessed August 14, 2015].

Levitan, I. & Barrantes, F., 2012. *Cholesterol Regulation of Ion Channels and Receptors*, John Wiley & Sons. Available at: https://books.google.com/books?id=T4Zr3CfwBwYC&pgis=1 [Accessed August 27, 2015].

Lewis, R.S. & Cahalan, M.D., 1995. Potassium and calcium channels in lymphocytes. *Annual review of immunology*, 13, pp.623–53. Available at: http://www.ncbi.nlm.nih.gov/pubmed/7612237 [Accessed September 1, 2015].

Li, K. et al., 2005. Distinct poly(I-C) and virus-activated signaling pathways leading to interferon-beta production in hepatocytes. *The Journal of biological chemistry*, 280(17), pp.16739–47. Available at: http://www.jbc.org/content/280/17/16739.full [Accessed August 15, 2015].

Li, S., 2004. A Map of the Interactome Network of the Metazoan C. elegans. *Science*, 303(5657), pp.540–543. Available at: http://www.pubmedcentral.nih.gov/articlerender.fcgi?artid=1698949&tool=pmcentrez&rendertype=abstract [Accessed October 2, 2015].

Li, Y. et al., 2013. Human apolipoprotein A-I is associated with dengue virus and enhances virus infection through SR-BI. *PloS one*, 8(7), p.e70390. Available at: http://journals.plos.org/plosone/article?id=10.1371/journal.pone.0070390 [Accessed April 7, 2016].

Libraty, D.H. et al., 2002. High Circulating Levels of the Dengue Virus Nonstructural Protein NS1 Early in Dengue Illness Correlate with the Development of Dengue Hemorrhagic Fever. *The Journal of Infectious Diseases*, 186(8), pp.1165–1168. Available at: http://jid.oxfordjournals.org/content/186/8/1165.long [Accessed October 17, 2015].

Lima, M. da R.Q. et al., 2010. Comparison of three commercially available dengue NS1 antigen capture assays for acute diagnosis of dengue in Brazil. *PLoS neglected tropical diseases*, 4(7), p.e738. Available at: http://www.pubmedcentral.nih.gov/articlerender.fcgi?artid=2897844&tool=pmcentrez&rendertype=abstract [Accessed October 28, 2015].

Lin, C.S., 1993. Voltage-gated potassium channels regulate calcium-dependent pathways involved in human T lymphocyte activation. *Journal of Experimental Medicine*, 177(3), pp.637–645. Available at: http://jem.rupress.org/content/177/3/637.abstract?ijkey=7ac43e3fb467e86ad7b5c8e8ee36d2a4f7a990b1&keytype2=tf_ipsecsha [Accessed August 31, 2015].

Lin, M.-H. et al., 2014. Membrane undulation induced by NS4A of Dengue virus: a molecular dynamics simulation study. *Journal of biomolecular structure & dynamics*, 32(10), pp.1552–62. Available at: http://www.ncbi.nlm.nih.gov/pubmed/23964591 [Accessed October 27, 2015].

Lindenbach, B.D. & Rice, C.M., 1999. Genetic Interaction of Flavivirus Nonstructural Proteins NS1 and NS4A as a Determinant of Replicase Function. *J. Virol.*, 73(6), pp.4611–4621. Available at: http://jvi.asm.org/content/73/6/4611.abstract [Accessed October 26, 2015].

Lindenbach, B.D. & Rice, C.M., 2003. Molecular biology of flaviviruses. *Advances in virus research*, 59, pp.23–61. Available at: http://www.ncbi.nlm.nih.gov/pubmed/14696326 [Accessed September 7, 2015].

Linnen, J.M. et al., 2008. Dengue viremia in blood donors from Honduras, Brazil, and Australia. *Transfusion*, 48(7), pp.1355–62. Available at: http://www.ncbi.nlm.nih.gov/pubmed/18503610 [Accessed October 25, 2015].

Linthicum, K.J. et al., 1996. Dengue 3 virus distribution in the mosquito Aedes aegyptl: an immunocytochemical study. *Medical and Veterinary Entomology*, 10(1), pp.87–92. Available at: http://doi.wiley.com/10.1111/j.1365-2915.1996.tb00086.x [Accessed October 22, 2015].

Lisova, O. et al., 2007. Mapping to completeness and transplantation of a group-specific, discontinuous, neutralizing epitope in the envelope protein of dengue virus. *The Journal of general virology*, 88(Pt 9), pp.2387–97. Available at: http://jgv.microbiologyresearch.org/content/journal/jgv/10.1099/vir.0.83028-0 [Accessed November 2, 2015].

Liu, J. et al., 2012. A synthetic double-stranded RNA, poly I:C, induces a rapid apoptosis of human CD34(+) cells. *Experimental hematology*, 40(4), pp.330–41. Available at: http://www.exphem.org/article/S0301472X11005947/fulltext [Accessed August 13, 2015].

Liu, J. et al., 2013. HIV-1 Tat protein increases microglial outward K(+) current and resultant neurotoxic activity. *PloS one*, 8(5), p.e64904. Available at: http://journals.plos.org/plosone/article?id=10.1371/journal.pone.0064904 [Accessed September 1, 2015].

Liu, J. et al., 2012. Involvement of Kv1.3 and p38 MAPK signaling in HIV-1 glycoprotein 120-induced microglia neurotoxicity. *Cell death & disease*, 3, p.e254. Available at: http://www.pubmedcentral.nih.gov/articlerender.fcgi?artid=3270274&tool=pmcentrez&rendertype=abstract [Accessed September 1, 2015].

Liu, S. et al., 2013. MAVS recruits multiple ubiquitin E3 ligases to activate antiviral signaling cascades. *eLife*, 2, p.e00785. Available at: http://elifesciences.org/content/2/e00785.abstract [Accessed November 19, 2015].

Liu, W.J. et al., 2006. A single amino acid substitution in the West Nile virus nonstructural protein NS2A disables its ability to inhibit alpha/beta interferon induction and attenuates virus virulence in mice. *Journal of virology*, 80(5), pp.2396–404. Available at: http://jvi.asm.org/content/80/5/2396.long [Accessed July 7, 2015].

Liu, W.J. et al., 2004. Analysis of adaptive mutations in Kunjin virus replicon RNA reveals a novel role for the flavivirus nonstructural protein NS2A in inhibition of beta interferon promoter-driven transcription. *Journal of virology*, 78(22), pp.12225–35. Available at: http://jvi.asm.org/content/78/22/12225.long [Accessed October 27, 2015].

Ma, H. et al., 1987. Plasmid construction by homologous recombination in yeast. *Gene*, 58(2-3), pp.201–16. Available at: http://www.ncbi.nlm.nih.gov/pubmed/2828185 [Accessed November 7, 2015].

Ma, L. et al., 2004. Solution structure of dengue virus capsid protein reveals another fold. *Proceedings of the National Academy of Sciences of the United States of America*, 101(10), pp.3414–9. Available at: http://www.pnas.org/content/101/10/3414.abstract [Accessed October 19, 2015].

Macharia, R.W., Ombura, F.L. & Aroko, E.O., 2015. Insects' RNA Profiling Reveals Absence of "Hidden Break" in 28S Ribosomal RNA Molecule of Onion Thrips, Thrips tabaci. *Journal of Nucleic Acids*, 2015. Available at: https://doaj.org/article/c99b90cd973c45b081bfcdec6d639601 [Accessed September 27, 2015].

Mackenzie, J., Jones, M. & Young, P., 1996. Immunolocalization of the Dengue Virus Nonstructural Glycoprotein NS1 Suggests a Role in Viral RNA Replication. *Virology*, 220(1), pp.232–240. Available at: http://www.sciencedirect.com/science/article/pii/S0042682296903074 [Accessed September 28, 2015].

Mackenzie, J.M. et al., 1998. Subcellular localization and some biochemical properties of the flavivirus Kunjin nonstructural proteins NS2A and NS4A. *Virology*, 245(2), pp.203–15. Available at: http://www.sciencedirect.com/science/article/pii/S0042682298991565 [Accessed August 14, 2015].

Macpherson, I. & Stoker, M., 1962. Polyoma transformation of hamster cell clones—an investigation of genetic factors affecting cell competence. *Virology*, 16(2), pp.147–151. Available at: http://www.sciencedirect.com/science/article/pii/0042682262902908 [Accessed July 30, 2015].

Mairiang, D. et al., 2013. Identification of new protein interactions between dengue fever virus and its hosts, human and mosquito. *PloS one*, 8(1), p.e53535. Available at: http://journals.plos.org/plosone/article?id=10.1371/journal.pone.0053535 [Accessed August 7, 2015].

Malavige, G.N. & Ogg, G.S., 2013. T cell responses in dengue viral infections. *Journal of clinical virology : the official publication of the Pan American Society for Clinical Virology*, 58(4), pp.605–11. Available at: http://www.journalofclinicalvirology.com/article/S138665321300471X/fulltext [Accessed November 2, 2015].

Malonia, S.K. et al., 2014. Chromatin remodeling protein SMAR1 regulates NF-κB dependent Interleukin-8 transcription in breast cancer. *The international journal of biochemistry & cell biology*, 55, pp.220–6. Available at: http://www.ncbi.nlm.nih.gov/pubmed/25239884 [Accessed November 13, 2015].

Malonia, S.K. et al., 2011. Gene regulation by SMAR1: Role in cellular homeostasis and cancer. *Biochimica et Biophysica Acta - Reviews on Cancer*, 1815(1), pp.1–12. Available at: http://www.sciencedirect.com/science/article/pii/S0304419X10000600 [Accessed June 30, 2015].

Mankouri, J. et al., 2009. Suppression of a pro-apoptotic K+ channel as a mechanism for hepatitis C virus persistence. *Proceedings of the National Academy of Sciences of the United States of America*, 106(37), pp.15903–8. Available at: http://www.pubmedcentral.nih.gov/articlerender.fcgi?artid=2747216&tool=pmcentrez&rendertype=abstract [Accessed September 1, 2015].

Mao, Y. et al., 2000. SUMO-1 conjugation to topoisomerase I: A possible repair response to topoisomerase-mediated DNA damage. *Proceedings of the National Academy of Sciences of the United States of America*, 97(8), pp.4046–51. Available at: http://www.pubmedcentral.nih.gov/articlerender.fcgi?artid=18143&tool=pmcentrez&rendertype=abstract [Accessed November 3, 2015].

Martins, V.E.P. et al., 2012. Occurrence of natural vertical transmission of dengue-2 and dengue-3 viruses in Aedes aegypti and Aedes albopictus in Fortaleza, Ceará, Brazil. *PloS one*, 7(7), p.e41386. Available at: http://journals.plos.org/plosone/article?id=10.1371/journal.pone.0041386 [Accessed October 23, 2015].

Massé, N. et al., 2010. Dengue virus replicons: production of an interserotypic chimera and cell lines from different species, and establishment of a cell-based fluorescent assay to screen inhibitors, validated by the evaluation of ribavirin's activity. *Antiviral research*, 86(3), pp.296–305. Available at: http://www.ncbi.nlm.nih.gov/pubmed/20307577 [Accessed November 6, 2015].

Mathew, A. & Rothman, A.L., 2008. Understanding the contribution of cellular immunity to dengue disease pathogenesis. *Immunological reviews*, 225, pp.300–13. Available at: http://www.ncbi.nlm.nih.gov/pubmed/18837790 [Accessed November 2, 2015].

Matsumoto, M. & Seya, T., 2008. TLR3: interferon induction by double-stranded RNA including poly(I:C). *Advanced drug delivery reviews*, 60(7), pp.805–12. Available at: http://www.sciencedirect.com/science/article/pii/S0169409X07003833 [Accessed May 18, 2015].

Matter, N., Herrlich, P. & König, H., 2002. Signal-dependent regulation of splicing via phosphorylation of Sam68. *Nature*, 420(6916), pp.691–5. Available at: http://www.ncbi.nlm.nih.gov/pubmed/12478298 [Accessed November 3, 2015].

Matz, M. V, 2002. Amplification of representative cDNA samples from microscopic amounts of invertebrate tissue to search for new genes. *Methods in molecular biology (Clifton, N.J.)*, 183, pp.3–18. Available at: http://www.ncbi.nlm.nih.gov/pubmed/12136765 [Accessed September 29, 2015].

Mayhew, G.F. et al., 2007. Construction and characterization of an expressed sequenced tag library for the mosquito vector Armigeres subalbatus. *BMC genomics*, 8(1), p.462. Available at: http://www.biomedcentral.com/1471-2164/8/462 [Accessed September 5, 2015].

Mazzon, M. et al., 2009. Dengue virus NS5 inhibits interferon-alpha signaling by blocking signal transducer and activator of transcription 2 phosphorylation. *The Journal of infectious diseases*, 200(8), pp.1261–70. Available at: http://jid.oxfordjournals.org/content/200/8/1261.full [Accessed August 15, 2015].

McCloskey, C. et al., 2010. Kv1.3 is the exclusive voltage-gated K+ channel of platelets and megakaryocytes: roles in membrane potential, Ca2+ signalling and platelet count. *The Journal of physiology*, 588(Pt 9), pp.1399–406. Available at: http://www.pubmedcentral.nih.gov/articlerender.fcgi?artid=2876798&tool=pmcentrez&rendertype=abstract [Accessed August 29, 2015].

McFarlane, M. et al., 2014. Characterization of Aedes aegypti innate-immune pathways that limit Chikungunya virus replication. *PLoS neglected tropical diseases*, 8(7), p.e2994. Available at: http://journals.plos.org/plosntds/article?id=10.1371/journal.pntd.0002994 [Accessed September 9, 2015].

McLean, J.E. et al., 2011. Flavivirus NS4A-induced autophagy protects cells against death and enhances virus replication. *The Journal of biological chemistry*, 286(25), pp.22147–59. Available at: http://www.jbc.org/content/286/25/22147 [Accessed September 9, 2015].

McMeniman, C.J. et al., 2009. Stable introduction of a life-shortening Wolbachia infection into the mosquito Aedes aegypti. *Science (New York, N.Y.)*, 323(5910), pp.141–4. Available at: http://www.sciencemag.org/content/323/5910/141.abstract [Accessed June 17, 2015].

van Meerloo, J., Kaspers, G.J.L. & Cloos, J., 2011. Cell sensitivity assays: the MTT assay. *Methods in molecular biology (Clifton, N.J.)*, 731, pp.237–45. Available at: http://www.ncbi.nlm.nih.gov/pubmed/21516412 [Accessed June 11, 2015].

Meertens, L. et al., 2012. The TIM and TAM families of phosphatidylserine receptors mediate dengue virus entry. *Cell host & microbe*, 12(4), pp.544–57. Available at: http://www.sciencedirect.com/science/article/pii/S1931312812003046 [Accessed August 17, 2015].

Mendoza, M.Y. et al., 2002. A putative receptor for dengue virus in mosquito tissues: Localization of a 45-KDA glycoprotein. *American Journal of Tropical Medicine and Hygiene*, 67(1), pp.76–84.

von Mering, C. et al., 2002. Comparative assessment of large-scale data sets of protein-protein interactions. *Nature*, 417(6887), pp.399–403. Available at: http://www.ncbi.nlm.nih.gov/pubmed/12000970 [Accessed November 6, 2015].

Messina, J.P. et al., 2014. Global spread of dengue virus types: mapping the 70 year history. *Trends in microbiology*, 22(3), pp.138–46. Available at: http://www.pubmedcentral.nih.gov/articlerender.fcgi?artid=3946041&tool=pmcentrez&rendertype=abstract [Accessed July 14, 2014].

Mia, M.S. et al., 2013. Trends of dengue infections in Malaysia, 2000-2010. *Asian Pacific journal of tropical medicine*, 6(6), pp.462–6. Available at: http://www.sciencedirect.com/science/article/pii/S1995764513600759 [Accessed October 27, 2015].

Michels, M. et al., 2014. Platelet function alterations in dengue are associated with plasma leakage. *Thrombosis and haemostasis*, 112(2), pp.352–62. Available at: http://th.schattauer.de/en/contents/archive/issue/1895/manuscript/21012.html [Accessed August 31, 2015].

Miller, C., 2000. An overview of the potassium channel family. *Genome biology*, 1(4), p.REVIEWS0004.

Available at: http://europepmc.org/articles/PMC138870/?report=abstract [Accessed August 31, 2015].

Miller, J.L. et al., 2008. The mannose receptor mediates dengue virus infection of macrophages. *PLoS pathogens*, 4(2), p.e17. Available at: http://www.pubmedcentral.nih.gov/articlerender.fcgi?artid=2233670&tool=pmcentrez&rendertype=abstract [Accessed October 26, 2015].

Miller, M.B. & Tang, Y.-W., 2009. Basic Concepts of Microarrays and Potential Applications in Clinical Microbiology. *Clinical Microbiology Reviews*, 22(4), pp.611–633. Available at: http://www.pubmedcentral.nih.gov/articlerender.fcgi?artid=2772365&tool=pmcentrez&rendertype=abstract [Accessed April 15, 2015].

Miller, S. et al., 2007. The non-structural protein 4A of dengue virus is an integral membrane protein inducing membrane alterations in a 2K-regulated manner. *The Journal of biological chemistry*, 282(12), pp.8873–82. Available at: http://www.jbc.org/content/282/12/8873.abstract [Accessed October 24, 2015].

Miller, S., Sparacio, S. & Bartenschlager, R., 2006. Subcellular localization and membrane topology of the Dengue virus type 2 Non-structural protein 4B. *The Journal of biological chemistry*, 281(13), pp.8854–63. Available at: http://www.jbc.org/content/281/13/8854 [Accessed October 27, 2015].

Modis, Y. et al., 2003. A ligand-binding pocket in the dengue virus envelope glycoprotein. *Proceedings of the National Academy of Sciences of the United States of America*, 100(12), pp.6986–91. Available at: http://www.pnas.org/content/100/12/6986.full [Accessed October 20, 2015].

Modis, Y. et al., 2004. Structure of the dengue virus envelope protein after membrane fusion. *Nature*, 427(6972), pp.313–9. Available at: http://dx.doi.org/10.1038/nature02165 [Accessed October 20, 2015].

Modis, Y. et al., 2005. Variable surface epitopes in the crystal structure of dengue virus type 3 envelope glycoprotein. *Journal of virology*, 79(2), pp.1223–31. Available at: http://jvi.asm.org/content/79/2/1223.short [Accessed October 20, 2015].

Mohammed, H. et al., 2008. Dengue virus in blood donations, Puerto Rico, 2005. *Transfusion*, 48(7), pp.1348–54. Available at: http://www.ncbi.nlm.nih.gov/pubmed/18503611 [Accessed October 25, 2015].

Morrison, J., Aguirre, S. & Fernandez-Sesma, A., 2012. Innate Immunity Evasion by Dengue Virus. *Viruses*, 4(12), pp.397–413. Available at: http://www.pubmedcentral.nih.gov/articlerender.fcgi?artid=3347034&tool=pmcentrez&rendertype=abstract [Accessed April 6, 2015].

Mosmann, T., 1983. Rapid colorimetric assay for cellular growth and survival: Application to proliferation and cytotoxicity assays. *Journal of Immunological Methods*, 65(1-2), pp.55–63. Available at: http://www.sciencedirect.com/science/article/pii/0022175983903034 [Accessed August 21, 2014].

Mounier, N. et al., 1992. Insect muscle actins differ distinctly from invertebrate and vertebrate cytoplasmic actins. *Journal of Molecular Evolution*, 34(5), pp.406–415. Available at: http://link.springer.com/10.1007/BF00162997 [Accessed November 5, 2015].

Mukhopadhyay, S., Kuhn, R.J. & Rossmann, M.G., 2005. A structural perspective of the flavivirus life cycle. *Nature Reviews Microbiology*, 3(1), pp.13–22. Available at: http://www.nature.com/nrmicro/journal/v3/n1/full/nrmicro1067.html#B2 [Accessed October 20, 2015].

Müller, P. et al., 2005. Identification of JAK/STAT signalling components by genome-wide RNA interference. *Nature*, 436(7052), pp.871–5. Available at: http://dx.doi.org/10.1038/nature03869 [Accessed July 31, 2015].

Müller, S. & Dejean, A., 1999. Viral immediate-early proteins abrogate the modification by SUMO-1 of PML and Sp100 proteins, correlating with nuclear body disruption. *Journal of virology*, 73(6), pp.5137–43. Available at:

http://www.pubmedcentral.nih.gov/articlerender.fcgi?artid=112559&tool=pmcentrez&rendertype=abstract [Accessed November 3, 2015].

Mungrue, K., 2014. The laboratory diagnosis of dengue virus infection, a review. *Advance Laboratory Medicine International*, 4(1), pp.1–8. Available at: http://www.scopemed.org/?mno=48483 [Accessed May 31, 2015].

Muñoz-Jordan, J.L. et al., 2003. Inhibition of interferon signaling by dengue virus. *Proceedings of the National Academy of Sciences of the United States of America*, 100(24), pp.14333–8. Available at: http://www.pnas.org/content/100/24/14333.full [Accessed August 14, 2015].

Muñoz-Jordán, J.L. et al., 2005. Inhibition of alpha/beta interferon signaling by the NS4B protein of flaviviruses. *Journal of virology*, 79(13), pp.8004–13. Available at: http://jvi.asm.org/content/79/13/8004.long [Accessed August 15, 2015].

Muñoz-Jordán, J.L., 2010. Subversion of interferon by dengue virus. *Current topics in microbiology and immunology*, 338, pp.35–44. Available at: http://www.ncbi.nlm.nih.gov/pubmed/19802576 [Accessed August 15, 2015].

Mustafa, M.S. et al., 2014. Discovery of fifth serotype of dengue virus (DENV-5): A new public health dilemma in dengue control. *Medical Journal Armed Forces India*, 71(1), pp.67–70. Available at: http://www.sciencedirect.com/science/article/pii/S0377123714001725 [Accessed January 11, 2015].

Muylaert, I.R. et al., 1996. Mutagenesis of the N-linked glycosylation sites of the yellow fever virus NS1 protein: effects on virus replication and mouse neurovirulence. *Virology*, 222(1), pp.159–68. Available at: http://www.sciencedirect.com/science/article/pii/S0042682296904067 [Accessed October 26, 2015].

Nam, D.K. et al., 2002. Oligo(dT) primer generates a high frequency of truncated cDNAs through internal poly(A) priming during reverse transcription. *Proceedings of the National Academy of Sciences of the United States of America*, 99(9), pp.6152–6. Available at: http://www.pubmedcentral.nih.gov/articlerender.fcgi?artid=122918&tool=pmcentrez&rendertype=abstract [Accessed November 7, 2015].

Nam, V. et al., 2012. Community-based control of Aedes aegypti by using Mesocyclops in southern Vietnam. *The American Journal of Tropical Medicine and Hygiene*, 86(5), pp.850–9. Available at: http://www.pubmedcentral.nih.gov/articlerender.fcgi?artid=3335693&tool=pmcentrez&rendertype=abstract [Accessed October 28, 2015].

Nam, V.S. et al., 2000. National progress in dengue vector control in Vietnam: survey for Mesocyclops (Copepoda), Micronecta (Corixidae), and fish as biological control agents. *The American journal of tropical medicine and hygiene*, 62(1), pp.5–10. Available at: http://www.ncbi.nlm.nih.gov/pubmed/10761718 [Accessed October 28, 2015].

Nasirudeen, A.M.A. et al., 2011. RIG-I, MDA5 and TLR3 Synergistically Play an Important Role in Restriction of Dengue Virus Infection E. Harris, ed. *PLoS Neglected Tropical Diseases*, 5(1), p.e926. Available at: http://journals.plos.org/plosntds/article?id=10.1371/journal.pntd.0000926 [Accessed November 19, 2015].

Nayak, V. et al., 2009. Crystal structure of dengue virus type 1 envelope protein in the postfusion conformation and its implications for membrane fusion. *Journal of virology*, 83(9), pp.4338–44. Available at: http://jvi.asm.org/content/83/9/4338 [Accessed October 21, 2015].

Nene, V. et al., 2007. Genome sequence of Aedes aegypti, a major arbovirus vector. *Science (New York, N.Y.)*, 316(5832), pp.1718–23. Available at: http://www.sciencemag.org/content/316/5832/1718.abstract [Accessed November 6, 2015].

Netsawang, J. et al., 2010. Nuclear localization of dengue virus capsid protein is required for DAXX interaction and apoptosis. *Virus research*, 147(2), pp.275–83. Available at: http://www.sciencedirect.com/science/article/pii/S0168170209004134 [Accessed October 27, 2015].

Nicolaou, S.A. et al., 2009. Localization of Kv1.3 channels in the immunological synapse modulates

the calcium response to antigen stimulation in T lymphocytes. *Journal of immunology (Baltimore, Md. : 1950)*, 183(10), pp.6296–302. Available at: http://www.pubmedcentral.nih.gov/articlerender.fcgi?artid=2783516&tool=pmcentrez&rendertype=abstract [Accessed August 27, 2015].

Noisakran, S. et al., 2008. Identification of human hnRNP C1/C2 as a dengue virus NS1-interacting protein. *Biochemical and biophysical research communications*, 372(1), pp.67–72. Available at: http://www.sciencedirect.com/science/article/pii/S0006291X08008589 [Accessed October 24, 2015].

Noisakran, S. et al., 2012. Infection of bone marrow cells by dengue virus in vivo. *Experimental hematology*, 40(3), pp.250–259.e4. Available at: http://www.sciencedirect.com/science/article/pii/S0301472X11005935 [Accessed August 31, 2015].

Nojima, T. et al., 2009. Herpesvirus protein ICP27 switches PML isoform by altering mRNA splicing. *Nucleic acids research*, 37(19), pp.6515–27. Available at: http://www.pubmedcentral.nih.gov/articlerender.fcgi?artid=2770646&tool=pmcentrez&rendertype=abstract [Accessed November 23, 2015].

Normile, D., 2013. Tropical medicine. Surprising new dengue virus throws a spanner in disease control efforts. *Science (New York, N.Y.)*, 342(6157), p.415. Available at: http://www.ncbi.nlm.nih.gov/pubmed/24159024 [Accessed November 19, 2015].

O'Neill, L.A.J. & Bowie, A.G., 2010. Sensing and signaling in antiviral innate immunity. *Current biology : CB*, 20(7), pp.R328–33. Available at: http://www.sciencedirect.com/science/article/pii/S0960982210000874 [Accessed November 11, 2015].

Ohara, O. & Temple, G., 2001. Directional cDNA library construction assisted by the in vitro recombination reaction. *Nucleic acids research*, 29(4), p.E22. Available at: http://www.pubmedcentral.nih.gov/articlerender.fcgi?artid=29629&tool=pmcentrez&rendertype=abstract [Accessed November 4, 2015].

Oldenburg, K.R. et al., 1997. Recombination-mediated PCR-directed plasmid construction in vivo in yeast. *Nucleic acids research*, 25(2), pp.451–2. Available at: http://www.pubmedcentral.nih.gov/articlerender.fcgi?artid=146432&tool=pmcentrez&rendertype=abstract [Accessed November 5, 2015].

Oliphant, T. et al., 2006. Antibody recognition and neutralization determinants on domains I and II of West Nile Virus envelope protein. *Journal of virology*, 80(24), pp.12149–59. Available at: http://www.pubmedcentral.nih.gov/articlerender.fcgi?artid=1676294&tool=pmcentrez&rendertype=abstract [Accessed November 2, 2015].

Osorio, J.E. et al., 2011. Development of DENVax: a chimeric dengue-2 PDK-53-based tetravalent vaccine for protection against dengue fever. *Vaccine*, 29(42), pp.7251–60. Available at: http://www.pubmedcentral.nih.gov/articlerender.fcgi?artid=4592106&tool=pmcentrez&rendertype=abstract [Accessed November 21, 2015].

Osorio, J.E. et al., 2014. Safety and immunogenicity of a recombinant live attenuated tetravalent dengue vaccine (DENVax) in flavivirus-naive healthy adults in Colombia: a randomised, placebo-controlled, phase 1 study. *The Lancet Infectious Diseases*, 14(9), pp.830–838. Available at: http://www.pubmedcentral.nih.gov/articlerender.fcgi?artid=4648257&tool=pmcentrez&rendertype=abstract [Accessed October 6, 2015].

Otsuki, K. et al., 1979. Studies on avian infectious bronchitis virus (IBV). III. Interferon induction by and sensitivity to interferon of IBV. *Archives of virology*, 60(3-4), pp.249–55. Available at: http://www.ncbi.nlm.nih.gov/pubmed/228636 [Accessed September 25, 2015].

Pahl, H.L., 1999. Activators and target genes of Rel/NF-kappaB transcription factors. *Oncogene*, 18(49), pp.6853–66. Available at: http://www.nature.com/onc/journal/v18/n49/full/1203239a.html [Accessed November 13, 2015].

Pando-Robles, V. et al., 2014. Quantitative proteomic analysis of Huh-7 cells infected with Dengue

virus by label-free LC-MS. *Journal of proteomics*, 111, pp.16–29. Available at: http://www.sciencedirect.com/science/article/pii/S1874391914003443 [Accessed November 6, 2015].

Panyasrivanit, M. et al., 2009. Co-localization of constituents of the dengue virus translation and replication machinery with amphisomes. *The Journal of general virology*, 90(Pt 2), pp.448–56. Available at: http://jgv.microbiologyresearch.org/content/journal/jgv/10.1099/vir.0.005355-0;jsessionid=3sncfmf4d8g3j.x-sgm-live-02#tab2 [Accessed April 9, 2016].

Panyi, G. et al., 2003. Colocalization and nonrandom distribution of Kv1.3 potassium channels and CD3 molecules in the plasma membrane of human T lymphocytes. *Proceedings of the National Academy of Sciences of the United States of America*, 100(5), pp.2592–7. Available at: http://www.pubmedcentral.nih.gov/articlerender.fcgi?artid=151385&tool=pmcentrez&rendertype=abstract [Accessed August 27, 2015].

Panyi, G. et al., 2004. Kv1.3 potassium channels are localized in the immunological synapse formed between cytotoxic and target cells. *Proceedings of the National Academy of Sciences of the United States of America*, 101(5), pp.1285–90. Available at: http://www.pnas.org/content/101/5/1285.full [Accessed August 29, 2015].

Patel, V.J. et al., 2009. A comparison of labeling and label-free mass spectrometry-based proteomics approaches. *Journal of proteome research*, 8(7), pp.3752–9. Available at: http://pubs.acs.org/doi/abs/10.1021/pr900080y [Accessed April 12, 2016].

Patramool, S. et al., 2011. Proteomic analysis of an Aedes albopictus cell line infected with Dengue serotypes 1 and 3 viruses. *Parasites & Vectors*, 4(1), p.138. Available at: http://www.pubmedcentral.nih.gov/articlerender.fcgi?artid=3151224&tool=pmcentrez&rendertype=abstract [Accessed September 30, 2015].

Pattanakitsakul, S.-N. et al., 2007. Proteomic analysis of host responses in HepG2 cells during dengue virus infection. *Journal of proteome research*, 6(12), pp.4592–600. Available at: http://dx.doi.org/10.1021/pr070366b [Accessed November 22, 2015].

Peeling, R.W. et al., 2010. Evaluation of diagnostic tests: dengue. *Nature Reviews Microbiology*, 8(12), pp.S30–S37. Available at: http://www.nature.com/nrmicro/journal/v8/n12_supp/full/nrmicro2459.html#top [Accessed October 19, 2015].

Peleg, J., 1968. Growth of arboviruses in monolayers from subcultured mosquito embryo cells. *Virology*, 35(4), pp.617–619. Available at: http://www.sciencedirect.com/science/article/pii/0042682268902936 [Accessed July 30, 2015].

Peng, X. et al., 2009. Virus-host interactions: from systems biology to translational research. *Current opinion in microbiology*, 12(4), pp.432–8. Available at: http://www.pubmedcentral.nih.gov/articlerender.fcgi?artid=2742299&tool=pmcentrez&rendertype=abstract [Accessed November 19, 2015].

Perich, M.J. et al., 2000. Behavior of Resting Aedes aegypti (Culicidae: Diptera) and Its Relation to Ultra-low Volume Adulticide Efficacy in Panama City, Panama. *Journal of Medical Entomology*, 37(4), pp.541–546. Available at: http://jme.oxfordjournals.org/content/37/4/541.abstract [Accessed October 22, 2015].

Petersen, K. et al., 2002. Matrix attachment regions (MARs) enhance transformation frequencies and reduce variance of transgene expression in barley. *Plant molecular biology*, 49(1), pp.45–58. Available at: http://www.ncbi.nlm.nih.gov/pubmed/12008898 [Accessed October 30, 2015].

Pherez, F.M., 2007. Factors affecting the emergence and prevalence of vector borne infections (VBI) and the role of vertical transmission (VT). *Journal of vector borne diseases*, 44(3), pp.157–63. Available at: http://www.ncbi.nlm.nih.gov/pubmed/17896618 [Accessed October 23, 2015].

Phuc, H.K. et al., 2007. Late-acting dominant lethal genetic systems and mosquito control. *BMC biology*, 5(1), p.11. Available at: http://www.biomedcentral.com/1741-7007/5/11 [Accessed September 28, 2015].

Platanias, L.C., 2005. Mechanisms of type-I- and type-II-interferon-mediated signalling. *Nature*

reviews. Immunology, 5(5), pp.375–86. Available at: http://dx.doi.org/10.1038/nri1604 [Accessed December 8, 2014].

Pokidysheva, E. et al., 2006. Cryo-EM reconstruction of dengue virus in complex with the carbohydrate recognition domain of DC-SIGN. *Cell*, 124(3), pp.485–93. Available at: http://www.sciencedirect.com/science/article/pii/S0092867406000079 [Accessed November 14, 2015].

Pongs, O. et al., 1988. Shaker encodes a family of putative potassium channel proteins in the nervous system of Drosophila. *The EMBO journal*, 7(4), pp.1087–96. Available at: http://europepmc.org/articles/PMC454441/?report=abstract [Accessed August 31, 2015].

Pouliot, S. et al., 2010. Maternal dengue and pregnancy outcomes: a systematic review. *Obstetrical & gynecological survey*, 65(2), pp.107–18. Available at: http://www.ncbi.nlm.nih.gov/pubmed/20100360 [Accessed October 25, 2015].

Preußat, K. et al., 2003. Expression of voltage-gated potassium channels Kv1.3 and Kv1.5 in human gliomas. *Neuroscience Letters*, 346(1-2), pp.33–36. Available at: http://www.sciencedirect.com/science/article/pii/S0304394003005627 [Accessed August 29, 2015].

Pryor, M.J. et al., 2004. Histidine 39 in the dengue virus type 2 M protein has an important role in virus assembly. *Journal of General Virology*, 85(12), pp.3627–3636.

Pryor, M.J. & Wright, P.J., 1994. Glycosylation mutants of dengue virus NS1 protein. *The Journal of general virology*, 75 (Pt 5)(5), pp.1183–7. Available at: http://jgv.microbiologyresearch.org/content/journal/jgv/10.1099/0022-1317-75-5-1183 [Accessed October 26, 2015].

Punzel, M. et al., 2014. Dengue virus transmission by blood stem cell donor after travel to Sri Lanka; Germany, 2013. *Emerging infectious diseases*, 20(8), pp.1366–9. Available at: http://www.pubmedcentral.nih.gov/articlerender.fcgi?artid=4111198&tool=pmcentrez&rendertype=abstract [Accessed October 25, 2015].

Ramanathan, M.P. et al., 2006. Host cell killing by the West Nile Virus NS2B-NS3 proteolytic complex: NS3 alone is sufficient to recruit caspase-8-based apoptotic pathway. *Virology*, 345(1), pp.56–72. Available at: http://www.sciencedirect.com/science/article/pii/S0042682205005258 [Accessed October 29, 2015].

Rampalli, S. et al., 2005. Tumor suppressor SMAR1 mediates cyclin D1 repression by recruitment of the SIN3/histone deacetylase 1 complex. *Molecular and cellular biology*, 25(19), pp.8415–29. Available at: http://www.pubmedcentral.nih.gov/articlerender.fcgi?artid=1265755&tool=pmcentrez&rendertype=abstract [Accessed August 15, 2015].

Redman, P.T. et al., 2007. Apoptotic surge of potassium currents is mediated by p38 phosphorylation of Kv2.1. *Proceedings of the National Academy of Sciences of the United States of America*, 104(9), pp.3568–73. Available at: http://www.pubmedcentral.nih.gov/articlerender.fcgi?artid=1805571&tool=pmcentrez&rendertype=abstract [Accessed September 1, 2015].

Reggiori, F. et al., 2010. Coronaviruses Hijack the LC3-I-positive EDEMosomes, ER-derived vesicles exporting short-lived ERAD regulators, for replication. *Cell host & microbe*, 7(6), pp.500–8. Available at: http://www.sciencedirect.com/science/article/pii/S1931312810001769 [Accessed March 23, 2016].

Reikine, S., Nguyen, J.B. & Modis, Y., 2014. Pattern Recognition and Signaling Mechanisms of RIG-I and MDA5. *Frontiers in immunology*, 5, p.342. Available at: http://www.pubmedcentral.nih.gov/articlerender.fcgi?artid=4107945&tool=pmcentrez&rendertype=abstract [Accessed November 19, 2015].

Reimer, T. et al., 2008. poly(I:C) and LPS induce distinct IRF3 and NF-kappaB signaling during type-I IFN and TNF responses in human macrophages. *Journal of leukocyte biology*, 83(5), pp.1249–57. Available at: http://www.jleukbio.org/content/83/5/1249.long [Accessed July 1, 2015].

Reyes-Del Valle, J. et al., 2005. Heat shock protein 90 and heat shock protein 70 are components of dengue virus receptor complex in human cells. *Journal of virology*, 79(8), pp.4557–67. Available at: http://www.pubmedcentral.nih.gov/articlerender.fcgi?artid=1069525&tool=pmcentrez&rendertype=abstract [Accessed November 14, 2015].

Robert Putnak, J. et al., 2005. An evaluation of dengue type-2 inactivated, recombinant subunit, and live-attenuated vaccine candidates in the rhesus macaque model. *Vaccine*, 23(35), pp.4442–4452. Available at: http://www.sciencedirect.com/science/article/pii/S0264410X0500441X [Accessed November 2, 2015].

Rodríguez, M.M., Bisset, J.A. & Fernández, D., 2007. Levels of insecticide resistance and resistance mechanisms in Aedes aegypti from some Latin American countries. *Journal of the American Mosquito Control Association*, 23(4), pp.420–9. Available at: http://www.ncbi.nlm.nih.gov/pubmed/18240518 [Accessed October 28, 2015].

Rodriguez-Madoz, J.R. et al., 2010. Inhibition of the type I interferon response in human dendritic cells by dengue virus infection requires a catalytically active NS2B3 complex. *Journal of virology*, 84(19), pp.9760–74. Available at: http://jvi.asm.org/content/84/19/9760.long [Accessed August 16, 2015].

Roosendaal, J. et al., 2006. Regulated cleavages at the West Nile virus NS4A-2K-NS4B junctions play a major role in rearranging cytoplasmic membranes and Golgi trafficking of the NS4A protein. *Journal of virology*, 80(9), pp.4623–32. Available at: http://jvi.asm.org/content/80/9/4623 [Accessed October 27, 2015].

Rutschmann, S., Kilinc, A. & Ferrandon, D., 2002. Cutting Edge: The Toll Pathway Is Required for Resistance to Gram-Positive Bacterial Infections in Drosophila. *The Journal of Immunology*, 168(4), pp.1542–1546. Available at: http://www.jimmunol.org/content/168/4/1542.full [Accessed October 1, 2015].

Sabin, L.R., Hanna, S.L. & Cherry, S., 2010. Innate antiviral immunity in Drosophila. *Current Opinion in Immunology*, 22(1), pp.4–9. Available at: http://www.pubmedcentral.nih.gov/articlerender.fcgi?artid=2831143&tool=pmcentrez&rendertype=abstract [Accessed October 1, 2015].

Salazar, C. et al., 2007. A cytoskeletal actin gene in the mosquito Anopheles gambiae. *Insect Molecular Biology*, 3(1), pp.1–13. Available at: http://doi.wiley.com/10.1111/j.1365-2583.1994.tb00145.x [Accessed November 5, 2015].

Salazar, M.I. et al., 2007. Dengue virus type 2: replication and tropisms in orally infected Aedes aegypti mosquitoes. *BMC microbiology*, 7(1), p.9. Available at: http://www.biomedcentral.com/1471-2180/7/9 [Accessed September 29, 2015].

Salinas, M. et al., 1997. New Modulatory Subunits for Mammalian ShabK+ Channels. *Journal of Biological Chemistry*, 272(39), pp.24371–24379. Available at: http://europepmc.org/abstract/MED/9305895 [Accessed August 28, 2015].

Samsa, M.M. et al., 2009. Dengue virus capsid protein usurps lipid droplets for viral particle formation. *PLoS pathogens*, 5(10), p.e1000632. Available at: http://www.pubmedcentral.nih.gov/articlerender.fcgi?artid=2760139&tool=pmcentrez&rendertype=abstract [Accessed April 23, 2015].

Sánchez-Vargas, I. et al., 2009. Dengue virus type 2 infections of Aedes aegypti are modulated by the mosquito's RNA interference pathway. *PLoS pathogens*, 5(2), p.e1000299. Available at: http://journals.plos.org/plospathogens/article?id=10.1371/journal.ppat.1000299 [Accessed September 29, 2015].

Sands, S.B., 1989. Charybdotoxin blocks voltage-gated K+ channels in human and murine T lymphocytes. *The Journal of General Physiology*, 93(6), pp.1061–1074. Available at: http://jgp.rupress.org/content/93/6/1061 [Accessed August 31, 2015].

Sasaki, T. et al., 2013. Dengue virus neutralization and antibody-dependent enhancement activities of human monoclonal antibodies derived from dengue patients at acute phase of secondary infection. *Antiviral research*, 98(3), pp.423–31. Available at:

http://www.sciencedirect.com/science/article/pii/S0166354213000727 [Accessed October 28, 2015].

Schexneider, K.I. & Reedy, E.A., 2005. Thrombocytopenia in dengue fever. *Current hematology reports*, 4(2), pp.145–8. Available at: http://www.ncbi.nlm.nih.gov/pubmed/15720964 [Accessed August 31, 2015].

Schlake, T. et al., 1994. Gene expression within a chromatin domain: the role of core histone hyperacetylation. *Biochemistry*, 33(14), pp.4197–206. Available at: http://www.ncbi.nlm.nih.gov/pubmed/8155635 [Accessed October 30, 2015].

Schmitz, A. et al., 2005. Design of PAP-1, a selective small molecule Kv1.3 blocker, for the suppression of effector memory T cells in autoimmune diseases. *Molecular pharmacology*, 68(5), pp.1254–70. Available at: http://molpharm.aspetjournals.org/content/68/5/1254.abstract [Accessed September 3, 2015].

Scott, J.C. et al., 2010. Comparison of Dengue Virus Type 2-Specific Small RNAs from RNA Interference-Competent and –Incompetent Mosquito Cells S. L. O'Neill, ed. *PLoS Neglected Tropical Diseases*, 4(10), p.e848. Available at: http://www.pubmedcentral.nih.gov/articlerender.fcgi?artid=2964303&tool=pmcentrez&rendertype=abstract [Accessed October 5, 2015].

Seo, J.S. et al., 2014. Cell cycle-dependent SUMO-1 conjugation to nuclear mitotic apparatus protein (NuMA). *Biochemical and biophysical research communications*, 443(1), pp.259–65. Available at: http://www.ncbi.nlm.nih.gov/pubmed/24309115 [Accessed November 23, 2015].

Sessions, O.M. et al., 2009. Discovery of insect and human dengue virus host factors. *Nature*, 458(7241), pp.1047–50. Available at: http://dx.doi.org/10.1038/nature07967 [Accessed April 17, 2015].

Shafee, N. & AbuBakar, S., 2003. Dengue virus type 2 NS3 protease and NS2B-NS3 protease precursor induce apoptosis. *The Journal of general virology*, 84(Pt 8), pp.2191–5. Available at: http://jgv.microbiologyresearch.org/content/journal/jgv/10.1099/vir.0.19022-0#tab2 [Accessed October 27, 2015].

Shagin, D.A. et al., 2002. A novel method for SNP detection using a new duplex-specific nuclease from crab hepatopancreas. *Genome research*, 12(12), pp.1935–42. Available at: http://www.pubmedcentral.nih.gov/articlerender.fcgi?artid=187582&tool=pmcentrez&rendertype=abstract [Accessed November 6, 2015].

Shcheglov, A. et al., 2007. *Normalization of cDNA libraries* A. A. Buzdin & S. A. Lukyanov, eds., Dordrecht: Springer Netherlands. Available at: http://www.springerlink.com/index/10.1007/978-1-4020-6040-3 [Accessed October 3, 2015].

Shepard, D.S. et al., 2011. Economic impact of dengue illness in the Americas. *The American journal of tropical medicine and hygiene*, 84(2), pp.200–7. Available at: http://www.pubmedcentral.nih.gov/articlerender.fcgi?artid=3029168&tool=pmcentrez&rendertype=abstract [Accessed November 4, 2015].

Shepard, D.S., Undurraga, E.A. & Halasa, Y.A., 2013. Economic and disease burden of dengue in Southeast Asia. *PLoS neglected tropical diseases*, 7(2), p.e2055. Available at: http://journals.plos.org/plosntds/article?id=10.1371/journal.pntd.0002055 [Accessed February 17, 2015].

Shera, K.A., Shera, C.A. & McDougall, J.K., 2001. Small tumor virus genomes are integrated near nuclear matrix attachment regions in transformed cells. *Journal of virology*, 75(24), pp.12339–46. Available at: http://www.pubmedcentral.nih.gov/articlerender.fcgi?artid=116130&tool=pmcentrez&rendertype=abstract [Accessed November 10, 2015].

Shi, P.-Y., 2014. Flavivirus NS5 Prevents the InSTATement of IFN. *Cell host & microbe*, 16(3), pp.269–71. Available at: http://www.sciencedirect.com/science/article/pii/S1931312814003035 [Accessed November 3, 2015].

Shu, P.Y. et al., 2000. Dengue NS1-specific antibody responses: isotype distribution and serotyping in

patients with Dengue fever and Dengue hemorrhagic fever. *Journal of medical virology*, 62(2), pp.224–32. Available at: http://www.ncbi.nlm.nih.gov/pubmed/11002252 [Accessed November 2, 2015].

Silva, E.M. et al., 2013. Mapping the interactions of dengue virus NS1 protein with human liver proteins using a yeast two-hybrid system: identification of C1q as an interacting partner. *PloS one*, 8(3), p.e57514. Available at: http://www.pubmedcentral.nih.gov/articlerender.fcgi?artid=3597719&tool=pmcentrez&rendertype=abstract [Accessed June 19, 2015].

Sim, S. & Dimopoulos, G., 2010a. Dengue virus inhibits immune responses in Aedes aegypti cells. *PloS one*, 5(5), p.e10678. Available at: http://journals.plos.org/plosone/article?id=10.1371/journal.pone.0010678 [Accessed September 14, 2015].

Sim, S. & Dimopoulos, G., 2010b. Dengue virus inhibits immune responses in Aedes aegypti cells. *PloS one*, 5(5), p.e10678. Available at: http://www.pubmedcentral.nih.gov/articlerender.fcgi?artid=2872661&tool=pmcentrez&rendertype=abstract [Accessed September 14, 2015].

Sim, S., Jupatanakul, N. & Dimopoulos, G., 2014. Mosquito Immunity against Arboviruses. *Viruses*, 6(11), pp.4479–4504. Available at: http://www.mdpi.com/1999-4915/6/11/4479/.

Singh, K. et al., 2007. p53 target gene SMAR1 is dysregulated in breast cancer: its role in cancer cell migration and invasion. *PloS one*, 2(7), p.e660. Available at: http://www.pubmedcentral.nih.gov/articlerender.fcgi?artid=1924604&tool=pmcentrez&rendertype=abstract.

Singh, K. et al., 2009. Tumor suppressor SMAR1 represses IkappaBalpha expression and inhibits p65 transactivation through matrix attachment regions. *The Journal of biological chemistry*, 284(2), pp.1267–78. Available at: http://www.jbc.org/content/284/2/1267.long [Accessed July 7, 2015].

Singh, M.P. et al., 2010. NS1 antigen as an early diagnostic marker in dengue: report from India. *Diagnostic microbiology and infectious disease*, 68(1), pp.50–4. Available at: http://www.sciencedirect.com/science/article/pii/S0732889310001276 [Accessed October 26, 2015].

Singh, S. et al., 2010. SMAR1 regulates free radical stress through modulation of AKR1a4 enzyme activity. *The international journal of biochemistry & cell biology*, 42(7), pp.1105–14. Available at: http://www.ncbi.nlm.nih.gov/pubmed/20097305 [Accessed November 12, 2015].

Sinha, S. et al., 2012. Chromatin remodelling protein SMAR1 inhibits p53 dependent transactivation by regulating acetyl transferase p300. *The international journal of biochemistry & cell biology*, 44(1), pp.46–52. Available at: http://www.sciencedirect.com/science/article/pii/S1357272511002937 [Accessed August 15, 2015].

Sinha, S. et al., 2010. Coordinated regulation of p53 apoptotic targets BAX and PUMA by SMAR1 through an identical MAR element. *The EMBO journal*, 29(4), pp.830–42. Available at: http://www.pubmedcentral.nih.gov/articlerender.fcgi?artid=2829167&tool=pmcentrez&rendertype=abstract [Accessed November 12, 2015].

Siu, R.W.C. et al., 2011. Antiviral RNA interference responses induced by Semliki Forest virus infection of mosquito cells: characterization, origin, and frequency-dependent functions of virus-derived small interfering RNAs. *Journal of virology*, 85(6), pp.2907–17. Available at: http://www.pubmedcentral.nih.gov/articlerender.fcgi?artid=3067965&tool=pmcentrez&rendertype=abstract [Accessed September 30, 2015].

Sobhanifar, S., 2003. Yeast two hybrid assay: A fishing tale. *BioTeach Journal*, 1(Figure 3), pp.81–88. Available at: http://scholar.google.com/scholar?hl=en&btnG=Search&q=intitle:Yeast+Two+Hybrid+Assay+:+A+Fishing+Tale#0.

Sokolov, Y., 1997. Purification, Visualization, and Biophysical Characterization of Kv1.3 Tetramers.

Journal of Biological Chemistry, 272(4), pp.2389–2395. Available at: http://www.jbc.org/content/272/4/2389.long [Accessed August 25, 2015].

Souza-Neto, J.A., Sim, S. & Dimopoulos, G., 2009. An evolutionary conserved function of the JAK-STAT pathway in anti-dengue defense. *Proceedings of the National Academy of Sciences of the United States of America*, 106(42), pp.17841–6. Available at: http://www.pubmedcentral.nih.gov/articlerender.fcgi?artid=2764916&tool=pmcentrez&rendertype=abstract [Accessed August 24, 2015].

Spiker, S. & Thompson, W.F., 1996. Nuclear Matrix Attachment Regions and Transgene Expression in Plants. *Plant physiology*, 110(1), pp.15–21. Available at: http://www.pubmedcentral.nih.gov/articlerender.fcgi?artid=157689&tool=pmcentrez&rendertype=abstract [Accessed October 30, 2015].

Sreenath, K. et al., 2010. Nuclear matrix protein SMAR1 represses HIV-1 LTR mediated transcription through chromatin remodeling. *Virology*, 400(1), pp.76–85. Available at: http://www.ncbi.nlm.nih.gov/pubmed/20153010 [Accessed November 3, 2015].

Sriburi, R. et al., 2004. XBP1: a link between the unfolded protein response, lipid biosynthesis, and biogenesis of the endoplasmic reticulum. *The Journal of cell biology*, 167(1), pp.35–41. Available at: http://jcb.rupress.org/content/167/1/35.long [Accessed November 20, 2015].

Stadler, K. et al., 1997. Proteolytic activation of tick-borne encephalitis virus by furin. *Journal of virology*, 71(11), pp.8475–81. Available at: http://www.pubmedcentral.nih.gov/articlerender.fcgi?artid=192310&tool=pmcentrez&rendertype=abstract [Accessed October 20, 2015].

Szabò, I. et al., 2005. A novel potassium channel in lymphocyte mitochondria. *The Journal of biological chemistry*, 280(13), pp.12790–8. Available at: http://www.jbc.org/content/280/13/12790.long#F1 [Accessed August 30, 2015].

Tahoun, A. et al., 2011. Comparative analysis of EspF variants in inhibition of Escherichia coli phagocytosis by macrophages and inhibition of E. Coli translocation through human- and bovine-derived M cells. *Infection and Immunity*, 79(11), pp.4716–4729.

Taimen, P. et al., 2004. NuMA and nuclear lamins are cleaved during viral infection--inhibition of caspase activity prevents cleavage and rescues HeLa cells from measles virus-induced but not from rhinovirus 1B-induced cell death. *Virology*, 320(1), pp.85–98. Available at: http://www.sciencedirect.com/science/article/pii/S0042682203008651 [Accessed June 15, 2015].

Tambyah, P.A. et al., 2008. Dengue hemorrhagic fever transmitted by blood transfusion. *The New England journal of medicine*, 359(14), pp.1526–7. Available at: http://www.ncbi.nlm.nih.gov/pubmed/18832256 [Accessed October 25, 2015].

Tan, F.L.-S. et al., 2005. Dengue haemorrhagic fever after living donor renal transplantation. *Nephrology, dialysis, transplantation : official publication of the European Dialysis and Transplant Association - European Renal Association*, 20(2), pp.447–8. Available at: http://ndt.oxfordjournals.org/content/20/2/447.long [Accessed October 25, 2015].

Tanabe, M. et al., 2003. Mechanism of up-regulation of human Toll-like receptor 3 secondary to infection of measles virus-attenuated strains. *Biochemical and Biophysical Research Communications*, 311(1), pp.39–48. Available at: http://www.sciencedirect.com/science/article/pii/S0006291X03019600 [Accessed November 12, 2015].

Tassaneetrithep, B. et al., 2003. DC-SIGN (CD209) mediates dengue virus infection of human dendritic cells. *The Journal of experimental medicine*, 197(7), pp.823–9. Available at: http://jem.rupress.org/content/197/7/823.long [Accessed August 27, 2015].

Tauszig, S. et al., 2000. Toll-related receptors and the control of antimicrobial peptide expression in Drosophila. *Proceedings of the National Academy of Sciences of the United States of America*, 97(19), pp.10520–5. Available at: http://www.pnas.org/content/97/19/10520 [Accessed July 8, 2015].

Tavalai, N. & Stamminger, T., 2009. Interplay between Herpesvirus Infection and Host Defense by PML Nuclear Bodies. *Viruses*, 1(3), pp.1240–64. Available at: http://www.mdpi.com/1999-4915/1/3/1240/htm [Accessed November 23, 2015].

Taylor, M.P. & Kirkegaard, K., 2007. Modification of cellular autophagy protein LC3 by poliovirus. *Journal of virology*, 81(22), pp.12543–53. Available at: http://www.pubmedcentral.nih.gov/articlerender.fcgi?artid=2169029&tool=pmcentrez&rendertype=abstract [Accessed April 9, 2016].

Teixeira, M.G. et al., 2013. Epidemiological Trends of Dengue Disease in Brazil (2000–2010): A Systematic Literature Search and Analysis T. R. Unnasch, ed. *PLoS Neglected Tropical Diseases*, 7(12), p.e2520. Available at: http://journals.plos.org/plosntds/article?id=10.1371/journal.pntd.0002520 [Accessed October 4, 2015].

Tergaonkar, V., 2006. NFκB pathway: A good signaling paradigm and therapeutic target. *The International Journal of Biochemistry & Cell Biology*, 38(10), pp.1647–1653. Available at: http://www.ncbi.nlm.nih.gov/pubmed/16766221 [Accessed September 21, 2015].

Thaithumyanon, P. et al., 1994. Dengue infection complicated by severe hemorrhage and vertical transmission in a parturient woman. *Clinical infectious diseases : an official publication of the Infectious Diseases Society of America*, 18(2), pp.248–9. Available at: http://www.ncbi.nlm.nih.gov/pubmed/8161636 [Accessed October 2, 2015].

Tham, H.-W. et al., 2014. CPB1 of Aedes aegypti interacts with DENV2 E protein and regulates intracellular viral accumulation and release from midgut cells. *Viruses*, 6(12), pp.5028–46. Available at: http://www.pubmedcentral.nih.gov/articlerender.fcgi?artid=4276941&tool=pmcentrez&rendertype=abstract [Accessed September 29, 2015].

Thomas, P. & Smart, T.G., 2005. HEK293 cell line: a vehicle for the expression of recombinant proteins. *Journal of pharmacological and toxicological methods*, 51(3), pp.187–200. Available at: http://www.ncbi.nlm.nih.gov/pubmed/15862464 [Accessed July 9, 2014].

Thompson, B.S. et al., 2009. A therapeutic antibody against west nile virus neutralizes infection by blocking fusion within endosomes. *PLoS pathogens*, 5(5), p.e1000453. Available at: http://www.pubmedcentral.nih.gov/articlerender.fcgi?artid=2679195&tool=pmcentrez&rendertype=abstract [Accessed November 2, 2015].

Thongrungkiat, S. et al., 2011. Prospective field study of transovarial dengue-virus transmission by two different forms of Aedes aegypti in an urban area of Bangkok, Thailand. *Journal of vector ecology : journal of the Society for Vector Ecology*, 36(1), pp.147–52. Available at: http://www.bioone.org/doi/abs/10.1111/j.1948-7134.2011.00151.x [Accessed October 23, 2015].

Tsai, Y.-T. et al., 2009. Human TLR3 recognizes dengue virus and modulates viral replication in vitro. *Cellular Microbiology*, 11(4), pp.604–15. Available at: http://www.ncbi.nlm.nih.gov/pubmed/19134117 [Accessed October 9, 2015].

Tu, Y.-C. et al., 2012. Blocking double-stranded RNA-activated protein kinase PKR by Japanese encephalitis virus nonstructural protein 2A. *Journal of virology*, 86(19), pp.10347–58. Available at: http://jvi.asm.org/content/86/19/10347.long [Accessed August 15, 2015].

Uetz, P. et al., 2000. A comprehensive analysis of protein-protein interactions in Saccharomyces cerevisiae. *Nature*, 403(6770), pp.623–7. Available at: http://dx.doi.org/10.1038/35001009 [Accessed August 7, 2015].

Umareddy, I. et al., 2007. Dengue virus serotype infection specifies the activation of the unfolded protein response. *Virology journal*, 4, p.91. Available at: http://www.pubmedcentral.nih.gov/articlerender.fcgi?artid=2045667&tool=pmcentrez&rendertype=abstract [Accessed November 20, 2015].

Vicente, R. et al., 2006. Association of Kv1.5 and Kv1.3 contributes to the major voltage-dependent K+ channel in macrophages. *The Journal of biological chemistry*, 281(49), pp.37675–85. Available at: http://www.jbc.org/content/281/49/37675.long [Accessed August 31, 2015].

Wallis, T.P. et al., 2004. Determination of the disulfide bond arrangement of dengue virus NS1 protein. *The Journal of biological chemistry*, 279(20), pp.20729–41. Available at: http://www.jbc.org/content/279/20/20729.long [Accessed October 26, 2015].

Wang, E. et al., 2000. Evolutionary Relationships of Endemic/Epidemic and Sylvatic Dengue Viruses. *Journal of Virology*, 74(7), pp.3227–3234. Available at: http://jvi.asm.org/content/74/7/3227 [Accessed October 17, 2015].

Wang, T.-Y. et al., 2010. A mini review of MAR-binding proteins. *Molecular biology reports*, 37(7), pp.3553–60. Available at: http://www.ncbi.nlm.nih.gov/pubmed/20174991 [Accessed July 27, 2015].

Wang, Y., Tong, X. & Ye, X., 2012. Ndfip1 negatively regulates RIG-I-dependent immune signaling by enhancing E3 ligase Smurf1-mediated MAVS degradation. *Journal of immunology (Baltimore, Md. : 1950)*, 189(11), pp.5304–13. Available at: http://www.ncbi.nlm.nih.gov/pubmed/23087404 [Accessed November 3, 2015].

Wasinpiyamongkol, L. et al., 2012. Protein expression in the salivary glands of dengue-infected Aedes aegypti mosquitoes and blood-feeding success. *The Southeast Asian journal of tropical medicine and public health*, 43(6), pp.1346–57. Available at: http://www.ncbi.nlm.nih.gov/pubmed/23413697 [Accessed September 30, 2015].

Watanabe, T., Watanabe, S. & Kawaoka, Y., 2010. Cellular networks involved in the influenza virus life cycle. *Cell host & microbe*, 7(6), pp.427–39. Available at: http://www.sciencedirect.com/science/article/pii/S193131281000171X [Accessed May 27, 2015].

Watson, A.A. et al., 2011. Structural flexibility of the macrophage dengue virus receptor CLEC5A: implications for ligand binding and signaling. *The Journal of biological chemistry*, 286(27), pp.24208–18. Available at: http://www.jbc.org/content/286/27/24208.full [Accessed April 7, 2016].

Watterson, D., Kobe, B. & Young, P.R., 2012. Residues in domain III of the dengue virus envelope glycoprotein involved in cell-surface glycosaminoglycan binding. *The Journal of general virology*, 93(Pt 1), pp.72–82. Available at: http://jgv.microbiologyresearch.org/content/journal/jgv/10.1099/vir.0.037317-0#tab2 [Accessed March 22, 2016].

Wellenreuther, R. et al., 2004. SMART amplification combined with cDNA size fractionation in order to obtain large full-length clones. *BMC genomics*, 5(1), p.36. Available at: /pmc/articles/PMC436056/?report=abstract [Accessed September 29, 2015].

Welsch, S. et al., 2009. Composition and three-dimensional architecture of the dengue virus replication and assembly sites. *Cell host & microbe*, 5(4), pp.365–75. Available at: http://www.cell.com/article/S1931312809000985/fulltext [Accessed May 15, 2015].

White, L.A., 1987. Susceptibility of Aedes albopictus C6/36 cells to viral infection. *Journal of clinical microbiology*, 25(7), pp.1221–4. Available at: http://www.pubmedcentral.nih.gov/articlerender.fcgi?artid=269180&tool=pmcentrez&rendertype=abstract [Accessed September 14, 2015].

WHO, 2011. Comprehensive Guidelines for Prevention and Control of Dengue and Dengue Haemorrhagic Fever. , pp.1–196. Available at: http://www.searo.who.int/entity/vector_borne_tropical_diseases/documents/SEAROTPS60/en/ [Accessed October 28, 2015].

WHO, 1997. Dengue haemorrhagic fever: diagnosis, treatment, prevention and control. 2nd edition. Geneva : World Health Organization. Available at: http://www.who.int/csr/resources/publications/dengue/Denguepublication/en/ [Accessed August 31, 2015].

WHO, 2012. Global Strategy for dengue prevention and control, 2012–2020. *WHO Press*. Available at: http://www.who.int/denguecontrol/9789241504034/en/ [Accessed October 17, 2015].

Wilder-Smith, A. & Gubler, D.J., 2008. Geographic expansion of dengue: the impact of international

travel. *The Medical clinics of North America*, 92(6), pp.1377–90. Available at: http://www.sciencedirect.com/science/article/pii/S0025712508000989 [Accessed September 28, 2015].

Winnebeck, E.C., Millar, C.D. & Warman, G.R., 2010. Why does insect RNA look degraded? *Journal of insect science (Online)*, 10, p.159. Available at: http://www.pubmedcentral.nih.gov/articlerender.fcgi?artid=3016993&tool=pmcentrez&rendertype=abstract [Accessed September 21, 2015].

Wise de Valdez, M.R. et al., 2011. Genetic elimination of dengue vector mosquitoes. *Proceedings of the National Academy of Sciences of the United States of America*, 108(12), pp.4772–5. Available at: http://www.pubmedcentral.nih.gov/articlerender.fcgi?artid=3064365&tool=pmcentrez&rendertype=abstract [Accessed October 25, 2015].

Wong, K. et al., 2012. Susceptibility and response of human blood monocyte subsets to primary dengue virus infection. *PloS one*, 7(5), p.e36435. Available at: http://journals.plos.org/plosone/article?id=10.1371/journal.pone.0036435 [Accessed October 1, 2015].

Wong, S.S. et al., 2012. The dengue virus M protein localises to the endoplasmic reticulum and forms oligomers. *FEBS letters*, 586(7), pp.1032–7. Available at: http://www.sciencedirect.com/science/article/pii/S0014579312001718 [Accessed October 25, 2015].

Wu, J. et al., 2013. Voltage-gated potassium channel Kv1.3 is highly expressed in human osteosarcoma and promotes osteosarcoma growth. *International journal of molecular sciences*, 14(9), pp.19245–56. Available at: http://www.pubmedcentral.nih.gov/articlerender.fcgi?artid=3794831&tool=pmcentrez&rendertype=abstract [Accessed August 29, 2015].

Wu, S.J. et al., 2000. Comparison of two rapid diagnostic assays for detection of immunoglobulin M antibodies to dengue virus. *Clinical and diagnostic laboratory immunology*, 7(1), pp.106–10. Available at: http://www.pubmedcentral.nih.gov/articlerender.fcgi?artid=95832&tool=pmcentrez&rendertype=abstract [Accessed October 29, 2015].

Wulff, H. et al., 2004. K+ Channel Expression during B Cell Differentiation: Implications for Immunomodulation and Autoimmunity. *The Journal of Immunology*, 173(2), pp.776–786. Available at: http://www.jimmunol.org/content/173/2/776.full [Accessed August 31, 2015].

Wulff, H. et al., 2003. The voltage-gated Kv1.3 K(+) channel in effector memory T cells as new target for MS. *The Journal of clinical investigation*, 111(11), pp.1703–13. Available at: http://www.pubmedcentral.nih.gov/articlerender.fcgi?artid=156104&tool=pmcentrez&rendertype=abstract [Accessed November 17, 2015].

Xi, Z., Ramirez, J.L. & Dimopoulos, G., 2008. The Aedes aegypti toll pathway controls dengue virus infection. *PLoS pathogens*, 4(7), p.e1000098. Available at: http://www.pubmedcentral.nih.gov/articlerender.fcgi?artid=2435278&tool=pmcentrez&rendertype=abstract [Accessed May 12, 2015].

Xie, X. et al., 2013. Membrane topology and function of dengue virus NS2A protein. *Journal of virology*, 87(8), pp.4609–22. Available at: http://www.pubmedcentral.nih.gov/articlerender.fcgi?artid=3624351&tool=pmcentrez&rendertype=abstract [Accessed August 14, 2015].

Xie, X. et al., 2015. Two distinct sets of NS2A molecules are responsible for dengue virus RNA synthesis and virion assembly. *Journal of virology*, 89(2), pp.1298–313. Available at: http://jvi.asm.org/content/early/2014/11/06/JVI.02882-14 [Accessed October 24, 2015].

Xu, C. et al., 2011. HIV-1 gp120 enhances outward potassium current via CXCR4 and cAMP-dependent protein kinase A signaling in cultured rat microglia. *Glia*, 59(6), pp.997–1007. Available at: http://www.pubmedcentral.nih.gov/articlerender.fcgi?artid=3077451&tool=pmcentrez&rendertype=abstract [Accessed September 1, 2015].

Xu, J., 2003. The voltage-gated potassium channel Kv1.3 regulates energy homeostasis and body weight. *Human Molecular Genetics*, 12(5), pp.551–559. Available at: http://hmg.oxfordjournals.org/content/12/5/551.full [Accessed August 29, 2015].

Yamamoto, M. et al., 2003. Role of adaptor TRIF in the MyD88-independent toll-like receptor signaling pathway. *Science (New York, N.Y.)*, 301(5633), pp.640–3. Available at: http://www.ncbi.nlm.nih.gov/pubmed/12855817 [Accessed September 22, 2015].

Yao, R. et al., 2001. Identification of a PDZ domain containing Golgi protein, GOPC, as an interaction partner of frizzled. *Biochemical and biophysical research communications*, 286(4), pp.771–8. Available at: http://www.ncbi.nlm.nih.gov/pubmed/11520064 [Accessed November 3, 2015].

Yao, X. et al., 1996. Molecular cloning of a glibenclamide-sensitive, voltage-gated potassium channel expressed in rabbit kidney. *The Journal of clinical investigation*, 97(11), pp.2525–33. Available at: http://www.jci.org/articles/view/118700 [Accessed August 30, 2015].

Yap, G., Sil, B.K. & Ng, L.-C., 2011. Use of saliva for early dengue diagnosis. *PLoS neglected tropical diseases*, 5(5), p.e1046. Available at: http://journals.plos.org/plosntds/article?id=10.1371/journal.pntd.0001046 [Accessed October 28, 2015].

Yauch, L.E. et al., 2009. A protective role for dengue virus-specific CD8+ T cells. *Journal of immunology (Baltimore, Md. : 1950)*, 182(8), pp.4865–73. Available at: http://www.pubmedcentral.nih.gov/articlerender.fcgi?artid=2674070&tool=pmcentrez&rendertype=abstract [Accessed October 20, 2015].

Yellen, G., 2002. The voltage-gated potassium channels and their relatives. *Nature*, 419(6902), pp.35–42. Available at: http://dx.doi.org/10.1038/nature00978 [Accessed July 12, 2015].

Yoneyama, M. et al., 1996. Autocrine amplification of type I interferon gene expression mediated by interferon stimulated gene factor 3 (ISGF3). *Journal of biochemistry*, 120(1), pp.160–9. Available at: http://www.ncbi.nlm.nih.gov/pubmed/8864859 [Accessed July 31, 2015].

Yoneyama, M. et al., 1998. Direct triggering of the type I interferon system by virus infection: activation of a transcription factor complex containing IRF-3 and CBP/p300. *The EMBO journal*, 17(4), pp.1087–95. Available at: http://www.pubmedcentral.nih.gov/articlerender.fcgi?artid=1170457&tool=pmcentrez&rendertype=abstract [Accessed July 31, 2015].

Yong, Y.K. et al., 2007. Rapid detection and serotyping of dengue virus by multiplex RT-PCR and real-time SYBR green RT-PCR. *Singapore medical journal*, 48(7), pp.662–8. Available at: http://www.ncbi.nlm.nih.gov/pubmed/17609830 [Accessed October 28, 2015].

Yu, C.-Y. et al., 2006. Flavivirus infection activates the XBP1 pathway of the unfolded protein response to cope with endoplasmic reticulum stress. *Journal of virology*, 80(23), pp.11868–80. Available at: http://www.pubmedcentral.nih.gov/articlerender.fcgi?artid=1642612&tool=pmcentrez&rendertype=abstract [Accessed November 20, 2015].

Yu, I.-M. et al., 2008. Structure of the immature dengue virus at low pH primes proteolytic maturation. *Science (New York, N.Y.)*, 319(5871), pp.1834–1837.

Yu, S.P. & Kerchner, G.A., 1998. Endogenous voltage-gated potassium channels in human embryonic kidney (HEK293) cells. *Journal of neuroscience research*, 52(5), pp.612–7. Available at: http://www.ncbi.nlm.nih.gov/pubmed/9632317 [Accessed August 13, 2015].

Yusof, R., 2000. Purified NS2B/NS3 Serine Protease of Dengue Virus Type 2 Exhibits Cofactor NS2B Dependence for Cleavage of Substrates with Dibasic Amino Acids in Vitro. *Journal of Biological Chemistry*, 275(14), pp.9963–9969. Available at: http://www.jbc.org/content/275/14/9963.long [Accessed October 27, 2015].

Zahn-Zabal, M. et al., 2001. Development of stable cell lines for production or regulated expression using matrix attachment regions. *Journal of Biotechnology*, 87(1), pp.29–42. Available at: http://www.sciencedirect.com/science/article/pii/S0168165600004235 [Accessed October 30, 2015].

Zambon, R.A. et al., 2005. The Toll pathway is important for an antiviral response in Drosophila. *Proceedings of the National Academy of Sciences of the United States of America*, 102(20), pp.7257–62. Available at: http://www.pnas.org/content/102/20/7257.long [Accessed October 1, 2015].

Zhang, L. et al., 2009. Analysis of vaccinia virus-host protein-protein interactions: validations of yeast two-hybrid screenings. *Journal of proteome research*, 8(9), pp.4311–8. Available at: http://www.pubmedcentral.nih.gov/articlerender.fcgi?artid=2738428&tool=pmcentrez&rendertype=abstract [Accessed June 19, 2015].

Zhang, M. et al., 2013. Differential proteomics of Aedes albopictus salivary gland, midgut and C6/36 cell induced by dengue virus infection. *Virology*, 444(1-2), pp.109–18. Available at: http://www.sciencedirect.com/science/article/pii/S0042682213003462 [Accessed September 10, 2015].

Zhang, M. et al., 2012. TRAF-interacting protein (TRIP) negatively regulates IFN-β production and antiviral response by promoting proteasomal degradation of TANK-binding kinase 1. *The Journal of experimental medicine*, 209(10), pp.1703–11. Available at: http://jem.rupress.org/content/209/10/1703.figures-only [Accessed August 13, 2015].

Zhang, W. et al., 2003. Visualization of membrane protein domains by cryo-electron microscopy of dengue virus. *Nature Structural Biology*, 10(11), pp.907–912. Available at: http://dx.doi.org/10.1038/nsb990 [Accessed October 19, 2015].

Zhang, X. et al., 2013. Cryo-EM structure of the mature dengue virus at 3.5-Å resolution. *Nature Structural & Molecular Biology*, 20(1), pp.105–10. Available at: http://www.pubmedcentral.nih.gov/articlerender.fcgi?artid=3593067&tool=pmcentrez&rendertype=abstract [Accessed February 28, 2016].

Zhu, Y.Y. et al., 2001. Reverse transcriptase template switching: a SMART approach for full-length cDNA library construction. *BioTechniques*, 30(4), pp.892–7. Available at: http://www.ncbi.nlm.nih.gov/pubmed/11314272 [Accessed July 9, 2015].

Zong, R.T., Das, C. & Tucker, P.W., 2000. Regulation of matrix attachment region-dependent, lymphocyte-restricted transcription through differential localization within promyelocytic leukemia nuclear bodies. *The EMBO journal*, 19(15), pp.4123–33. Available at: http://www.pubmedcentral.nih.gov/articlerender.fcgi?artid=306587&tool=pmcentrez&rendertype=abstract [Accessed November 1, 2015].

Żyżyńska-Granica, B. & Koziak, K., 2012. Identification of suitable reference genes for real-time PCR analysis of statin-treated human umbilical vein endothelial cells. *PloS one*, 7(12), p.e51547. Available at: http://journals.plos.org/plosone/article?id=10.1371/journal.pone.0051547 [Accessed July 10, 2015].